Dendroclimatic Response of High-Elevation Conifers, Vancouver Island, British Columbia

by

Colin Peter Laroque
B.Sc., University of Saskatchewan, 1993
M.Sc., University of Victoria, 1995

A Dissertation Submitted in Partial Fulfillment of the
Requirements for the Degree of

DOCTOR OF PHILOSOPHY

in the Department of Geography

We accept this thesis as conforming to the required standard

Dr. D.J. Smith, Supervisor (Department of Geography)

Dr. M.C. Edgell, Departmental Member (Department of Geography)

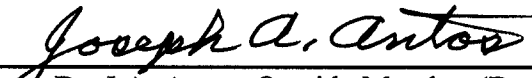

Dr. J.A. Antos, Outside Member (Department of Biology)

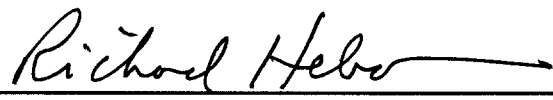

Dr. R.J. Hebda, Outside Member (School of Earth and Ocean Sciences)

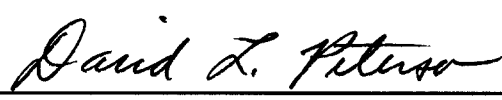

Dr. D. L. Peterson, External Examiner (College of Forest Resources, University of Washington)

Supervisor: Dr. D.J. Smith

ABSTRACT

The aim of this research program was to examine the growth response of high-elevation conifers on Vancouver Island to past, present and future climates. Forty locations were sampled and 88 chronologies were used to describe radial-growth changes over time and space. Radial-growth trends have been similar across Vancouver Island for most of the past 500 years. Large-scale oceanic influences on climate were shown to be strong forcing mechanism to radial growth.

Master chronologies were constructed for each of the five tree species examined: mountain hemlock, *Tsuga mertensiana* (Bong.) Carr., yellow-cedar, *Chamaecyparis nootkatensis* (D. Don) Spach, western hemlock, *Tsuga heterophylla* (Raf.) Sarg., Douglas-fir, *Pseudotsuga menziesii* (Mirb.) Franco, and western red-cedar, *Thuja plicata* Donn. The response of these species to climate were combined to develop multiple aggregate chronologies (MACs). The MACs are able to record a stronger relationship to climate than all but the best single-species chronologies, with relationships to seasonalized parameters improved to a greater degree than those of single-month variables.

Using these MAC relationships, proxy information was derived for four climate parameters (April 1 snowpack depth, June-July temperature, July temperature, July precipitation). The explained variance of the models was higher in the two seasonal reconstructions (April 1 snowpack depth r^2 = 41 %, June-July temperature r^2 = 34 %) than for individual monthly reconstructions (July precipitation r^2 = 15 %, July

than for individual monthly reconstructions (July precipitation $r^2 = 15$ %, July temperature $r^2 = 24$ %). A wavelet analysis showed that each of the four models contains dominant modes of variability throughout time at approximately16, 32, 65 and 130-150 year periods. Each mode of variability seems to be linked to ocean forcing mechanisms.

Climate/radial-growth relationships were used to predict radial growth under various future climate scenarios. *TREE* (Tree-ring Radial Expansion Estimator) was developed to present an interactive, internet-based radial-growth model, which calculates the short-term radial-growth response for each tree species to user-defined climate change scenarios. Long-term radial-growth responses were produced using data from general circulation models to develop relationships that predict future radial growth of each tree species. These predictions highlight which species are susceptible to future shifts in climate and indicate which climate parameters may drive changes in radial growth.

Dr. D.J. Smith, Supervisor (Department of Geography)

Dr. M.C. Edgell, Departmental Member (Department of Geography)

Dr. J.A. Antos, Outside Member (Department of Biology)

Dr. R.J. Hebda, Outside Member (Department of Earth and Ocean Sciences)

Dr. D. L. Peterson, External Examiner (College of Forest Resources, University of Washington)

Table of Contents

List of Tables

List of Figures

Acknowledgements

Grateful appreciation is given to my committee members: Dan Smith, Mike Edgell, Joe Antos, and Richard Hebda. Their comments and criticism throughout the process of writing my dissertation were invaluable. Comments from my external examiner, Dave Peterson, were also extremely helpful.

I have learned three important life lessons while completing my Ph.D. The first is that I like my sleeping bags warm. The second is that I like my beer cold. The third, and most important, is that I can never value too highly the people who have trusted me with their keys, and who have accepted mine. Keys to my office doors were always happily shared with (in alphabetical order) Jackie, Jason, Kent, and Rosaline. I shared keys to the door of the UVTRL with my good friends Alexis, Chris, Dan, Dave, Deanna, Jen, Karen, Laurel, Lisa, Rochelle, Sonya, Travis, Trisalyn and Ze ev. I ll gladly share my keys with any of you anytime. For all other doors at school that were important for me to get into, Cathy always shared the keys. For that I thank her.

My family always welcomed me with open arms and openly shared with me the keys to their homes. Although these keys were not used as often as I would have liked, it was comforting to know that I always had their keys jingling on the key chain in my pocket. To Mom and Dad Laroque and Loewen, and to Grandma Laroque, thank you so much for your open-door policies (both front door and fridge door). I can never repay you.

And lastly without a firstly, I thank Dawn. Thanks for sharing all of your keys with me wherever we moved. Thanks for sharing the key to your bank account. Thanks for sharing your editorial skills, for me they were key. Thanks for sharing the keys to your thoughts and your dreams. In return I will always share with you the key to my heart.

1.0 Introduction

The maritime climate of coastal British Columbia is regulated by the Pacific Ocean through a complex suite of forcing processes (Hanawa 1995). There is a growing recognition that the climate of the region is not static, and that shifts between climatic states have occurred not only repeatedly but often abruptly within the last millennium (Charles 1998, Gedalof and Smith 2001a). These patterns are largely a response to El Niño / Southern Oscillation (ENSO) related teleconnections and interdecadal climate variability driven by the Pacific Decadal Oscillation (PDO) (Hare 1996, Zhang *et al.* 1997, Gedalof 1999). If future climatic patterns continue in the same manner, it is likely that there will continue to be significant interannual variations in climate that will in turn influence the ecosystems of coastal British Columbia.

The potential for rapid climatic change in British Columbia over the next century makes it imperative to investigate the growth response of the province s forests to predicted climate conditions (Leung and Ghan 1999, Flato and Boer 2001). In addition to ENSO and PDO shifts, general circulation models predict increases of 2 to 5 °C in mean summer and winter temperatures within this region (Flato and Boer 2001) and increases in precipitation from 0.4 to 2 mm per day (Leung and Ghan 1999). Given that much smaller temperature and precipitation increases over the last 100 years appear to have had major impacts on the productivity of conifer forests in nearby Washington state (Graumlich *et al.* 1989), it is essential that forest managers in British Columbia understand how climate changes have and may influence forest productivity.

Climate plays an important role in limiting tree growth in coastal British Columbia, and dendroclimatological and dendroecological techniques provide a robust

tool for assessing the potential impacts of climatic change. Mature conifers contain within their annual growth rings a biological time series describing a response to a variety of site factors, including competition, tree and stand age, fire and other disturbances, and climate. Fritts (1976) established a methodological framework that uses statistical methods to decipher the climatic influences on radial growth. By comparing the annual variations in ring width to variations in monthly and seasonal climatic data, descriptive dendroclimatic models can be developed. These models can then be used to predict likely growth responses to different climate change scenarios.

Dendroclimatological investigations on Vancouver Island on the west coast of British Columbia have excellent potential for establishing climate change effects on trees. Many of the high-elevation tree species present are extremely long-lived and have a proven ability to retain a climate signal (Laroque and Smith 1999, Lewis and Smith 1999, Gedalof and Smith 2001b). The research presented in this dissertation investigates past, present and potential future climate/radial-growth relationships on Vancouver Island and strengthens the understanding of these relationships with new techniques.

1.1 Background

Although previous studies have established that trees on Vancouver Island can be used to describe past climates, proxy reconstructions from this area retain large amounts of unexplained variance (Laroque 1995, Zhang 1996, Smith and Laroque 1998a, Lewis and Smith 1999). In the response functions used to generate the proxy reconstructions, climate data generally explain between one-half and three-quarters of the variation in radial growth, with multiple, combined climate parameters necessary to explain this much

variation. The study with the fewest significant climate parameters needed to explain the variance in radial growth used only two climate parameters and a prior growth variable to explain the annual variance of mountain hemlock radial growth ($r^2 = 0.76$) (Lewis and Smith 1999) (All tree species scientific names are listed in Appendix A.). In contrast, six climate parameters and a prior growth variable were needed to explain the annual variance in radial growth of both yellow-cedar ($r^2 = 0.61$) (Laroque 1995) and Douglas-fir ($r^2 = 0.61$) (Zhang 1996).

The approach used in all of these studies was developed by Fritts *et al.* (1971) and was intended for individual tree species that are sensitive to a single dominant climate factor. In the Pacific Northwest of North America, oceanic influences result in a subdued environment where no one dominating effect consistently limits growth from year to year (Hanawa 1995). It appears that radial growth, and consequent reconstructions derived from this growth, do not consistently capture the same type or magnitude of climate signal from year to year.

With no single environmental limitation on radial growth consistently present, the single-species methodology has delivered poor results (i.e., low r^2) when reconstructing climate variables on Vancouver Island. These reconstructions are weak, with individual monthly parameters being reconstructed less reliably than seasonal climate parameters. In these studies, the strongest explained variance of a single climate parameter when modeled gave a poor result, i.e., mountain hemlock reconstructing July temperature, $r^2 = 0.25$ (Lewis and Smith 1999); yellow-cedar reconstructing August temperature, $r^2 = 0.25$ (Laroque 1995); Douglas-fir reconstructing April through July precipitation, $r^2 = 0.47$

(Zhang 1996). It may be possible to produce better proxy climate reconstructions either by means of a better statistical interpretation of climate/radial-growth relationships using a single-species methodology, or by developing new approaches that account for the varying time frame of growth from year to year in a tree-ring series.

Multiple regression (Fritts *et al.* 1971) and principal components analysis (PCA) (Peters *et al.* 1981) remain the most commonly used statistical methods to relate tree-ring widths to climate conditions. These techniques are generally able to reconstruct a large portion of the explained variance in a relationship, but they are limited by the signal strength and noise inherent in a tree-ring series. Artificial neural network (ANN) relationships have recently been employed to improve our ecological understanding of the relationships between climate and tree-rings (Keller *et al.* 1998, Woodhouse 1999), but they are limited in their ability and cannot produce proxy climate reconstructions (Zhang 2000).

One remedy is to develop climate/radial-growth relationships that use the annually variable biological clock of each species to better define targeted climate parameters. Co-occurring tree species are likely to incorporate parts of the same climate information, but under slightly different time frames depending on the particular climate dynamics of a given year and on the tolerance limits of each tree species. If each climate/radial-growth signal could be understood, then a multiple tree species approach should be able to define a stronger climate signal together than a single species could define independently.

The growth of individual coniferous tree species on Vancouver Island follows a

predictable cycle from year to year (Allen and Owens 1972, Owens 1973, Owens and Molder 1984a, Owens and Molder 1984b, Owens and Molder 1985). Nevertheless, the interval over which radial growth occurs for each species does not always coincide with the same calendar dates or progress at the same rate through the season (Laroque and Smith 1999, Gedalof and Smith 2001b). The use of the term tree-time is introduced in this dissertation to refer to a species natural schedule: when in its phenological cycle trees start to produce xylem, when they form the different types of woody tissue that make up a season s radial-growth increment, and when they allocate energy needed to produce xylem the following season. Individual tree-times may help define what climate factors are likely to be most important to radial-growth in a given year, and consequently may help predict which climate parameters can be reconstructed accurately for a given relationship.

A shortcoming of previous dendroclimatological research in the Pacific Northwest region is that researchers have derived climate proxies by assuming that calendar-time consistently matched tree-time. If trees do not consistently form rings in the same calendar-time interval, the year-to-year climate/radial-growth relationship will contain excess noise. Noise is defined as extraneous information that weakens a direct tree-ring relationship to a particular climate variable (Fritts 1976).

With each half of the climate/radial-growth relationship using a different method of keeping track of time, it is not surprising that reconstructions derived from these relationships do not produce strong results. Because seasonally variable climate conditions in a maritime location can greatly alter the timing and rate of tree growth from

year to year, setting both the meteorological collection of data and the initiation of growth onto the same timing system does not seem possible. To get better results, some form of compensation for the different timing of growth processes must be built into climate reconstructions. With this in mind, this dissertation focuses on, first, determining whether better climate/radial-growth relationships can in fact be established using multiple species, and if so, to then see how these newly derived relationships can be applied to dendroclimatological research in maritime locations.

1.2 Research Purpose

The aim of this research program is to examine the growth response of high-elevation conifers on Vancouver Island to climate. Building on the success of previous tree-ring studies in this setting (Smith and Laroque 1998b, Laroque and Smith 1999, Lewis and Smith 1999, Gedalof and Smith 2001b), this research explores ways to derive more reliable proxy climate reconstructions from multiple species in a maritime climate.

This research is distinct from past studies in two ways:

(1) The sampling density of the coastal tree-ring network is unprecedented in the literature (Blasing and Fritts 1976; Briffa *et al.* 1992). Such a sampling density is important in its own right, because previous dendroclimatological studies have assumed that limited sample sizes can adequately represent a coastal region. This assumption has never been tested. Furthermore, extensive sampling is particularly important on Vancouver Island because previous research has suggested that this area may be a meeting point for various large-scale climatic patterns (Wiles *et al.* 1996). Distinctly different chronologies have been found to the north and south of Vancouver Island along

the coast, and to the east in the interior of British Columbia (Wiles *et al.* 1996, Beaubien and Freeland 2000, Watson *et al.* 2000). Tree-ring records on Vancouver Island consequently should be examined to see if they are distinct from those found in these other regions, and to what extent they may differ across Vancouver Island.

(2) The use of multiple species from the same location, to derive better proxy climatic parameters, has yet to be attempted anywhere. This approach is used to derive reconstructions with stronger signal-to-noise ratios, which are then able to increase the amount of explained variance that characterize existing dendroclimatic proxy reconstructions from Vancouver Island.

1.3 Research Objectives

The research has four key objectives:

A. to collect increment cores from high-elevation conifer species from an extensive network of coastal sites on Vancouver Island;

B. to describe radial-growth changes over time and space on Vancouver Island;

C. to establish individual tree-times of each species by relating the timing and responses of the radial growth of these trees to known climatic parameters; and

D. to develop improved climate/radial-growth models capable of predicting the effects of past, present and future climates on selected conifer species.

Chapter 2 discusses the study sites on Vancouver Island. Chapter 3 documents the chronology development and describes the dendrochronological utility of each species. It also describes the trees ages and radial-growth characteristics. Chapter 4

investigates the spatial and temporal patterns of the network. Chapter 5 explores the individual response of each species to climatic inputs, the timing of ring growth and how it relates to the physiological incorporation of climate into radial growth. Chapter 6 derives and tests a new multiple species modelling method to improve upon existing single-species climate/radial-growth models. Chapter 7 uses the derived models from Chapter 6 to hindcast past climate conditions using the established relationships. Chapter 8 then incorporates climate data from historical records and forecasted general circulation models to predict the response of radial growth under future climates in both the short and long term. The last chapter, Chapter 9, summarizes the dissertation, and concludes by discussing the strengths, weaknesses, and implications of the various steps that were taken.

2.0 Study Sites

2.1 Study Area

Vancouver Island is a 450 km long and 75 km wide island on the west coast of British Columbia, Canada (located between 47° and 52° north latitude, 123° and 128° west longitude), with a northwest-southeast orientation (Figure 2.1). Elevation rises from sea level to a maximum of 2200 m asl in the Vancouver Island Insular Mountain Range. These mountains run the length of Vancouver Island and help modify the large-scale climatic forcing mechanisms that play a role in the island s biogeography.

2.2 Biogeoclimatic Zones

The British Columbia Ministry of Forests has developed a system of classification for forested and rangeland areas (i.e., Biogeoclimatic Ecosystem Classification, Pojar and Meidinger 1991). The system incorporates various factors such as major climate elements, characteristic plant species, and drainage characteristics of individual locations to better describe the province s natural environment (Krajina 1965, 1969). Four biogeoclimatic zones are present on Vancouver Island (Pojar and Meidenger 1991): the Coastal Douglas-fir (CDF) zone, the Coastal Western Hemlock (CWH) zone, the Mountain Hemlock (MH) zone, and the Alpine Tundra (AT) zone (Figures 2.2 and 2.3).

The CDF zone is restricted to the relatively dry, low-elevation area of southeastern Vancouver Island, which has cool, wet winters, and warm, dry summers (Pojar *et al.* 1987, Klinka *et al.* 1991). The area is dominated by Douglas-fir with smaller components of western red-cedar, grand fir, shore pine, Garry oak, western yew, big leaf maple, red alder, black cottonwood, and arbutus (Nuszdorfer *et al.* 1991). The forest

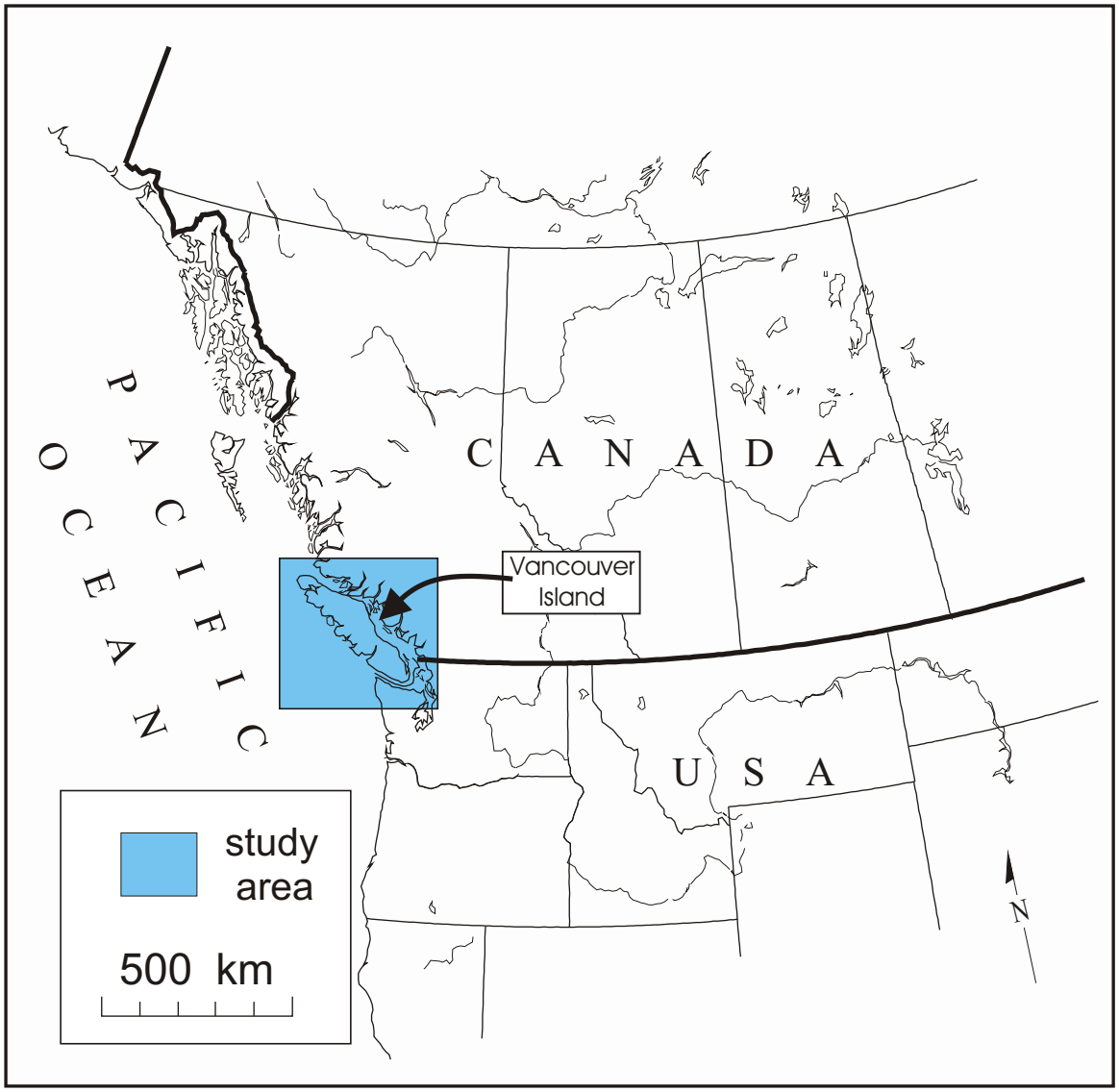

Figure 2.1 - Map of northwestern North America highlighting the Vancouver Island study area.

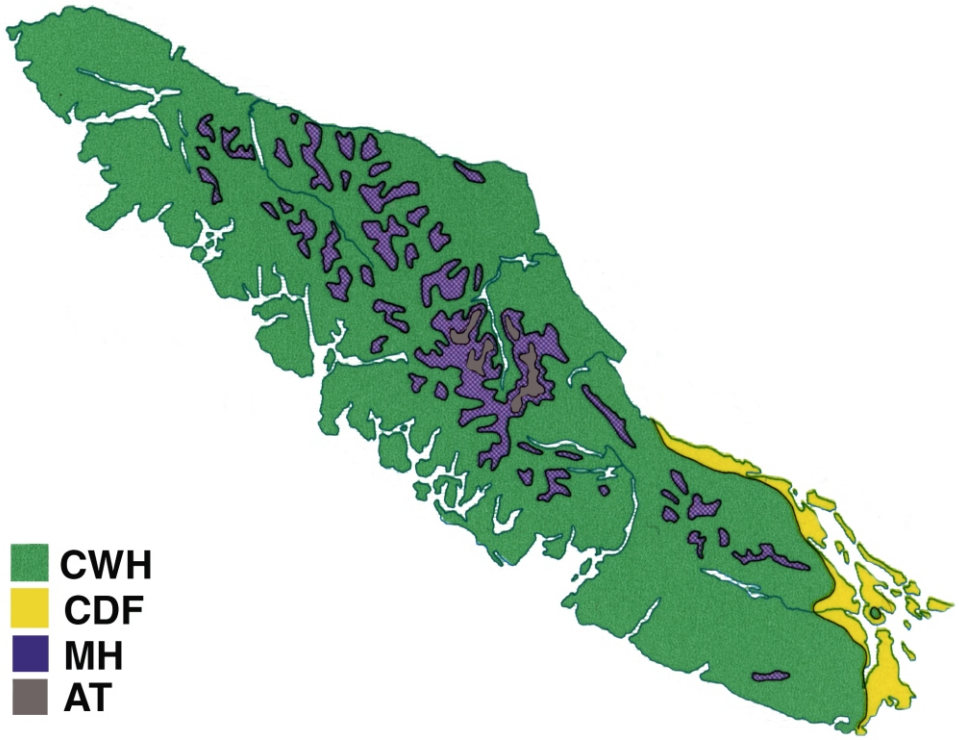

Figure 2.2 - The four biogeoclimatic zones on Vancouver Island. CWH = Coastal Western Hemlock zone, CDF = Coastal Douglas-fir zone, MH = Mountain Hemlock zone, AT = Alpine Tundra zone (adapted from Pojar and Meidinger 1991: 52).

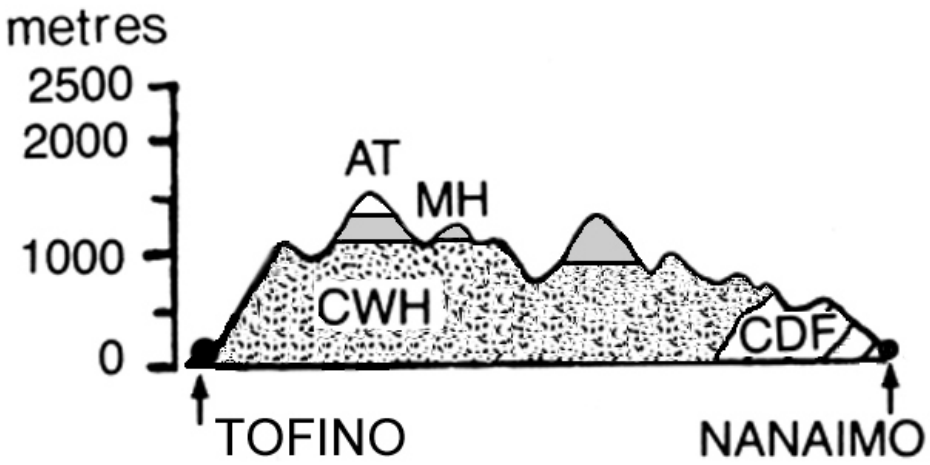

Figure 2.3 -The altitudinal separation of the four biogeoclimatic zones on Vancouver Island according to the existing Biogeoclimatic Ecosystem Classification system (adapted from Pojar and Meidinger 1991: 55).

structure in this zone is a mixture of open and multi-storied canopies, but is hard to typify because it is also the most heavily influenced by human impacts (Nuszdorfer *et al.* 1991).

The CWH zone is by far the wettest and largest of all Vancouver Island zones. The CWH has mild winters and cool summers, although short hot periods are possible in the summer months (Pojar *et al.* 1987, Klinka *et al.* 1991). This zone is the most diverse on Vancouver Island in terms of number of tree species present, with western hemlock, western red-cedar, amabilis fir, western white pine, yellow-cedar, grand fir, shore pine, red alder, black cottonwood, bigleaf maple, western yew, Sitka spruce, and Douglas-fir all present in various numbers throughout the zone (Pojar *et al.* 1991a). CWH forests are typified by a continuous, multi-storied canopy with some gaps.

The MH zone has short, cool summers and cool winters with a deep snowpack (Klinka *et al.* 1991). On Vancouver Island the dominant trees in the MH zone are mountain hemlock and yellow-cedar, with a minor component of amabilis fir or subalpine fir. Most trees grow in open areas as individuals or as part of small tree islands, but they can also be found in more continuously treed areas in their lower elevations (Pojar *et al.* 1991b).

The AT zone on Vancouver Island is limited to mountain summits where ice and snow remain nearly all year. The AT zone is predominantly treeless except for krummholz mountain hemlock and yellow-cedar that occur above 1500 m asl. In the AT zone, frost can occur at any time of the year, soil development is limited, and harsh wind conditions contribute to make seedling survival and tree growth nearly impossible (Pojar and Stewart 1991).

The biogeoclimatic zones are presented as distinct, but sharp boundaries do not usually exist. While each zone is characterized by tree species that tolerate some degree of variability in their environmental requirements, these factors tend to shift gradually from zone to zone. The environmental factors that differentiate the zones include temperature, precipitation, elevation, aspect, and snowpack accumulations. Most of these factors are ultimately controlled by the large-scale physiographic effects of Vancouver Island.

2.3 Physiographic Effects

On the west coast of Vancouver Island, prevailing winds bring moisture-laden air masses onshore, providing conditions that are cool and very wet. More moisture condenses out of these air masses as they reach further inland to the higher central areas of the island. On northern portions of the island, similar cool and wet conditions dominate, but a more gradual elevation gain somewhat diminishes the high amounts of moisture received. On the eastern side of Vancouver Island a rainshadow effect is created by the central Insular Mountain Range, making for drier localized conditions. The southeastern portion of the Island is the driest of all regions, largely because it is influenced from the north and northwest by a rainshadow effect of the Insular Mountains, and is protected from the southwest by rainshadow effects of the Olympic Peninsula. The central portion of the island contains the highest elevations and, therefore, has the coolest temperatures and the largest snowpack accumulations (Hnytka 1990).

2.3 Study Site Locations

Tree-ring samples were collected at 40 high-elevation sites on Vancouver Island. At each study site, increment core samples from multiple tree species were collected.

Figure 2.4 shows the 40 sampling sites and Table 2.1 presents information about each site (number, name, code, species sampled, and location). The sites are from treeline locations found along a northwest-southeast longitudinal transect and three east-west latitudinal transects. Treeline areas were selected because strong climate signals are characteristically retained in the tree-ring records of trees growing at their tolerance limits (Fritts 1976). Potential sites were identified close to the axis of each transect, but because high-elevation sites did not always fall directly under the transects, sampling was sometimes carried out at the nearest suitable location. As much as possible, sites were positioned equidistant along the east-west transects. Sites were also positioned both east and west of the longitudinal transect to capture any wet-side/dry-side effects that might be present along the length of Vancouver Island.

The study sites were chosen so as to keep aspect, slope, and stand characteristics similar. Where possible, sampling took place at locations with a minimum 1000 m asl elevation and at the upper elevation limit of growth for each tree species at each particular site. At most sites the limit of growth was found at approximately 1250-1300 m asl for yellow-cedar, while for mountain hemlock sampling generally occurred at 1300 -1500 m asl or at the summit of the mountain. Whenever possible summit locations were chosen to reduce noise resulting from the ecological consequences of slope and aspect (Fonda and Bliss 1969). When locations other than the summit had to be sampled, areas with as little slope as possible were sought.

For mountain hemlock and yellow-cedar, sampling was limited to open subalpine tree islands (Figure 2.5a-c). Previous research found that sampling at scattered tree

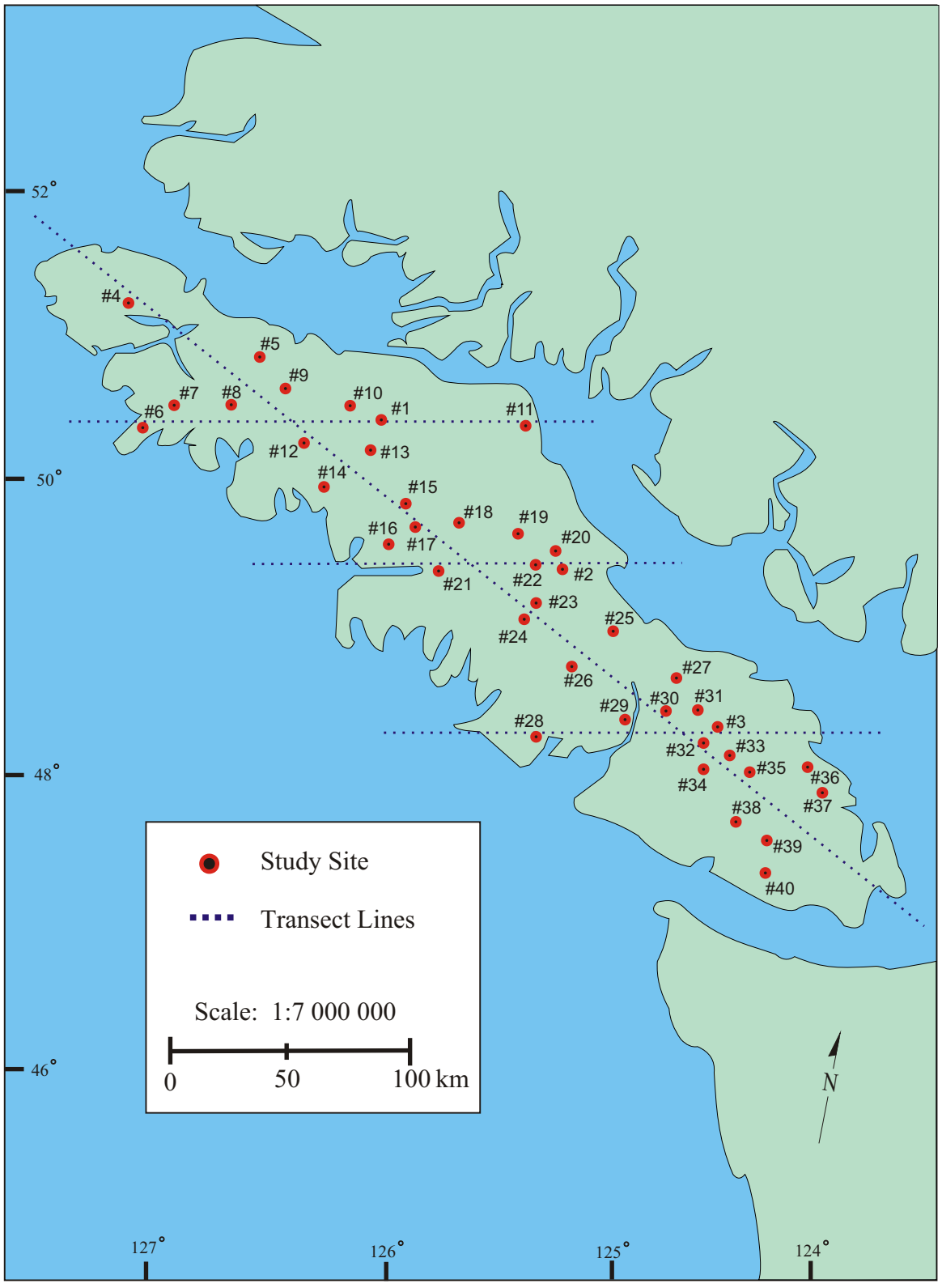

Figure 2.4 - Map of Vancouver Island showing the transect lines and study sites.

Table 2.1 - The 40 study sites and sampling information. Tree species sampled are abbreviated as follows:
MH = mountain hemlock, YC = yellow-cedar, WH = western hemlock, DF = Douglas-fir, WRC = western red-cedar.

No.	Name	Site Code	Tree Species Sampled					Site Description (Latitude, longitude, average elevation, NTS map sheet, UTM coordinate)
			MH	YC	WH	DF	WRC	
1	Mount Cain	96N / 97N	x	x	x			50 13' 55" N, 126 19' 30" W, 1100m asl, 92 L/1, 907670
2	Mount Becher	97I	x	x				49 39' 30" N, 125 12' 40" W, 1120 m asl, 92 F/11, 407023
3	Green Mountain	96V / 97C	x	x	x			49 03' 20" N, 124 20' 25" W, 1200m asl, 92 F/1, 021344
4	Mount MacIntosh	96K	x	x				50 40' 10" N, 127 51' 20" W, 696m asl, 92L/12, 808133
5	Castle Mountain	97M	x	x				50 28' 10" N, 127 03' 00" W, 1100m asl, 92 L/1, 907670
6	Butterfly / Wolf Ridge	96T / 96S	x	x				50 11' 10" N, 127 43' 05" W, 610m asl, 92 L/4, 899595 50 11' 00" N, 127 44' 20" W, 518m asl, 92 L/4, 916603
7	Colonial Creek	97K	x	x				50 17' 30" N, 127 33' 20" W, 915 m asl, 92 L/5, 031722
8	Bulldog Ridge	97L	x	x				50 17' 50" N, 127 14' 00" W, 870m asl, 92 L/6, 259731
9	Mrs. Wade Mountain	96L	x	x				50 21' 30" N, 126 53' 05" W, 1097m asl, 92 L/7, 503804
10	Mount Elliot	96M	x	x				50 17' 50" N, 126 29' 55" W, 1433m asl, 92L/8, 780744
11	Mount Menzies	97O	x	x				50 12' 15" N, 125 28' 10" W, 915m asl, 92 K/3, 232643
12	Apple Tree Hill	96P	x	x				50 08' 00" N, 126 46' 55" W, 1036m asl, 92 L/2, 582550
13	Maquilla Peak	97P	x	x				50 07' 55" N, 126 21' 45" W, 1220m asl, 92 L/1, 891563
14	Silver Spoon Saddle	96O	x	x				49 58' 30" N, 126 40' 45" W, 900m asl, 92 E/15, 664386
15	South Sheena Creek	96Q	x	x				49 55' 45" N, 126 09' 55" W, 1158m asl, 92 E/16, 032348
16	Nesook Creek	97Q		x	x		x	49 46' 45" N, 126 16' 50" W, 610m asl, 92 E/16, 964166
17	Mount Upana	96X	x	x				49 49' 10" N, 126 07' 20" W, 1025m asl, 92 E/16, 073225
18	Mount Heber	97E	x	x				49 53' 50" N, 125 55' 50" W, 1375m asl, 92 F/13, 89831
19	Lupine Mountain	97D	x	x				49 49' 15" N, 125 31' 00" W, 1300m asl, 92 F/13, 189215
20	Mount Washington	94MW / 97H	x	x				49 44' 35" N, 125 17' 30" W, 1400m asl, 92 F/11, 350130

Table 2.1- cont. The 40 study sites and sampling information. Tree species sampled are abbreviated as follows:
MH = mountain hemlock, YC = yellow-cedar, WH = western hemlock, DF = Douglas-fir, WRC = western red-cedar.

No.	Name	Site Code	Tree Species Sampled					Site Description (Latitude, longitude, average elevation, NTS map sheet, UTM coordinate)
			MH	YC	WH	DF	WRC	
21	Hanging Valley Creek	97F	x	x				49 40' 10" N, 125 58' 30" W, 1130m asl, 92 F/12, 855061
22	Circlet Lake	93CIR	x					49 41' 30" N, 125 23' 30" W, 1260m asl, 92 F/11, 280070
23	Milla Lake	94ML	x	x				49 33' 20" N, 125 23' 00" W, 1380m asl, 92 F/11, 265924
24	Cream Lake	95CRM	x					49 29' 00" N, 125 31' 00" W, 1280m asl, 92 F/5, 166846
25	Mount Apps	96G	x	x				49 26' 30" N, 124 57' 55" W, 1200m asl, 92 F/7, 578779
26	Mount Porter	96H	x	x				49 18' 30" N, 125 13' 45" W, 1140m asl, 92 F/6, 380645
27	Mount Arrowsmith	94MA / 97A	x	x	x			49 16' 15" N, 124 37' 30" W, 1120m asl, 92 F/7, 818585
28	Mount Redford	97B		x	x		x	49 01' 30" N, 125 24' 40" W, 680m asl, 92 F/3, 239333
29	Pirate Peak	97J	x	x				49 06' 20" N, 124 52' 55" W, 1010m asl, 92 F/2, 625407
30	Douglas Peak	96F	x	x				49 08' 10" N, 124 38' 45" W, 1365m asl, 92 F/2, 802432
31	Mount Moriarty	96E	x	x	x			49 08' 30" N, 124 28' 00" W, 1400m asl, 92 F/1, 932440
32	Wapiti Ridge	96C	x	x	x			48 59' 40" N, 124 26' 20" W, 1040m asl, 92 C/16, 948277
33	Haley Lake	96U	x		x			49 00' 30" N, 124 18' 45" W, 1320m asl, 92 F/1, 043293
34	Heather Mountain	94HM	x	x				48 57' 37" N, 124 27' 23" W, 1135m asl, 92 C/16, 936232
35	Mount Franklyn	96D	x			x		48 54' 40" N, 124 11' 00" W, 1060m asl, 92 C/16, 118163
36	Mount Brenton	96J	x	x				48 54' 00" N, 123 50' 50" W, 1305m asl, 92 B/13, 380166
37	Mount Prevost	95MP				x		48 49' 50" N, 123 43' 50" W, 780m asl, 92 B/13, 441089
38	T-A-D Ridge	96B	x	x	x			48 41' 40" N, 124 16' 40" W, 980m asl, 92 C/9, 062941
39	Mount Modeste	96I	x	x	x			48 38' 20" N, 124 06' 20" W, 1100m asl, 92 C/9, 183875
40	San Juan Ridge	96A	x	x	x			48 31' 15" N, 124 07' 50" W, 1000m asl, 92 C/9, 163748

A)

B)

C)

Figure 2.5 - Three representative sites from the study: A) A northern site, # 9, Mrs. Wade Mountain, B) A mid-island site, # 2, Mount Becher (Note: snow survey signs in the tree in the centre of the photograph), C) A southern site, # 3, Green Mountain.

islands greatly diminished the problems attendant with competition in closed stands (Laroque 1995; Smith and Laroque 1996, 1998a, 1998b; Laroque and Smith 1999) Sampling of other tree species in the study was conducted at as high an elevation as possible. Open stands were always sought but sampling often occurred under a more continuous canopy for western hemlock, western red-cedar, and Douglas-fir.

Field research took place in the summers of 1996 and 1997. Permission to access all of the sites was granted by either the timber license holder or BC Parks.

3.0 Chronology Development

3.1 Introduction

Crossdating is the technique whereby radial-growth patterns from individual cores in a series are matched to define a coherent group pattern. This chapter describes the methods used to collect the cores and to develop the crossdated chronologies. Detailed are the procedures used to process the cores, the analytical protocol followed, the site properties, and the crossdating results.

3.2 Methods

3.2.1 Sampling Protocol

Increment cores (two per tree at cross-slope positions at dbh) were collected from 20 trees per species at each site (Stokes and Smiley 1968). The largest and tallest canopy trees were selected for sampling, while trees with obvious structural damage were excluded. A minimum of two tree species were sampled at each site, except at three sites (# 22, # 24, and # 37) where only a single series was collected. Both mountain hemlock and yellow-cedar trees were sampled at 32 of the 40 locations. At the remaining sites only one of these species was sampled in conjunction with western hemlock, western red-cedar, subalpine fir or Douglas-fir (Table 2.1). In all, 88 sets of cores from 40 locations make up the sampling network.

3.2.2 Sample Preparation

Individual increment cores were transported in plastic straws to the University of Victoria Tree-Ring Laboratory where they were air dried. Once dry, the cores were glued to slotted mounting boards (Fritts 1976). All samples were initially sanded using coarse-

grade sandpaper (50 or 80 grit) with a belt sander. Following this, a hand-held orbital sander with progressively finer grades of sandpaper (120, 240, 400 grit) and a final hand polish with very fine sandpaper (600 grit) were used to finish preparing the samples.

3.2.3 Measurement

An image of each tree core, created using a high-resolution Agfa Duoscan!" scanner (2000 dpi x 1000 dpi), was analyzed by WinDENDRO (Version 6.1b, 1996) software to assign ring boundaries. Once each ring boundary was visually confirmed by the operator, WinDendro measured every ring width to the nearest thousandth of a millimetre. These WinDendro-formatted data files were converted to the Tucson decadal format using the program CONVERT (Version 1.3, 1996), which rounded the data to the nearest hundredth of a millimetre.

3.2.4 Crossdating

The ring-width data were checked for signal homogeneity using the International Tree-Ring Data Bank (ITRDB) program routine COFECHA (Version 3.0, Holmes 1999). COFECHA correlates incremental sections of ring-width data with the average result from the entire group of cores. Using this program an operator can identify where a possible problem exists in the measurement data, or where a missing or false ring location might be located.

Individual cores from a series that did not show a common growth signal and detracted from a site s homogeneity were eliminated from further analysis. Common characteristics that forced the removal of a core from analysis included: broken pieces that could not be interpreted; discolourations in the wood sequences that did not produce

distinct ring boundaries; or growth sequences limited by factors other than climate.

COFECHA provides statistics useful for describing the collective radial-growth signal present in a set of data. The *mean series correlation* describes the average of the correlations of each core s ring-width data to the overall master series in question. In this study positive values of the mean series correlation above 0.328 are significant at a $p < 0.01$ level of confidence (based on 50-year segments) and indicate a series chronology that contains a homogeneous growth signal.

Mean sensitivity is defined as a measure of "mean percentage change from each measured yearly ring value to the next" (Douglass 1936, cited by Fritts 1976: 258). It shows how sensitive a tree or group of trees is to the year-to-year changes in factors affecting its growth. A value of 0.0 indicates complacency or little year-to-year sensitivity, and a value of 1.0 indicates extreme ring-width change from year-to-year.

Mean measurement is simply the average measurement of all of the ring widths in all cores within each site series. The statistic gives further information on the individual growing characteristics for each series, and it is a helpful measure for comparing site and species chronologies.

Autocorrelation is a measure of the relationship of one year's radial-growth on radial-growth in the following year. This measurement has a scale of 0.0 to 1.0. A value of 0.0 indicates that no autocorrelation exists in the data, and would signify that the growth in one year has no effect on the next year's growth. A measure of 1.0 indicates that each year's growth completely dictates growth in the following year (Holmes *et al.* 1986; Colenutt and Luckman 1991).

3.2.5 Standardization

Standardization is a two-step process that eliminates variation in ring widths resulting from changes associated with aging, and then combines the detrended data into a series index by calculating a robust mean (Cook 1999). Detrending, for example, provides a way to make the wide rings of a young tree more comparable to narrower rings from an older tree (Schweingruber 1988, 1993). Standardization, then, reduces the age-dependent variation in ring widths, ensuring that they reflect environmental constraints as much as possible. By averaging the standardized ring-width measurements into an index, a homogeneous series chronology is created.

The program TURBO ARSTAN V2.07 (Cook 1999) was used to detrend (remove the biological growth trend) and standardize the tree-ring data sets to eliminate any inherent growth patterns. The detrending function of the program provides a best-fit growth curve that maximizes the signal-to-noise ratio of each core using three possible methods.

- A *negative exponential curve* describes a ring-width decrease as trees grow older and was the detrending method used for most cores in this study. This is the most common trend in trees that are growing in open-canopy stands (Figure 3.1a).
- A *cubic smoothing spline curve* corresponds to radial-growth trends in trees with a slow early growth, a peak in radial-growth rate in the middle of the life cycle, and then reduced radial-growth in old age. This type of growth trend is common in closed-canopy stands, in which trees exhibit a growth spurt as a result of gaining sufficient height in the upper canopy to take advantage of more available sunlight (Figure 3.1b) (Cook and Peters 1981).

" *Linear regression equations* are straight lines that approximate the radial-growth trend of trees with highly irregular growth rates. This type of detrending is most often used when tree growth has occurred in a closed-canopy stand in which a disturbance event alters the regular growth cycles (Figure 3.1c) (Cook and Briffa 1990).

A single detrending often eliminates only the age-related growth trend, leaving noise in the tree-ring chronologies from exogenous disturbances (e.g., fire damage to a stand) and endogenous processes (e.g., gap-phase responses by a tree). To eliminate this noise, it is standard practice to detrend each sample a second time using a second detrending method (Cook and Briffa 1990). Some form of a smoothing spline, with either a high-frequency cutoff response or a high series length scaling factor, is used to highlight the climate signal. The common level of spline stiffness uses a scaling factor of two-thirds the length of the data set (66 %). In this study, a second detrending was undertaken using different scaling factors depending upon the species. Because the mountain hemlock samples were found at the highest elevation at sites where little exogenous and endogenous disturbance occurs (Fowells 1965), the stiffest, and most conservative scaling spline was used (80 % series length cutoff). For other species sampled at lower elevations, the scaling factor was reduced to account for increases in competition effects in areas of more continuous canopy (Cook and Peters 1981). Yellow-cedar chronologies were detrended a second time using a 70 percent series length cutoff, while the western hemlock, western red-cedar, subalpine fir and Douglas-fir were

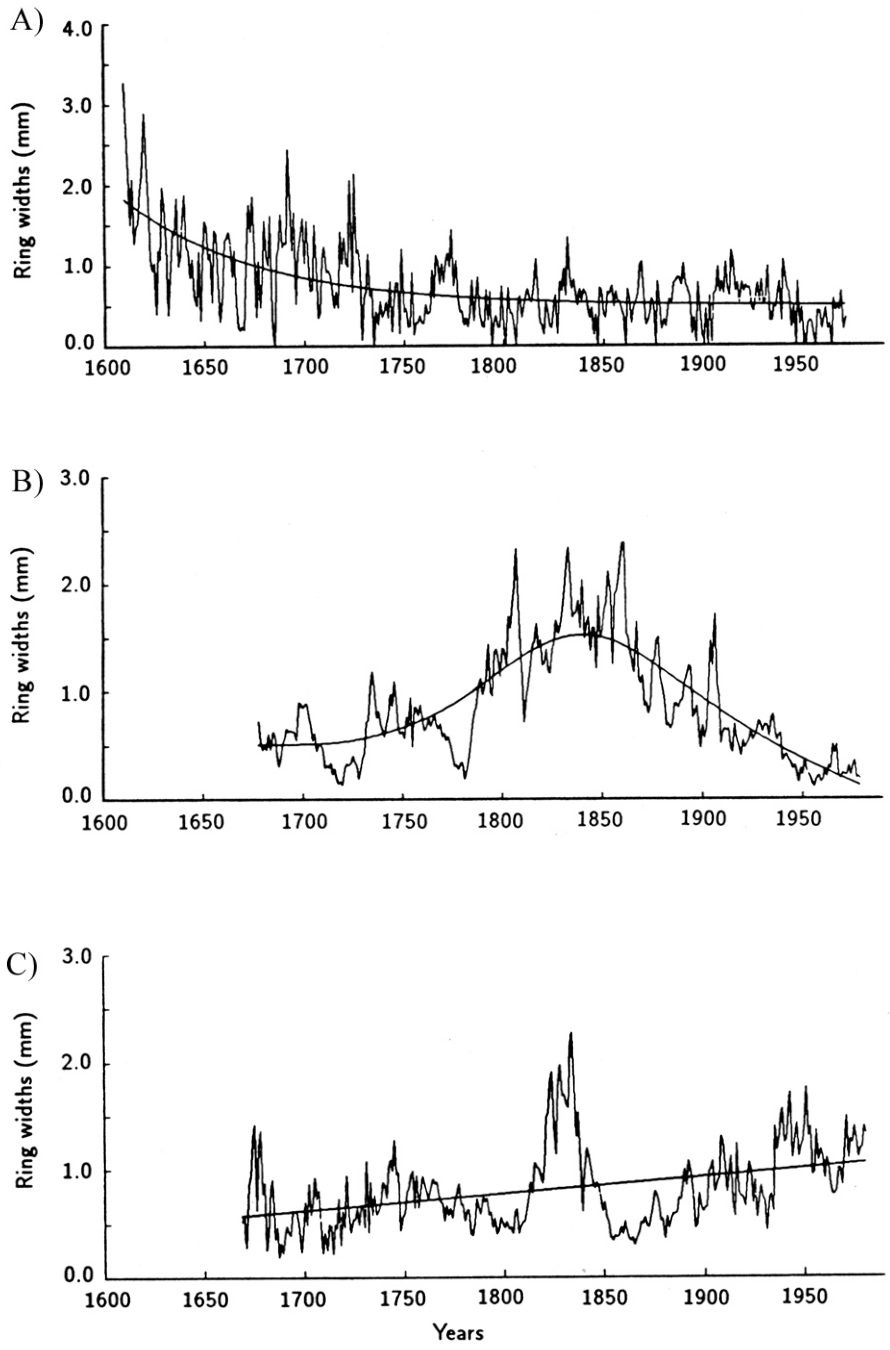

Figure 3.1 - The three methods of detrending used in this study: A) The negative exponential curve, B) The cubic smoothing spline, C) The linear regression equation (adapted from Cook and Briffa 1990: 99).

detrended a second time using a 66 percent series length cutoff. Once all of the individual cores were double detrended, all cores in a series were compiled into standardized tree-ring chronologies (one per species per site) using Turbo ARSTAN (Cook 1999).

3.2.6 Estimated Population Signals

A basic assumption of dendrochronology is that the tree-ring data collected provides a good representation of the overall population signal strength at the site. A simple test of this assumption can be derived from the Estimated Population Signal (EPS) statistic. EPS is a measure that determines how well a chronology based on a finite number of trees approximates the theoretical population chronology from which it is assumed to have been drawn. EPS values are favoured over other statistical tests (e.g., ANOVA) in dendrochronology, as the EPS can be calculated on series made up of variable core depths and lengths and even when the number of cores per tree differs (Briffa and Jones 1990). EPS takes into account the increasing uncertainty in a tree-ring chronology as the sampling depth lessens (Wigley *et al.* 1984). If the EPS remains between 0.80 to 0.85 (Briffa and Jones 1990, Wigley *et al.* 1984), then the chronology is regarded as robust to allow for climatic reconstruction. The remaining portion of the chronology can still be used in a climate reconstruction, but the confidence placed in that portion of the reconstruction is not as strong (Briffa and Jones 1990, Wigley *et al.* 1984).

3.3 Results

3.3.1 Tree Age Characteristics

The ages of the oldest individual trees found at each site are mapped in Figure 3.2,

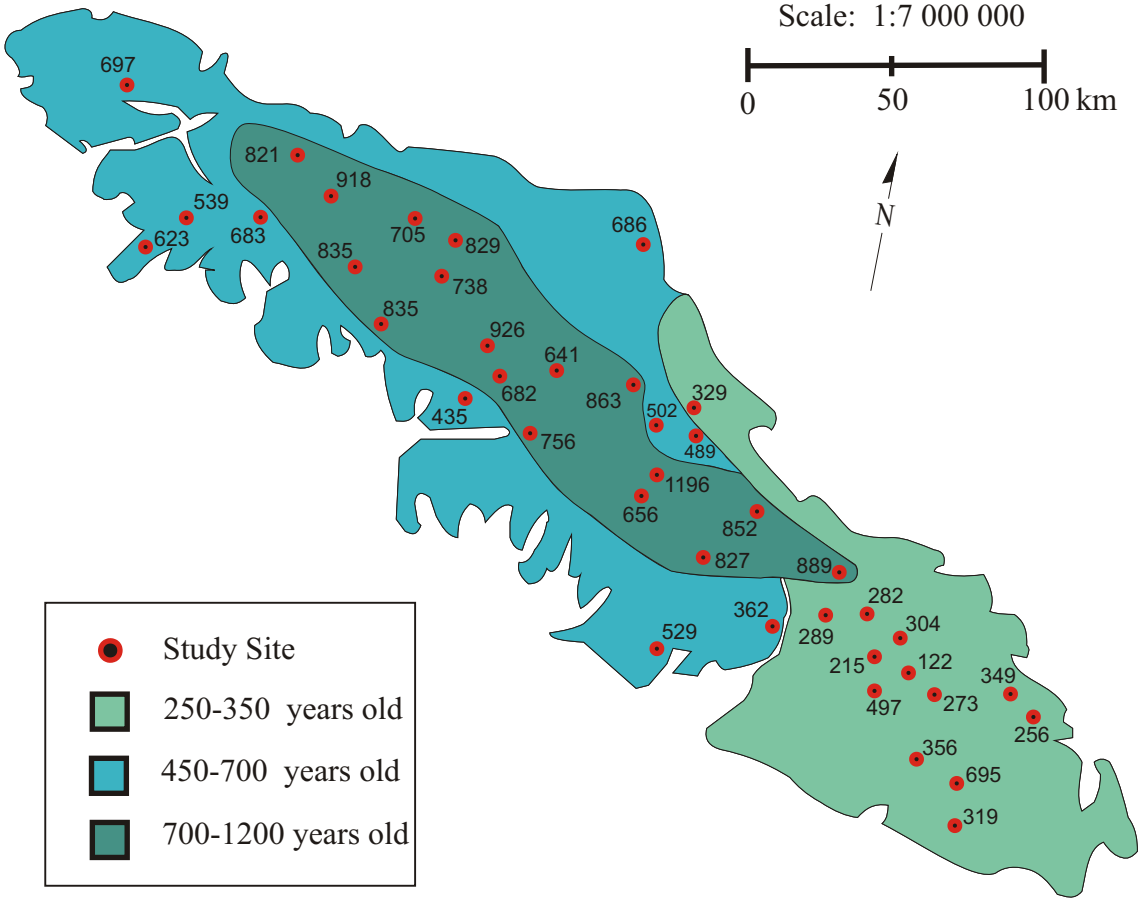

Figure 3.2 - The oldest trees sampled at each study site in the study. Ages were grouped and were broken into three classes and mapped.

revealing three general Vancouver Island age groups. On the north end of the island and southward along the western coast to the Alberni Inlet, the high-elevation trees ranged in age from 400 to 700 years old. This group also occurs on the east side of Vancouver Island from the northern tip southward to the Campbell River Lakes area. The oldest trees were found in the north-central and central parts of the island. This area encompasses Strathcona Provincial Park and the highest relief on the island. In this region trees up to 1200 years of age were found, with individuals over 700 years of age common at most sampling location. In the eastern and southern areas of Vancouver

Island the youngest high-elevation forests were found. From the Nanaimo Lowlands southward along the east side of the Beaufort Range, and south of the Alberni Inlet, high-elevation trees rarely exceeded 330 years. Two exceptions occurred: a 497-year-old yellow-cedar found in a high-elevation bog at the Heather Mountain site, and a 695-year-old mountain hemlock above a rocky ledge at the Mount Modeste site.

These three age groups have likely resulted from dominant climate forcing mechanisms and past disturbance events. In the southern and eastern regions, conditions are generally drier and snowpacks much shallower (Hnytka 1990). These conditions likely result in a higher local forest fire frequency compared to regions on the north and west coast of the island, where greater precipitation lessens the fire hazard (Gavin 2000). The age distribution on southern Vancouver Island is thought to be an artifact of fires in the 17th century. Laroque and Smith (1999) show evidence for a fire at high elevations in this region in the late summer of 1669 AD. Schmidt (1957) and Parminter (1990) concur and describe a large regional fire that occurred in the 1660s over the same region at low elevation. In general, montane areas exhibit cool, wet, rocky, and isolated drainage basins that help to curtail any forest fire activity (Pew and Larson 2001).

3.3.2 Altitudinal Boundaries

A significant biogeoclimatic boundary on Vancouver Island is the one that separates western hemlock stands from those dominated by mountain hemlock. Although the Biogeoclimatic Ecosystem Classification system assumes that this change in forest composition occurs close to the 1000 m contour (BC Ministry of Forests 1993), data from this study show that this is rarely the case (Figure 3.3). Instead the transition occurs at

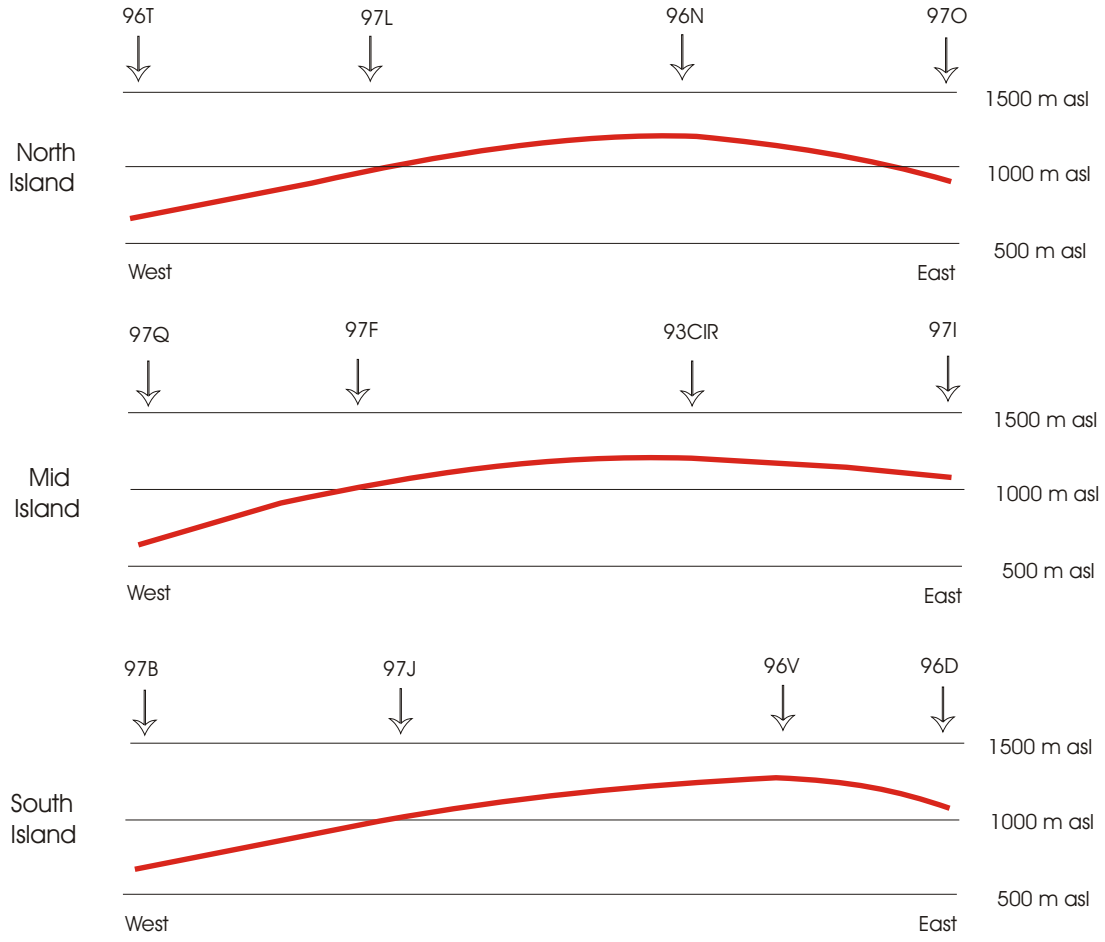

Figure 3.3 - The elevation of the western hemlock-mountain hemlock ecotonal boundary at each of the three east-west transect lines in the study.

3.3.3 Crossdating Results

Results of the crossdating analysis are presented in Tables 3.1, 3.2, and 3.3. The mean series correlations for mountain hemlock ranged from 0.323 to 0.623 (overall average 0.490); yellow-cedar had a slightly lower range (0.259 to 0.533, overall average 0.433). The western hemlock series had a range from 0.328 to 0.592 (overall average 0.447) for the 11 sites sampled, but limited sampling precluded defining ranges for the other species. In general, signals from all of the chronologies were statistically significant and presented homogeneous patterns from each group of cores. In some cases there were a few sites where the cores did not crossdate well, likely due to the impact of local variation within the site (e.g., local soil variability).

Yellow-cedar was as sensitive (average mean sensitivity 0.253) as mountain hemlock (0.251) and slightly more sensitive than western hemlock (0.234). All three measures are considered high in previous dendrochronological analyses completed in the Pacific Northwest (Ettl and Peterson 1995, Laroque 1995). While western hemlock had the highest average autocorrelation value (0.779), both yellow-cedar (0.764) and mountain hemlock (0.729) also had relatively high values, indicating that the previous year s growth had a strong relationship to the annual growth of these species.

3.3.4 Species Utility

The chronologies in this study crossdate well and have good dendrochronological utility. Of the 88 original chronologies, 80 provide a statistically reliable signal over a multi-century time period. Mountain hemlock trees seem to be the best suited for dendrochronological applications and were the easiest of the species examined to

crossdate. Only one site (Mt. Upana) yielded a poor chronology for mountain hemlock.

Mountain hemlock trees produce a strong, coherent group signal when 18 or more cores are present in a chronology (Table 3.4). The relatively low autocorrelation (compared with the other species studied) and high mean sensitivity values recorded are positive features of the species for dendroclimatological analysis in the region. Mountain hemlock also had the strongest EPS among the species studied (Table 3.4). Average values of 0.938 were recorded when 33 or more cores were used to construct a chronology. The species consistently showed the same radial-growth pattern (noted by recurring conspicuous rings) in almost all samples, and once these pointer rings were established, easier crossdating was facilitated (Figure 3.4a).

The only deviation from a normal ring structure in mountain hemlock occurred when a black ring was encountered. The term black ring describes a crystallized resinous zone of dark growth without normal wood cell structures (Figure 3.4b). This narrow ring could be confused with a zone of latewood, but in fact it represents an entire year s growth and must be counted as such for proper crossdating. Although the crystallized material in the ring has not been positively identified, there is some indication that it may be styloid crystals grown out from the previous year s last formed latewood cells (Kellogg and Rowe 1981). The black rings do not occur in a continuous radius around the bole, nor do they seem to occur in the same year of growth in more than one tree. The formation of the ring is not thought to be related to climate as it occurs infrequently and never in the same year in different cores at a site.

Yellow-cedar is more difficult to crossdate than mountain hemlock. In the pith

Table 3.1- Parameters for the crossdated mountain hemlock chronologies in the study.

Site No.	Name	n = Trees (cores)	Range (years AD)	Chronology length (years)	Mean series correlation	Mean sensitivity	Mean measurement	Auto-correlation
1	Mount Cain	49 (81)	1166-1997	832	0.510	0.292	0.410	0.596
2	Mount Becher	18 (32)	1668-1997	330	0.550	0.284	0.620	0.759
3	Green Mountain	20 (38)	1749-1996	248	0.561	0.298	0.690	0.595
4	Mount MacIntosh	19 (30)	1294-1996	703	0.440	0.235	0.330	0.795
5	Castle Mountain	18 (33)	1543-1997	455	0.450	0.234	0.570	0.739
6	Butterfly Ridge	15 (25)	1655-1996	342	0.473	0.262	0.710	0.838
7	Colonial Creek	15 (28)	1533-1997	465	0.431	0.278	0.530	0.759
8	Bulldog Ridge	19 (32)	1445-1997	553	0.437	0.247	0.480	0.769
9	Mrs. Wade Mountain	19 (32)	1370-1997	627	0.473	0.224	0.460	0.780
10	Mount Elliot	23 (41)	1292-1996	705	0.467	0.270	0.520	0.568
11	Mount Menzies	17 (28)	1491-1997	507	0.403	0.249	0.500	0.787
12	Apple Tree Hill	20 (39)	1339-1996	658	0.423	0.215	0.440	0.793
13	Maquilla Peak	19 (34)	1320-1997	678	0.426	0.230	0.410	0.712
14	Silver Spoon Saddle	19 (35)	1362-1996	635	0.483	0.244	0.470	0.740
15	South Sheena Creek	19 (33)	1553-1996	444	0.408	0.212	0.630	0.772
16	Nesook Creek	n/a	n/a	n/a	n/a	n/a	n/a	n/a
17	Mount Upana	16 (24)	1337-1996	660	0.323	0.239	0.500	0.779
18	Mount Heber	19 (37)	1410-1997	588	0.544	0.257	0.450	0.684
19	Lupine Mountain	15 (27)	1520-1997	478	0.413	0.232	0.450	0.710
20	Mount Washington	19 (37)	1504-1997	494	0.558	0.277	0.570	0.732
21	Hanging Valley Creek	18 (32)	1375-1997	623	0.443	0.219	0.440	0.795

Table 3.1, cont.- Parameters for the crossdated mountain hemlock chronologies in the study.

Site No.	Name	n = Trees (cores)	Range (years AD)	Chronology length (years)	Mean series correlation	Mean sensitivity	Mean Measurement	Auto-correlation
22	Circlet Lake	45 (67)	1557-1993	437	0.521	0.255	0.720	0.610
23	Milla Lake	21 (24)	1558-1993	436	0.525	0.262	0.640	0.661
24	Cream Lake	23 (39)	1412-1995	584	0.606	0.270	0.580	0.666
25	Mount Apps	16 (30)	1552-1996	445	0.518	0.298	0.760	0.694
26	Mount Porter	20 (36)	1747-1996	250	0.537	0.227	1.010	0.720
27	Mount Arrowsmith	18 (35)	1648-1997	350	0.619	0.263	0.620	0.714
28	Mount Redford	n/a	n/a	n/a	n/a	n/a	n/a	n/a
29	Pirate Peak	20 (38)	1777-1997	221	0.531	0.258	0.670	0.716
30	Douglas Peak	20 (38)	1708-1996	289	0.572	0.225	0.890	0.826
31	Mount Moriarty	20 (36)	1738-1996	260	0.613	0.287	0.770	0.731
32	Wapiti Ridge	21 (38)	1784-1996	213	0.623	0.236	1.270	0.754
33	Haley Lake	22 (41)	1876-1996	121	0.502	0.237	1.310	0.687
34	Heather Mountain	11 (16)	1754-1993	240	0.470	0.307	0.780	0.592
35	Mount Franklyn	17 (28)	1751-1996	246	0.499	0.249	0.890	0.797
36	Mount Brenton	17 (28)	1641-1996	356	0.444	0.240	0.580	0.813
37	Mount Prevost	n/a	n/a	n/a	n/a	n/a	n/a	n/a
38	T-A-D Ridge	18 (32)	1699-1996	298	0.489	0.230	0.790	0.735
39	Mount Modeste	20 (38)	1301-1996	696	0.441	0.237	0.520	0.722
40	San Juan Ridge	15 (23)	1490-1996	507	0.420	0.239	0.590	0.835
			mean	459	0.490	0.251	0.637	0.729
			median	455	0.483	0.247	0.580	0.735

Table 3.2 - Parameters for the crossdated yellow-cedar chronologies in the study.

Site No.	Name	n = Trees (cores)	Range (years AD)	Chronology length (years)	Mean series correlation	Mean sensitivity	Mean measurement	Auto-correlation
1	Mount Cain	42 (44)	1205-1994	789	0.450	0.257	0.360	0.619
2	Mount Becher	20 (34)	1509-1997	489	0.457	0.255	0.580	0.792
3	Green Mountain	13 (24)	1707-1996	290	0.533	0.263	0.670	0.785
4	Mount MacIntosh	12 (15)	1320-1996	677	0.357	0.261	0.310	0.784
5	Castle Mountain	17 (29)	1172-1997	826	0.409	0.240	0.370	0.767
6	Wolf Ridge	14 (23)	1470-1996	527	0.336	0.285	0.630	0.774
7	Colonial Creek	18 (31)	1459-1997	539	0.475	0.287	0.530	0.752
8	Bulldog Ridge	17 (32)	1421-1997	577	0.426	0.272	0.460	0.774
9	Mrs. Wade Mountain	17 (31)	1065-1996	932	0.458	0.271	0.310	0.743
10	Mount Elliot	21 (31)	1290-1996	707	0.501	0.264	0.370	0.725
11	Mount Menzies	18 (31)	1390-1997	608	0.439	0.245	0.700	0.782
12	Apple Tree Hill	18 (27)	1154-1996	843	0.401	0.258	0.330	0.782
13	Maquilla Peak	17 (30)	1257-1997	741	0.358	0.222	0.560	0.799
14	Silver Spoon Saddle	16 (30)	1237-1996	760	0.463	0.277	0.450	0.740
15	South Sheena Creek	10 (16)	1067-1996	930	0.407	0.231	0.370	0.788
16	Nesook Creek	n/a	n/a	n/a	n/a	n/a	n/a	n/a
17	Mount Upana	16 (28)	1305-1996	692	0.401	0.251	0.490	0.793
18	Mount Heber	16 (30)	1354-1997	644	0.473	0.257	0.350	0.694
19	Lupine Mountain	17 (28)	1133-1997	865	0.397	0.259	0.290	0.758
20	Mount Washington	48 (91)	1702-1994	292	0.464	0.209	0.880	0.806
21	Hanging Valley Creek	16 (25)	1243-1997	755	0.447	0.243	0.420	0.777

Table 3.2, cont. - Parameters for the crossdated yellow-cedar chronologies in the study.

Site No.	Name	n = Trees (cores)	Range (years AD)	Chronology length (years)	Mean series correlation	Mean sensitivity	Mean Measurement	Auto-correlation
22	Circlet Lake	n/a	n/a	n/a	n/a	n/a	n/a	n/a
23	Milla Lake	22 (24)	798-1994	1196	0.300	0.279	0.430	0.692
24	Cream Lake	n/a	n/a	n/a	n/a	n/a	n/a	n/a
25	Mount Apps	18 (32)	1145-1996	852	0.450	0.236	0.500	0.820
26	Mount Porter	17 (30)	1452-1996	545	0.404	0.236	0.670	0.829
27	Mount Arrowsmith	44 (61)	1105-1994	889	0.433	0.238	0.520	0.720
28	Mount Redford	10 (18)	1761-1997	237	0.259	0.245	1.180	0.866
29	Pirate Peak	22 (39)	1634-1997	364	0.479	0.257	0.570	0.773
30	Douglas Peak	19 (36)	1752-1996	245	0.552	0.254	0.890	0.725
31	Mount Moriarty	17 (30)	1707-1996	290	0.414	0.209	0.960	0.851
32	Wapiti Ridge	17 (27)	1809-1996	188	0.484	0.261	0.950	0.670
33	Haley Lake	n/a	n/a	n/a	n/a	n/a	n/a	n/a
34	Heather Mountain	14 (25)	1497-1994	498	0.430	0.269	0.670	0.728
35	Mount Franklyn	n/a	n/a	n/a	n/a	n/a	n/a	n/a
36	Mount Brenton	18 (31)	1704-1996	293	0.458	0.264	0.540	0.771
37	Mount Prevost	n/a	n/a	n/a	n/a	n/a	n/a	n/a
38	T-A-D Ridge	18 (33)	1641-1996	356	0.500	0.234	0.620	0.762
39	Mount Modeste	21 (34)	1327-1996	670	0.521	0.279	0.570	0.778
40	San Juan Ridge	13 (20)	1533-1996	464	0.416	0.258	0.570	0.758
			mean	605	0.433	0.253	0.560	0.764
			median	626	0.443	0.257	0.535	0.773

Table 3.3 -Parameters for crossdated chronologies of the other species in the study. Species codes are as follows: WH = western hemlock, WRC = western red-cedar, DF = Douglas-fir, and SAF = subalpine fir.

Site No.	Name	Species	n = Trees (cores)	Range (years AD)	Chronology length (years)	Mean series correlation	Mean sensitivity	Mean measurement	Auto-correlation
1	Mount Cain	WH	15 (24)	1320-1997	678	0.328	0.218	0.470	0.788
3	Green Mountain	WH	17 (32)	1696-1997	302	0.500	0.232	0.810	0.805
16	Nesook Creek	WH	17 (27)	1615-1997	383	0.370	0.230	0.600	0.75
16	Nesook Creek	WRC	13 (23)	1616-1997	382	0.474	0.178	0.940	0.789
27	Mount Arrowsmith	WH	8 (15)	1705-1997	293	0.512	0.215	0.820	0.796
28	Mount Redford	WH	13 (25)	1469-1997	529	0.447	0.264	0.850	0.781
28	Mount Redford	WRC	10 (18)	1672-1997	326	0.501	0.189	1.140	0.86
31	Mount Moriarty	WH	19 (33)	1760-1996	237	0.471	0.231	1.440	0.797
32	Wapiti Ridge	WH	13 (24)	1791-1996	206	0.592	0.232	1.320	0.865
33	Haley Lake	SAF	35 (35)	1922-1996	75	0.474	0.243	2.200	0.412
33	Haley Lake	WH	24 (29)	1791-1996	206	0.448	0.293	2.250	0.609
35	Mount Franklyn	DF	17 (30)	1724-1996	274	0.575	0.213	1.130	0.882
37	Mount Prevost	DF	32 (35)	1740-1996	257	0.472	0.263	1.420	0.721
38	T-A-D Ridge	WH	17 (21)	1648-1996	349	0.400	0.225	0.630	0.801
39	Mount Modeste	WH	8 (14)	1601-1996	396	0.354	0.208	0.790	0.728
40	San Juan Ridge	WH	19 (27)	1708-1996	289	0.497	0.235	0.780	0.852

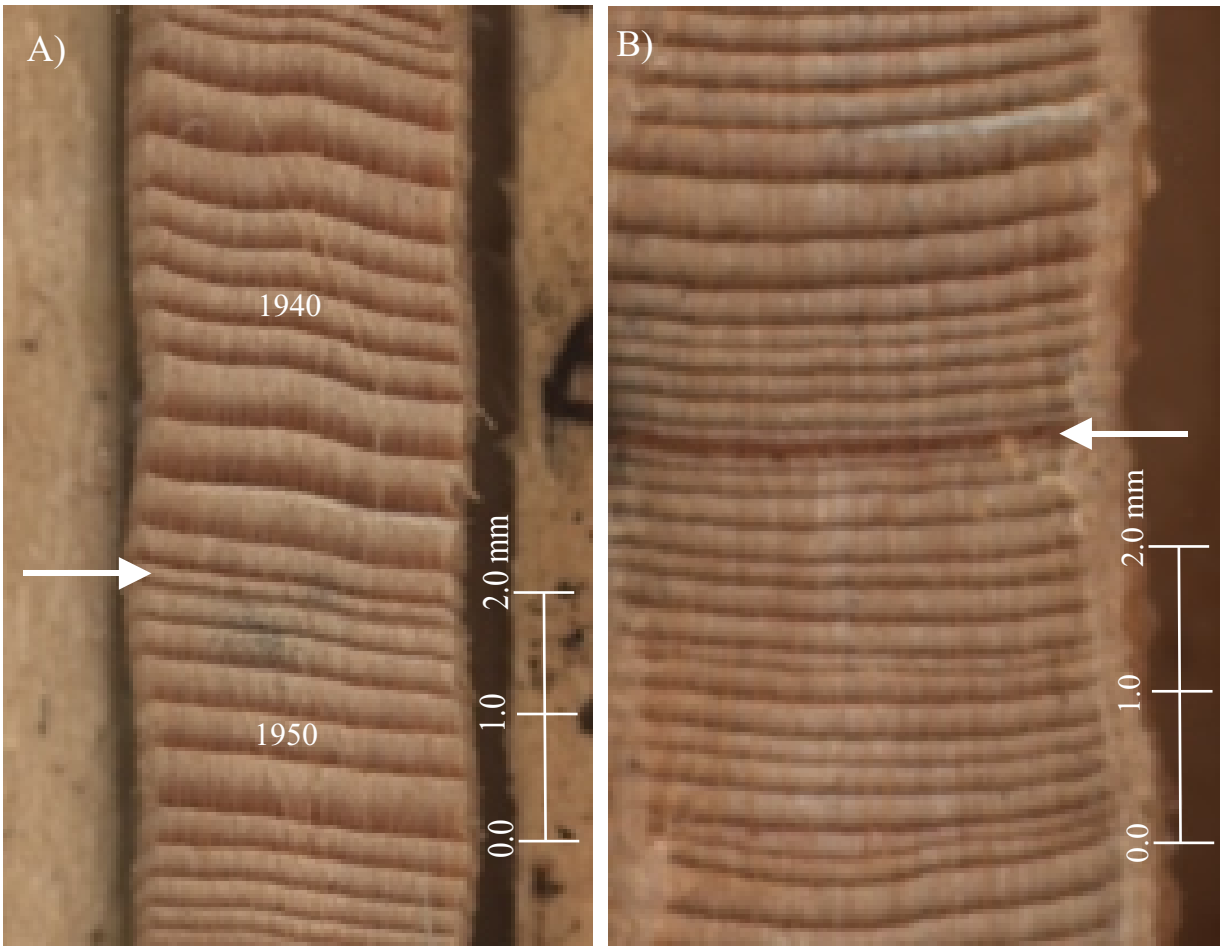

Figure 3.4 - A) a consistent pointer year in all mountain hemlock samples was the 1946 ring. The arrow points to the 1946 ring. B) a "black-ring" which was occasionally found only in mountain hemlock ring sequences. Through crossdating, all black rings were found to contain the growth increment of a single year. The arrow points to the black-ring.

area of many yellow-cedar trees, it is hard to distinguish between actual ring changes and the often highly variable cell and wood colours. Wood tissue is often full of reaction wood because of the pliable nature of saplings under deep snowpacks (Grossnickle 1992, Koppenaal and Mitchell 1992, Klinka and Chourmouzis 2001). In addition, near the bark of very old trees, the rings of earlywood and latewood are not always easily discernable; the density of the two is similar (Josza 1992), the rings are small (< 0.10 mm), and the

Table 3.4 - The estimated population signal strength of all of the mountain hemlock chronologies in the study.

Site No.	Name	Estimated Population Signal	Number of cores	EPS 0.80 - 0.85	Number of cores	Date EPS is > 0.80-0.85 (AD)	Range (AD)
1	Mount Cain	0.98	80	0.85	27	1470	1166-1997
2	Mount Becher	0.96	32	0.89	10	1720	1668-1997
3	Green Mountain	0.97	34	0.90	16	1800	1749-1996
4	Mount MacIntosh	0.93	30	0.83	9	1600	1294-1996
5	Castle Mountain	0.92	30	0.86	10	1675	1543-1997
6	Butterfly Ridge	0.92	25	0.80	12	1860	1655-1996
7	Colonial Creek	0.92	28	0.80	22	1790	1533-1997
8	Bulldog Ridge	0.94	32	0.81	11	1650	1445-1997
9	Mrs. Wade Mountain	0.95	31	0.88	88	1680	1370-1997
10	Mount Elliot	0.95	40	0.88	25	1700	1292-1996
11	Mount Menzies	0.92	28	0.81	19	1725	1491-1997
12	Apple Tree Hill	0.93	39	0.85	19	1565	1339-1996
13	Maquilla Peak	0.95	34	0.83	15	1555	1320-1997
14	Silver Spoon Saddle	0.95	35	0.81	16	1520	1362-1996
15	South Sheena Creek	0.91	33	0.88	28	1785	1553-1996
16	Nesook Creek	n/a	n/a	n/a	n/a	n/a	n/a
17	Mount Upana	0.85	24	0.81	22	1865	1337-1996
18	Mount Heber	0.96	37	0.81	9	1520	1410-1997
19	Lupine Mountain	0.89	26	0.85	17	1755	1520-1997
20	Mount Washington	0.97	33	0.89	25	1785	1504-1997
21	Hanging Valley Creek	0.94	32	0.88	19	1680	1375-1997

Table 3.4, cont. - The estimated population signal strength of all of the mountain hemlock chronologies in the study.

Site No.	Name	Estimated Population Signal	Number of cores	EPS 0.80 - 0.85	Number of cores	Date EPS is > 0.80-0.85 (AD)	Range (AD)
22	Circlet Lake	0.96	38	0.87	9	1710	1557-1993
23	Milla Lake	n/a	n/a	n/a	n/a	n/a	1558-1993
24	Cream Lake	0.97	38	0.84	8	1570	1412-1995
25	Mount Apps	0.94	30	0.85	10	1760	1552-1996
26	Mount Porter	0.96	36	0.89	20	1825	1747-1996
27	Mount Arrowsmith	0.97	35	0.89	14	1725	1648-1997
28	Mount Redford	n/a	n/a	n/a	n/a	n/a	n/a
29	Pirate Peak	0.95	38	0.90	30	1830	1777-1997
30	Douglas Peak	0.95	38	0.89	15	1760	1708-1996
31	Mount Moriarty	0.97	35	0.94	26	1790	1738-1996
32	Wapiti Ridge	0.97	38	0.91	19	1840	1784-1996
33	Haley Lake	0.94	40	0.91	34	1930	1876-1996
34	Heather Mountain	0.89	15	0.81	9	1860	1754-1993
35	Mount Franklyn	0.93	28	0.89	12	1810	1751-1996
36	Mount Brenton	0.91	27	0.81	20	1775	1641-1996
37	Mount Prevost	n/a	n/a	n/a	n/a	n/a	n/a
38	T-A-D Ridge	0.93	29	0.90	12	1750	1699-1996
39	Mount Modeste	0.94	38	0.82	13	1660	1301-1996
40	San Juan Ridge	0.92	22	0.84	10	1725	1490-1996
	mean	0.94	33.5	0.86	18.8	1722	
	median	0.94	33	0.86	16	1737	

boundaries between successive rings are hard to discern because each ring is only a few cells wide. These problems are common concerns when crossdating yellow-cedar but are easy to rectify when the investigator is aware of their occurrence.

Yellow-cedar chronologies yield strong EPS statistics provided there are sufficient samples (n > 16) (Table 3.5). Signal strengths of 0.909 were possible when 29 cores made up a chronology. This species high mean sensitivity and low number of crossdating problems secure its utility to dendrochronology. Another positive characteristic of upper-elevation yellow-cedar on Vancouver Island is that the wood structure remains intact for a long time (Kellner *et al.* 2000). This means that even sections of rings that are partially decomposed can still be easily distinguished, polished and measured (Figure 3.5). Although it has a weaker mean series correlation than mountain hemlock, the extreme longevity of yellow-cedar trees on Vancouver Island (commonly > 750 years) makes it a useful species to study.

Yellow-cedar chronologies from four sites (Mt. Macintosh, Wolf Ridge, Maquilla Peak, and Mt. Redford) proved to have weak mean series correlation. In these cases, low core numbers and site-specific characteristics (e.g., soil characteristics) are probably to blame for the poor results.

High-elevation western hemlock proved difficult to crossdate, even though the ring boundaries are easily discernable. The biggest problem encountered with this species is the frequent interruption of the ring sequence by one or more pinched out (locally absent) rings. Because western hemlock typically grows under a canopy, it commonly shuts down cambium development at various points of its circumference, or

Table 3.5 - The estimated population signal strength of all of the yellow-cedar chronologies in the study.

Site No.	Name	Estimated Population Signal	Number of cores	EPS 0.80 - 0.85	Number of cores	Date EPS is > 0.80-0.85 (AD)	Range (AD)
1	Mount Cain	0.97	53	0.84	29	1635	1205-1994
2	Mount Becher	0.91	25	0.83	13	1655	1509-1997
3	Green Mountain	0.95	24	0.83	19	1810	1707-1996
4	Mount MacIntosh	0.81	15	0.81	13	1780	1320-1996
5	Castle Mountain	0.90	24	0.83	13	1555	1172-1997
6	Wolf Ridge	0.85	21	0.80	20	1805	1470-1996
7	Colonial Creek	0.93	30	0.84	12	1710	1459-1997
8	Bulldog Ridge	0.91	30	0.83	13	1655	1421-1997
9	Mrs. Wade Mountain	0.94	30	0.84	9	1395	1065-1996
10	Mount Elliot	0.96	31	0.83	22	1650	1290-1996
11	Mount Menzies	0.91	31	0.86	14	1775	1390-1997
12	Apple Tree Hill	0.91	25	0.81	20	1635	1154-1996
13	Maquilla Peak	0.89	29	0.86	16	1610	1257-1997
14	Silver Spoon Saddle	0.95	24	0.84	17	1690	1237-1996
15	South Sheena Creek	0.87	16	0.82	14	1620	1067-1996
16	Nesook Creek	0.57	n/a	n/a	n/a	n/a	n/a
17	Mount Upana	0.92	18	0.82	12	1585	1305-1996
18	Mount Heber	0.92	30	0.84	11	1560	1354-1997
19	Lupine Mountain	0.93	27	0.82	25	1565	1133-1997
20	Mount Washington	0.97	82	0.87	22	1785	1702-1994
21	Hanging Valley Creek	0.91	20	0.85	14	1650	1243-1997

Table 3.5, cont. - The estimated population signal strength of all of the yellow-cedar chronologies in the study.

Site No.	Name	Estimated Population Signal	Number of cores	EPS 0.80 - 0.85	Number of cores	Date EPS is > 0.80-0.85 (AD)	Range (AD)
22	Circlet Lake	n/a	n/a	n/a	n/a	n/a	n/a
23	Milla Lake	0.83	22	0.83	22	1850	798-1994
24	Cream Lake	n/a	n/a	n/a	n/a	n/a	n/a
25	Mount Apps	0.94	31	0.87	25	1675	1145-1996
26	Mount Porter	0.92	28	0.81	20	1785	1452-1996
27	Mount Arrowsmith	0.97	57	0.84	27	1760	1105-1994
28	Mount Redford	0.66	18	n/a	n/a	n/a	1761-1997
29	Pirate Peak	0.92	31	0.83	24	1835	1634-1997
30	Douglas Peak	0.96	36	0.84	14	1810	1752-1996
31	Mount Moriarty	0.90	30	0.87	10	1810	1707-1996
32	Wapiti Ridge	0.94	27	0.86	16	1860	1809-1996
33	Haley Lake	n/a	n/a	n/a	n/a	n/a	n/a
34	Heather Mountain	0.91	22	0.84	14	1800	1497-1994
35	Mount Franklyn	n/a	n/a	n/a	n/a	n/a	n/a
36	Mount Brenton	0.92	31	0.83	1835	24	1704-1996
37	Mount Prevost	n/a	n/a	n/a	n/a	n/a	n/a
38	T-A-D Ridge	0.95	32	0.82	1700	15	1641-1996
39	Mount Modeste	0.95	29	0.80	1580	10	1327-1996
40	San Juan Ridge	0.88	18	0.86	1840	17	1533-1996
	mean	0.91	29	0.83	17	1705	
	median	0.92	28.5	0.83	16	1700	

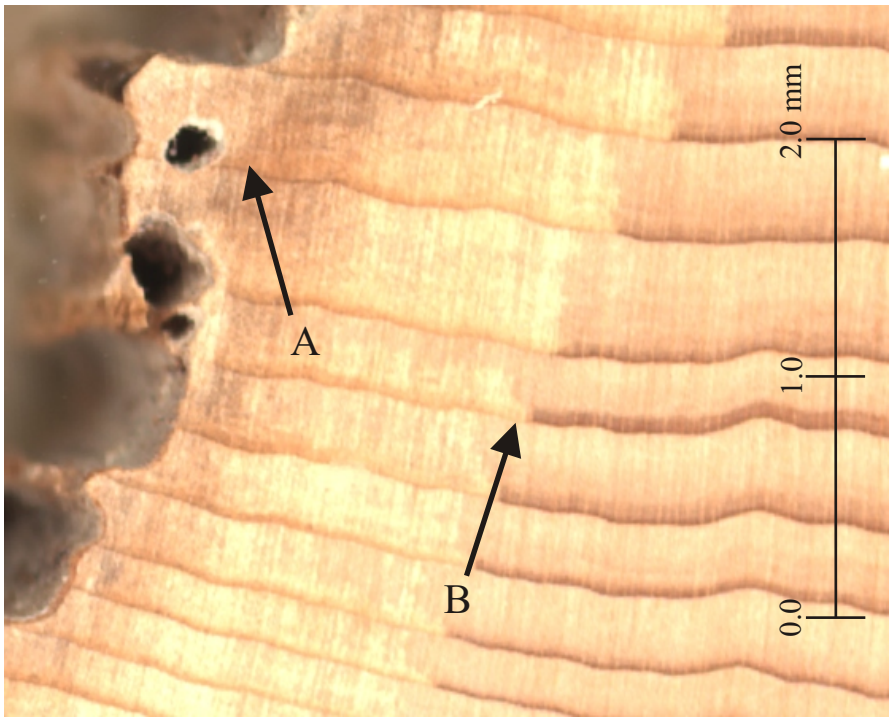

Figure 3.5 - An example from a 1582 years old yellow-cedar from northern Vancouver Island. A) The arrow points to the boundary where deteriorating wood turns to rot and where ring boundaries can no longer be distinguished. B) The arrow points to where sound wood begins to transform into deteriorated woody tissue. Note that the ring boundaries are still visible in the deteriorated wood.

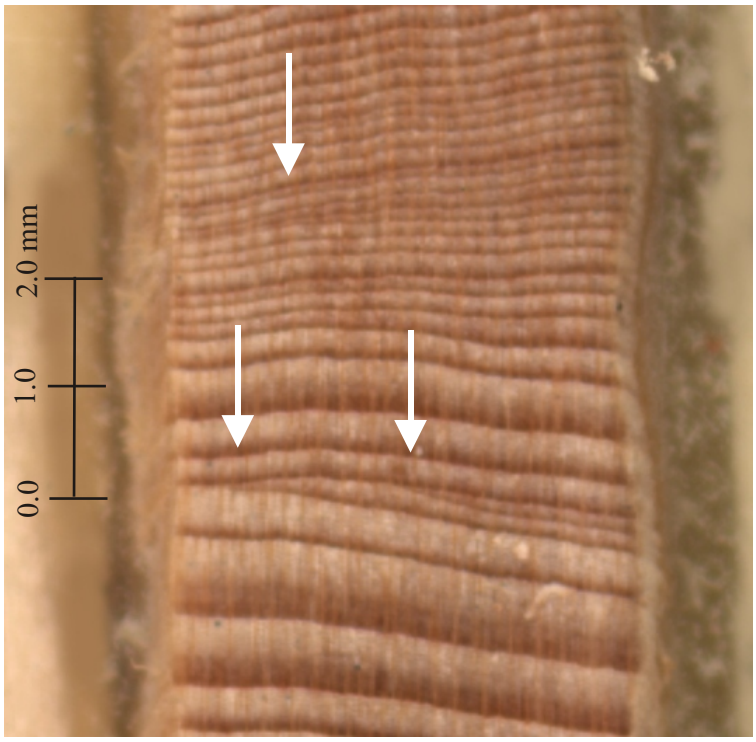

Figure 3.6 - A sample of western hemlock showing pinched out rings. The three arrows all point to rings that are pinched out in this small section of the sample.

concentrates growth in areas best positioned to maximize the collection of light and nutrients (Schweingruber 1996, van Pelt and Franklin 1999). These uneven patterns of growth are reflected in the ring structures (Figure 3.6), and make crossdating difficult. When constructing crossdated chronologies from western hemlock trees it is almost impossible to find ring-width sequences that do not contain inherent problems. On average 25 cores were needed to attain a signal strength of 0.895. Three of the 11 western hemlock chronologies (from Mount Cain, Nesook Creek, and Mount Modeste) remain suspect, even though these sites have high core counts. The weak EPS values at these three sites, and in general for all western hemlock sites, show that this species is not the best candidate to use in dendrochronological analyses from high-elevation environments (Table 3.6).

An associated problem is that western hemlock trees appear to alter some of their visual characteristics at the upper-elevation limit of their range. They appear in a gradient from a common western hemlock expression, to a hybrid-like western hemlock/mountain hemlock appearance. These changes include leaf and bark characteristics, and also show up in the pattern of radial increments. Hybrid-like samples from Mt. Arrowsmith crossdated better with visually pure western hemlock samples from 100 m lower in elevation than with pure mountain hemlock from 100 m higher in elevation. This was true even though, on a whole, the mountain hemlock samples crossdated more reliably and produced better chronologies (mean series correlation = 0.619 from 35 cores) than western hemlock (mean series correlation = 0.512 from 15 cores). Although western hemlock and mountain hemlock are reported to hybridize (e.g.,

Table 3.6 - The estimated population signal strength of all of the other species chronologies in the study. Species codes are as follows: WH = western hemlock, WRC = western red-cedar, DF = Douglas-fir, SAF = subalpine fir.

Site No.	Name	Species	Estimated Population Signal	Number of cores	EPS 0.80 - 0.85	Number of cores	Date EPS is > 0.80-0.85 (AD)	Range (AD)
1	Mount Cain	WH	0.81	24	0.80	22	1880	1320-1997
3	Green Mountain	WH	0.92	32	0.83	11	1750	1696-1997
16	Nesook Creek	WH	0.88	27	0.84	23	1845	1615-1997
16	Nesook Creek	WRC	0.92	21	0.81	15	1820	1616-1997
27	Mount Arrowsmith	WH	0.90	15	0.85	11	1835	1705-1997
28	Mount Redford	WH	0.90	25	0.83	20	1870	1469-1997
28	Mount Redford	WRC	0.90	16	0.82	14	1830	1672-1997
31	Mount Moriarty	WH	0.93	33	0.87	16	1820	1760-1996
32	Wapiti Ridge	WH	0.94	24	0.87	14	1850	1791-1996
33	Haley Lake	SAF	n/a	n/a	n/a	n/a	n/a	n/a
33	Haley Lake	WH	n/a	n/a	n/a	n/a	n/a	n/a
35	Mount Franklyn	DF	0.97	32	0.82	17	1780	1724-1996
37	Mount Prevost	DF	0.90	25	0.81	10	1825	1740-1996
38	T-A-D Ridge	WH	0.90	27	0.83	11	1775	1648-1996
39	Mount Modeste	WH	0.82	14	0.82	13	1885	1601-1996
40	San Juan Ridge	WH	0.95	27	0.88	17	1760	1708-1996
		WH mean	0.90	25	0.84	16	1827	
		WH median	0.90	26	0.83	15	1840	

Tsuga X jeffreyi), it is thought to only occur rarely in nature (Taylor 1972). The consensus is that the hybrid-looking individuals commonly encountered are genetically more similar to western hemlock (Taylor 1972), and this seems to be the case in this study, especially with regard to ring characteristics and ring sequences.

Ring characteristics of high-elevation western red-cedar are more similar in crossdating characteristics to western hemlock than to yellow-cedar. As with western hemlock, boundaries between earlywood and latewood are highly visible and so the problem commonly encountered is incomplete ring sequences due to locally absent rings (Figure 3.7). As with western hemlock, these ring aberrations can account for a single or many missing rings. Typically, when crossdating western red cedar, a ring sequence either crossdates well, or it does not crossdate at all. As with western hemlock, these effects most likely result from competition for light in the closed canopy (van Pelt and Franklin 1999).

High-elevation Douglas-fir sampled in this study presented no significant problems in crossdating. The boundaries between the rings were well defined, and earlywood and latewood separation was equally distinct. Because upper-elevation Douglas-fir were near their altitudinal limit, few of the problems associated with crossdating low-elevation Douglas-fir (e.g., due to insect damage) seem to be encountered (Alfaro and Macdonald 1988).

Subalpine fir generally grow in open subalpine meadows on Vancouver Island, and when trees large enough to sample were found, few aberrant effects were present in their ring structures. It is common to find predictably tight early-stage growth in the

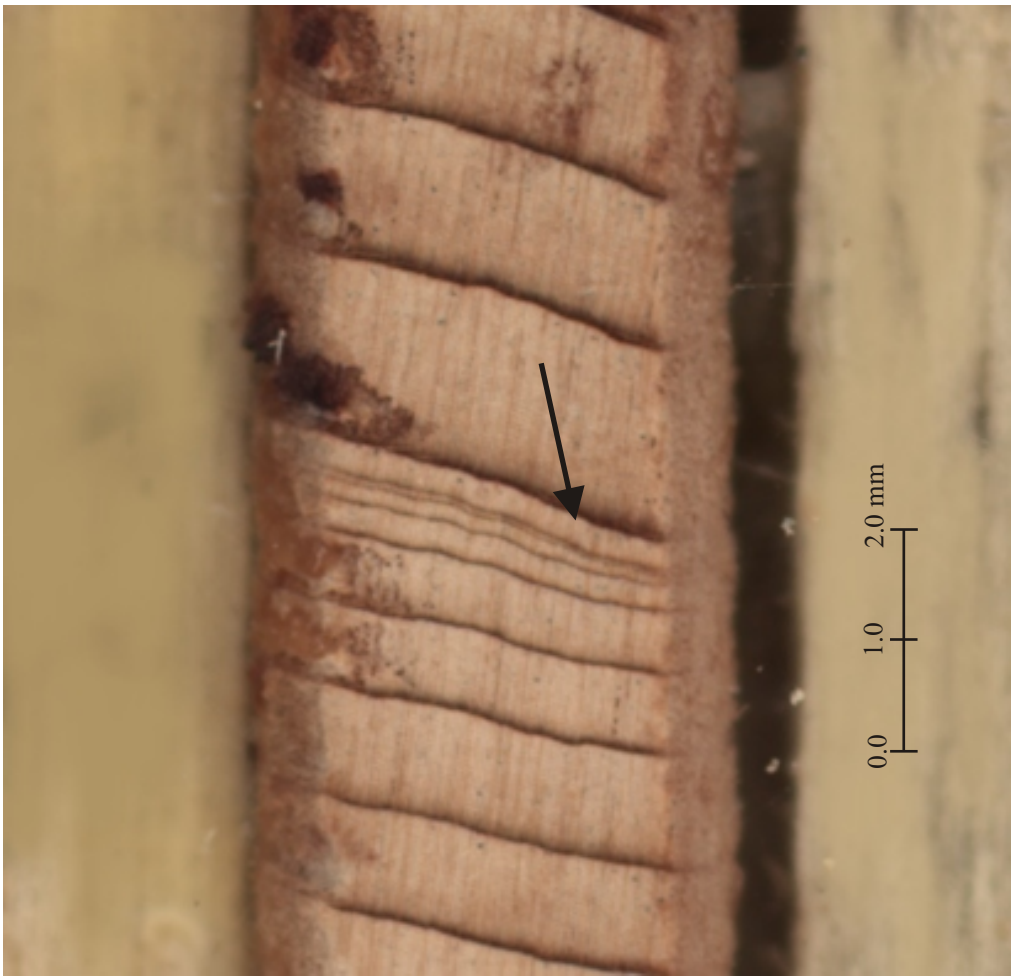

Figure 3.7 - The arrow points to a location on a sample of western red-cedar where rings pinch out. This characteristic in western red-cedar ring structures does not occur as frequently as in western hemlock.

species, which results from growing in the deep snowpack environment (Laroque *et al.* 2000/01). Once past the sapling stage, the ring structures are well defined and provide no problems in crossdating. No further analyses of subalpine fir were undertaken, as no tree over 100 years was found.

The limited Douglas-fir, subalpine fir, and western red-cedar in these environments show chronology characteristics in the same range as those of western hemlock (Table 3.6). If more samples could be found, these species may be well suited for dendrochronological analysis in upper-elevation areas of Vancouver Island.

4.0 Spatial and Temporal Dimensions

4.1 Introduction

Tree-ring chronologies are known to share common signals over distances as great as 700 km. Cropper and Fritts (1982) show that similar radial-growth trends occur within trees distributed from the American Southwest to the interior of British Columbia. Nevertheless, Wiles *et al.* (1996) found two distinct patterns of radial growth in the Pacific Northwest and suggested these represented the direct convergence of oceanic circulation patterns. This suggestion provided the impetus behind ongoing dendroclimatological research in the region (e.g., Wiles *et al.* 1996, Wiles *et al.* 1998, Gedalof 1999).

An objective of this study was to distinguish which climatic parameters influence the spatial growth patterns of high-elevation trees on Vancouver Island. Once the spatial dimension of radial-growth patterns was better understood, it was important to ascertain whether and how this pattern has changed through time. This chapter documents the complex spatial and temporal relationships between climate and radial growth on Vancouver Island.

4.2 Spatial Analysis

The crossdated chronologies established in Chapter 3 were analyzed to see if any spatial patterns existed. An 88 x 88 chronology correlation matrix was constructed to compare these relationships over a common time frame from 1793 to 1993, a well-replicated 200-year interval in all the chronologies. Values found above 0.24 over the 200-year interval indicate that the radial-growth patterns are similar to a high degree ($p <$

0.0001). Each species was grouped inside the matrix to assist in the comparison of within- and between-species correlations spatially in the network (Appendix B).

Most within-species cross correlations were highly significant, with very few site-to-site chronologies failing to show the same 200-year pattern in the test. The strongest correlations were usually from nearby sites of the same species. Between-species tests often showed a high correlation, especially when the two chronologies came from the same or nearby locations. The strongest correlations between species pairs were for mountain hemlock and western hemlock, and between mountain hemlock and yellow-cedar.

To try to understand if there was any north-to-south variation in these relationships, a second test was conducted comparing six sites from northern Vancouver Island to six sites from southern Vancouver Island. The 6 x 6 matrix was selected from sites containing both a mountain hemlock and a yellow-cedar chronology (Figure 4.1). In general there is a strong similarity within each species group, with all the northern mountain hemlock and yellow-cedar chronologies indicating significance above the $p < 0.0001$ level (Tables 4.1 and 4.2). The southern within-group matrix again shows a high degree of similarity (Tables 4.3 and 4.4).

Tables 4.5 and 4.6 present correlations between sites in the northern and southern group for each species. In this case, very strong patterns again dominate (e.g., Apple Tree Hill vs. San Juan Ridge for mountain hemlock and Castle Mountain vs. Mount Modeste for yellow-cedar), with only a few values not exhibiting a strong significantly similar signal. The chronology comparisons are shown in Figure 4.2 and 4.3.

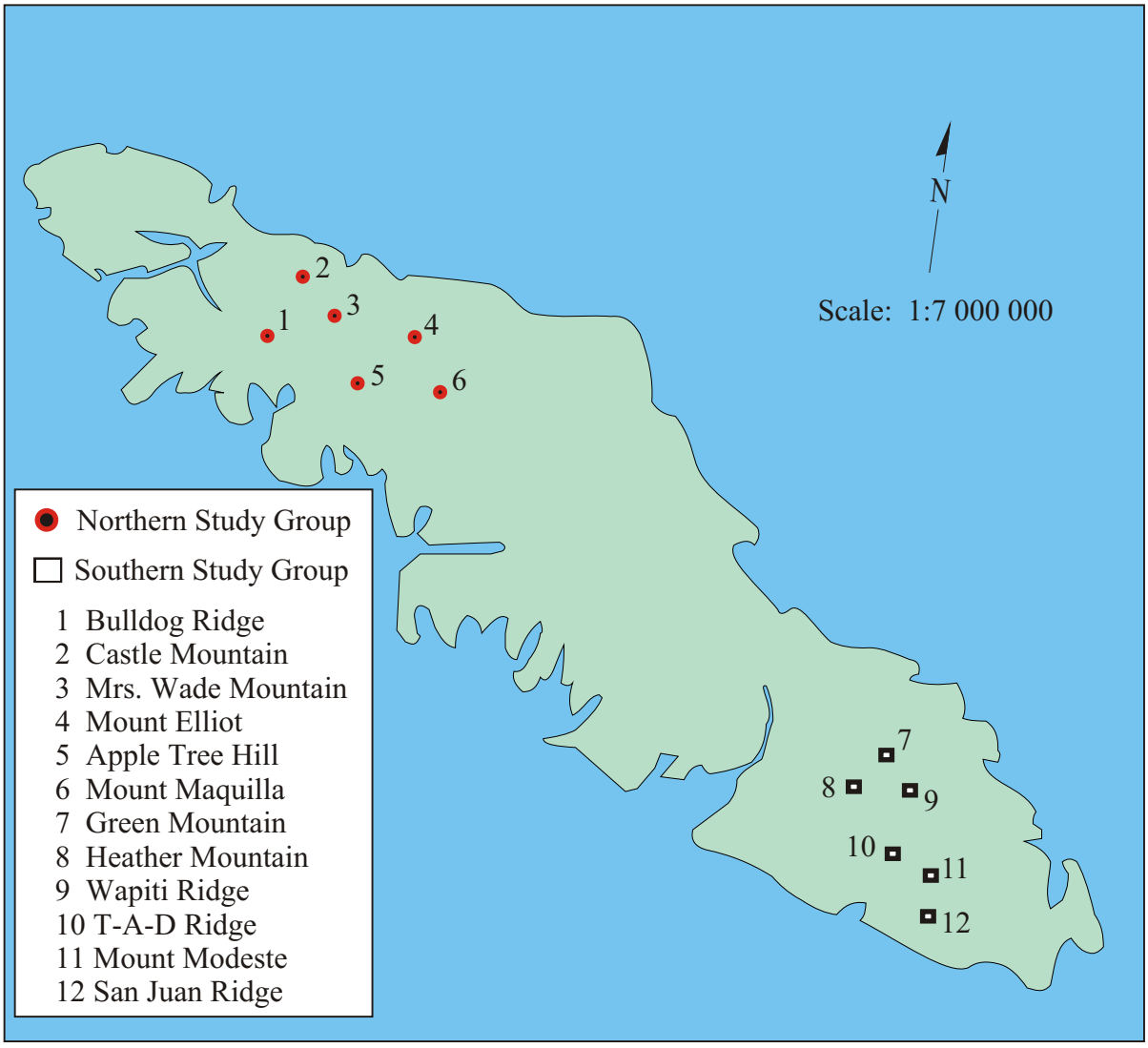

Figure 4.1- The location of the six most northern and six most southern sites that have both mountain hemlock and yellow-cedar chronologies available for spatial comparison on Vancouver Island.

Table 4.1- Correlation matrix of the northern group of mountain hemlock chronologies (all values are above 0.24 and significant at $p < 0.0001$).

Name	Bulldog Ridge	Castle Mountain	Mrs. Wade Mountain	Mount Elliot	Apple Tree Hill	Mount Maquilla
Bulldog Ridge	1.00					
Castle Mountain	0.55	1.00				
Mrs. Wade Mountain	0.26	0.56	1.00			
Mount Elliot	0.36	0.56	0.57	1.00		
Apple Tree Hill	0.39	0.52	0.66	0.51	1.00	
Mount Maquilla	0.58	0.51	0.36	0.31	0.42	1.00

Table 4.2 - Correlation matrix of the northern group of yellow-cedar chronologies (all values are above 0.24 and significant $p < 0.0001$).

Name	Bulldog Ridge	Castle Mountain	Mrs. Wade Mountain	Mount Elliot	Apple Tree Hill	Mount Maquilla
Bulldog Ridge	1.00					
Castle Mountain	0.67	1.00				
Mrs. Wade Mountain	0.49	0.70	1.00			
Mount Elliot	0.52	0.52	0.56	1.00		
Apple Tree Hill	0.85	0.64	0.56	0.57	1.00	
Mount Maquilla	0.56	0.48	0.44	0.59	0.54	1.00

Table 4.3 - Correlation matrix of the southern group of mountain hemlock chronologies with values above 0.24 significant at $p < 0.0001$. Shaded areas are values with $r < 0.24$ and individual p-values contained in brackets.

Name	Green Mountain	Heather Mountain	Wapiti Ridge	T-A-D Ridge	Mount Modeste	San Juan Ridge
Green Mountain	1.00					
Heather Mountain	0.52	1.00				
Wapiti Ridge	0.50	0.36	1.00			
T-A-D Ridge	0.35	0.22 (0.005)	0.70	1.00		
Mount Modeste	0.44	0.30	0.50	0.52	1.00	
San Juan Ridge	0.36	0.33	0.22 (0.004)	0.27	0.58	1.00

Table 4.4 - Correlation matrix of the southern group of yellow-cedar chronologies (all values are above 0.24 and significant $p < 0.0001$).

Name	Green Mountain	Heather Mountain	Wapiti Ridge	T-A-D Ridge	Mount Modeste	San Juan Ridge
Green Mountain	1.00					
Heather Mountain	0.72	1.00				
Wapiti Ridge	0.36	0.42	1.00			
T-A-D Ridge	0.42	0.44	0.47	1.00		
Mount Modeste	0.63	0.74	0.38	0.64	1.00	
San Juan Ridge	0.45	0.65	0.43	0.53	0.67	1.00

Table 4.5 - Correlation matrix of the northern versus southern group of mountain hemlock chronologies with values above 0.24 significant at $p < 0.0001$. Shaded areas are values with $r < 0.24$ and individual p-values contained in brackets.

Name	Bulldog Ridge	Castle Mountain	Mrs. Wade Mountain	Mount Elliot	Apple Tree Hill	Mount Maquilla
Green Mountain	0.39	0.46	0.38	0.62	0.28	0.49
Heather Mountain	0.35	0.40	0.29	0.41	0.27	0.19 (0.006)
Wapiti Ridge	0.52	0.42	0.52	0.27	0.21 (0.003)	0.37
T-A-D Ridge	0.52	0.38	0.29	0.14 (0.04)	0.22 (0.002)	0.42
Mount Modeste	0.61	0.57	0.50	0.41	0.58	0.49
San Juan Ridge	0.37	0.48	0.37	0.57	0.73	0.32

Table 4.6 - Correlation matrix of the northern versus southern group of yellow-cedar chronologies with values above 0.24 significant at $p < 0.0001$. Shaded areas are values with $r < 0.24$ and individual p-values contained in brackets.

Name	Bulldog Ridge	Castle Mountain	Mrs. Wade Mountain	Mount Elliot	Apple Tree Hill	Mount Maquilla
Green Mountain	0.38	0.50	0.48	0.46	0.39	0.31
Heather Mountain	0.47	0.57	0.51	0.61	0.50	0.49
Wapiti Ridge	0.06 (0.385)	0.28	0.34	0.33	0.19 (0.008)	0.23 (0.001)
T-A-D Ridge	0.41	0.55	0.57	0.48	0.41	0.35
Mount Modeste	0.66	0.70	0.57	0.68	0.68	0.61
San Juan Ridge	0.45	0.49	0.52	0.52	0.59	0.51

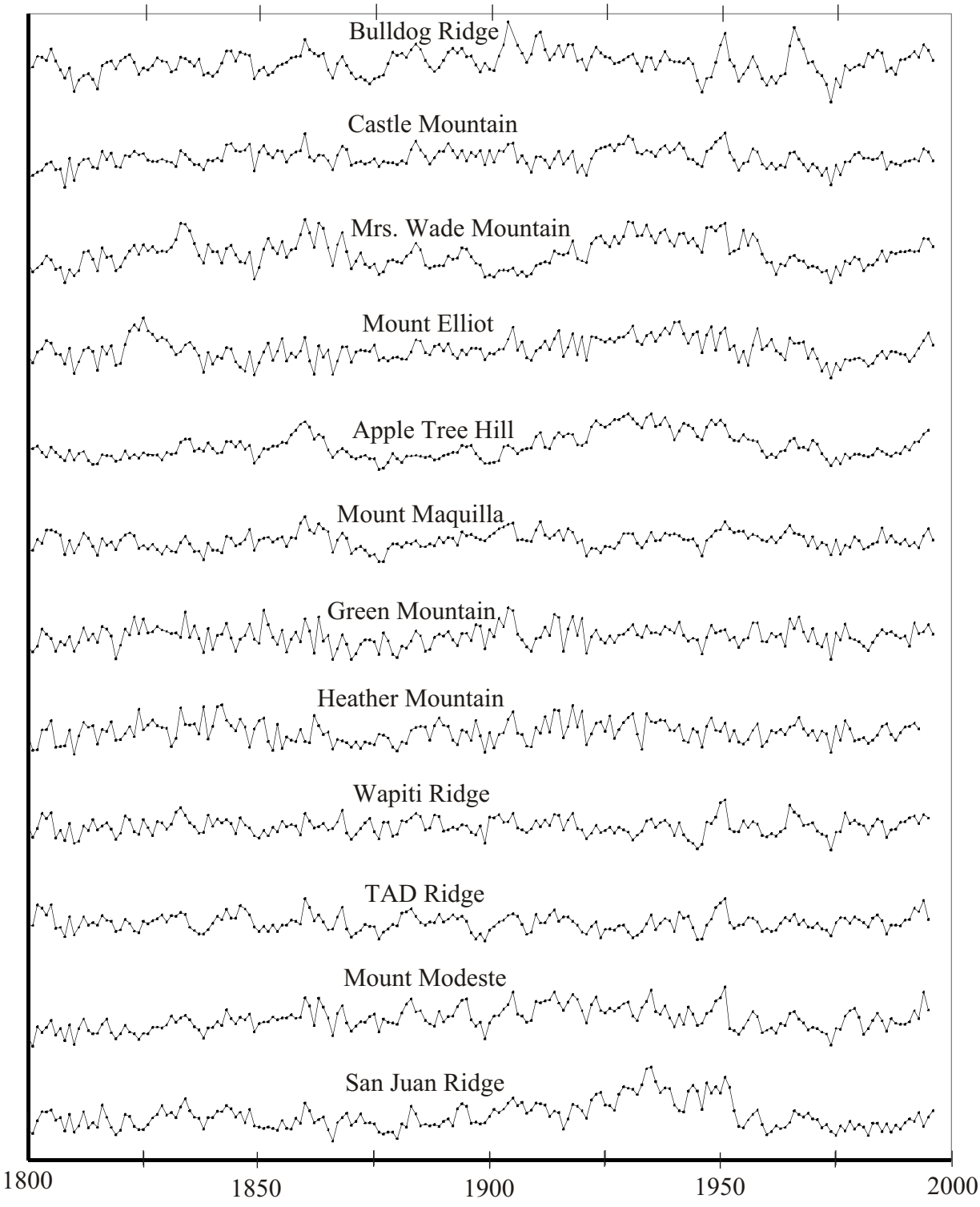

Figure 4.2 - The 12 mountain hemlock chronologies in the north- to south-island comparison. The chronologies are displayed from north to south and encompass the time frame from 1795-1995.

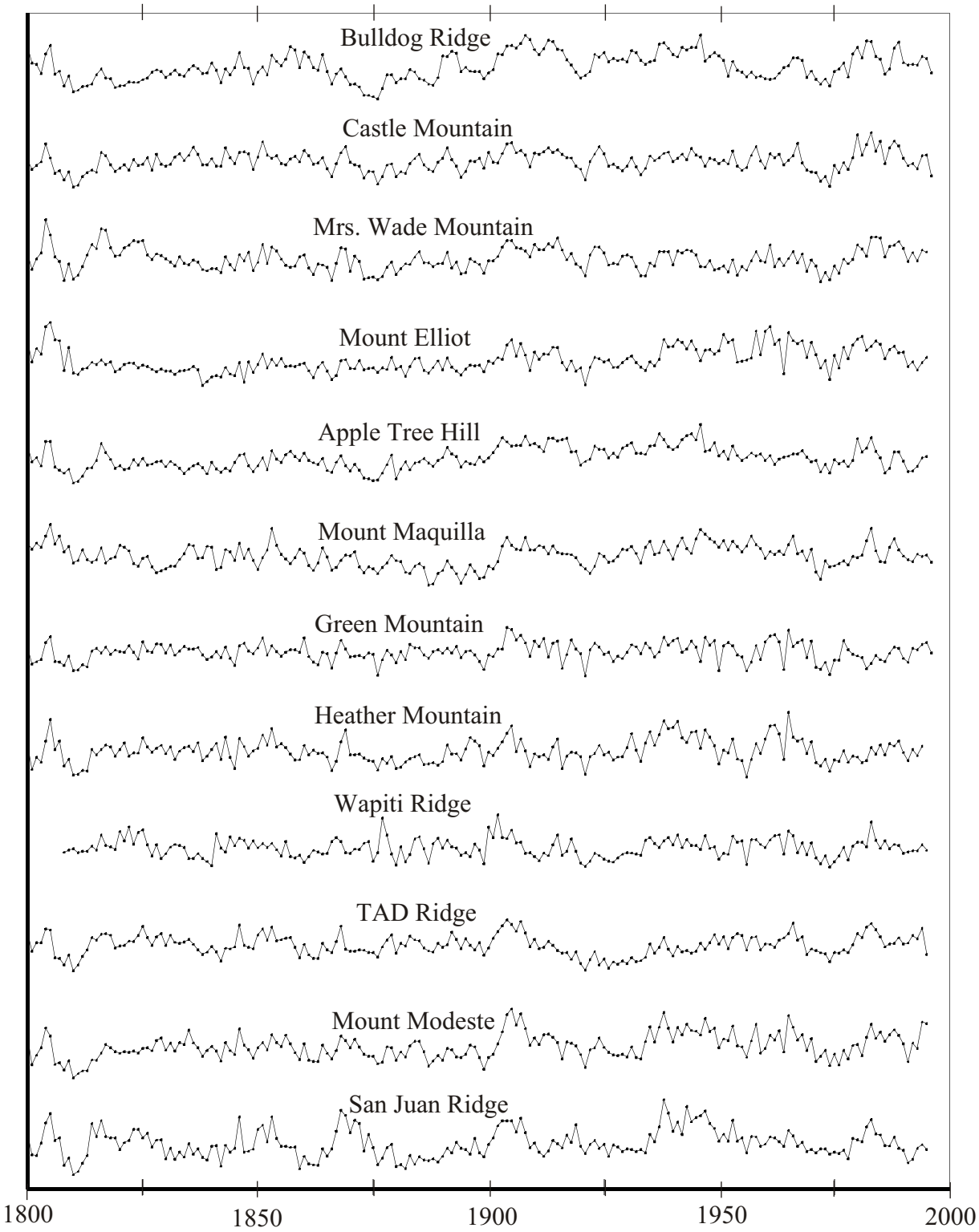

Figure 4.3 - The 12 yellow-cedar chronologies in the north- to south-island comparison. The chronologies are displayed from north to south and encompass the time frame from 1795-1995.

These results show that the radial-growth trends are similar from the northern to the southern areas of Vancouver Island over the 200-year interval. This spatial pattern is similar to the single homogeneous pattern described by Cropper and Fritts (1982), and unlike the distinct-zone model proposed by Wiles *et al.* (1996).

4.3 Temporal Analysis

The results from the above analysis suggest that over the last 200 years, radial-growth patterns on Vancouver Island have been similar. The correlation matrices demonstrated that most sites were strongly similar to each other but not perfectly related, so an analysis was undertaken to examine the year to year changes to the pattern of growth over time. To test for changes in past growth, the 32 sites that contained both a mountain hemlock and yellow-cedar chronology were analyzed (Figure 4.4). The program SURFER™ (Version 6.04, 1997) was used to map the spatial co-ordinates of each site and to distinguish when radial growth was greater or less than one standard deviation from the average ARSTAN index of each species for the year. A mapped image for each year (1493 AD to 1993 AD) was constructed (data before this period are too intermittent for a complete network analysis).

A year-by-year analysis of the mapped deviations of radial growth for each year shows there are four basic growth patterns (Figure 4.5a-d):

- Years where no pattern existed (Figure 4.5a).
- Years when radial growth was greater or less at the northern study sites when compared to those on southern Vancouver Island (Figure 4.5b).

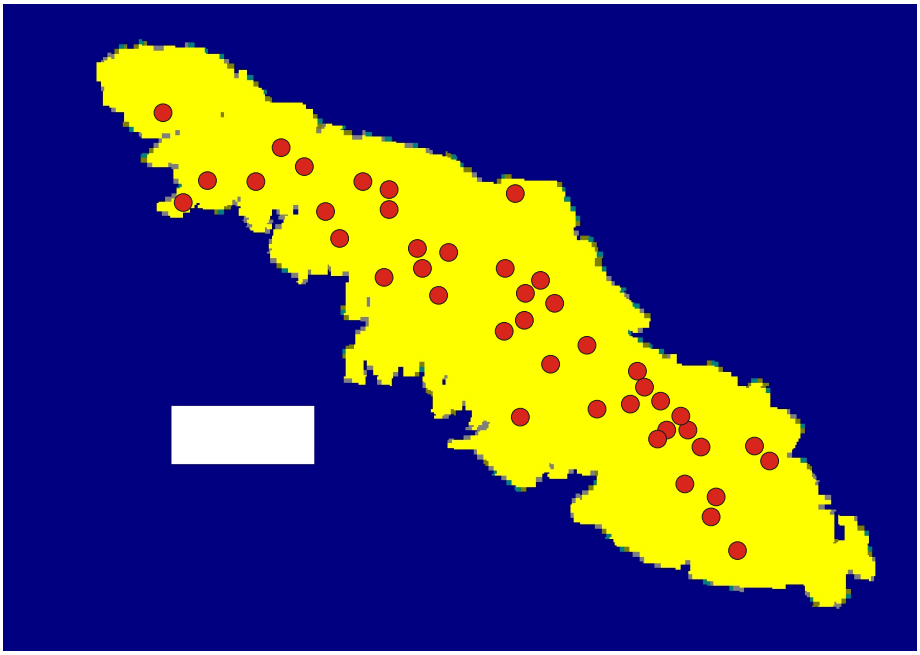

Figure 4.4 - A mapped image from the Surfer analysis in which all sites that contain both a mountain hemlock and yellow-cedar chronology and were used in the spatial analysis are displayed by a circular symbol.

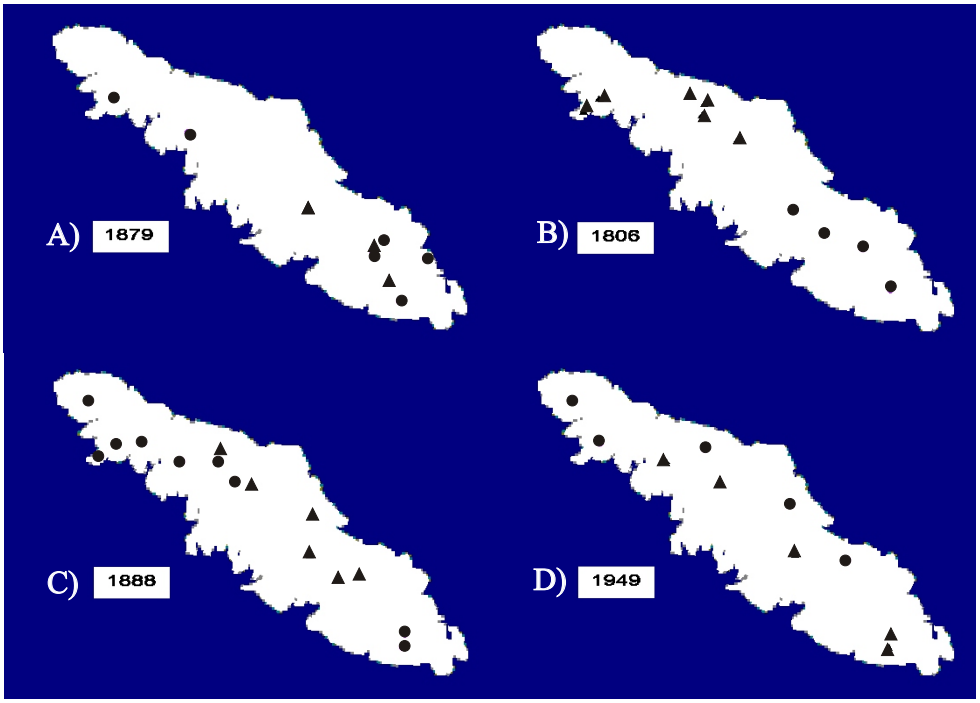

Figure 4.5 - The growth patterns found within the last 500 years on Vancouver Island as revealed by the Surfer spatial analysis. Sites with radial growth above one standard deviation are indicated by a triangle symbol (▲). Sites with radial growth below one standard deviation are indicated by a circular symbol (●). The sample patterns are : A) no spatial pattern, B) greater growth in the north or the south, C) greater growth in central Vancouver Island, D) greater growth in the east or west coast of the island.

- Years when radial growth was greater than normal on central Vancouver Island, and lower than normal at northern and southern sites (Figure 4.5c).
- Years when radial growth was greater along one coast than the other (Figure 4.5d).

Overall there was no systematic deviation in the pattern of growth across Vancouver Island. The dominant yearly growth trend was that no pattern existed (occurring over 90 % of the time). No clear deviation from a pattern of similarity makes sense since most sites were so closely correlated. When differences in radial growth did appear, it never repeated in subsequent years and were always interrupted by years where no coherent pattern existed. Moreover, the year-by-year analysis produced no obvious cyclical time frame for any of the recognizable patterns.

These results indicate that, although specific weather conditions may influence radial-growth patterns on Vancouver Island in an individual year, there has been no overall change in the frequency or magnitude of these patterns in the last 500 years. They exist only for a year and do not signal any latitudinal persistence that might be associated with large shifts in the dominating climate-forcing mechanisms as was suggested by Wiles *et al.* (1996). Vancouver Island appears to have been influenced by the same predominant forcing mechanisms throughout the past, suggesting that Vancouver Island is not under the influence of two or more systems in a given year (i.e. one system dominating the north, and a different system dominating the south) as was originally hypothesised (Wiles *et al.* 1996). Instead, a single forcing mechanism influences radial growth over the entire island.

4.4 Island-wide Master Chronologies

Because radial-growth patterns for each species have remained similar across Vancouver Island for at least the last 500 years, and because the growth patterns for all species were similar within species across the island as established by the correlation matrix, the 88 chronologies developed in Chapter 3 were averaged into island-wide master chronologies (one for each species). Each master chronology was constructed by averaging all yearly values from all sites into a master Vancouver Island value for the year. The five master chronologies are displayed in Figures 4.6.

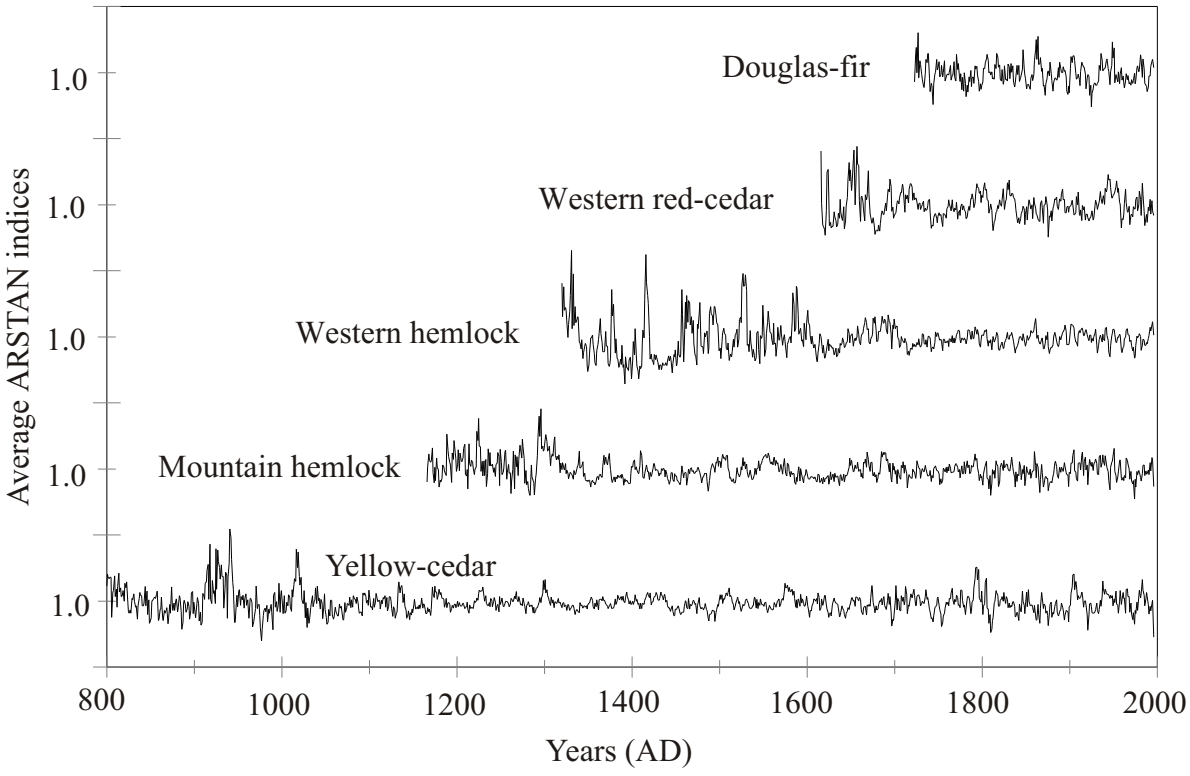

Figures 4.6 - The five master Vancouver Island chronologies developed in the study.

Table 4.7 illustrates the cross-species correlation of the master chronologies over a 200-year interval from 1793-1993. The relationships that existed between the species from the 88 x 88 chronology matrix is maintained within the master chronologies, with mountain hemlock and western hemlock continuing to share the greatest similarity. The significant similarities between most species provide a rationale for investigating common mechanisms that might control similar characteristics of the master chronologies. The non-significant relationships also provide a justification for looking at species-specific factors in climate/radial-growth relationships.

Table 4.7 - Interspecies correlations from 1793-1993 for master chronologies. Values above 0.24 are significant at $p < 0.0001$. Note that because of the very short interval for subalpine fir it could not be used in the comparison.

	mountain hemlock	yellow-cedar	western hemlock	western red-cedar	Douglas-fir
mountain hemlock	1.00				
yellow-cedar	0.50	1.00			
western hemlock	0.64	0.24	1.00		
western red-cedar	0.20	0.38	0.15	1.00	
Douglas-fir	0.22	0.14	0.36	0.11	1.00

4.5 Large-scale Forcing Mechanisms

Due to the close proximity of the Pacific Ocean, the radial-growth of trees on Vancouver Island is likely affected by large-scale oceanic forcing mechanisms (Wiles *et*

al. 1996, Peterson *et al.* 1999, Wiles *et al.* 1998, Gedalof and Smith 2001a). Three such mechanisms have been documented:

- an equatorial sea surface temperature (SST) mechanism, found in oceanic effects such as El Nino and the southern oscillation (ENSO) phenomenon. One of the ways these phenomena are measured is by their relation to the 27° C SSTs in the equatorial Pacific, where spatial and temporal fluctuations cooler than this temperature are linked to many climate-forcing patterns (e.g., precipitation fluctuations along the coast of Peru). A widely used index of the variation of the cooler phases of ENSO as measured in SSTs is the Cold Tongue Index (CTI) (Smith *et al.* 1996). The updated Smith *et al.* (1996) data set is available from the Joint Institute of the Study of the Atmosphere and the Oceans (JISAO) website (http://www.jisao.washington.edu/main.html, accessed November 16/2001) and has a continuous record of monthly values from 1896 to present.

- an interannual to interdecadal recurring pattern of climate variability centred in the mid-latitudes of the Pacific Ocean, called the Pacific Decadal Oscillation (PDO) (Mantua *et al.* 1997). The pattern has two distinct phases, a warm/dry phase and a cool/moist phase. The PDO is characterized by sudden dramatic phase reversals. Instrumental data from the region indicate phase switches took place around 1925, 1947 and 1977. Proxy records indicate that these phase switches have occurred for at least the last 350 years (Biondi *et al.* 2001, Gedalof and Smith 2001a). The updated Mantua *et al.* (1997) data set is available from the JISAO website (http://www.jisao.washington.edu/main.html, accessed November 16/2001) and has a continuous record of monthly values from 1900 to present.

- a variability pattern across North America especially accurate for winter climates, measured by the Pacific North American (PNA) index (Wallace and Gutzler 1981). The PNA index is a measure of the standardized 500 hPa geopotential heights over 4 grid points in the northern Pacific Ocean and North American continent (Wallace and Gutzler 1981). The PNA index is used to relate stationary air pressure patterns over the defined area in the winter months to various types of climate related processes happening at the surface. The updated Wallace and Gutzler (1981) data set is available from the JISAO website (http://www.jisao.washington.edu/main.html, accessed November 16/2001) and has a continuous record of monthly values from 1948 to present.

Monthly values, as well as seasonal averages (DJF, MAM, JJA, SON), for each climate index were correlated with the five master chronologies established in section 4.4 (80 correlations in the matrix; 12 monthly and four seasonal variables by the five master

chronologies). Values significant at the 95 and 99 percent confidence intervals are displayed in Table 4.8, 4.9 and 4.10 for each of the three matrices.

Table 4.8 - Relationships between the Cold Tongue Index and the master chronologies for five species. Significant values of single monthly or seasonal CTI parameters are listed at either the 99 or 95 percent confidence interval (p-values are listed in brackets).

	99 %	99 %	95 %	95 %	95 %	95 %	95 %	95 %	95 %
Mountain hemlock	MAM (0.002)	Mar (0.004)	Apr (0.01)	Aug (0.045)	DJF (0.049)	Jan (0.048)	JJA (0.023)	Jul (0.021)	May (0.018)
Yellow-cedar			DJF (0.035)	Feb (0.033)					
Western hemlock			Dec (0.023)	DJF (0.027)	JJA (0.031)	Jul (0.019)	Oct (0.024)	SON (0.047)	
Western red-cedar	SON (0.007)	Dec (0.008)	Oct (0.011)	Nov (0.012)	Jul (0.045)	JJA (0.046)			
Douglas-fir									

Table 4.9 - Relationships between the Pacific Decadal Oscillation and the master chronologies for five species. Significant values of single monthly or seasonal PDO parameters are listed at either the 99 or 95 percent confidence interval (p-values are listed in brackets).

	99 %	99 %	95 %	95 %	95 %	95 %	95 %	95 %
Mountain hemlock	Apr (0.002)		Jun (0.029)					
Yellow-cedar	Apr (0.009)	Feb (0.003)	Mar (0.039)	Jan (0.015)	JJA (0.048)	SON (0.010)	MAM (0.048)	Jul (0.027)
Western hemlock								
Western red-cedar								
Douglas-fir								

Table 4.10 - Relationships between the Pacific North American Index and the master chronologies for five species. Significant values of single monthly or seasonal PNA parameters are listed at either the 99 or 95 percent confidence (p-values are listed in brackets).

	99 %	95 %	95 %
Mountain hemlock		JJA (0.010)	Jun (0.042)
Yellow-cedar	Jan (0.007)	JJA (0.040)	
Western hemlock			
Western red-cedar		Nov (0.018)	SON (0.040)
Douglas-fir		May (0.034)	

The index that displayed the most similarity to radial growth was the CTI. All tree species, except Douglas-fir, were related to this index over the interval 1896-1996 in some manner. Mountain hemlock showed a strong spring signal, while western red-cedar has a strong autumn/winter signal (Table 4.8). Both yellow-cedar and western hemlock have relationships significant at the 95 percent interval, with yellow-cedar s correlation being more prominent in the winter compared to western hemlock s stronger summer and autumn signals.

The PDO signal was correlated significantly with only yellow-cedar and mountain hemlock (Table 4.9). Both species have a strong relationship to April PDO values, and yellow-cedar also correlates strongly to spring, summer and autumn seasonal parameters and January, February, March, and July values. Mountain hemlock shows a strong relationship to the June index in addition to the very strong relationship to the April values. All other high-elevation species did not show any significant relationships to the

PDO index during the correlated period 1900-1996.

The PNA correlation matrix had the fewest relationships of the three indices to radial-growth of the Vancouver Island master chronologies (Table 4.10). Only yellow-cedar had a correlation to the index at the 99 percent level, and that was for the January parameter. Yellow-cedar also had a relationship significant to the PNA at the 95 percent level, in this case to the JJA seasonal parameter, and it shared this distinction with mountain hemlock. Mountain hemlock was also significantly correlated with the June monthly index values at the 95 percent confidence level. Western hemlock had no significant relationships with the PNA and western red-cedar and Douglas-fir had only one significant relationship each. Western red-cedar s relationship was with the autumn seasonal variable, while Douglas-fir s was with the May monthly index values.

4.6 Discussion

Tests of the spatial dimensions of the Vancouver Island tree-ring series reveal that there is no spatial pattern or difference in ring-width growth over the island in the montane zone. This characteristic has been constant for at least the last 500 years, and is evidence for long-term stability of the uniformitarianism principle in tree-ring response on Vancouver Island. It also suggests that if an outside regulator of climate does influence the growing conditions, all high-elevation trees are similarly affected. Years with distinguishable patterns are apparently produced by synoptic weather patterns or local extreme events that influenced radial-growth in individual years. As such, they are not likely to be part of a larger overall dominating pattern.

The process influencing radial growth on Vancouver Island is not clearly evident.

It was hoped that one mechanism could be identified as key to radial-growth across the montane zone, since the patterns had remained the same over the last 500 years. Instead, different species of trees seem to be more sensitive to different forcing mechanisms (i.e., mountain hemlock more so to the CTI and yellow-cedar more so to the PDO). Each species, therefore, must be producing cambium based on different climatic influences on their growing cycles. Each climatic affect that is linked to an oceanic mechanism must dominate the climate of Vancouver Island to varying degrees in different parts of the year or in varying degrees in different years (e.g., mountain hemlock more so to changes in spring CTI changes). Because statistically significant differences in the relationship of each species to oceanic links are detectable, a more detailed phenological investigation into the specific requirements of each tree species is needed in order to understand its connections to climate. These specific requirements are the subject of the next chapter.

5.0 Dendroecology of the Mountain Hemlock Zone on Vancouver Island

5.1 Background: Conifer Growth Characteristics

The climate/radial-growth relationship for all coniferous tree species in the Vancouver Island MH zone can be described by reference to a generalized annual cycle of growth (Figure 5.1). During the minimum photoperiod in December, trees in the MH zone are dormant and by early January achieve their maximum frost hardiness (Hawkins 1993). As conditions warm in spring and the photoperiod lengthens, dehardening processes begin (Hawkins 1993) and, for most species, continue until March, when warming temperatures and snowmelt initiate a new cycle of growth. By mid-March and early April, pollen release and fertilization are underway in most species (Owens *et al.* 1980). Infiltrating meltwater/precipitation and/or warming soil temperatures trigger a period of root growth in April, which continues for several weeks (Coleman *et al.* 1992). Bud burst and shoot elongation begin in mature trees by late April, and shoot elongation continues as the dominant growth process until early to mid-June (Owens and Molder 1984a, 1984b). Although shoot growth is typically replaced by cambium development after needle growth begins, the period when earlywood production commences is highly variable (Fritts 1976). Earlywood cell production continues for three to four weeks, starting sooner and lasting longer at lower elevations than at higher elevations. Following earlywood development, latewood cells begin to form, and the initiation and duration of this stage again vary with elevation, individual tree species, and climatic conditions. At most sites, and for most species on Vancouver Island, latewood growth continues until mid-July or mid-August (Laroque and Smith 1999, Gedalof and Smith 2001b), when tree

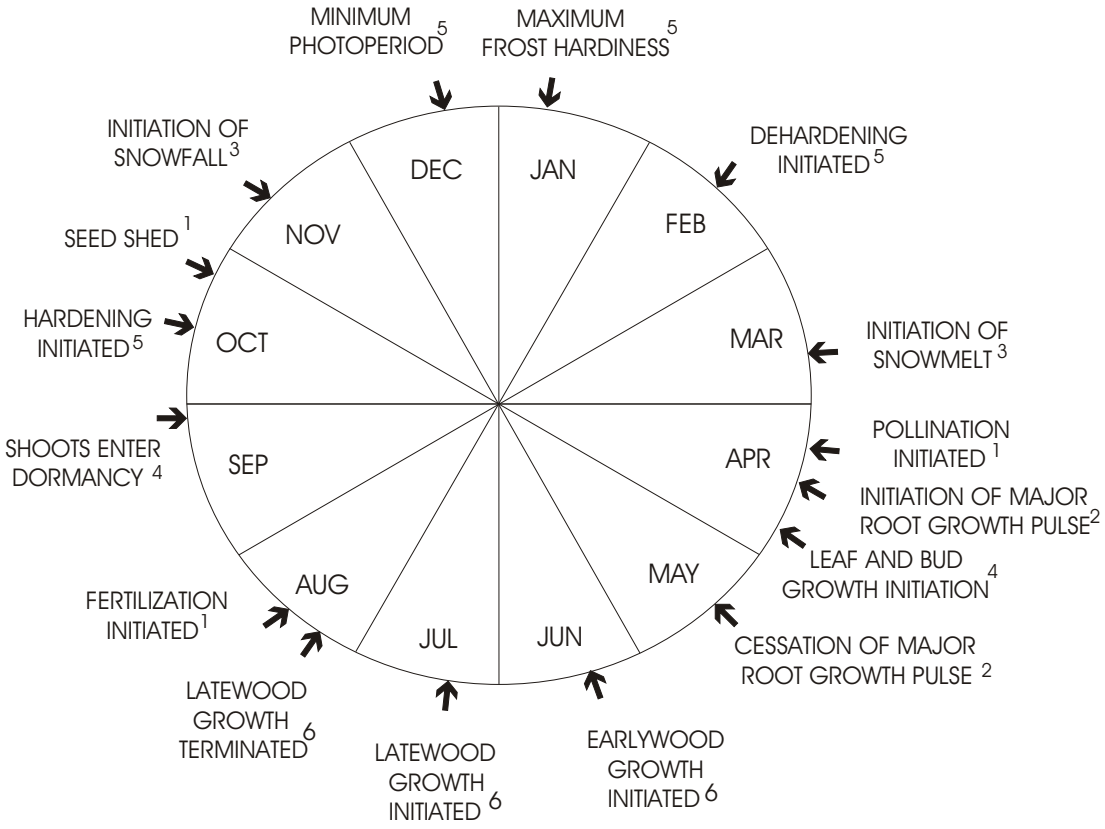

Figure 5.1 - Generalized yearly growth cycle of upper-elevation trees on Vancouver Island [1 = Owens *et al.* (1980), 2 = Coleman *et al*. (1992), 3 = Moore and McKendry (1995), 4 = Owens and Molder (1984a), 5 = Hawkins (1993), 6 = Laroque and Smith (1999) and Gedalof and Smith (2001b)].

energy is diverted into reproduction (cone development) for the following year (Owens *et al.* 1980), or into nutrient storage. This late-summer activity is followed by pre-dormancy (Owens and Molder 1984a, 1984b) and winter hardening processes in autumn (Hawkins 1993).

While this scenario outlines the general growth cycle of high-elevation trees on Vancouver Island, each tree species has its own timing and takes advantage of a particular

niche in habitat and its associated climate. In these niches individual tree species are able to either out compete or co-exist with other trees and, in doing so, may dominate or exist as a minor component of stands in a particular ecological zone.

This chapter will explore the climate/radial-growth relationship of each tree species to assess which climate parameters are important to its growth during each stage of radial growth. The chapter will first determine the significant climate parameters, and then interpret this information in relation to each tree s growth cycle.

5.2 Methods

5.2.1 PRECON Analysis

PRECON!" (Version 5.17.0, 1999) was used to recalculate matrices of climatic data using principal components analysis to form new orthogonal variables that maximize the variance in monthly climate parameters. The new orthogonal variables were then regressed with master tree-ring chronologies (Fritts *et al.* 1971). Each orthogonal variable explains successively lesser amounts of variance in the tree-ring data, and these new orthogonal variables were used in a stepwise multiple regression, a procedure that required that the predictor variables be independent (Guiot *et al.* 1982). The predictor variables were then tested for significance using a bootstrap method in PRECON (Efron 1979, Guiot 1991), which constructed a probability distribution of the predicted variables and standard error estimates. The end result of this process is that greater confidence can be placed in the predictor climate variables driving radial growth than if no cross-validation is carried out (Guiot 1990, 1991).

PRECON then uses matrix algebra to calculate which significant regression

coefficients are related to which initial monthly climate inputs. A matrix of significant variables from the bootstrapped procedure is multiplied by a principal component scores matrix (constructed from initial input variables and their eigenvector loadings), to express the significant regression coefficients into a new set of terms expressed in original climate variables rather than principal components. The output from PRECON then graphically represents the significant initial climate variables as a response function that demonstrates the calculated relationship between monthly climate variables and radial-growth (Fritts 1976).

Climate Data

Two inputs are needed for PRECON, climate data and tree-ring chronologies. This study used homogenized temperature and precipitation data available from Environment Canada from each of the five stations on Vancouver Island (http://www.cccma.bc.ec.gc.ca/hccd/data/access_data.html, accessed November 16/2001): 1) Port Alberni, 2) Quatsino, 3) Comox , 4) Nanaimo, and 5) Victoria (Environment Canada 1996, Mekis and Hogg 1999, Vincent 1998, Vincent and Gullett 1999) (Table 5.1 and Figure 5.2). Homogenization of the data was carried out by Environment Canada to adjust and correct for changes in gauge type, station movement, density and phase changes (snow to precipitation), etc. (see Mekis and Hogg 1999, Vincent 1998, Vincent and Gullett 1999 for more details). This was completed on a daily measurement scale to generate as high a quality time series for each set of station data as possible. Monthly values were calculated from the homogenized daily data, and were used in this study. In addition to the station data, snowpack data from two upper-

elevation locations on Vancouver Island were collected. The two data sets are from BC provincial snow survey sites (http://www.elp.gov.bc.ca/rib/wat/rfc/archive/historic.html, accessed November 16/2001) at Forbidden Plateau and Sno-bird Lake (Figure 5.2 and Table 5.1).

Tree-ring Chronologies

The master chronologies developed in Chapter 4 were used in the PRECON analysis. Previous research indicated that it is likely each species would have a specific climate/radial-growth signature (Smith and Laroque 1998, Laroque and Smith 1999, Gedalof and Smith 1999, Lewis and Smith 1999) and so each master chronology was tested against data from each climate station.

5.2.2 Estimating the Phenology of Wood Growth

In trying to understand which climate conditions trees reflect in their ring structures, it is important to appreciate the calendar time frame under which each grows. Normally this type of growth information is estimated by repetitive sampling at a single site throughout a growth season (Schweingruber 1996). In this study a similar type of estimate was possible by sampling throughout two complete growing seasons. At each location, all of the sampled cores were examined to estimate the stage of radial growth. The majority at each site consistently exhibited the same stage of radial-growth development.

In this way an estimated stage was assigned for each species sampled at a site and the progression of ring development followed throughout the growing season (Figure 5.3). An evaluation of radial growth stage was conducted for each of the two sampling

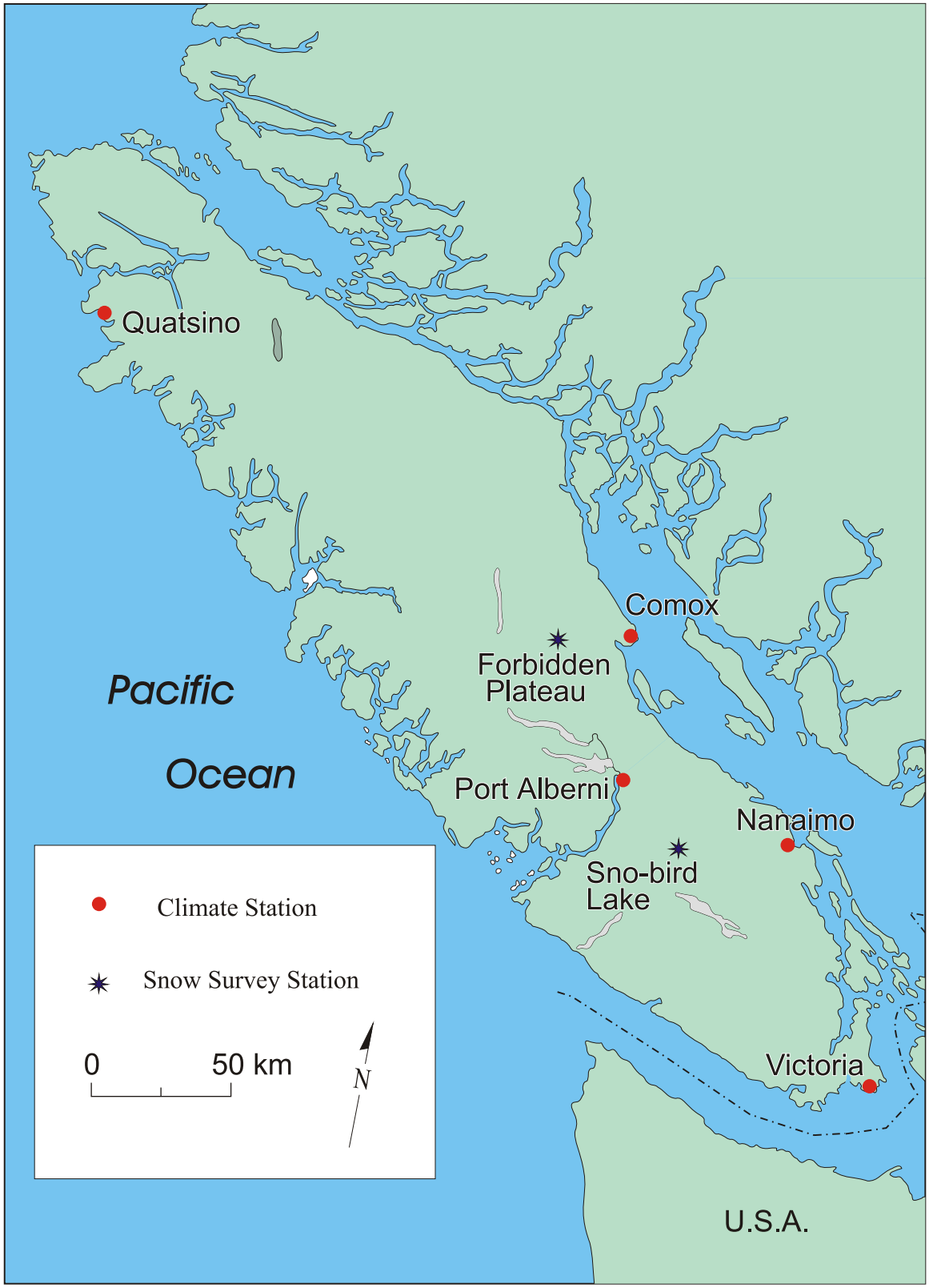

Figure 5.2 - Location of five climate stations and two snowpack stations used in this study.

Table 5.1 - The station name and number, duration of record, location and elevation of the five Vancouver Island climate stations and two montane snow survey sites from Vancouver Island.

Station Name	Station Number	Duration of Record	Latitude / Longitude	Elevation (m asl)
Port Alberni	1030180	1894-2000	49° 15' N / 124° 50' W	2
Quatsino	1036570	1895-2000	50° 32' N / 127° 39' W	8
Comox	1021830	1944-2000	49° 39' N / 124° 54' W	24
Nanaimo	1025C70	1902-2000	49° 3' N / 123° 1' W	30
Victoria Gonzales	1018620	1898-2000	48° 39' N / 123° 30' W	70
Forbidden Plateau (snow survey)	3B01	1954-2000	49° 39' N / 125° 13' W	1130
Sno-bird Lake (snow survey)	3B16	1966-2000	49° 03' N / 124° 20' W	1400

seasons. In general a similar progression in radial growth was seen, with initiation and cessation dates varying by about a week from the 1996 to 1997 season.

5.3 Results

5.3.1 Mountain Hemlock

Figure 5.4 illustrates the five response function analyses of the mountain hemlock master chronology compared to each climate station s data. The relationships are similar to those developed by Smith and Laroque (1998), Gedalof and Smith (2001b), and Lewis (2001). Approximately 65 percent of the variance in mountain hemlock growth can be

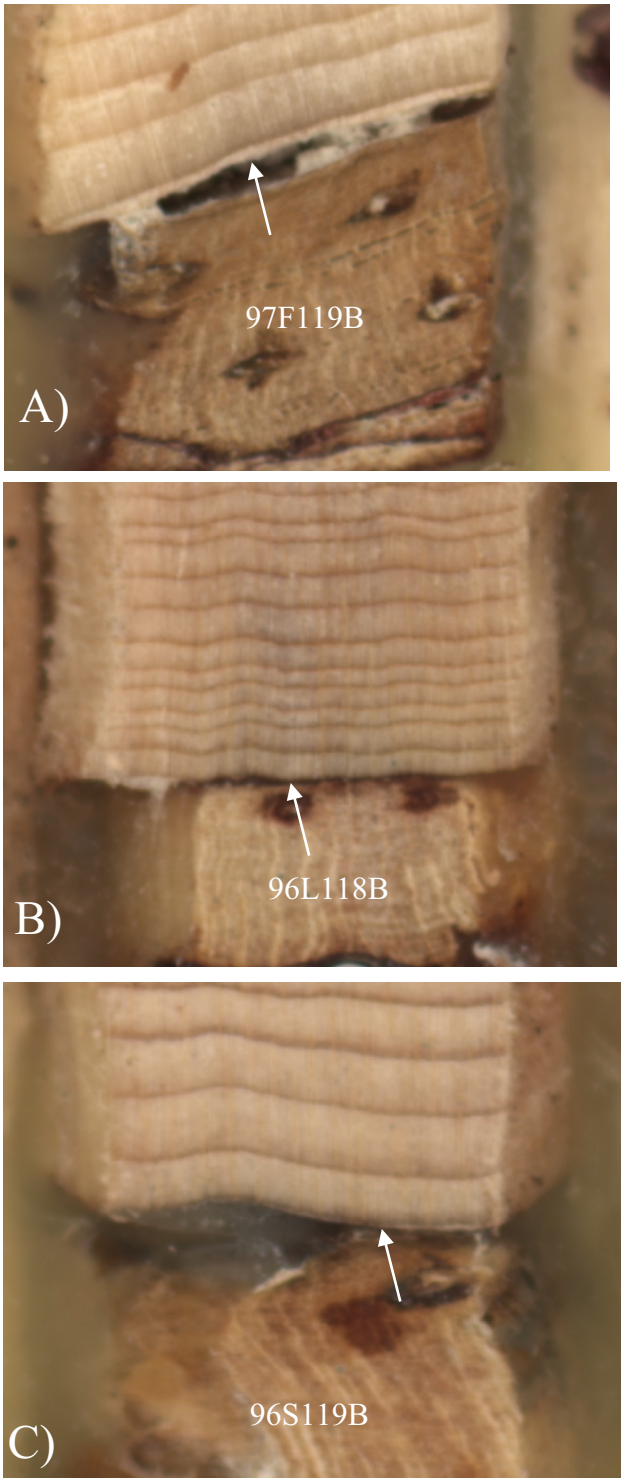

Figure 5.3 - Three yellow-cedar cores showing the extent of growth at the time of sampling. A) the arrow points to the earlywood growth on core 97F119B illustrating growing conditions early in the radial-growth season, B) the arrow points to the first cells of latewood growth on core 96L118B illustrating growing conditions mid-way through the radial-growth season, C) the arrow points to the termination of latewood growth on core 96S119B illustrating growing conditions late in the radial-growth season.

explained by climatic factors (35 %) and prior growth characteristics (30 %). The relatively high percentage of the variance explained by prior growth confirms the high autocorrelation values found by COFECHA (Table 3.1).

In general, three different climate parameters relate significantly to ring width. There is a significant positive response to growing-season temperature in the current year, a significant negative response to July temperature of the previous year, and a weaker negative response to winter precipitation. The negative relationship to the prior winter moisture signal is believed to be related to deep snowpack depths at high elevations on Vancouver Island (Smith and Laroque 1998, Gedalof and Smith 2001b, Lewis 2001).

The ecological behaviour that underlies these climate/radial-growth relationships is related to the annual growth cycle of mountain hemlock in high-elevation stands (Figure 5.5). Mountain hemlock follows the generalized upper-elevation growth scheme previously outlined, but differs from other species in the precise timing of initiation and cessation of cambium development. It was found that mountain hemlock begins to form earlywood cells by the end of the first week of June, with latewood cell development typically beginning by the end of the first week of July. By early August, the latewood cells have thickened cambial and tracheid cells, and wood-tissue growth ceases.

This yearly cycle of radial growth appears to be triggered by seasonal snowpack depth (Smith and Laroque 1998, Gedalof and Smith 2001, Klinka and Chourmouzis 2001, Lewis 2001, Peterson and Peterson 2001). In seasons with limited snowpack, earlywood growth is initiated sooner in the calendar year. As temperatures warm in late June, earlywood growth continues. The cessation of melting snowpack moisture inputs

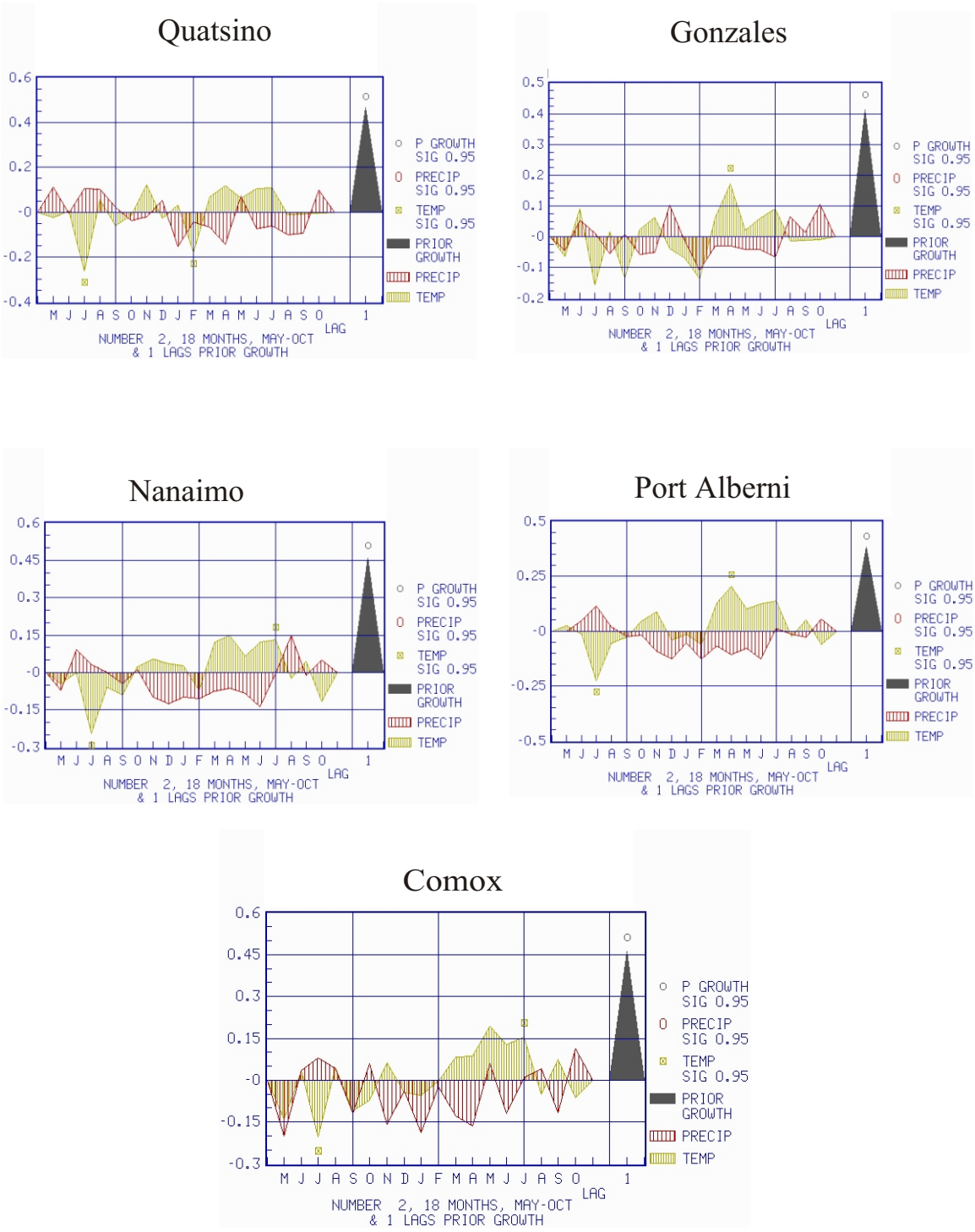

Figure 5.4 - Mountain hemlock response function analyses for the five climate stations in the study.

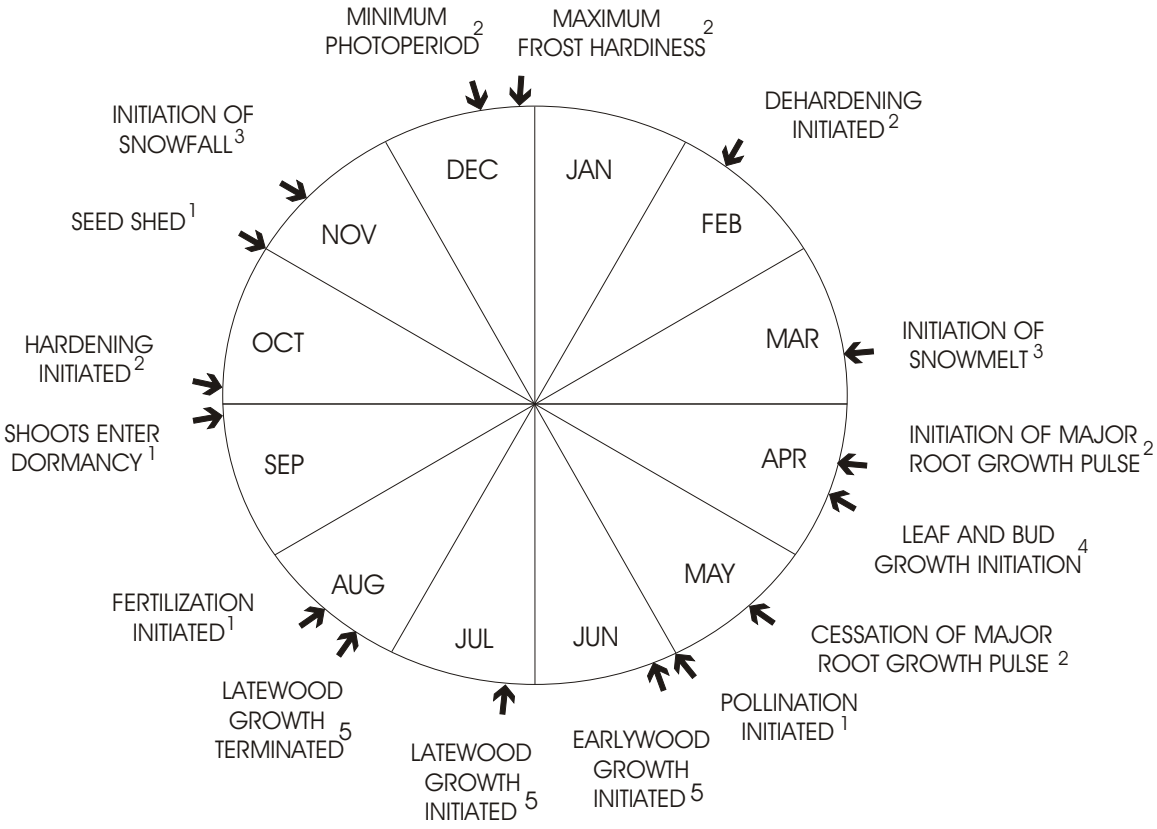

Figure 5.5 - Generalized yearly growth cycle of upper-elevation mountain hemlock on Vancouver Island [1 = Owens and Molder (1975), 2 = Coleman *et al*. (1992), 3 = Moore and McKendry (1995), 4 = Owens (1984), 5 = this study].

or the reduced photoperiod may help trigger the change of growth from earlywood to latewood. Depending on the interplay between growth inputs, the latewood-growth season continues until conditions dictate a switch in the utilization of photosynthetic products. These conditions usually occur by late July, when dominant ridges of high pressure tend to remain stable over Vancouver Island, and moisture input is at a yearly low (Klinka *et al.* 1991, Environment Canada 1996, Mekis and Hogg 1999).

The significantly correlated climate factors indicated by the response function analyses previous July temperature, spring growing-season temperatures, and winter moisture levels relate to these interpretations. Very warm temperatures in the previous July can negatively affect growth in the current year because of complex interactions with cone crops (Gedalof and Smith 2001b). Alternatively, this response could indicate an early termination of mountain hemlock radial growth resulting from moisture stress. Although unlikely in this type of environment, moisture stress at the end of the previous summer could have two effects: it could hamper proper storage of nutrients for subsequent years growth (e.g., Hale and Orcutt 1987), or it could limit or encourage root growth at the expense of above-ground growth in the fall and next spring (e.g., Pregitzer *et al.* 2000).

Response function analyses also indicate that spring temperature is important to the radial growth of mountain hemlock. Warm spring temperatures help to sustain greater radial growth during the time that earlywood production is most active. This factor has also been confirmed by other studies in the region (Heikkinen 1984, Heikkinen 1985, Smith and Laroque 1998a, Lewis and Smith 1999, Gedalof and Smith 2001a, 2001b).

Although no winter precipitation variables were shown to be significant at the 95 percent confidence interval (Figure 5.4), many individual chronologies from Vancouver Island have a significant negative relationship to winter precipitation (Smith and Laroque 1998a, Lewis and Smith 1999, Laroque *et al.* 2000/01, Gedalof and Smith 2001b). An important finding was the strong correlation between the April 1 snowpack levels at

Forbidden Plateau and the master mountain hemlock chronology ($r = -0.343$, $p < 0.025$). These results suggest that snowpack depth remains important to mountain hemlock growth, even though the response function using low-elevation precipitation data and the master chronology does not clearly exhibit this relationship.

Spring snowpack accumulation has been shown to be linked to winter moisture amounts at low elevations in other studies (Graumlich and Brubaker 1986, Smith and Laroque 1998a, Lewis and Smith 1999, Laroque *et al.* 2000/01, Gedalof and Smith 2001b). Winter snowpack accumulation at high elevations, and its consequent melt-out, have been regarded as a leading agent in initiating many of the physiological processes in mountain hemlock growth (Graumlich and Brubaker 1986, Smith and Laroque 1998a, Lewis and Smith 1999, Laroque *et al.* 2000/01, Gedalof and Smith 2001b). This may be because snowmelt and/or spring precipitation is needed to replenish soil moisture as spring growth processes are initiated (Gedalof and Smith 2001b), or because the snowpack needs to melt to permit the soil to warm to the temperatures required for optimum radial-growth (Fry and Phillips 1977, Oquist 1983, Tesky *et al.* 1984, Carter *et al.* 1987).

The dominance of the spring snowpack at high elevations on Vancouver Island can also influence growth by another means. Snowpack levels vary, from years with low to no spring snowpack accumulation (e.g., April 1 snowpack at Forbidden Plateau in 1981 = 127 cm), to others with large snowpack accumulation (e.g., April 1 snowpack at Forbidden Plateau in 1999 = 806 cm). For many trees at these elevations an 806 cm deep April 1 snowpack would mean that they are still almost completely buried at a time when

growth processes are normally initiated (Figure 5.5). Although many photosynthetic processes can occur at or near freezing soil temperatures, a lack of light reaching the needles of the buried trees, and soil temperatures well below optimum levels, would greatly hinder most above-ground growth processes (Havranek and Tranquillini 1995).

The timing of radial growth initiation depends, then, on spring snowpack depth and duration (Klinka and Chourmouzis 2001). If the depth of snow is too great, radial-growth processes are delayed. It is suspected that when the snowpack depth is lower than average, growth processes will occur earlier than normal (Klinka and Chourmouzis 2001). If this is true, and if the initiation of the growing cycle time frame fluctuates in anomalous snowpack years, then in these years radial-growth processes that follow initiation will also be altered.

Mountain hemlock radial growth is also significantly influenced by growing-season temperature. The temperature signal associated with radial growth also potentially varies in years of extreme snowpack events. In years of a high snowpack, radial growth would be delayed until later in the season, when normal processes could be initiated after snowmelt. In years such as these, the radial growth of mountain hemlock would still capture a temperature signal, but the interval in the calendar year that influence on growth would occur later in the growth season. Similarly, in years of an extremely low snowpack, all growth processes would be pushed closer to the beginning of the year and would again offset the calendar dates of the temperature signal captured. In this manner, mountain hemlock trees might contain some May, June, July, and potentially August temperature signals in their ring structures in anomalous snowpack years. This naturally

occurring shift in the growth season can add unwanted noise to a reconstructed climate signal particularly when reconstructing a single monthly variable.

5.3.2 Yellow-cedar

The climate/radial-growth relationship for yellow-cedar indicates that approximately 62 percent of the annual variance in radial growth can be explained by climatic factors (24 %) and prior growth characteristics (38 %) (Figure 5.6). The high percentage of the variance explained by prior growth confirms the significance of the previous year s growth and the high autocorrelation values found in previous analyses (Table 3.2, Laroque 1995).

Three different temperature variables and a precipitation variable were consistently shown to significantly influence radial growth. Yellow-cedar ring widths respond positively to warm growing season air temperatures, but negatively to warm August air temperatures in the current year (Figure 5.6). They also consistently show a positive response to warm previous October temperatures (Figure 5.6).

The physiological behaviour that underlies these climate/radial-growth relationships is related to the annual growth cycle of high-elevation yellow-cedar trees (Figure 5.7). Observations made during this study suggest that earlywood cell production generally begins in late June. Earlywood activity continues for three to four weeks until mid-July, after which latewood cell development begins. Latewood cells continue to be produced until mid-August, when reproductive processes divert tree energy from ring growth (Owens *et al.* 1980). It seems possible that the cessation of radial growth could be initiated by an increase in late July and early August air temperatures, or it could be

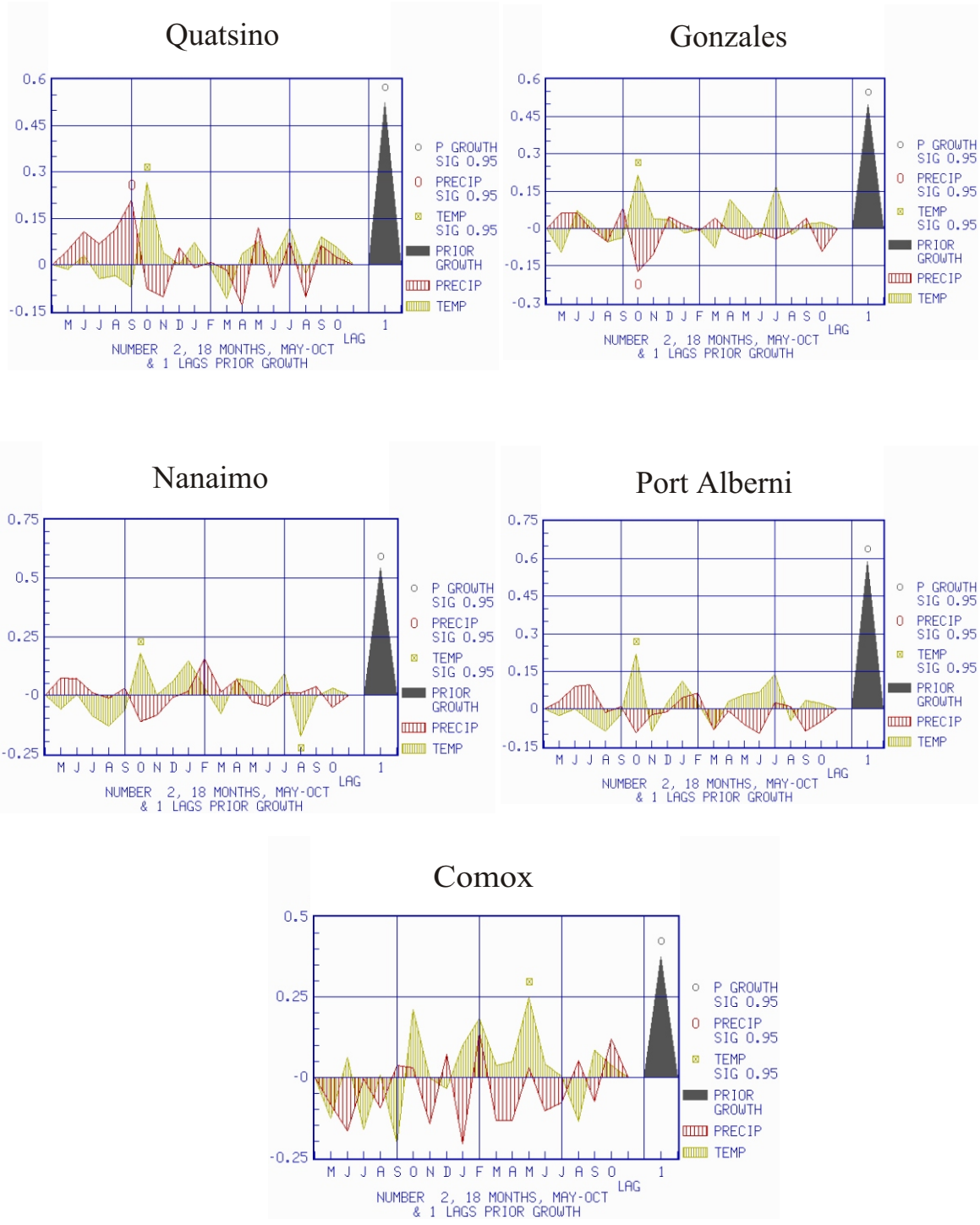

Figure 5.6- Yellow-cedar response function analyses for the five climate stations in the study.

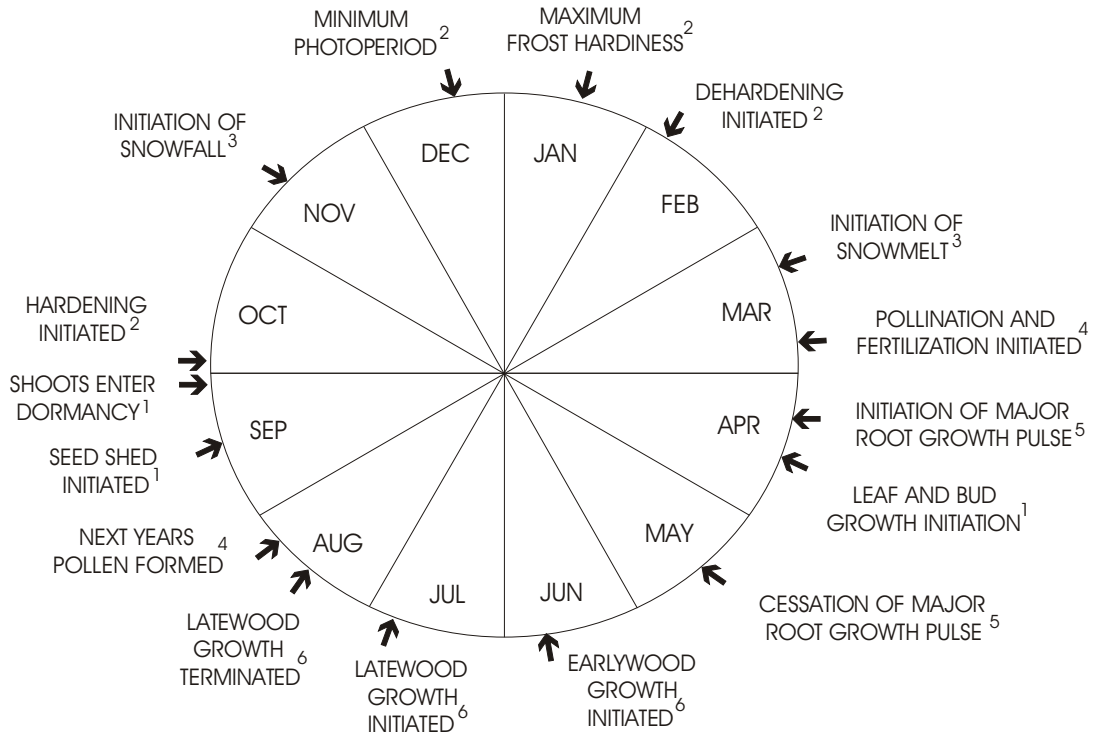

Figure 5.7 - Generalized yearly growth cycle of upper-elevation yellow-cedar on Vancouver Island [1 = Owens and Molder (1974a), 2 = Hawkins (19920, 3 = Moore and McKendry (1995), 4 = Owens *et al*. (1980), 5 = Coleman *et al*. (1992), 6 = this study]. Note: root growth is estimated from Coleman *et al.* (1992).

because of changes in the photoperiod.

The positive radial response to summer growing season air temperature presumably signifies an extension of the earlywood growth season and the delay of latewood production (Laroque and Smith 1999). Higher August air temperatures appear to stress yellow-cedar, bringing on latewood growth earlier than normal and ceasing radial growth shortly thereafter. If air temperatures are too high in August it negatively impacts radial growth, presumably by a reduction in soil moisture (Grossnickle and

Russell 1991). Finally, the significant positive relationship to temperature in the previous October is likely related to the enhanced ability of yellow-cedar to store photosynthate essential for radial growth in the following year.

A key point in the yellow-cedar radial-growth cycle is that it lags behind the rapid spring initiation and radial growth in mountain hemlock. Although yellow-cedar growth processes are active in early spring at the same time as those of mountain hemlock, wood production begins later in the growing season. This lag in cambium development suggests yellow-cedar makes a better candidate for capturing a late-season temperature signal.

5.3.3 Western Hemlock

The five response function analyses for western hemlock are presented in Figure 5.8. The relationships indicate that on average 68 percent of the annual variance in western hemlock growth can be explained by climatic factors and prior growth characteristics. Approximately 20 percent of the variance is explained by climate conditions in the current growth year, with 48 percent explained by growth in the prior growing season. As with the other species sampled, the high explained variance by the previous season s growth is expected due to high autocorrelation values recorded for the species (Table 3.3).

Two climate variables from the previous growing season are the only consistently significant variables. Western hemlock radial growth exhibits a positive response to August precipitation in the previous year and a negative response to the previous year s July temperature. April temperature is the only variable from the current growing season found to be significant or approach the 95 percent significance level in the PRECON

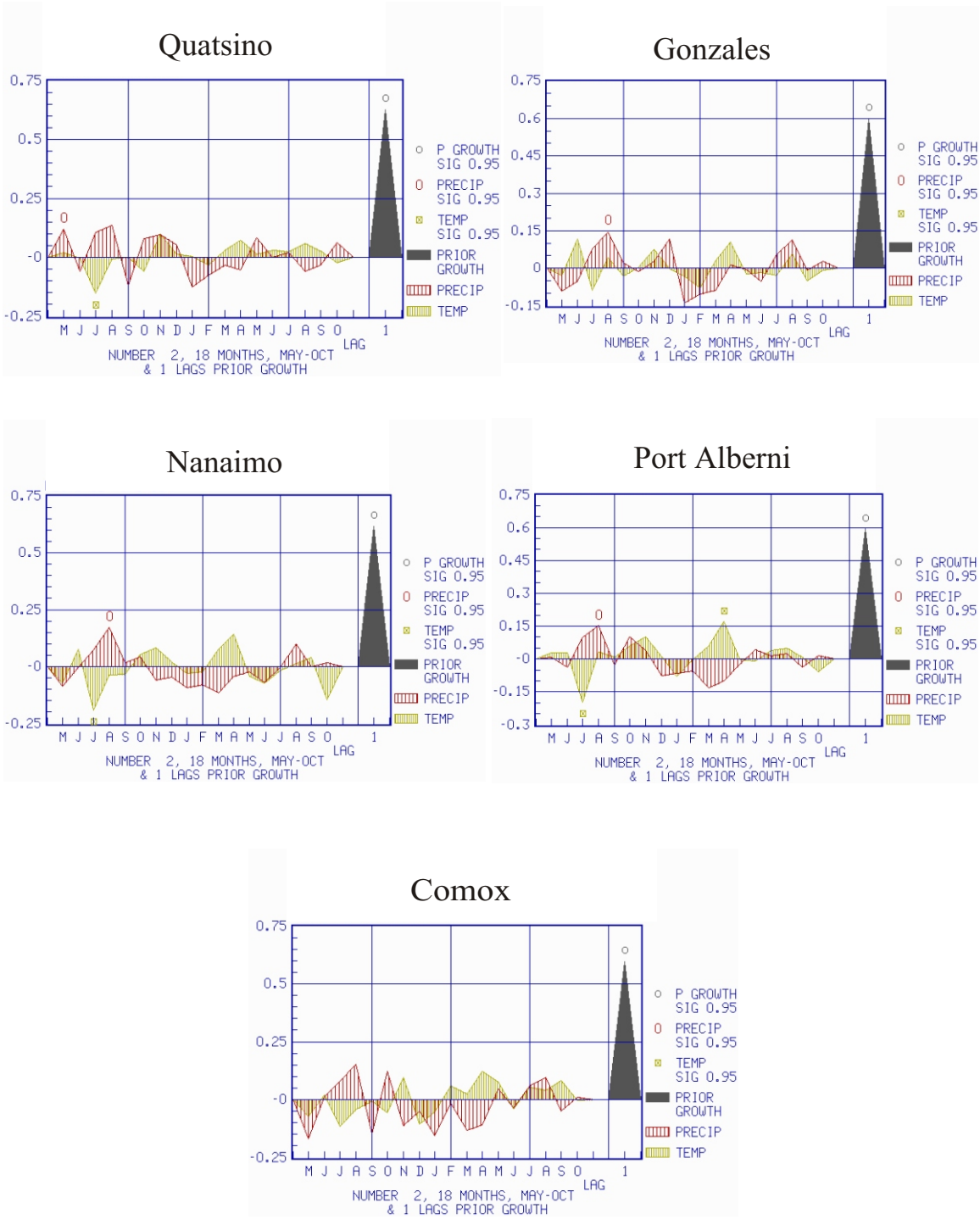

Figure 5.8- Western hemlock response function analyses for the five climate stations in the study.

response function tests.

The generalized model for the growth cycle of high-elevation western hemlock is presented in Figure 5.9. Previous research has established that western hemlock leaf growth commences in early July (Owens and Molder 1973). During the course of this study, it was found that western hemlock did not begin to produce earlywood cells until a similar time. Because of the late start in the growth of woody tissue, the highest elevation western hemlock seem to have a relatively short growing season. By early August either a combination of a lack of soil moisture and high air temperatures or changes in the photoperiod initiate the cessation of latewood growth which occurs by mid-August.

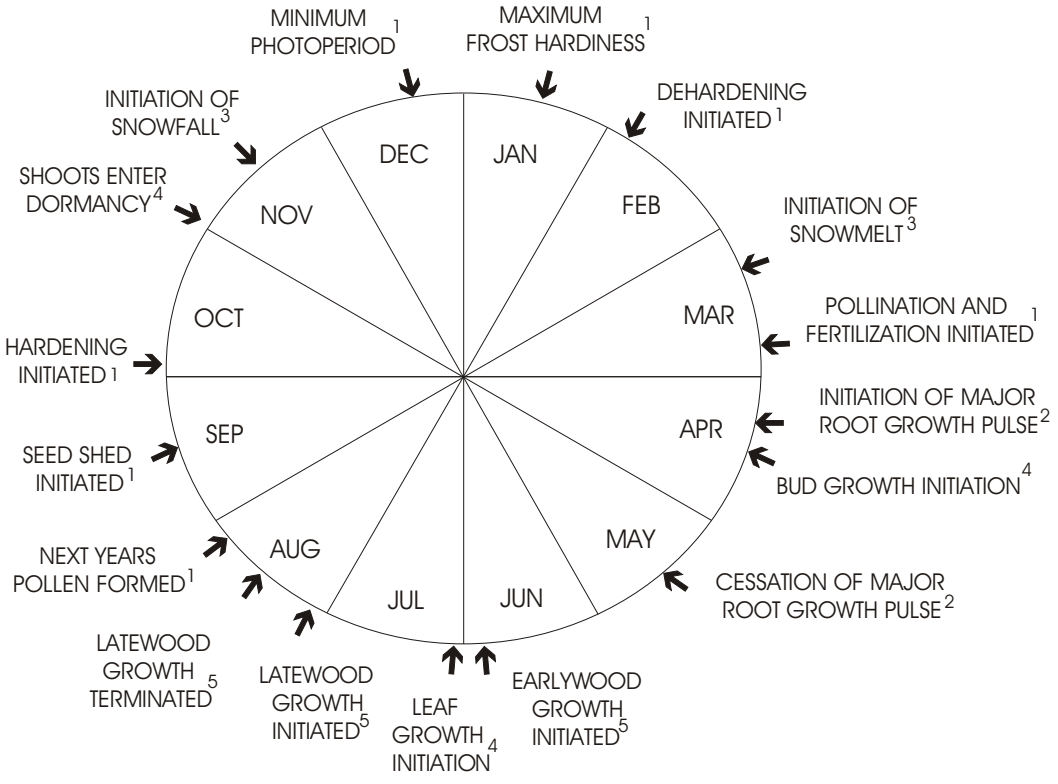

Figure 5.9 - Generalized yearly growth cycle of upper-elevation western hemlock on Vancouver Island [1 = Owens and Molder (1974b), 2 = Coleman *et al*. (1992), 3 = Moore and McKendry (1995), 4 = Owens and Molder (1973), 5 = this study]. Note: hardening and dehardening are adjusted for elevation differences from reported study, and root growth is estimated from Coleman *et al*. (1992).

Unlike mountain hemlock and yellow-cedar, western hemlock does not appear to be able to take full advantage of the short growing season. The response function analyses indicate that conditions in the previous summer are the most important to western hemlock growth in the current year. Proper needle enlargement may not be possible during short growing seasons, which in turn may limit a tree s ability to maximize fall nutrient storage for next year s growth (Margolis *et al.* 1995). This process is common in arid-site *Pinus* species, where needles are often grown mid-season and become a source of new energy only near the end of a growth season (Fritts 1976).

For western hemlock, if the previous year s growing conditions were wetter than normal in August, the extra available moisture, combined with the normally warm air temperatures of late summer, supports the full new needle development needed for growth in the following year. If the previous summer has warm air temperatures but is drier than normal, the lack of moisture in the shallow soils of the montane zone may prevent western hemlock from fully developing new needles.

The variable of current year s spring temperature is significant only at one location. The tendency, however, of the variable towards significance in all other response functions suggests that it is somewhat important to the radial growth of western hemlock (Figure 5.8). Positive spring temperatures likely melt snow sooner and raise the soil temperature, encouraging growth processes to begin earlier in the current growth season, thereby lengthening the overall growing season for the species.

5.3.4 Western Red-cedar

Western red-cedar produced three significant relationships in the response

function analyses (Figure 5.10). On average, growth in the previous year has almost twice the importance in explaining the variance of tree growth (42 %) as the present year s climate (27 %), a finding consistent with its high autocorrelation in Table 3.3.

Current and previous year summer moisture are both positively related to the radial growth of western red-cedar. Of significance are positive relationships to prior July precipitation and a negative relationship to prior July temperature (Figure 5.10). The same type of effect is seen with current June temperatures conditions, with western red-cedar s radial growth increasing if moisture levels are high and air temperatures are low. These factors give western red-cedar a response function more similar to that of western hemlock than to other species. Western red-cedar radial growth is also enhanced by high prior autumn temperatures. Warmer temperatures at this time of the year likely allow for a lengthened period of nutrient storage and uptake for the following year s growth.

The yearly cambial development cycle of western red-cedar closely follows that of yellow-cedar (Figure 5.11). At one site, earlywood growth commenced in late June, and at the other site, latewood growth had begun by late July. No data are available to indicate when western red-cedar ceases latewood cell production at high elevations.

5.3.5 Douglas-fir

Results from the Douglas-fir response functions indicate that, not just one but two years of prior growth are significant for radial growth in the current year (Figure 5.12). This result differs from studies of Douglas-fir at low-elevations on Vancouver Island, in which four years significance was found (Zhang 1996). The response functions indicate that prior years growth has more effect on current growing conditions than does the

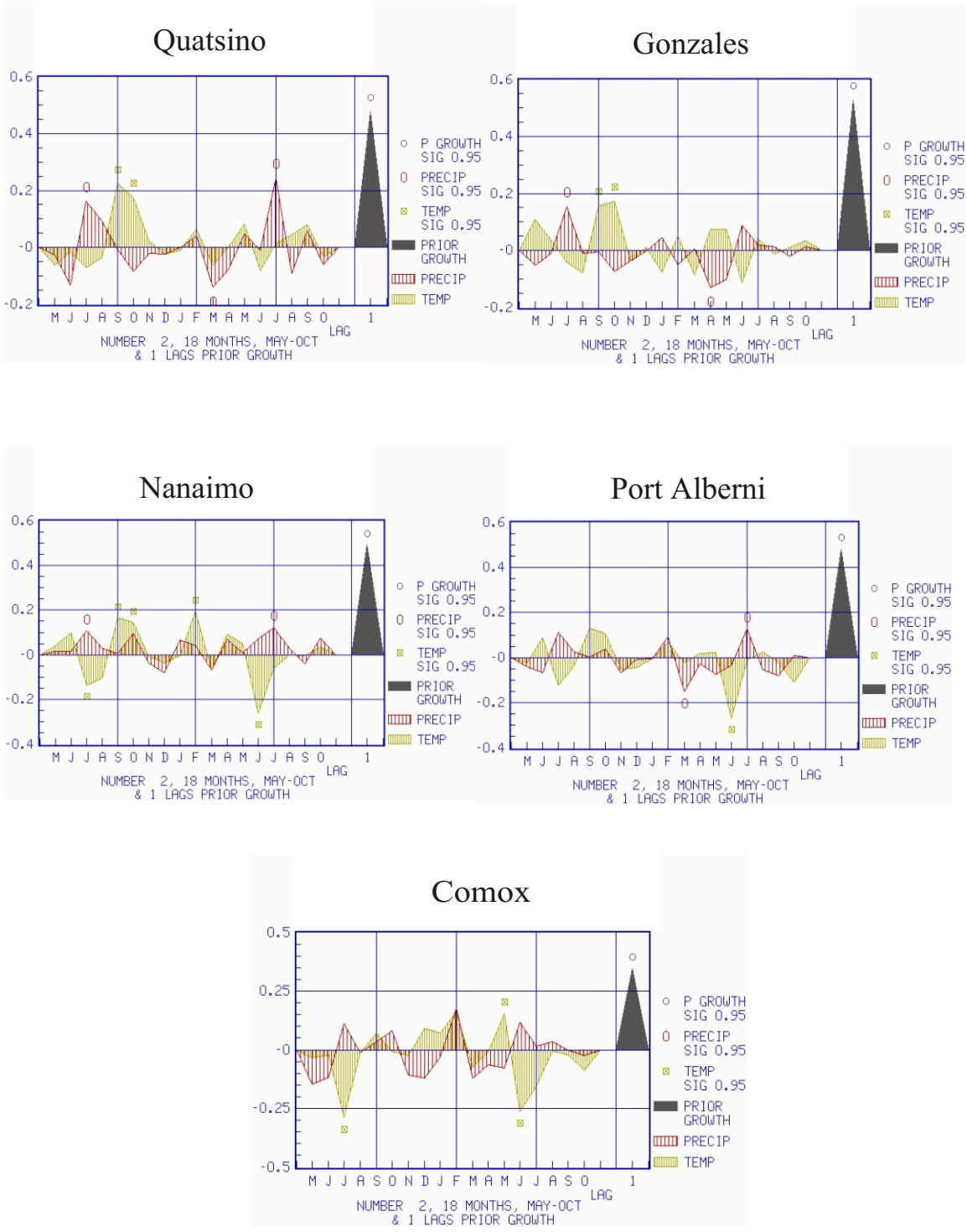

Figure 5.10 - Western red-cedar response function analyses for the five climate stations in the study.

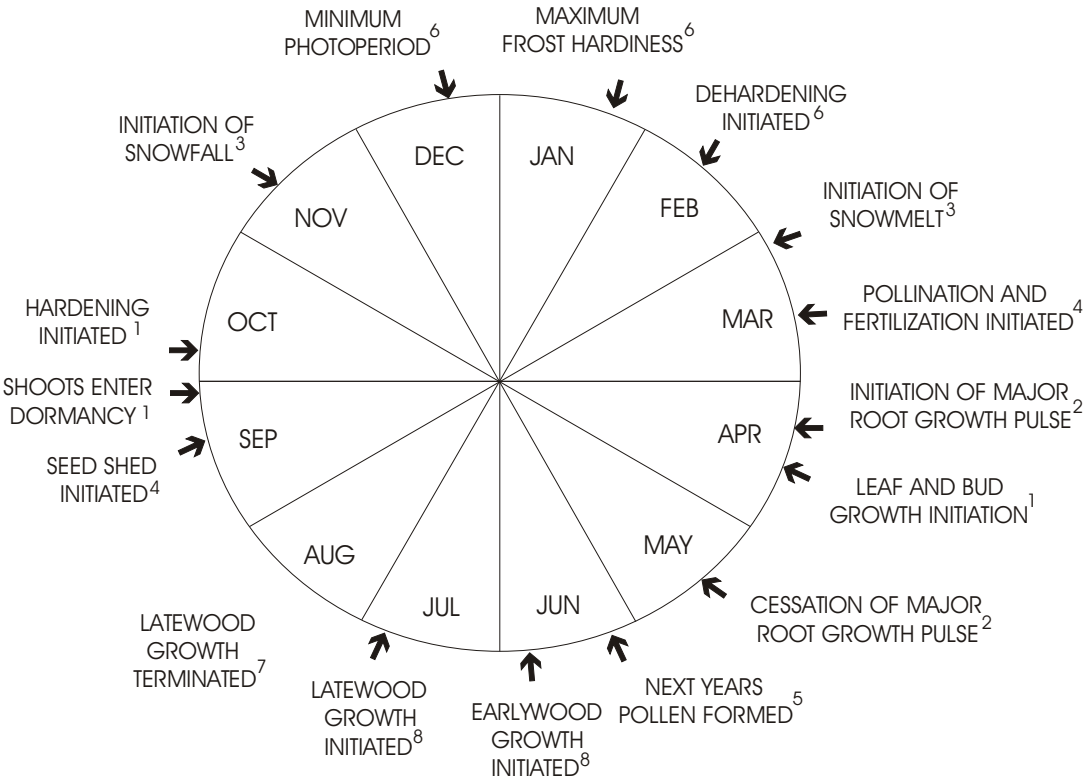

Figure 5.11 - Average yearly growth cycle of upper-elevation western red-cedar on Vancouver Island [1 = Owens and Molder (1984b), 2 = Coleman *et al*. (1992), 3 = Moore and McKendry (1995), 4 = Owens and Molder (1980), 5 = Owens and Pharis (1971), 6 = Silim and Lavender (1994), 7 = unknown, 8 = this study]. Note: root growth is estimated from Coleman *et al.* (1992).

current year's climate conditions. The master chronology explained approximately 64 percent of the variance, with previous growth years accounting for 42 percent of the explained variance and current year only 20 percent. Again this result agrees with the high autocorrelation values found with Douglas-fir (Table 3.3). The most common significant variables were positive relationships to previous spring and summer precipitation (Figure 5.12). Both current and previous years' autumn precipitation were also close to reaching a positive relationship at the 95 percent significance level.

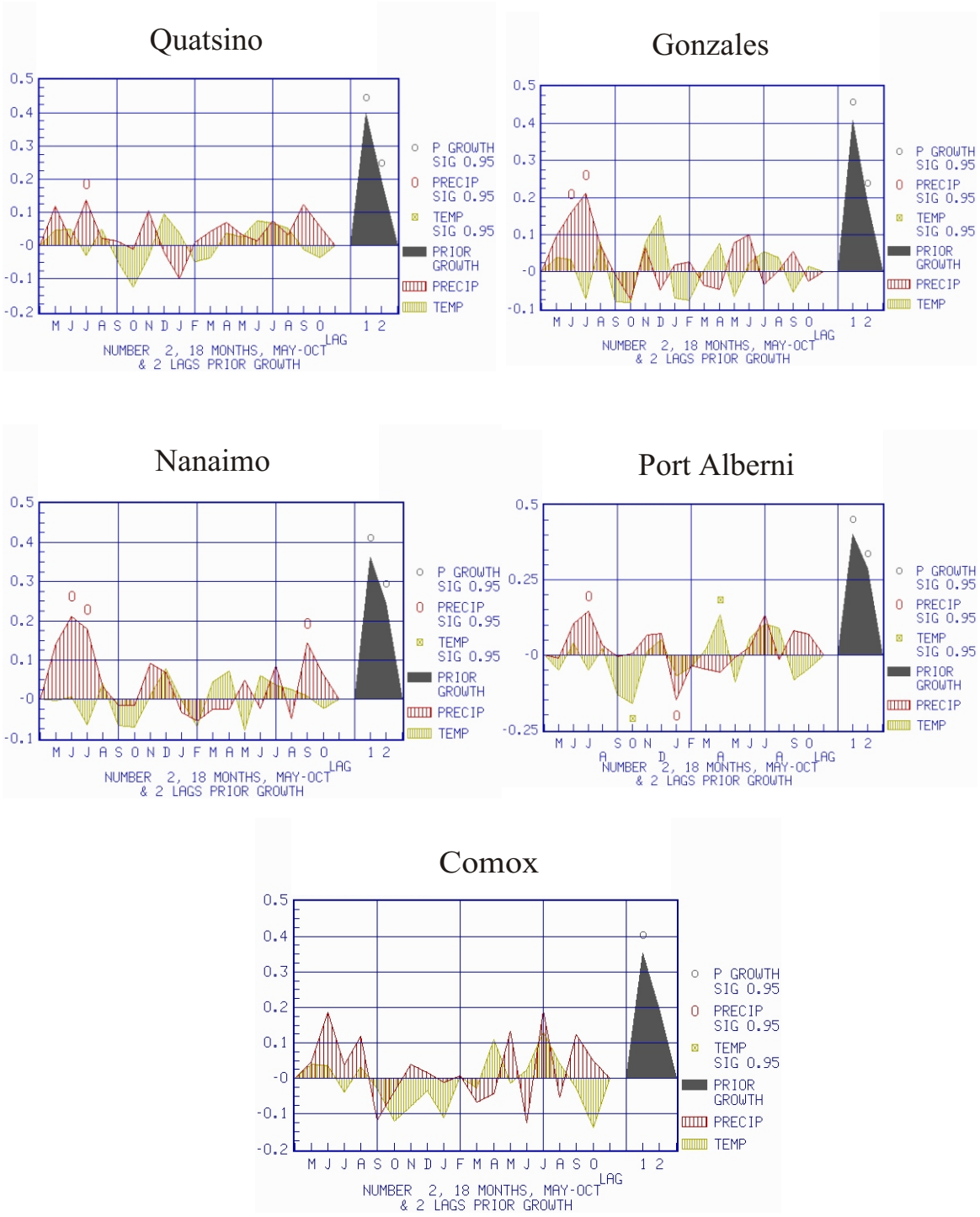

Figure 5.12 - Douglas-fir response function analyses for the five climate stations in the study.

The yearly growth cycle of Douglas-fir at low and mid-elevations is well documented (Allen and Owens 1972, Owens 1973), but no information is available for high-elevation studies. Figure 5.13 describes the growth processes as established by other researchers. In this study, earlywood growth was not documented until about mid-June for trees from one of the two sites. This is significantly different from observations made at approximately 800 m asl (end of May) (Livingston and Spittlehouse 1996) and sea level sites (beginning of May) (Rensing and Owens 1994). Similarly the transition from earlywood to latewood growth occurs later in the season in this study (end of July) compared with a mid-elevation study (mid-June to mid-July) (Livingston and Spittlehouse 1996) and one for sea-level Douglas-fir (mid-July) (Rensing and Owens 1994). The cessation of latewood growth at an upper-elevation location was not documented in this study but is estimated based on related Douglas-fir studies. Just as initiation of growth was delayed in high-elevation areas owing to the shorter growing season, it is estimated to cease earlier in the season too. Latewood growth was over by the end of August at mid-elevation (Livingston and Spittlehouse 1996) and sea-level sites (Rensing and Owens 1994).

Douglas-fir radial growth is positively influenced by a moist soil environment in spring and summer, as shown by the positive growth relationship to precipitation in the response function. This finding is consistent with four previous studies (McMinn 1960, Robertson *et al.* 1990, Livingstone and Spittlehouse 1996, Zhang *et al.* 2000). The positive relationship to late summer moisture in the current year can be explained by the maturation of the current year s needles, which provide a positive source of energy for

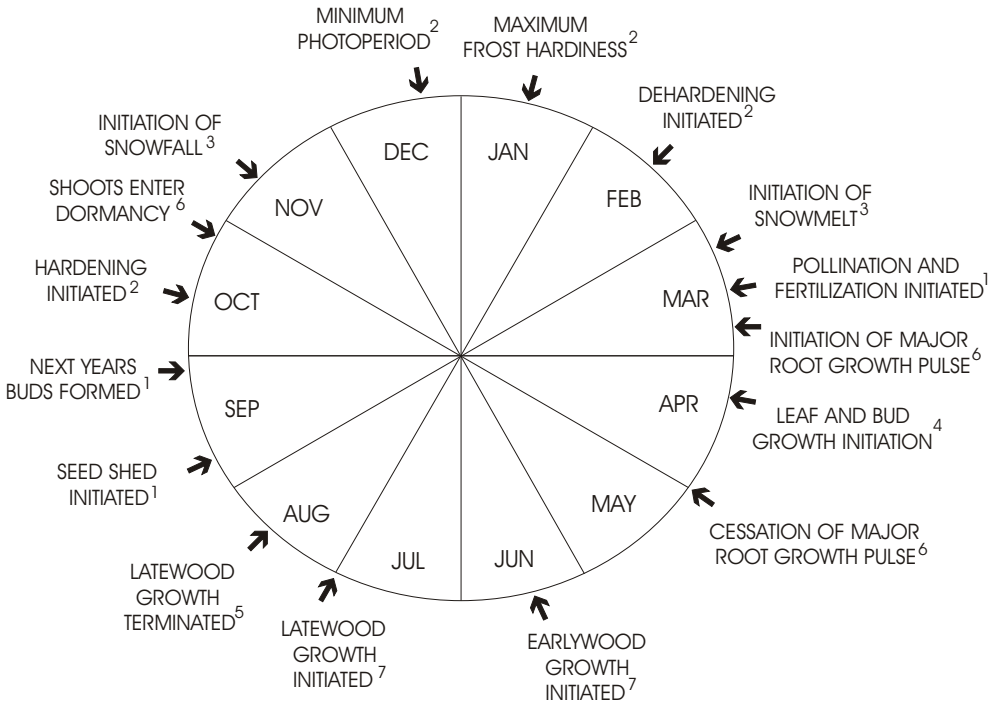

Figure 5.13 - Generalized yearly growth cycle of upper-elevation Douglas-fir on Vancouver Island [1 = Allen and Owens (1972), 2 = van den Driessche (1969) , 3 = Moore and McKendry (1995), 4 = Owens (1968), 5 = Livingston and Spittlehouse (1996), 6 = Fielder and Owens (1989), 7 = this study]. Note: termination of latewood is adjusted for elevation differences from Livingston and Spittlehouse (1996).

wood growth in the following year (Margolis *et al.* 1995). The positive relationship to current-year September precipitation is common for Douglas-fir. This is most likely the case because late-season moisture helps the tree prepare for winter dormancy, thereby allowing it to thicken cambial and tracheid cell walls and build up food reserves for the next year's growth (Rensing and Owens 1994).

5.4 Discussion

The findings of these dendroecological investigations shed light on the ability of upper-elevation trees to incorporate climatic information from their environment.

Although subjected to similar climate conditions, the different tree species from this region grow independently in reaction to environmental inputs on their own phenological schedule. Figure 5.14 shows a summary of the timing of radial growth for the five tree species, with dashed lines indicating that this timing has some variation in terms of the initiation and cessation of the tissue-forming processes in any given year. It is apparent that no species growth period begins or ends exactly on a calendar time boundary. For this reason, dendroclimatic analyses of individual tree species be less able to reconstruct monthly parameters without an additional measure to adjust for the missing portion of time in the given month. Added to this problem, is the fact that spring growth phenology for each tree species may be influenced annually by the melting of the highly variable spring snowpack. This variability in initiation and cessation of growth increases noise levels in climate/radial-growth relationships.

With the variation in timing of the onset and cessation of radial growth, a poor representation of monthly climate parameters is expected when compared to seasonally reconstructed climate parameters. The few seasonal reconstructions that have been assembled are better at explaining climatic variance than studies that have tried to reconstruct individual monthly parameters (e.g., Zhang 1996 vs. Laroque 1995). This is because seasonal parameters such as spring precipitation comprise multiple single-month parameters (e.g., spring = March + April + May), and in doing so encompass a larger amount of this natural variability. A wide enough calendar-defined season may more completely capture much of the tree-time spring growth. Unfortunately, it also captures other noise, resulting in a climate/radial-growth relationship that never grows exceedingly

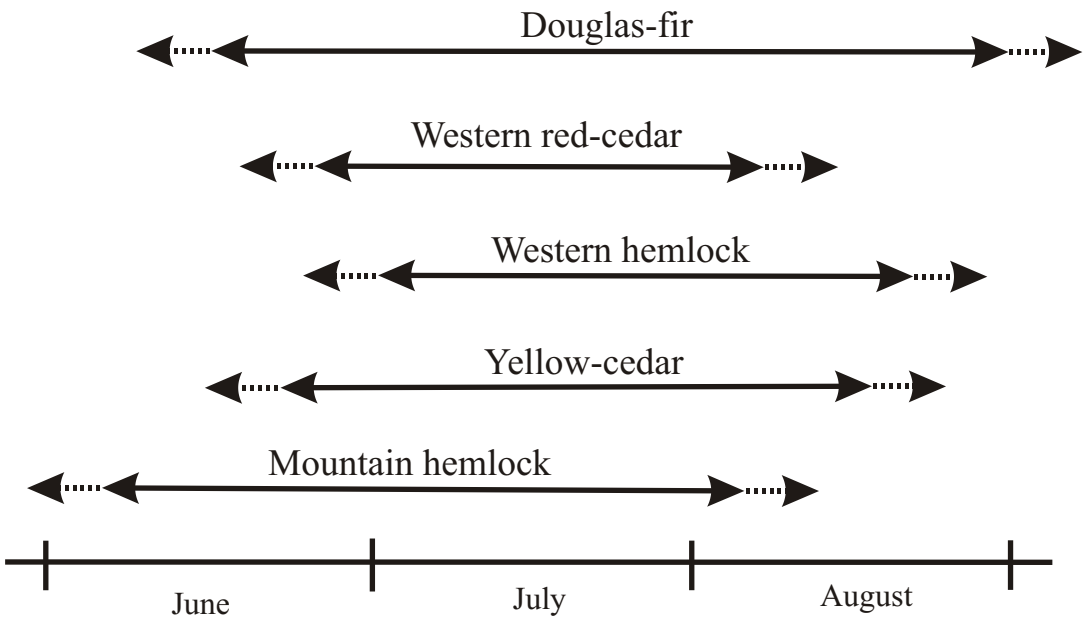

Figure 5.14 - The schematic presentation of the time period of radial growth for each species at high elevation on Vancouver Island. The dashed lines indicate the seasonally variable nature of initiation and cessation of xylem production in a growth year.

strong, and may not be particularly useful for climate reconstructions.

Trees in high-elevation settings on Vancouver Island do not have broad seasons of radial growth. Instead they have short growing windows (5-7 weeks) that can shorten or lengthen depending upon the climate in a given year. The insights into the complexities of each radial-growth/climate relationship gained in this chapter, provide the basis for developing a multiple-species approach to climate reconstruction in the next.

6.0 Multiple Aggregate Chronologies

6.1 Introduction

Multiple aggregate chronologies (MACs) are combined tree-ring series constructed in order to better model specific climate parameters. The proposed method strengthens a targeted signal and lessens unwanted noise by using *a priori* assumptions that are based on annual tree-growth cycles and climate/radial-growth relationships established in Chapter 5. These relationships are used to determine which indices should be aggregated to produce a stronger relationship with the targeted climate parameter.

MACs are simple mathematical additions of two or more single-species indices intended to form a new aggregate chronology. The MAC derives a simple linear function that has advantages over multiple regression or PCA analyses because it does not have as many required conditions upon its data (e.g., independence of multiple variables or uniform length of samples)(Fritts 1976, Fritts *et al.* 1990, Fritts 1991).

A priori assessments of species were conducted to target the reconstruction of four climate parameters and then the appropriate chronologies were aggregated to assess the range of possible relationships to climate. The methods and results are described below.

6.2 Methods

6.2.1 April 1 Snowpack Aggregates

As was shown in Chapter 5, snow depth is an important ecological parameter on Vancouver Island. It influences radial growth and plays an important role in the phenology of the spring growing season. The negative association of mountain hemlock radial growth with winter precipitation at high elevations is thought to provide insight

into spring snowpack depths (Smith and Laroque 1998a, Lewis and Smith 2000, Gedalof and Smith 2001b). The other species that indicated an association with snowpack was Douglas-fir. Like mountain hemlock, Douglas-fir does not demonstrate a clear relationship to spring snowpack depth *per se*, but the negative association with autumn and early spring moisture conditions bears a statistical relationship to the amount of snow accumulated by April 1 at high elevations. The assumption is that together mountain hemlock and Douglas-fir provide a stronger negative growth signal that reflects precipitation from autumn through spring, and so by proxy, spring snowpack accumulation. Since each species incorporates this signal differently, together they should produce a better indication of year to year April 1 snowpack variation than each does alone.

6.2.2 June-July Temperature Aggregates

The mountain hemlock response functions in Figure 5.4 show that summer growing season temperatures play a significant positive role in encouraging radial-growth. Mountain hemlock indices, then, should provide insight into the average June-July temperatures. In contrast, western red-cedar radial growth is negatively affected by higher growing season temperatures (Figure 5.10). By aggregating the two radial-growth indices, (mountain hemlock + [negative] western red-cedar), a better proxy record of average June-July temperature should result than either species defines alone.

6.2.3 July Precipitation Aggregates

Whereas radial growth of mountain hemlock relates negatively to July precipitation (Figure 5.4), western red-cedar has greater radial growth in summers with

larger amounts of moisture (Figure 5.10). By combining the two indices together to enhance the targeted July precipitation, the aggregated index should better represent stronger negative associations to the overall climate signal.

6.2.4 July Temperature Aggregates

This study shows that the radial growth of both mountain hemlock and yellow-cedar are positively related to July air temperature. Mountain hemlock consistently initiates radial growth early in the growing season and thus serves to capture an early-July temperature signal (Figure 5.4). On the other hand, yellow-cedar incorporates a late-July temperature signal into its ring structure (Figure 5.6). When years of earlier and later initiation of growth occur, aggregated mountain hemlock and yellow-cedar indices will better overlap the calendar date of July. The aggregated index should serve to capture more of the overall variation of a July temperature signal than each species would individually.

6.2.5 General Analysis Procedures

A series of MACs were developed to test the range of possible relationships to climate that the new aggregates formed. For the primary species in each test, all of the available single-species indices were selected as well as the master chronology. Aggregated to each of these indices was the most strongly correlated secondary species chronology, the least strongly correlated secondary species chronology and the master secondary species chronology to create three new sets of MACs. Climate data from Nanaimo and snow survey station from the Forbidden Plateau station (April 1 snow accumulation data) were selected. Collectively they are of long duration and explain a

large amount of the variance for the five stations tested (Table 6.1). The Comox station data generally has a higher r^2 value to the master chronologies than the other climate stations (Table 6.1), but its shorter record makes the significance level harder to attain. The longer duration of record also allows for more data with which to calibrate and verify reconstruction models. MACs were aggregated according to the parameters stipulated above and correlation matrices were then calculated between each set of constructed MACs and the targeted climate parameters.

Table 6.1 - The explained variance (r^2) values of each master tree species index to each climate station. The data is from the response function analysis tests in Chapter 5.0.

	Comox*	Nanaimo	Victoria	Port Alberni	Quatsino
Mountain hemlock	0.74	0.63	0.45	0.66	0.66
Yellow-cedar	0.70	0.62	0.60	0.63	0.68
Western hemlock	0.80	0.68	0.63	0.67	0.67
Western red-cedar	0.80	0.72	0.63	0.66	0.69
Douglas-fir	0.60	0.65	0.64	0.63	0.54

* Note that all station data is 95 years, except the Comox record which is only 55 years.

6.3 Results

6.3.1 April 1 Snowpack

The longest continuous period of upper-elevation snowpack information on Vancouver Island is from the Forbidden Plateau site near Mt. Becher (Figure 5.2). Pearson s correlations between the April 1 snowpack depth and 35 mountain hemlock

indices and the master mountain hemlock chronology were tested for their normality. Figure 6.1a illustrates that the correlation coefficients are organized in an approximate normal distribution. Although only 35 sites and the mean could be tested, this number of sites is high for a regional dendroclimatological study. The correlations between the snow depths and the indices show that most of the correlations for the mountain hemlock indices are negative, but that the range is large (0.14 to -0.59). Correlation of the master chronology to snowpack depth was found to be -0.34, on the higher end of the range of the correlations in the analysis (Figure 6.1a).

A histogram of correlations for Douglas-fir and April 1 snowpack depth was not constructed given that there are only two high-elevation Douglas-fir indices from this study, as well as two low-elevation chronologies from the Victoria area (DND = Smith and Lewis 1996, Heal Lake = Zhang 1996). A master index was calculated for the two high-elevation indices, as well as for the two indices from low-elevation. The range of correlations for all of the Douglas-fir indices was from 0.16 to -0.43. As with the mountain hemlock, the correlations were skewed towards negative relationships. The overall average from all Douglas-fir indices was correlated at -0.29.

MACs were created by adding the index values for each mountain hemlock chronology to, first the overall Douglas-fir master chronology, second, to the most strongly correlated Douglas-fir chronology in the test (Heal Lake = -0.47), and, third to the most weakly correlated Douglas-fir chronology in the test (DND = 0.16). The three types of MACs constructed (one constructed with all mountain hemlock indices and the overall Douglas-fir master index, and one constructed with all mountain hemlock indices

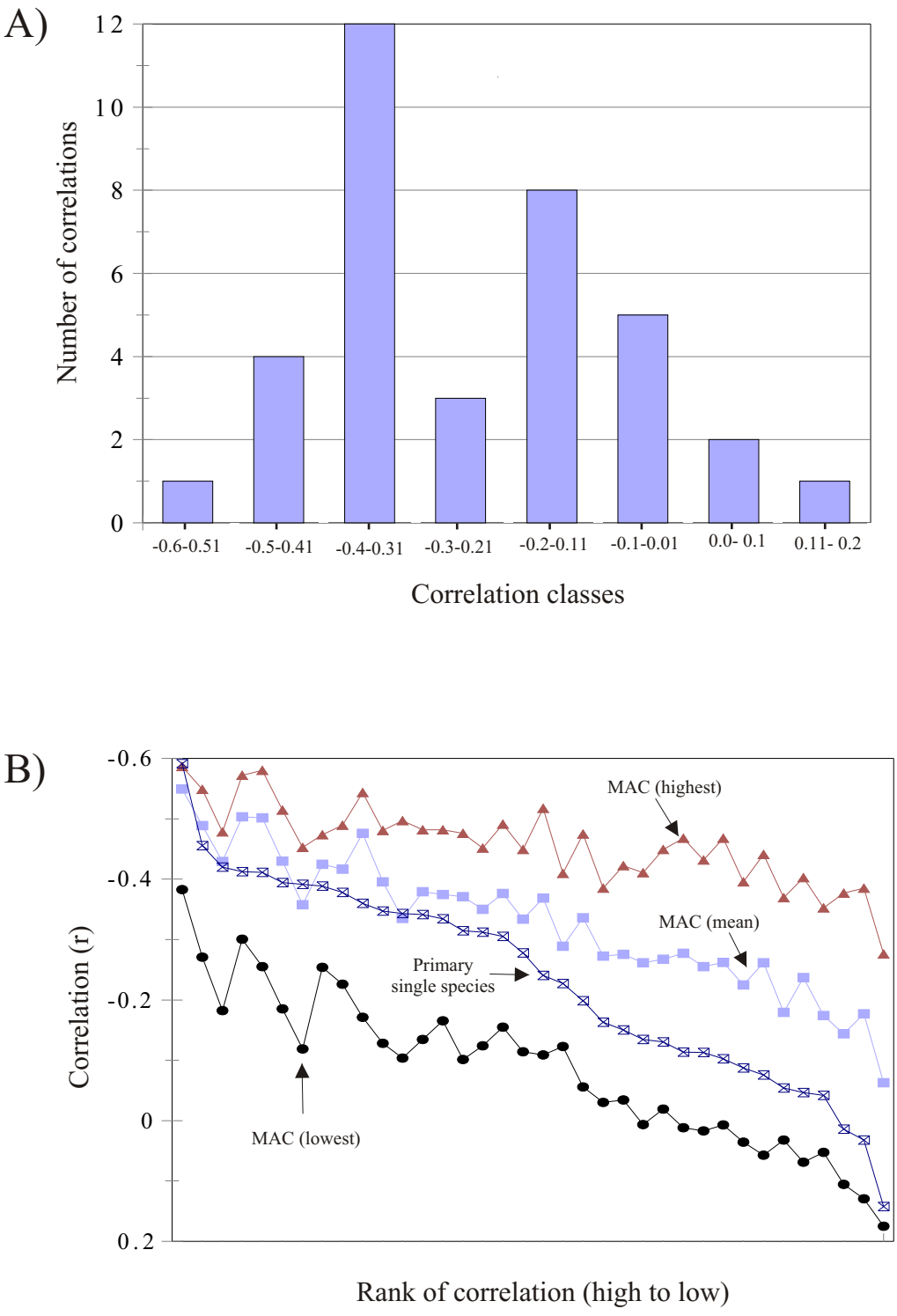

Figure 6.1 - A) A histogram of the correlations between the 36 mountain hemlock indices and the April 1 snowpack depths from Forbidden Plateau. B) The Pearson's r relationship of the original single-species index, and the MACs constructed with the mean, highest, and lowest secondary species indices, to snowpack depths at Forbidden Plateau.

and the highest correlated Douglas-fir index, and one constructed with all mountain hemlock indices and the lowest correlated Douglas-fir chronology) were evaluated.

Correlation matrices were calculated between the 36 MACs made with the master Douglas-fir index, the 36 MACs made with the most strongly correlated Douglas-fir index, and the 36 MACs made with the most weakly correlated Douglas-fir index and the snowpack data (Figure 6.1b).

For MACs using the Douglas-fir master index, improvement was seen in all indices but three, where the increases in the Pearson s r statistic ranged from -0.04 to 0.21. The new MACs constructed with the most strongly correlated Douglas-fir index had improved values ranging from 0.00 to 0.42. The new MACs constructed with the most weakly correlated Douglas-fir index showed no improvement over the single species correlations. The MACs created from the most weakly correlated Douglas-fir index showed reductions in correlations from 0.03 to 0.21.

6.3.2 June-July Temperature

A 95-year record of air temperature from the Nanaimo climate station was used to test correlations to the average June-July temperature. A histogram of correlations between the average temperature and the 35 mountain hemlock indices and the master mountain hemlock index are displayed in Figure 6.2a. The correlations approximate a normal distribution given the low number of values. A positive relationship is seen between the average temperature and mountain hemlock indices in all but four cases. The correlation values range from -0.22 to 0.52. The correlation of the master index to the June-July temperature average at Nanaimo was 0.39.

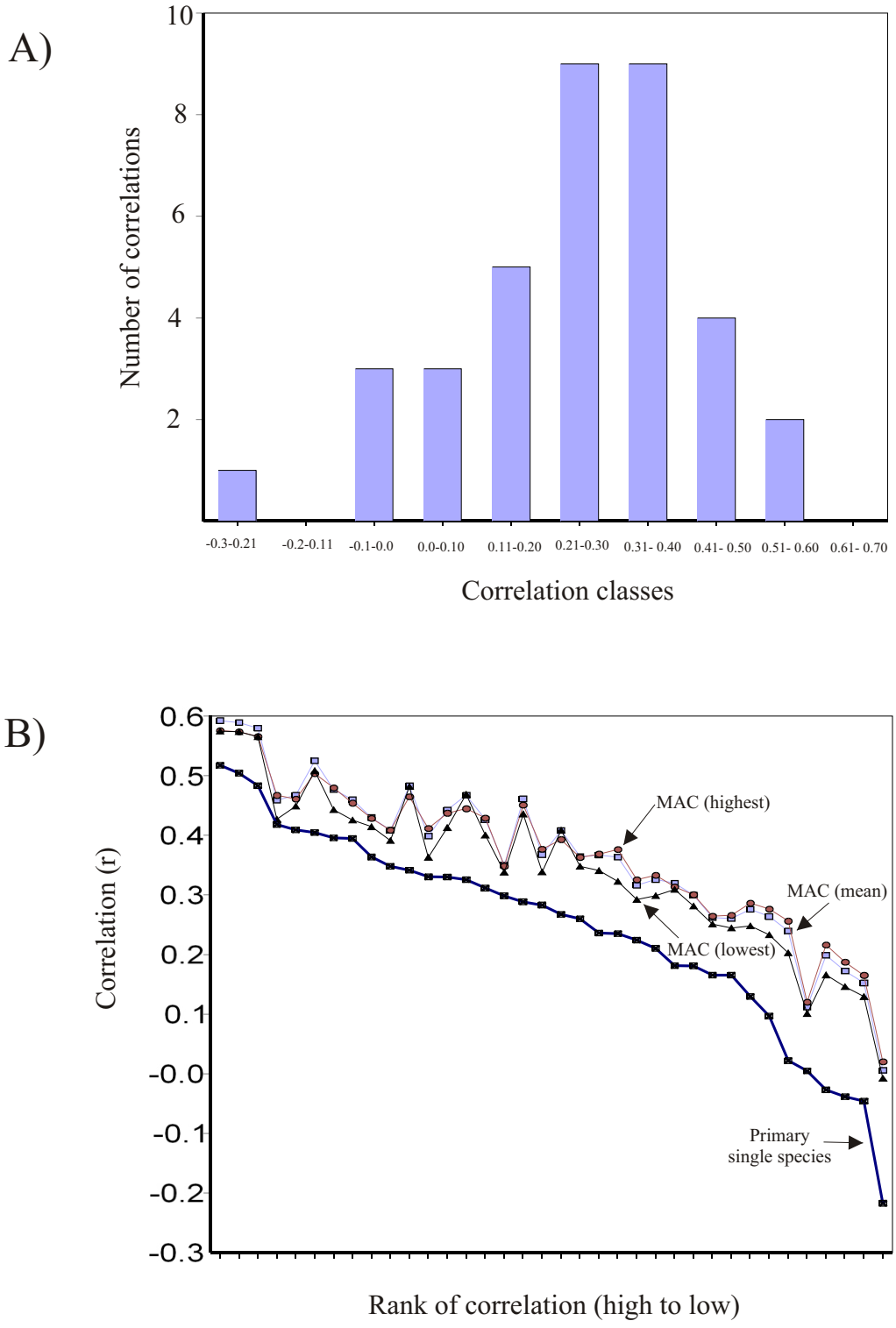

Figure 6.2 - A) A histogram of the correlations between the 36 mountain hemlock indices and the average June-July temperatures from Nanaimo station. B) The Pearson's r relationship of the original single-species index, and the MACs constructed with the mean, highest, and lowest secondary species indices, to average June-July temperatures at Nanaimo station.

A histogram was not constructed for the western red-cedar chronologies as there were only two series and the master series. The three values are all negatively associated with the seasonal temperature parameter and have a low range from -0.22 to -0.28. The western red-cedar master chronology has a median value of -0.27.

Thirty-six new MACs were constructed by subtracting the most strongly correlated western red-cedar chronology (Nesook Creek = -0.28) from each of the mountain hemlock chronologies. An additional 36 MACs were created by subtracting the master chronology for western red-cedar from each of the mountain hemlock chronologies, and 36 MACs were created by subtracting the most weakest correlated western red-cedar chronology (Mount Redford = -0.22) from each of the mountain hemlock chronologies. A correlation matrix was constructed for each set of new chronologies against the average June-July temperature. The results are displayed in Figure 6.2b. All of the new values at each site were higher than the single species average June-July temperature. The MACs created using the western red-cedar master chronology ranged from 0.01 to 0.59, while the MACs created using the most strongly correlated western red-cedar chronology ranged from 0.02 to 0.58. The MACs created from the weakest correlated chronologies ranged from -0.01 to 0.58, all very similar distributions since the three western red-cedar chronologies had a small range in variation.

6.3.3 July Precipitation

Climate data from the Nanaimo station were selected to construct correlation matrices of all of the mountain hemlock indices in this study with monthly July

precipitation results. The correlation matrix produced a histogram that once again approximates a normal distribution, ranging from 0.17 to -0.35 (Figure 6.3a). The mountain hemlock master index correlated at -0.11.

The two western red-cedar indices and their master index were also correlated against July precipitation values from the Nanaimo station. The three values ranged from 0.14 to 0.24, with the master index correlating at 0.21. No histogram was developed because of the low number of western red-cedar sites.

Three new sets of indices were constructed using the mountain hemlock indices, and subtracting the values for the western red-cedar master index, the Mount Redford site (strongest correlated = 0.24), and, the Nesook Creek site (weakest correlation = 0.14). In total, 3 new sets MACs were formed and their correlation values are displayed in Figure 6.3b. Values for the MACs created using the western red-cedar master index ranged from 0.06 to -0.37 , while the correlation values for the MACs created using the western red-cedar index at Mount Redford (strongest) ranged from 0.02 to -0.39. The MACs made up from the weakest correlated site (Nesook Creek) ranged from 0.09 to -0.33. The new MACs improved the correlation to the July precipitation amounts at Nanaimo from the single species chronologies in all cases.

6.3.4 July Temperature

July temperature was the second single-monthly variable tested. A histogram of the correlations between the monthly temperature values and the 35 mountain hemlock indices and the master index are displayed in Figure 6.4a. A histogram of the correlations between the July temperature values and 35 yellow-cedar indices and their master are

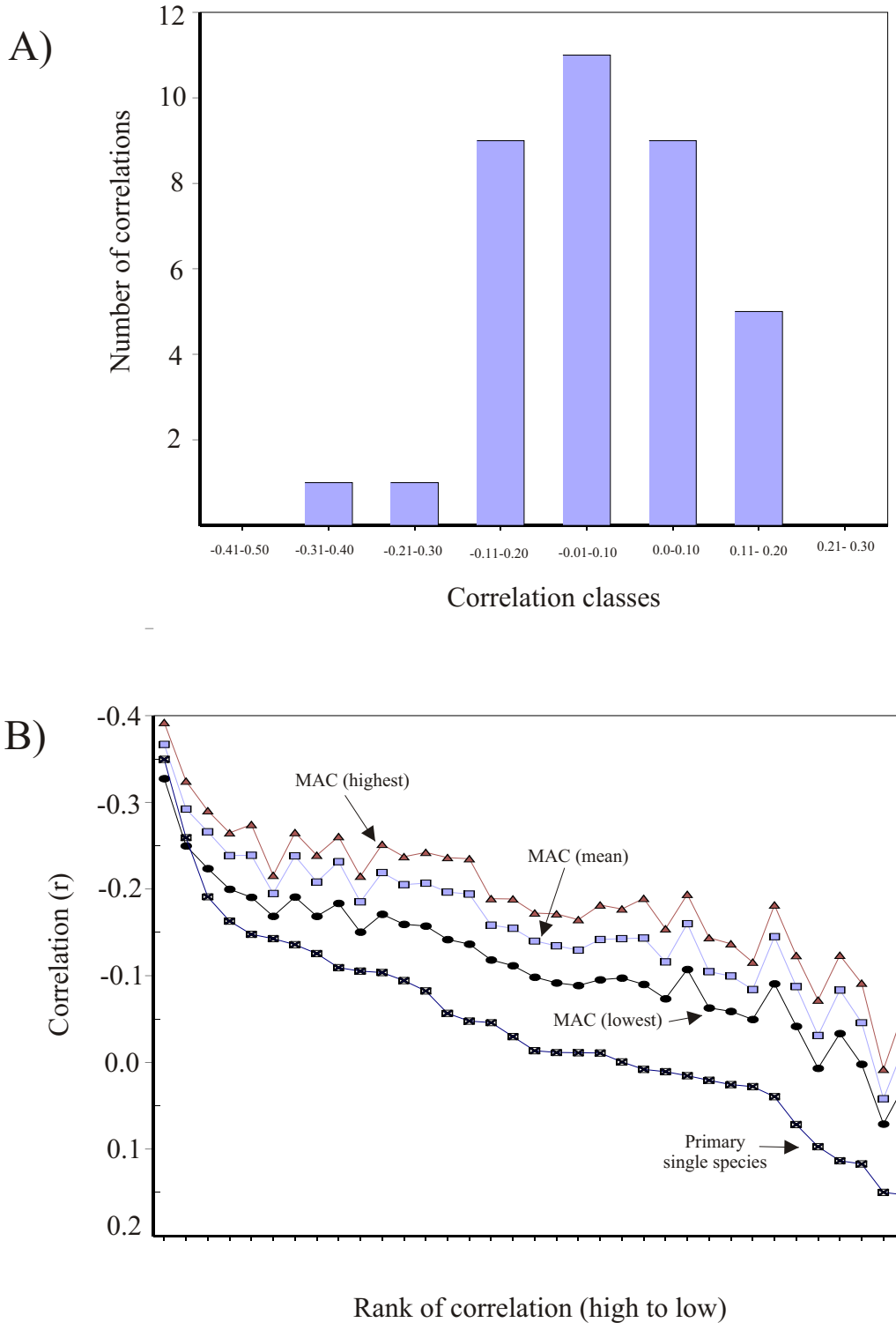

Figure 6.3 - A) A histogram of the correlations between the 36 mountain hemlock indices and July precipitation from Nanaimo station. B) The Pearson's r relationship of the original single-species index, and the MACs constructed with the mean, highest, and lowest secondary species indices, to July precipitation at Nanaimo station.

A)

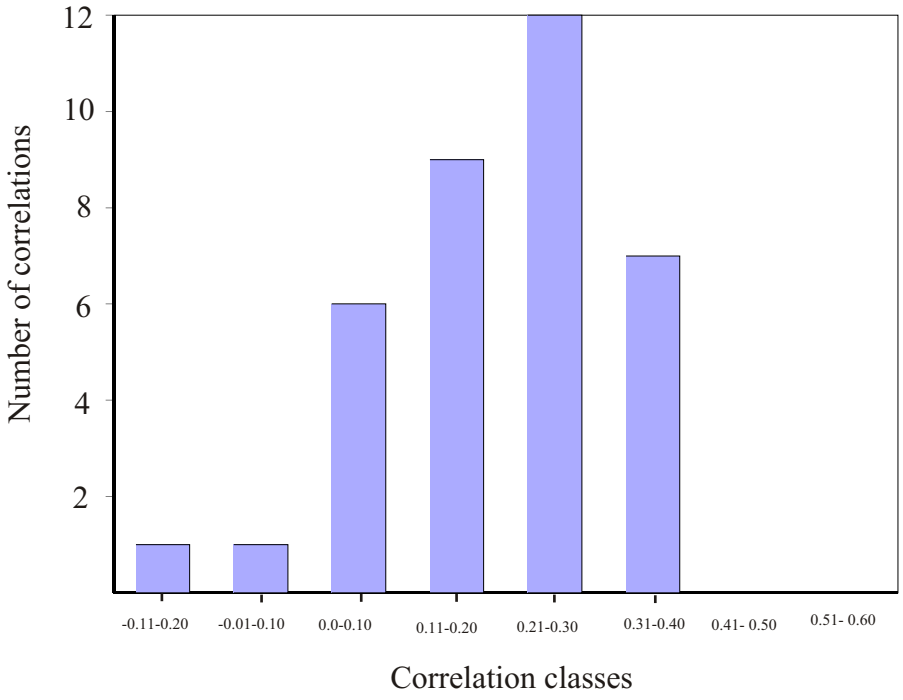

B)

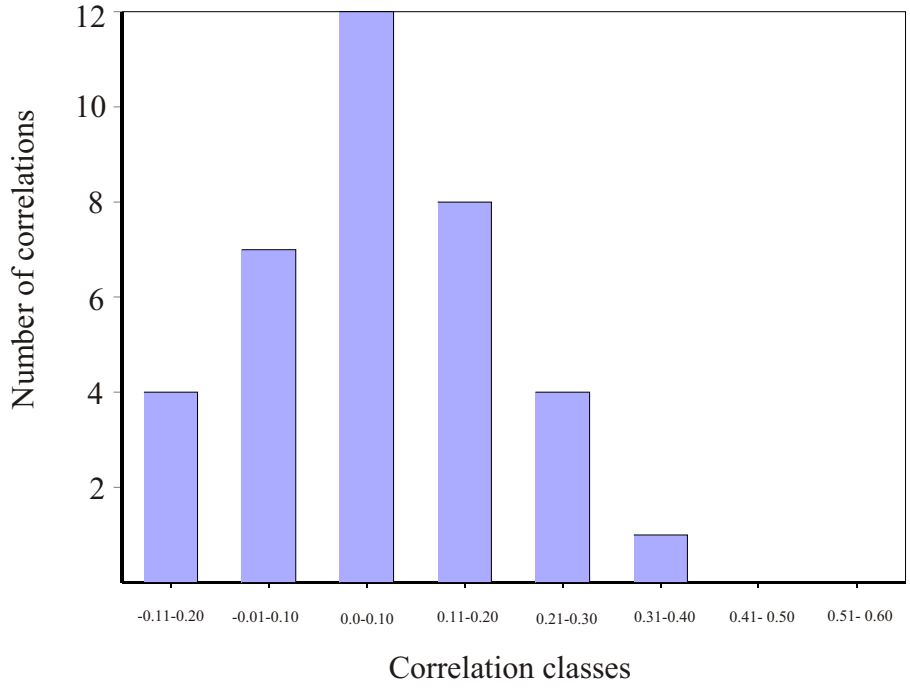

Figure 6.4 - A) A histogram of the correlations between the 36 mountain hemlock indices and July temperatures from Nanaimo station. B) A histogram of the correlations between the 36 yellow-cedar indices and July temperatures from Nanaimo station.

displayed in Figure 6.4b. In both cases the histograms approximate a normal distribution of the correlations to the climate parameter.

A positive relationship is seen between July temperature and all mountain hemlock indices except in two cases. The correlation values range from -0.18 to 0.39. Correlation of the mountain hemlock master index to July temperature at Nanaimo was 0.31. The yellow-cedar indices also had a wide range of correlations to July temperature, from -0.15 to 0.37. The master yellow-cedar index was correlated to July temperature at only 0.09.

MACs were created by adding the values from all the mountain hemlock indices to the values of the yellow-cedar master index, the most strongly correlated yellow-cedar index (Mount Cain = 0.37) to all of the mountain hemlock indices, and the weakest index (TAD ridge = -0.15) to all of the mountain hemlock indices. In total, three new sets of MACs were constructed (Figure 6.5). The new MACs constructed with the yellow-cedar master index had correlations to July temperature at Nanaimo, with values ranging from -0.09 to 0.33. These results were similar to the correlations from the mountain hemlock single-species to July temperature. A greater improvement was seen in the range of correlations from the MACs created using the most strongly correlated chronology of yellow-cedar, with values ranging from 0.12 to 0.46. Values for the MACs created using the most weakly correlated yellow-cedar index ranged from -0.20 to 0.18.

6.4 Discussion

With all climate parameters studied, a comparison of correlation matrices from single- vs multi-species indices displayed a consistent pattern. In all cases the greatest

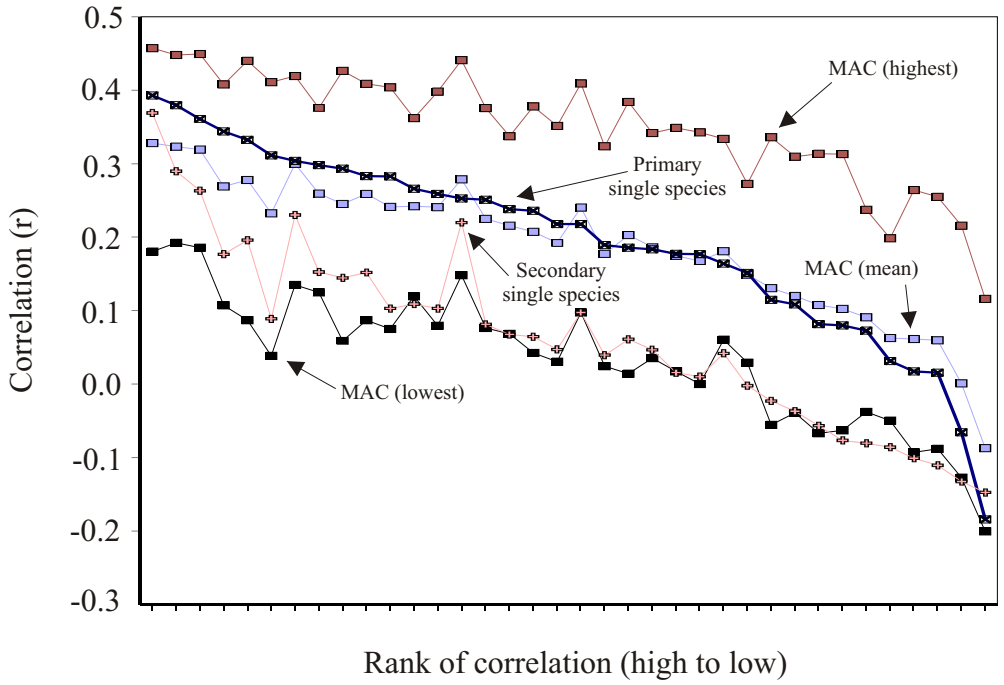

Figure 6.5- The Pearson's r relationship of the 36 original single-species indices of both mountain hemlock and yellow-cedar, and the MACs constructed with the mean, highest, and lowest secondary species indices, to July temperature at Nanaimo station.

improvements were seen when two species were used to explain a targeted climate parameter, *if* the initial index was poorly correlated with the climate parameter. If the single-species index was originally well correlated with the climate parameter, then the inclusion of another species either slightly improved or did not improve the overall correlation. This pattern was seen in all four tests, when using either the most strongly correlated MACs or the mean MACs. When using the most weakly correlated MACs, two patterns were apparent. In the first, two of the climate parameters (average June-July temperature and July precipitation) were improved by the most weakly correlated secondary species, while in the other two cases, the weakly correlated MACs produced correlations well below the single-species correlations. In the two cases where the correlations were below the single-species correlation (April 1 snow and July

temperature), there was a larger sample size of the secondary species to provide a better indication of a site with weak correlations.

In general the increase to the overall MAC correlation by the addition of the second species became less pronounced as ever more highly correlated single-species indices were encountered, until eventually the second species added little or altered the relationship negatively (Figure 6.6). This theoretical relationship was clearly shown where a larger sample size of secondary sites was tested (i.e., 36 yellow-cedar indices in the July temperature MAC), but was not as clearly indicated in the two tests with a low sample numbers (i.e., those using the three western red-cedar indices). This result suggests that, an upper threshold exists in the signal-to-noise ratio for relationships between a climate parameter and any tree-ring index. The signal captured by either the best single species or a combination of multiple species never exceeds this upper threshold limit. Conversely though, a lower threshold also exists. If a secondary species selected to be incorporated into a MAC was originally weakly correlated, it is likely that a MAC in which it is incorporated will display a correlation to climate that is worse than the original single-species correlation (Figure 6.6).

The MAC method can be limited in its ability to establish a better reconstruction than that resulting from a primary single-species index with a very strong signal-to-noise ratio. It does, however, have as likely a chance of improving the overall signal if a weak single-species index was originally employed. Unfortunately, there hardly ever exists a situation in dendrochronological studies where the study site sample size is large enough to correlate many sites to a climate station and then select only the most sensitive index.

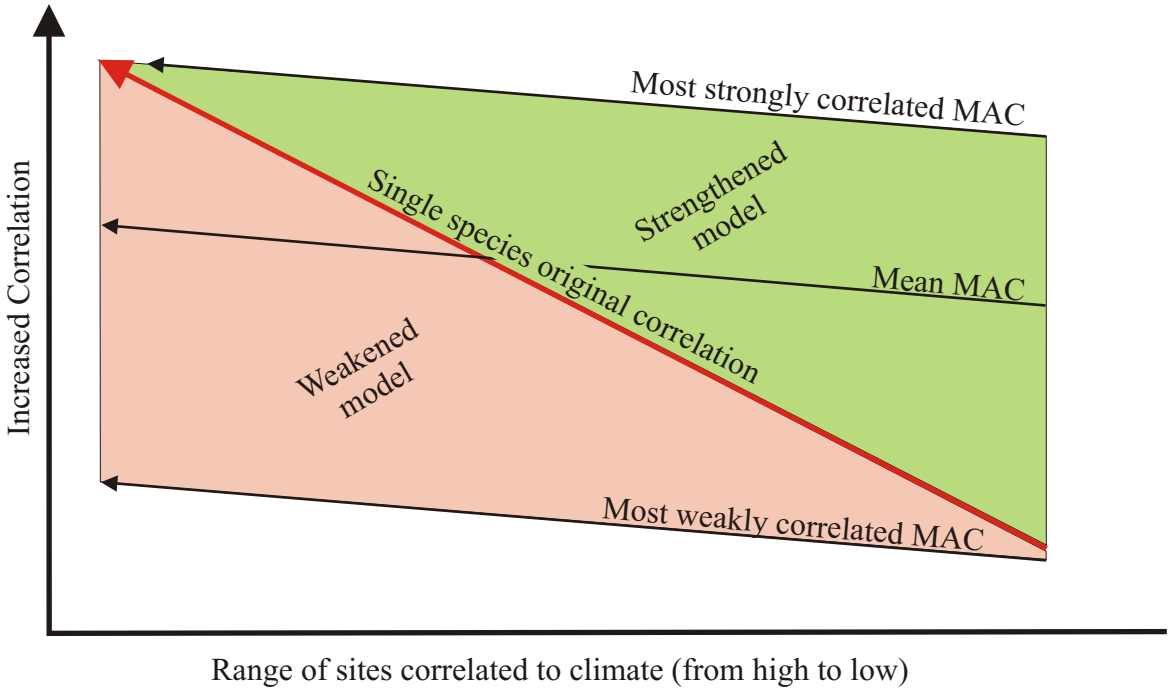

Figure 6.6 - The summarized theoretical distribution of a single-species index, and three MACs when correlated to a climate parameter in this study.

By developing the theoretical background of the normally distributed correlations, this chapter provides a justification for deciding when a multiple-species sampling approach would be advantageous over a single-species method. If time and resources are limited, then sampling two co-occurring species to target a related climate parameter will be more advantageous. This is because in a normally distributed population, the selection of two sites will most likely fall close to the mean, and two mean indices from the primary and secondary species seem to possess a better correlation to a climate parameter then the mean of a single-species. A researcher sampling two tree species may be fortunate and derive an improved reconstruction model, or if not, the single-species

chronology originally selected from the primary species was already highly correlated. In either case, the results will be better from a cost/benefit viewpoint than if the researcher visited multiple locations to find the site that correlated the best.

The procedures outlined in the MAC analysis have shown that better relationships to targeted climate parameters do exist when using multiple species, but the initial goal was to improve paleoreconstructions. In the next chapter, MAC-processed data will be put to the final test to see if conventional methods of calibration and verification using the new data sets will improve the overall reconstructions.

Chapter 7.0 Paleoreconstructions

7.1 Introduction

A primary objective of the study was to use tree rings to provide paleoclimatic models of climate conditions on Vancouver Island. The most common method of supplying this information is by using transfer function analysis (Fritts *et al.* 1971, Fritts 1976, Fritts 1991). Transfer functions are constructed by using tree-ring indices as predictor variables in regression equations to predict climate values.

In this chapter, reconstructions will be made for the four climate parameters explored in the previous chapter (April 1 snowpack depth, average June-July temperature, average July temperature, average July precipitation). Conventionally this is done with single-species indices, but in this chapter MACs will be used. The initial goal was to produce the best model possible of past climate conditions. To increase the statistical reliability in the reconstructions, instead of selecting the single best MAC to construct a proxy model, an average of the five highest correlated MACs for each climate parameter will be used.

7.2 Methods

Linear regression models were developed for MAC indices and climate parameters using SPSS (Version 7.5, 1996). For each of the four climate variables reconstructed, the top five correlated MACs were selected and averaged (Figure 7.1). This procedure allowed for a higher confidence to be placed in the independent variable, as the chance that an individual chronology would bias the data is greatly reduced by using a weighted average. Like most dendroclimatic reconstructions, limited sample

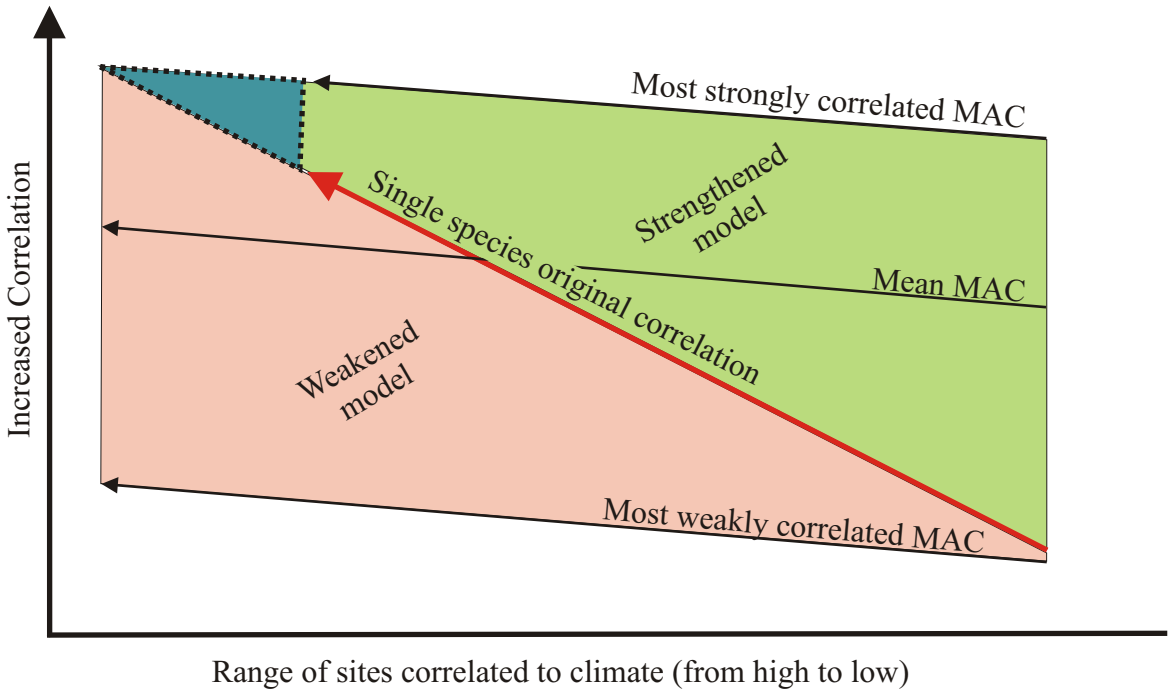

Figure 7.1 - The summarized theoretical distribution of a single species index, and three MAC indices when correlated to a climate parameter. The dashed triangle illustrates the theoretical area covered by the top five MACs which are combined to form the index that is used in each paleoreconstruction.

depth at the beginning of each chronology reduces the confidence placed in the model at that point, but by using two species this effect is reduced.

When developing a regression model for paleoclimatic reconstructions, it is standard dendroclimatological practice to divide the climate data set into two components, the calibration period and the verification period (Fritts 1976). A model is first constructed using a calibration data set and the derived relationship verifies the model's ability to reconstruct actual climate data (verifying data set). In this instance, calibration data consisted of 60 percent of the length of the climate data set for three of the four tests. Tests conducted for average June-July temperature, average monthly July

precipitation, and average monthly July temperature used a calibration interval from1937 to 1995. The verification data set consisted of climate data from 1901 to 1936. As the entire April 1 snow depth record was only 40 years long, 50 percent of the data was used for the calibration interval (1975 to 1995). Verification was conducted on the remaining 20 years of data (1955 to1974).

Six goodness-of-fit tests were then applied to the regression models using program VFY (Fritts 1976, Holmes 1999) which provides an indication of how well the reconstructed climates compare to the actual climate data. Once verified, each relationship was hindcasted over the entire chronology length to produce a proxy paleoreconstruction of climate.

7.3 Results

The calibration results are displayed in Figure 7.2, with the linear regression equations for each model listed in Table 7.1. Results of the six goodness-of-fit tests applied to each model are presented in Table 7.2. VFY ran analyses for simple Pearson r correlations at the 95 and 97.5 percent levels, as well as reduction of error tests, student t-tests, sign-product tests, and negative first differential tests (see Fritts 1976 for further description). As expected with models that were derived from the highest correlated MACs, the four models passed 22 of the 24 tests. Both the model for April 1 snowdepth and the model for July precipitation failed one verification test each (Table 7.2).

7.3.1 April 1 Snowpack

The April 1 snowpack reconstruction explained 41 percent of the variance in snowpack depth over the duration of the known record (Table 7.1). While calibration and

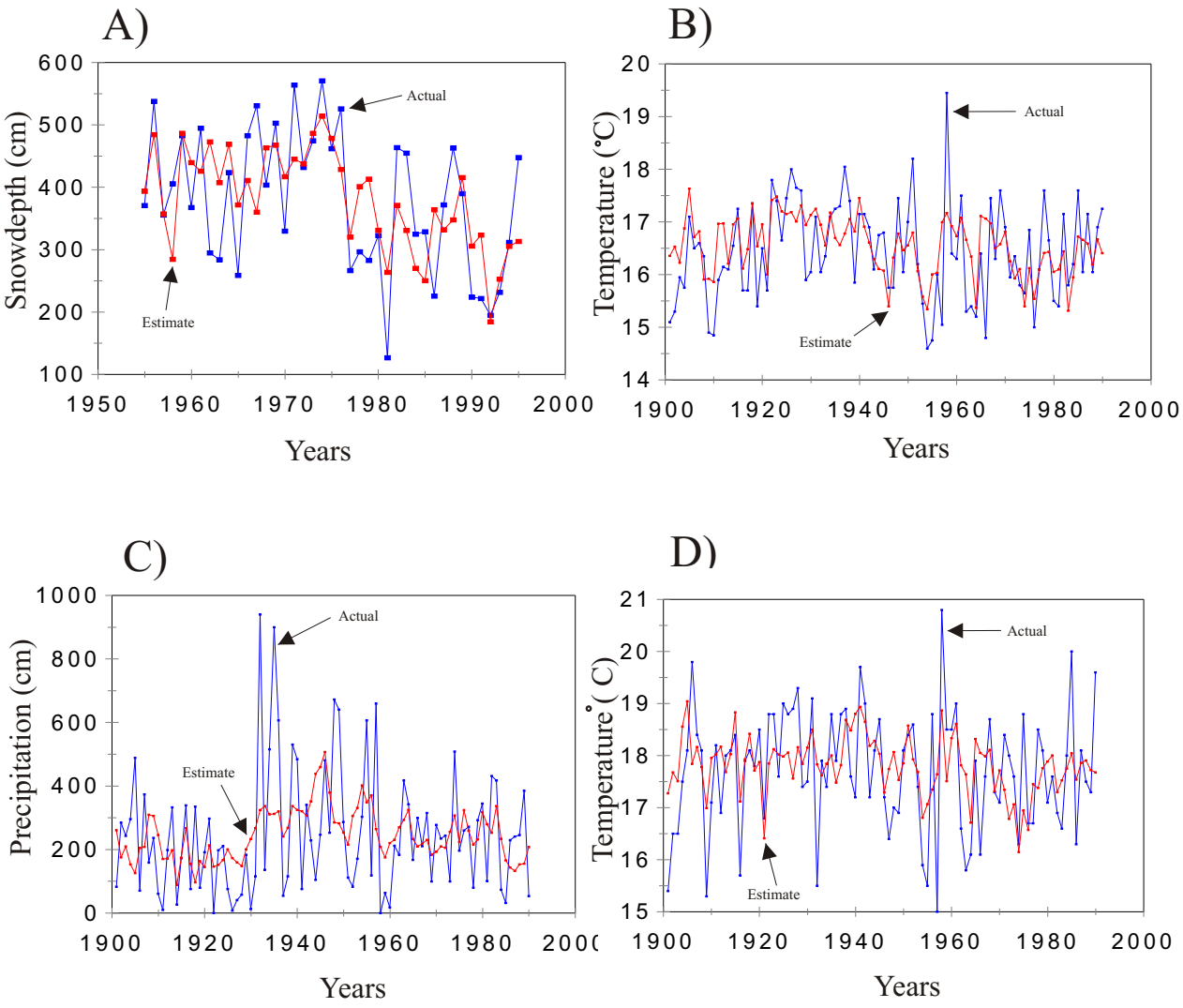

Figure 7.2 - The actual versus estimated reconstructions based on the calibration period for the climate parameters. A) April 1 snowpack, B) average June-July temperature, C) average July precipitation, D) average July temperature.

verification show that the model adequately represents significant shifts in snowpack depth, extreme events in the record were not well represented (Figure 7.2a).

Figure 7.3a shows the paleoreconstruction of April 1 snowdepth from 1500 to 1995. From 1500 until 1800 snow depths were for the most part above the 375 cm

Table 7.1 - The results of the linear regression analysis for each of the four climate parameters tested based on the calibration period.

Dependent variable	Explained r (r^2)	Equation
[1]April 1 Snow	0.64[a] (0.41)	MAC value * -205.398 + 827.719
[2]June-July Temperature	0.59[a] (0.34)	MAC value * 1.968 + 14.290
[2]July Precipitation	0.39[b] (0.15)	MAC value * -295.258 + 241.496
[2]July Temperature	0.49[a] (0.24)	MAC value * 1.740 + 14.290

Intervals and significance values for the one-tailed Pearson s r analysis were as follows: [1]Test interval = 1955-1995, [2]Test interval = 1901-1995, [a]Significant at $p < 0.0001$, [b]Significant at $p < 0.001$.

Table 7.2 - Results of the goodness-of-fit tests for the calibrated and verified models. Each test is listed as pass or fail with the statistical values in brackets.

	April 1 Snow[1]	June-July Temperature[2]	July Temperaure[2]	July Precipitation[2]
[a]Correlation (r)	pass (0.38)	pass (0.72)	pass (0.50)	pass (0.45)
[b]Correlation (r)	fail (0.38)	pass (0.72)	pass (0.50)	pass (0.45)
[a]Reduction of Error	pass (0.57)	pass (0.36)	pass (0.25)	pass (0.18)
[a]T-Value test	pass (4.12)	pass (3.52)	pass (3.67)	pass (2.53)
[a]Sign-product test	pass (5)	pass (10)	pass (12)	pass (12)
[a]Negative first differential test	pass (5)	pass (5)	pass (9)	fail (17)

Calibration intervals and significance levels for each test are noted as follows: [1]Calibration time period = 1975-1995 and verification time period = 1955-1974, [2]Calibration time period = 1937-1995 and verification time period = 1901-1936, [a]Significant at $p < 0.05$, [b]Significant at $p < 0.025$. Significance levels for the six tests are as follows: for April 1 snow, $r = 0.95 > 0.37$, $r = 0.975 > 0.44$, RE >0.14, T-value>1.73, S-P< 5, Neg F.D.< 5 , for all other tests, $r = 0.95 > 0.27$, $r = 0.975 > 0.32$, RE >0.07 T-value>1.69, S-P<= 12, Neg F.D.<= 12. Values of n are as follows: for snowpack test n = 20, for all other tests n = 35.

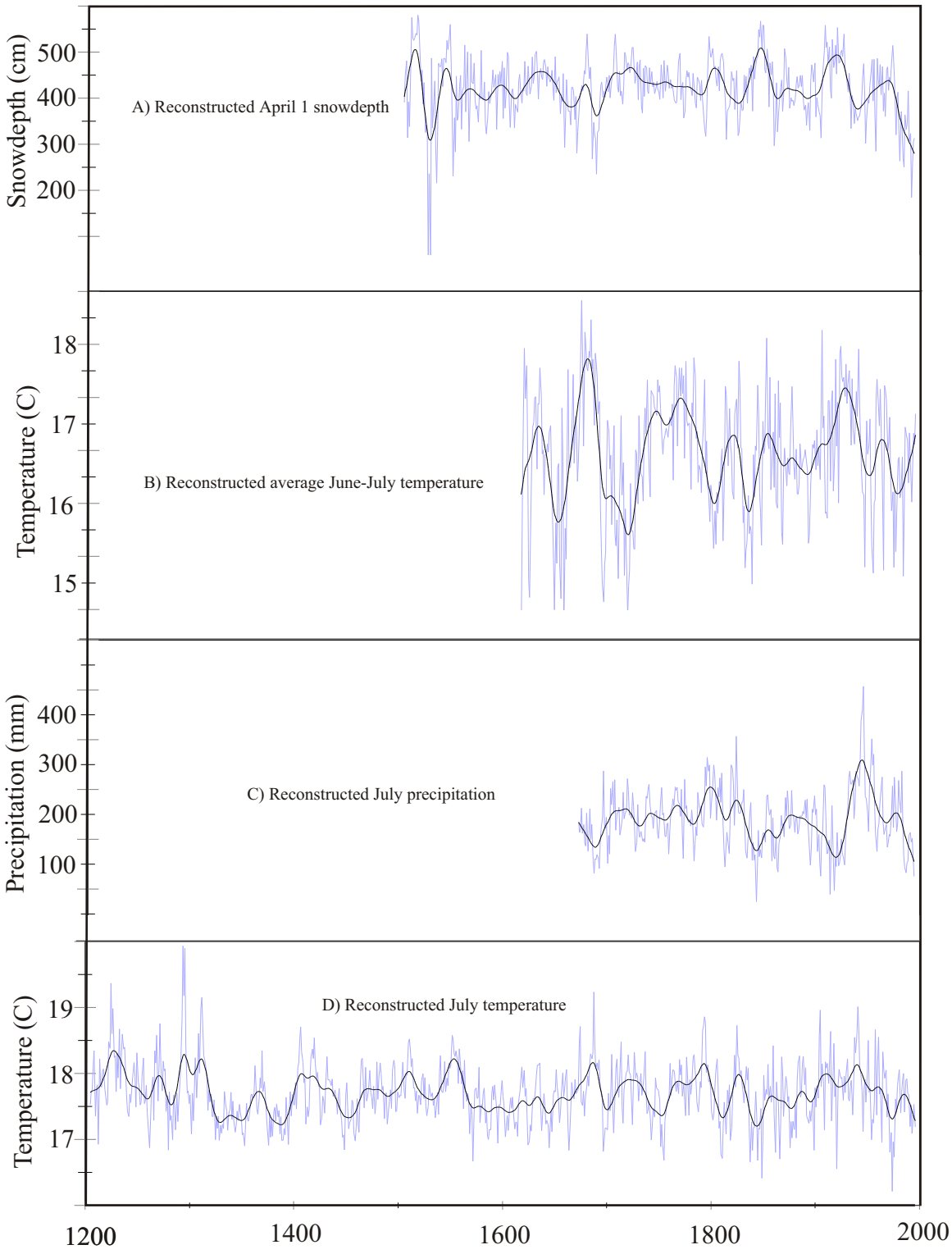

Figure 7.3 - The four reconstructed climate parameters from the study. The smoothed line in each reconstruction is a 25-year spline curve.

recorded mean value from Forbidden Plateau Station (Figure 7.4a). While above-average depths were infrequent during this time period, April 1 snow depths never exceeded 550 cm. Lower than average snowdepths (below 375 cm deep) were more common. Reduced snowpacks characterize the mid-1520s, and the late 1680s (Figures 7.3a, 7.4a). There were only a few consecutive years of above-average April 1 snow depths that stand out during this 300-year interval. From the mid-1530s to the early 1550s, late 1620s to mid-1660s, and late 1710s to mid-1780s April 1 snowpacks exceeded the historical mean (Figure 7.4a).

During the 1800s two intervals are recorded where April 1 snowpack depth was consistently above the historical average. From the late 1790s until the early 1810s and from the early 1830s until the early 1860s, April 1 snow depths remained above average with values in the mid- to late 1850s reaching above 450 cm. During the1900s, the April 1 snowpacks generally remained below the historical average, with 1909, 1921, 1927, and 1946 displaying April 1 snowpacks with depths more than 100 cm above the historical mean value.

7.3.2 June-July Temperature

The June-July reconstruction explained 34 percent of the variance in the historical temperature record from Nanaimo. The paleoreconstruction follows the general trend of the data, but as the lower level of explained variance suggests, the model fails to adequately represent extremes in the data set (Figure 7.2b).

The average June-July temperature paleoreconstruction is shown in Figure 7.3b. There were several notable periods in which the reconstruction departed from the long-term recorded mean (16.5 °C)(Figure 7.4b). Consecutive years of below-normal temperatures (>

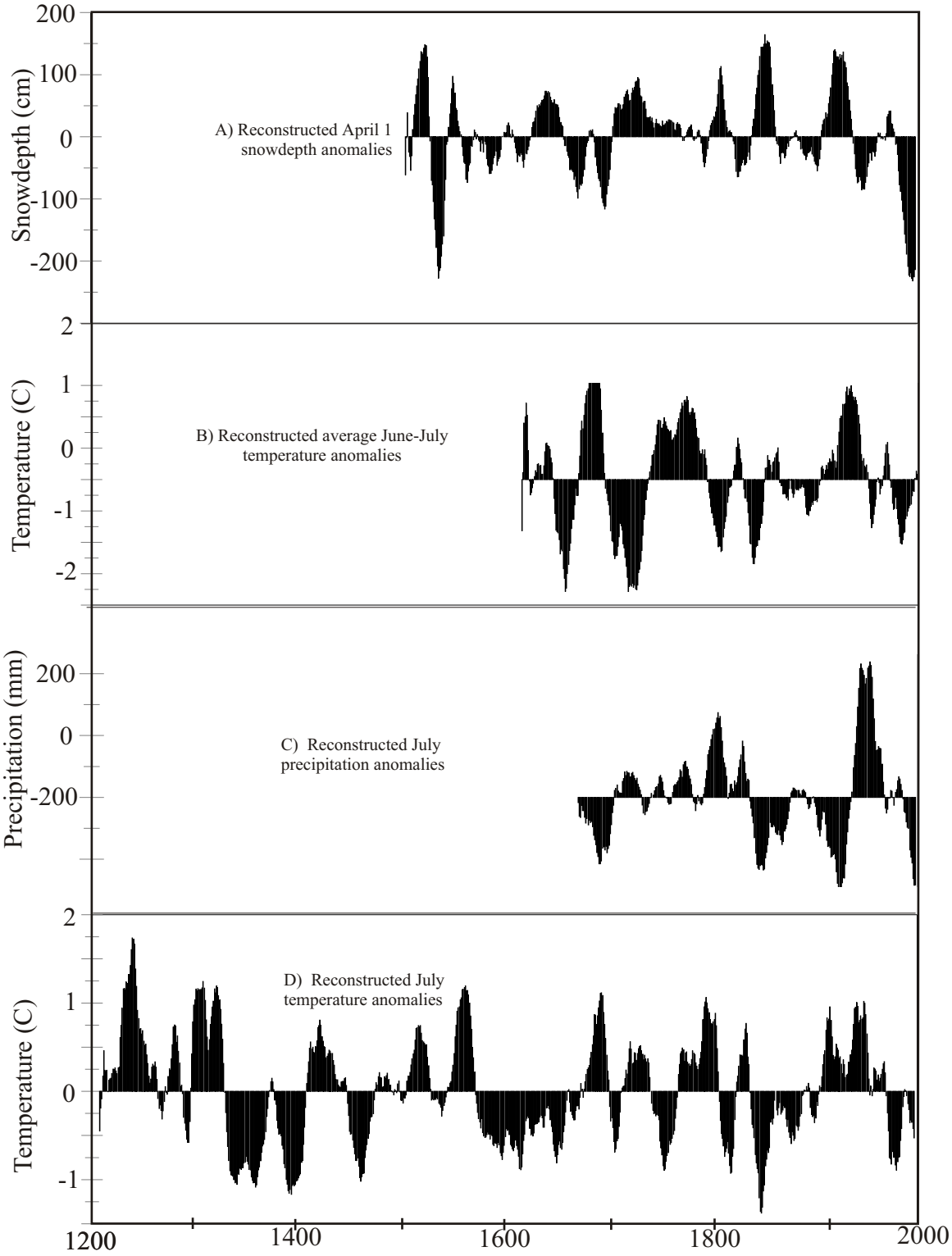

Figure 7.4 - The four reconstructed climate parameters from the study displayed as anomalies from their historical mean. The data are displayed with a 15-year moving average.

- 0.5 °C from the mean) were seen during the early 1650s to the early 1670s, the early 1690s to the late1730s, the early 1790s to the early 1810s, and the early 1830s to the mid-1840s. Periods of above-average temperatures (> + 0.5 °C from the mean) were as frequent but of longer duration (Figure 7.4b). They were seen during the early 1670s to early 1690s, early 1740s to the mid-1780s, and the mid-1910s to the mid-1940s.

7.3.3 July Precipitation

Figure 7.3c illustrates the reconstructed July precipitation which explained 15 percent of the variance in the actual precipitation data. The reconstruction does not provide detail into the highly variable extreme values contained within the historical data (range 0-940 mm) (Figure 7.2c). No zero or near-zero values were predicted in the paleoreconstruction, and no values ranged higher than 410 mm. Sustained above-average precipitation totals were identified from the early 1760s to the mid-1770s, the late 1780s to the early-1810s, the mid-1810s to the early 1830s, and the early 1930s to the mid-1950s (Figure 7.4c). Sustained below-average totals were more commonly seen, from the early 1670s to the mid-1690s, the early 1830s to the mid-1850s, the early 1860s to the mid-1870s, the early 1890s to the early 1930s, and the mid-1980s to present (Figure 7.4c).

7.3.4 July Temperature

Figure 7.3d displays the average July temperature record reconstructed using the averaged MACs. Since the two species that made up the MAC index were of long duration (yellow-cedar and mountain hemlock), the reconstruction covers the greatest interval of any of the proxy records. The model explains 24 percent of the actual variation in the July temperature data (Figure 7.2d). Sustained warmer-than-normal and cooler-than-normal

phases were evident during several periods, with cooler-than-normal phases outnumbering and outweighing warmer-than-normal phases. Intervals of more than ten years that averaged 0.5 °C warmer or cooler than the historical mean were identified. Sustained intervals of warmer-than-normal July temperatures were seen during the early 1220s to the early 1240s, the late 1540s to the early 1560, the mid-1670s to the early 1690s, and the mid-1930s to the early 1950s. Cooler-than-normal sustained periods were seen during the late 1270s to the mid-1290s, the late 1310s to the late 1350s, the mid-1370s to the late 1390s, the late 1430s to the mid-1460s, the early 1570s to the early 1690s, the late 1710s to the early 1730s, the mid-1740s to the early 1760s, the early 1830s to the early 1850s, and the mid-1960s to the mid-1970s.

7.4 Discussion

The MACs constructed to explain seasonal parameters were more robust than those created to model individual monthly parameters. This characteristic seems to be related to growth season plasticity. Radial growth records from trees in this setting appear to be able to withstand short-term climatic stresses (i.e., monthly or individual extreme events). Even though the monthly reconstructions are weaker, a correlation between the average June-July seasonal and the monthly average July temperature reconstructions were highly significant ($r = 0.36$, $p < 0.0001$, $n = 380$). Since these reconstructions are made up of different aggregates, and both reconstructions share the temperatures of July in common, it is seen as another reliable form of verification of at least those two models.

If short-term events are not well represented in the proxy records, then the strength of the reconstructions perhaps lies in the longer term trends they reveal. In Figure 7.4 the

four proxy data sets are illustrated as deviations from their historical mean. Cyclical events seem to be inherent in the longer-term time-series data. To explore if these apparent cycles are valid, a wavelet analysis of the four data sets was conducted.

Wavelet analysis provides a robust tool able to display the dominant modes of variability in a time series (Torrence and Compo 1998). Within dendroclimatology, wavelet analyses provide a methodology for understanding variabilities in climate that have changed in strength and frequency over time (e.g., Gedalof and Smith 2001a, Malamud 2001, Rigozo *et al.*, 2001).

Figures 7.5a-d illustrate the results of the wavelet analysis for each of the four proxy reconstruction data sets (http://paos.colorado.edu/research/wavelets/, accessed on November 16, 2001). A Gaussian filter was used to highlight areas in time where dominant modes of variability were found in each time series. The analyses display areas surrounded by solid black lines as significant at a 90 percent confidence interval compared to a red noise background (Torrence and Compo 1998). All four models have zero-padding added to each end of the time-series data set to offset edge effects. Since edge effects caused by the moving filter are inherent in the analyses, a cross-hatched pattern is overlain on each image to display where the reduction in confidence is placed in the time and frequency domains (Torrence and Compo 1998).

The wavelet analysis highlights cyclicity in all four data sets. Each modelled parameter displays a similarity to the other reconstructions by having modes of variability displayed at approximately 15, 25 and 65 year periods. Three models (average June-July temperature, average July precipitation, average July temperature) also display modes of

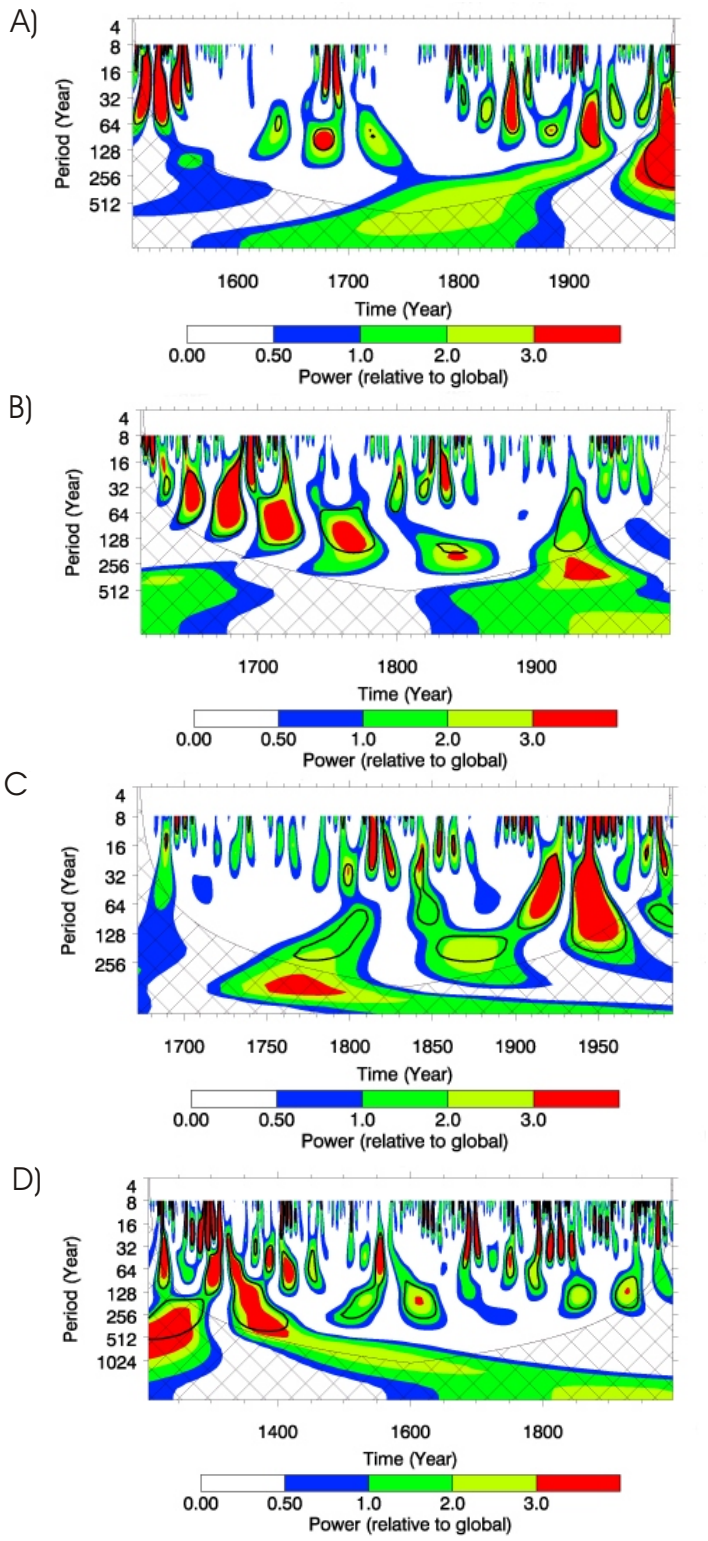

Figure 7.5 - The wavelet power spectrum of the four paleoreconstructions (A) April 1 snowpack depth, B) average June-July temperature, C) average July precipitation, D) average July temperature). The thick contour encloses regions significant at 90 percent confidence, relative to red noise. The cross-hatched region indicates where edge effects caused by zero-padding becomes significant.

variability at approximately 130-150 year periods. All of the models share similar modes of variability at particular intervals in each time series (e.g., a significant mode in the 1920s at a 32 year period, or two significant modes at a 16 year period in approximately the 1680s and 1690s).

The wavelet analysis highlights modes of variability in each of the four models that have also been shown to occur in the instrumental record. Modes connected to an eight year El Nino/Southern Oscillation (ENSO) signal (Moore and McKendry 1996), a 25 year multi-decadal PDO signal (Gedalof and Smith 2001a), and a 65 year sub-century signal (Kadonaga *et al.*, 1999) have been demonstrated. Evidence for a multi-century scale signal has also been documented from other proxy records, and the long length of the July temperature reconstruction highlights such a mode of variability that is not possible to detect with the short instrumental record.

Since all of the climate reconstruction parameters share similar modes of variability at the same temporal scale, an analysis of the characteristics of each mode is possible. For example, by comparing the July temperature and precipitation wavelet analyses (Figure 7.5) and the July temperature and precipitation anomaly analyses (Figure 7.4), characteristics of each mode in July can be made. The 16-year period of variability coincides with a warm/dry period in July on Vancouver Island. The 32-year period coincides with a warm/wet cycle, the 65-year period also with a warm/wet July climate, and the 130-year period with an enhanced cooler/dryer mode of variability. Although the characteristics are suggestive, strong significance cannot be put on the results until further analysis is completed.

The use of tree rings to develop climate indices is well established (D Arrigo *et al.* 1999, Biondi *et al.* 2001, Gedalof and Smith 2001a), but the adoption of MACs seems to provide another way to better target these climate-specific indices. The wavelet analyses provides evidence that the MAC paleoreconstructions have captured signatures of various oceanic forcing mechanisms during different intervals in time.

Having investigated the past relationships between tree rings and climate on Vancouver Island, the last remaining objective is to see if relationships between these two entities can be used to forecast future ring growth from forecasted climatic data. This objective will be addressed in the next chapter.

8.0 Radial-Growth Forecasting

8.1 Introduction

This chapter investigates the consequences of predicted future climates on the radial growth of trees on Vancouver Island using response function analyses (Blasing *et al.* 1984, Fritts *et al.* 1990). It first predicts the impact of short-term (< 10 years) climate changes upon the radial-growth rate of trees by using a model based on historical climate data. Second, this chapter investigates the likely impact of long-term (>10 to 100 years) climatic changes on radial-growth trends, as predicted by several different global circulation models.

8.2 Short-term Forecasting

The model *TREE* (Tree-ring Radial Expansion Estimator) was developed to forecast the impact of short-term climate changes on radial growth. *TREE* uses species-specific climate/radial-growth relationships and selected climate variables (temperature and precipitation) to predict radial-growth trends within the near future. Predictions are based upon stepwise multiple regression equations developed by SPSS (Version 7.5, 1996) that establish a relationship between 40 historical climate variables (current year and previous May to previous December monthly temperature and precipitation data) and a one year lag variable for each of the species tested, to historical radial-growth increments.

8.2.1 Methods

Regression models were developed for each species using the Nanaimo climate data from 1900 to 1995 (n=95). To select which of the 40 climate variables were the most important to each dependant variable, the following protocol was followed:

1) In the first step, a backward multiple regression model was developed using all 41 variables (40 climate and one lag variable). This process forced all the variables into a regression equation and then sequentially removed the variable that had the smallest partial correlation on the overall equation. In this manner the variables that have the least amount of consequence to the regression equation were highlighted first. In this step, all variables with a p-value greater than 0.50 where eliminated from further analysis to reduce the independent data set.

2) The second step was to enter all variables that were shown to be significant in the PRECON analysis with each master chronology and the remaining variables with p-values less than 0.50 into a forward stepwise multiple regression. Limits were placed on which data were entered into the regression equation by a F to Enter and F to Remove confidence levels set at 0.10 and 0.15 respectively.

3) The significant variables remaining from #2 were then incorporated into the master tree species multiple regression equations (Table 8.1). The calibration periods were set from 1900 to1959, while verification periods were fixed from 1960 to 1995. The results of this analysis is displayed in Table 8.2.

The models explained from 55 to 68 percent of the variance in radial growth (Table 8.1). As expected with the high amount of variance explained, all proxies were found to be significantly verified over the time frames modelled (Table 8.2). Two internet scripting languages, PERL and HTML, were used to implement the five *TREE* models. Predicted radial-growth increments are displayed as annual standardized measurements using an HTML interface. Script codes for both the PERL calculation engine and the HTML input/output interfaces are presented in Appendices C and D respectively.

8.2.2 Results

TREE (Version 2.1) [Http://cgrg.geog.uvic.ca/tree.htm] is able to explain over half of the variance in the radial-growth of all of the species studied (Table 8.1, Figure 8.1 a-e). The model works in a simple three-step process:

1. The user first selects either any or all of the five tree species for modelling in montane areas of Vancouver Island (Figure 8.2a).

Table 8.1 - Results of a stepwise multiple regression analysis between radial growth and precipitation and temperature variables from Nanaimo station (1900-1995). All models have a one year lag parameter included in each model and are significant at $p < 0.0001$.

Dependant variable	Explained r (r^2)	Equations
Master mountain hemlock	0.78 (0.60)	MH = (Apr temp * 0.0017) + (Aug precip* 0.0001362) + (Dec temp * 0.001423) + (July temp * 0.001287) + (June temp * 0.002033) + (March temp * 0.001764) + (May precip * -0.0000 7374) + (previous Dec precip * -0.00003426) + (previous July precip * -0.0001392)+ (previous July temp * -0.006888) + (previous June precip * 0.0001224) + (MH lag * 0.600) + (Constant) 0.820
Master yellow-cedar	0.78 (0.60)	YC = (Aug temp * -0.002083) + (Feb precip * 0.00004853) + (July temp * 0.002375) + (previous July temp * -0.002 667) + (previous Nov precip * -0.000 03721) + (previous Oct temp * 0.00325) + (previous Sept temp * -0.00217) + (YC lag * 0.703) + (Constant) 0.717
Master western hemlock	0.81 (0.66)	WH = (Apr temp * 0.001748) + (Aug precip * 0.00007632) + (Jan precip * -0.00002267) + (June temp * -0.001 128) + (previous Aug precip * 0.000 1395) + (previous July temp * -0.002 621) + (previous Sept precip * -0.00002694) + (WH lag * 0.765) + (Constant) 0.705
Master western red-cedar	0.82 (0.68)	WRC = (Feb temp * 0.003154) + (June temp * -0.003885) + (July precip*0.0001133) + (May precip * -0.0000543) + (previous Aug temp * -0.001977) + (previous Dec precip * -0.000 0246) + (previous July precip * 0.0002131) + (previous July temp * -0.001369) + (previous Nov precip * -0.00002821) + (previous Oct precip * 0.00003589) + (previous Oct temp * 0.002782) + (previous Sept temp * 0.001995) + (WRC lag * 0.580) + (Constant) 0.961
Master Douglas-fir	0.74 (0.55)	DF = (May precip * 0.00008060) + (Nov precip * 0.00001835) + (Previous June precip * 0.0002227) + (previous July precip * 0.0001801) + (previous May temp * -0.001733) + (Sept precip * 0.00006149) + (DF lag * 0.551) + (Constant) 0.426

Table 8.2 - Results of the goodness-of-fit tests for the forecast models developed by the calibrated data. Each test is listed as pass or fail with the statistical values in brackets.

	Mountain hemlock	Yellow-cedar	Western hemlock	Western red-cedar	Douglas-fir
[a]Correlation (r)	pass (0.73)	pass (0.74)	pass (0.90)	pass (0.77)	pass (0.69)
[b]Correlation (r)	pass (0.73)	pass (0.74)	pass (0.90)	pass (0.77)	pass (0.69)
[a]Reduction of Error test	pass (0.71)	pass (0.57)	pass (0.82)	pass (0.53)	pass (0.51)
[a]T-Value test	pass (4.29)	pass (3.56)	pass (4.73)	pass (4.40)	pass (1.80)
[a]Sign-product test	pass (5)	pass (8)	pass (2)	pass (7)	pass (4)
[a]Negative first differential test	fail (14)	fail (17)	fail (12)	fail (12)	fail (13)

Calibration intervals and significance levels for each test are noted as follows: [1]Calibration time period = 1900-1959 and verification time period = 1960-1995, [a]Significant at $p < 0.05$, [b]Significant at $p < 0.025$. Significance levels for the six tests are as follows: $r = 0.95 > 0.28$, $r = 0.975 > 0.33$, $RE > 0.08$ T-value > 1.7, Sign/product <= 12, Negative first differential <= 11. Values of n for all tests is n = 36.

2. The user next selects the climate parameters to be altered (Figure 8.2b), with the amount of alteration allowed based upon known seasonal patterns for Vancouver Island (Environment Canada 1996). For example, the user is able to make scaled precipitation adjustments of ± 3 to 75 mm in January to ± 1 to 30 mm for August. If no selection is made, future growth is predicted using the100-year temperature and precipitation averages from the Nanaimo climate station data.

3. Finally, the user selects a time interval (up to 20 years) over which the prediction is to be made (Figure 8.2c). In all cases, because the previous year s conditions have been shown to have a significant impact on growth in the current year, these conditions are incorporated in the model (i.e., previous year May to December temperature and precipitation). For the first year of a run, the previous year s climate parameter is based on the 100 year average of radial growth; for successive years the calculated increment is saved for use in the next year s calculation. Since all trees grow at different rates, based on age and species, the calculations are standardized so that average growth is equal to one. Departures above and below one standard deviation from the average signify when growth will be above or below normal growth rates.

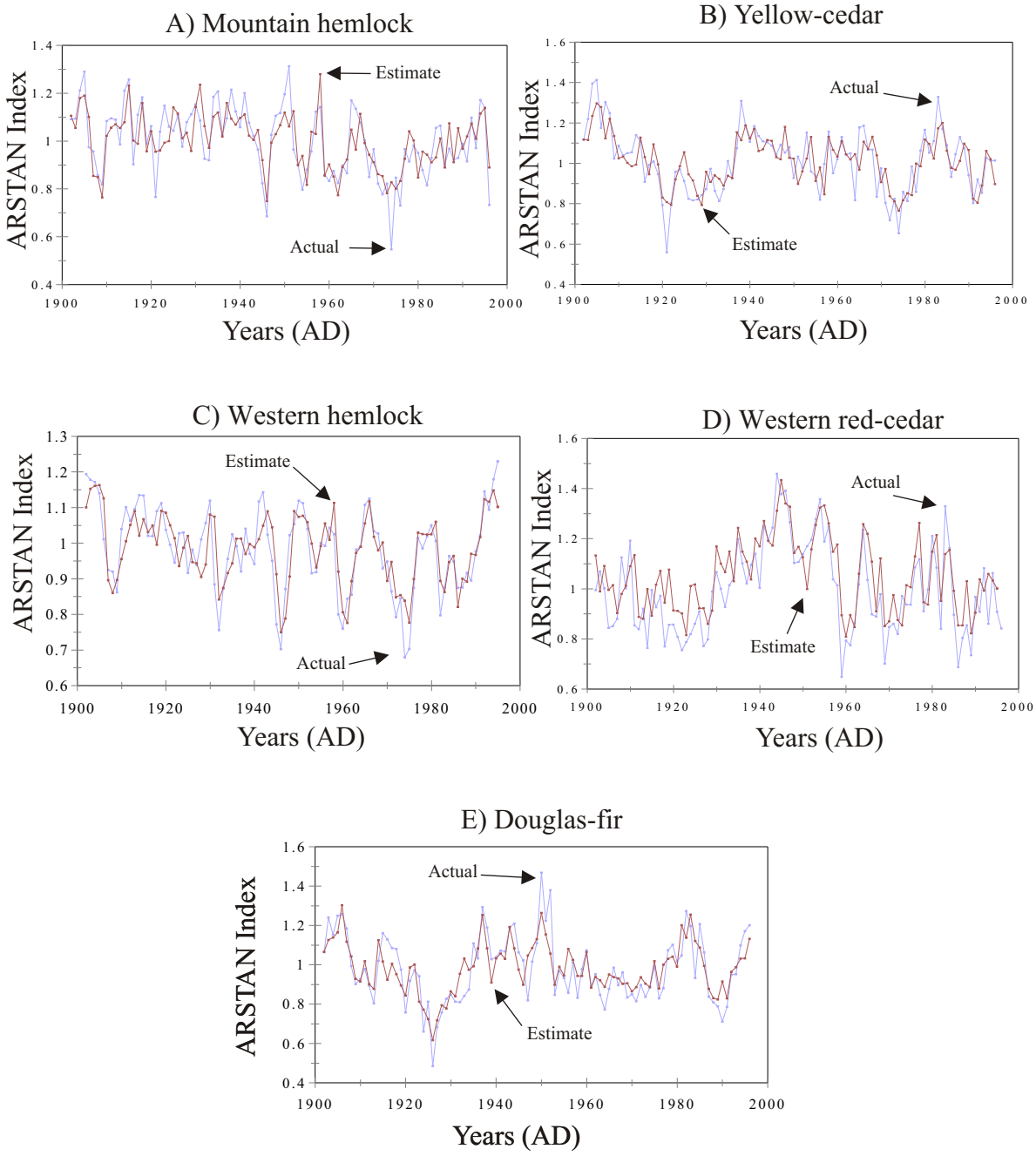

Figure 8.1 - The five reconstructions made with the multiple regression equations developed for the *TREE* model.

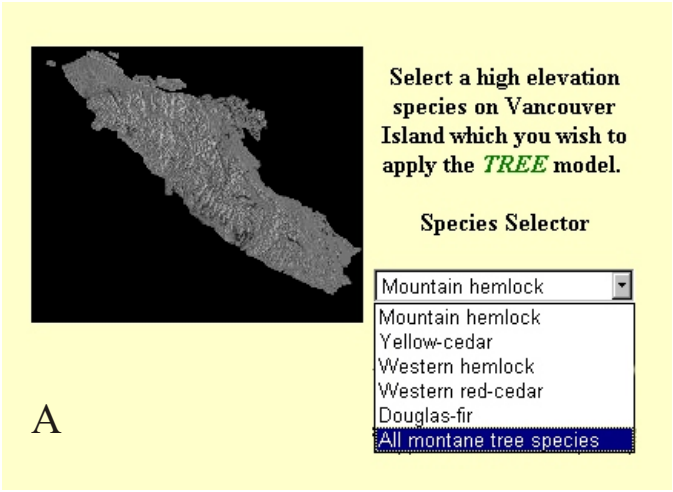

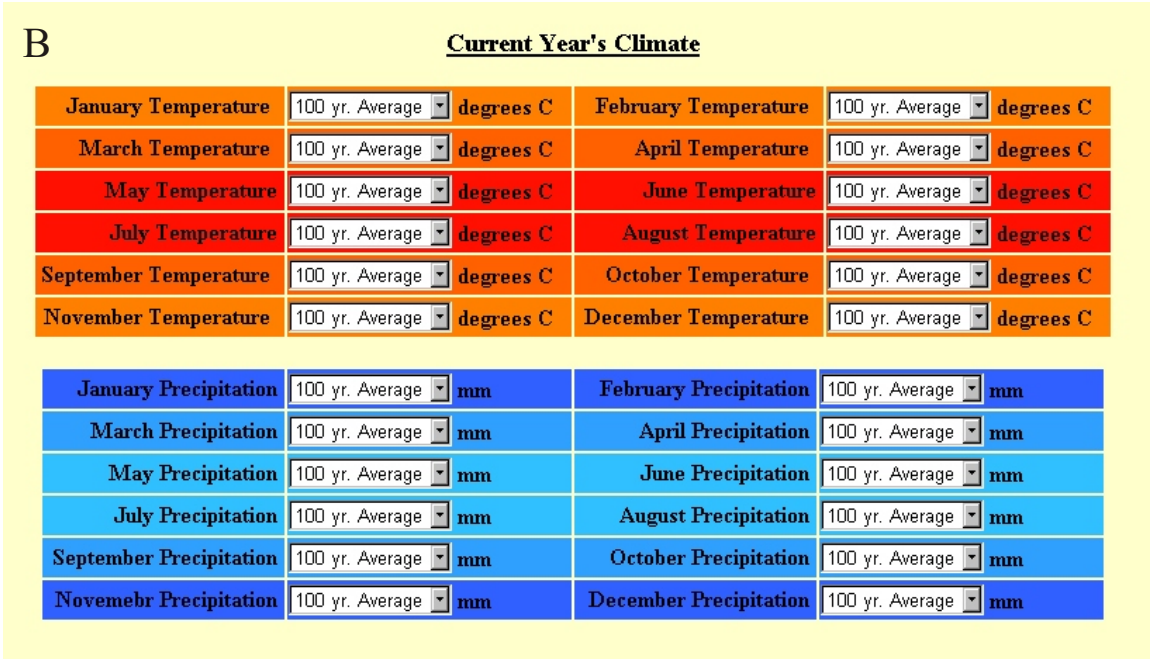

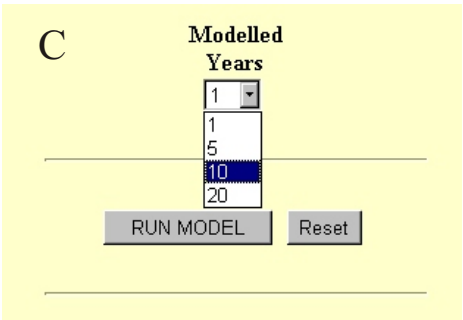

Figure 8.2 - Components of the input screen for the *TREE* model. A) The species selector. B) The climate parameter selector. C) The time interval selector.

The outputs of TREE are presented as schematic tree symbols which increase or decrease in size depending upon the predicted annual enhancement or reduction in radial growth, and as standardized ring-width values (Figure 8.3). Iterations are performed for the user-defined number of years and appropriate image sizes are displayed beside each year. Since the climate changes induced by the operator are static (i.e., they are altered from the past, but do not change in the future), most dramatic changes in radial-growth persist for only a few years, stabilizing in most cases by the 5th or 6th year.

8.3 Long-term Forecasting

A number of global circulation models (GCMs) have been developed in the last decade that are designed to forecast climatic changes likely to occur at the decade to century scale (e.g., Flato *et al.* 2000, Grassl 2000). These analyses have generated climate predictions that are, in most cases, quite different from the recorded historical changes for most regions (Allan *et al.* 2000, Hegerl *et al.* 2000).

This section presents a methodological framework that uses selected GCM outputs to forecast ring growth for the next century. These analyses provide an opportunity to forecast the radial-growth behaviour of selected species over the long term.

8.3.1. Methods

The following analyses were completed using GCM climate data generated by the Canadian Climate Centre (http://www.cccma.bc.ec.gc.ca/eng_index.html, accessed November 16, 2001). Sets of predicted temperature and precipitation data are considered under three different scenarios:

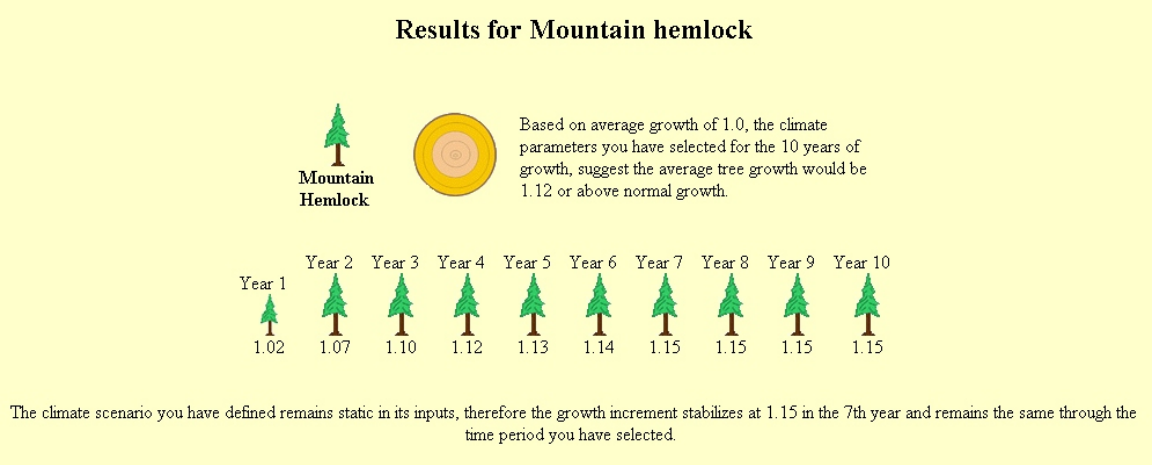

Figure 8.3 - Sample output screen from the *TREE* model. The output relates the average growth increment and whether the increment is above-, normal or below-average growth. It also relates the length of the analysis and each year's growth increment, as well as what year the growth increment stabilizes.

1. A 1x CO_2, second-generation Atmospheric General Circulation Model (AGCM2) for the period 2001-2020 AD. The outputs of this model are based on CO_2 changes in the atmosphere from 1850 to present (McFarlane *et al.* 1992), which are assumed to continue at the same rate into the future. The AGCM2 is used in seasonal climate forecasts and for modelling atmospheric changes (e.g., Boer *et al.* 1992, McFarlane *et al.* 1992, Zweirs 1996, Reader and Boer 1998, Holzer 1999).

2. A 2x CO_2, AGCM2 for the period 2001-2020 AD using the same model as above, except that the CO_2 forcing is calculated at a doubled rate.

3. A second generation Coupled General Circulation Model (CGCM2) with data provided from 1900 to 2100 AD. The CGCM2 couples the AGCM2 with an ocean component (a modular ocean module and a sea ice model) to better model ocean-atmosphere interactions (Flato *et al.* 2000, Flato and Boer 2001). CO_2 forcing in the CGCM2 model is derived from measured rates of change from 1900 to1996 and is calculated as annual one percent increases in CO_2 for the remaining years.

In order to apply the results, a 3.75 x 3.75 GCM grid was selected that is centred over 50 10' N latitude, 127 50' W longitude. The grid encompasses the northern two-thirds of Vancouver Island, a portion of the British Columbia Coast Mountains and a large portion of the nearby Pacific Ocean (Figure 8.4). Precipitation data from the grid are calculated in mm/day, which then have to be summed as monthly totals for comparison. Temperature data are reported as monthly means in C.

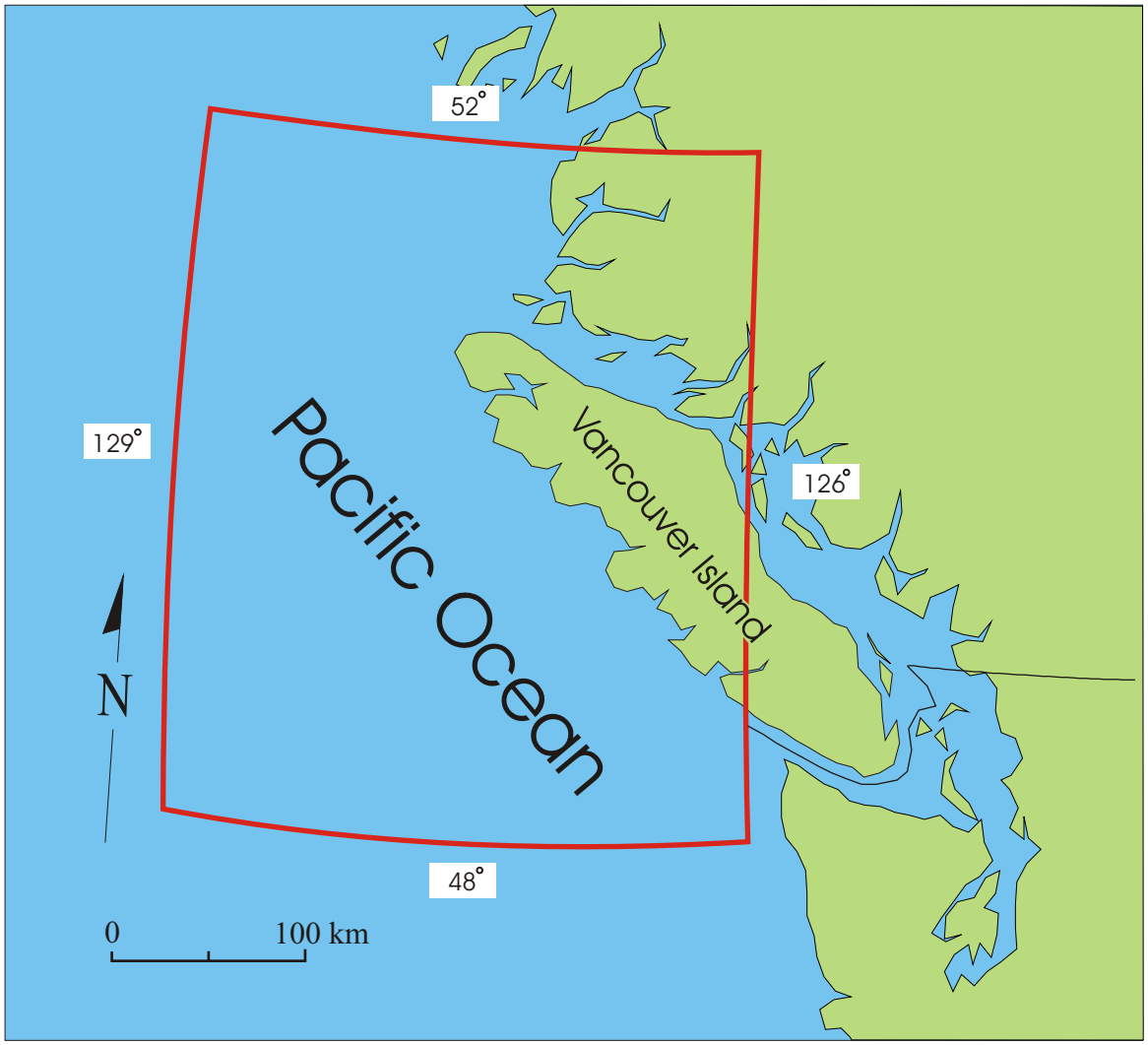

Figure 8.4 - A map of the area of the 3.75 ◦longitude x 3.75 ◦latitude grid square from which the GCM data was derived.

The CGCM2 data were compared to the Nanaimo and Quatsino climate data sets over the period 1900-2000. The GCM precipitation totals were found to be consistently higher in all months than were actually recorded at Nanaimo, most likely due to the large area of ocean covered by the grid square (Figures 8.4 and 8.5). Conversely, the Quatsino data set produced larger actual monthly average precipitation totals in all months compared to the GCM data (Figure 8.5). Recorded summer temperatures from the climate stations were equivalent to or exceeded the modelled data from the grid square (Figure 8.6). Autumn, winter and spring temperature data from the two stations indicated much cooler conditions existed at Nanimo and Quatsino than were predicted by the CGCM2 data from the grid (Figure 8.6). In December and January, the modelled temperatures were on average 6 °C warmer for the time period 1900-2000, and increased to 8 °C warmer for 2000-2100 forecast, when compared to the 1900-2000 temperature average from the station data. The forecasted temperature data for the grid square slowly warms from 2000 to 2100, attaining its highest levels at the end of the record.

The AGCM2 1x data generates precipitation values that closely follow those forecasted by the CGCM2 for 2000-2020, while the AGCM2 2x data set is considerably drier (Figure 8.7). Temperature values are more uniform among the three data sets. The 1x CO_2 data set produced the coolest forecasted temperatures, with the CGCM2 data predicting conditions approximately 2 °C warmer and the 2x data 1 °C warmer over the 20-year time period (Figure 8.8).

The three general circulation modelled data sets are regarded as reliable and consistent representations of the grid square climate over time. The duration of the

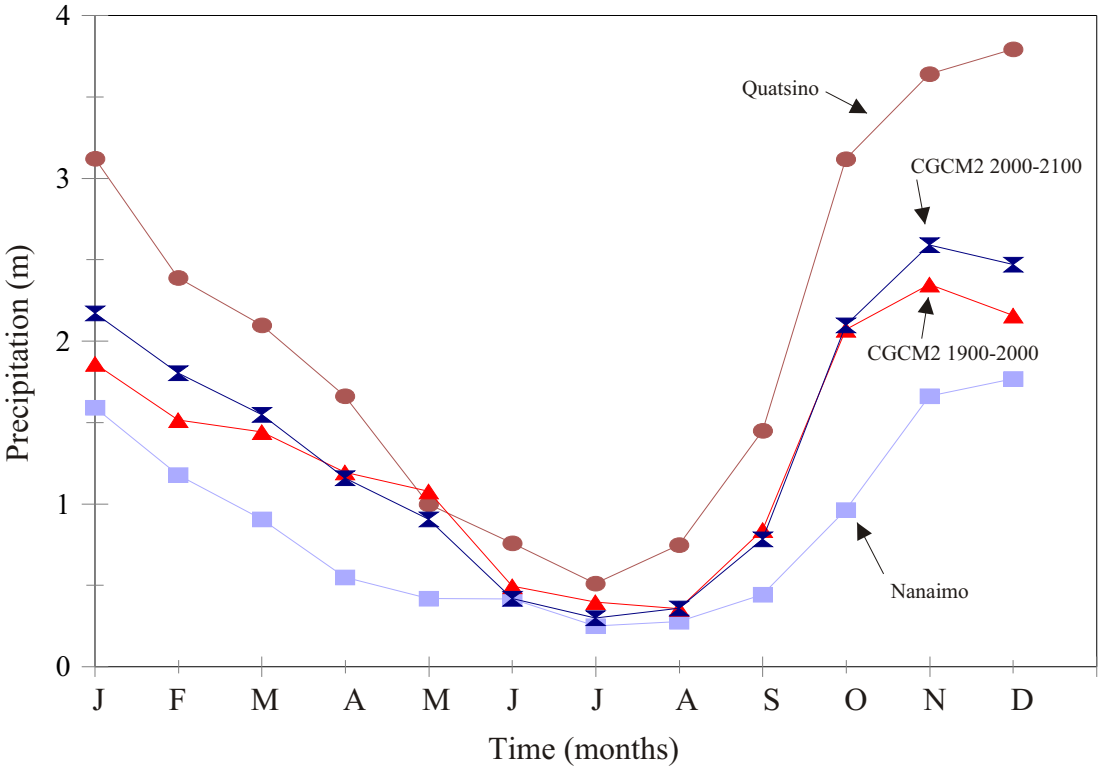

Figure 8.5 - Precipitation monthly averages from Nanaimo, Quatsino, and the CGCM2 data from 1900 to 2000, as well as the CGCM2 average monthly data from 2000 to 2100.

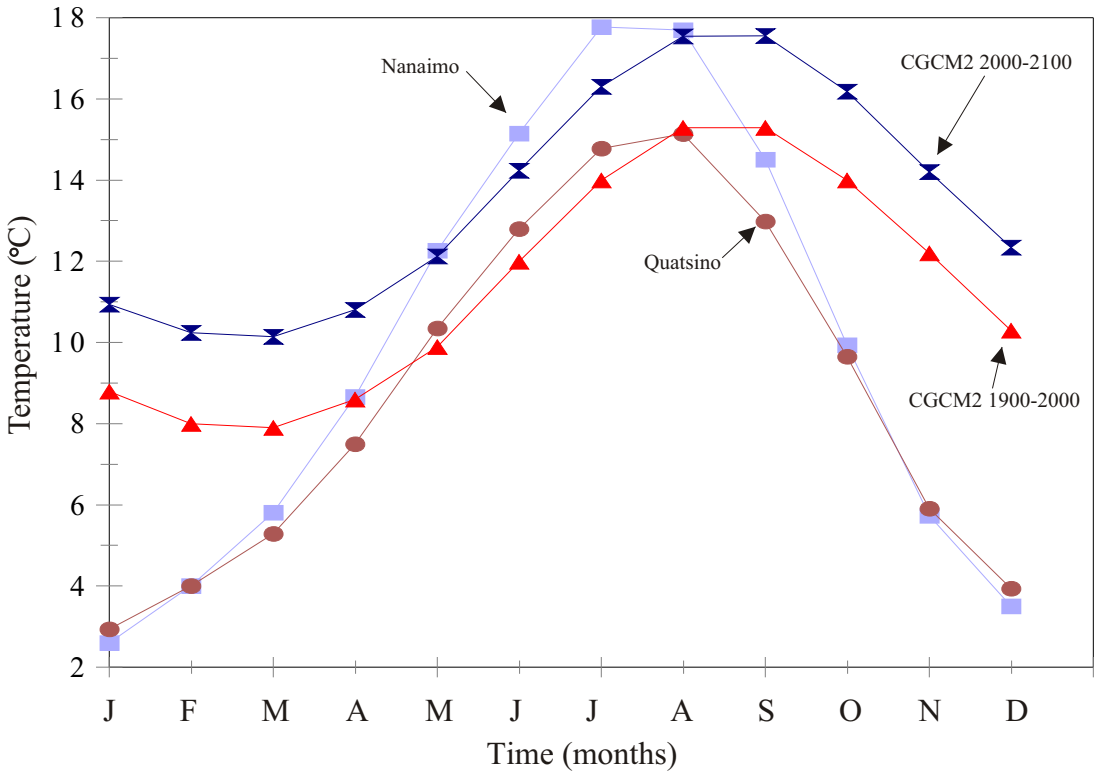

Figure 8.6 - Monthly temperature averages from Nanaimo, Quatsino, and the CGCM2 data from 1900 to 2000, as well as the CGCM2 monthly average data from 2000 to 2100.

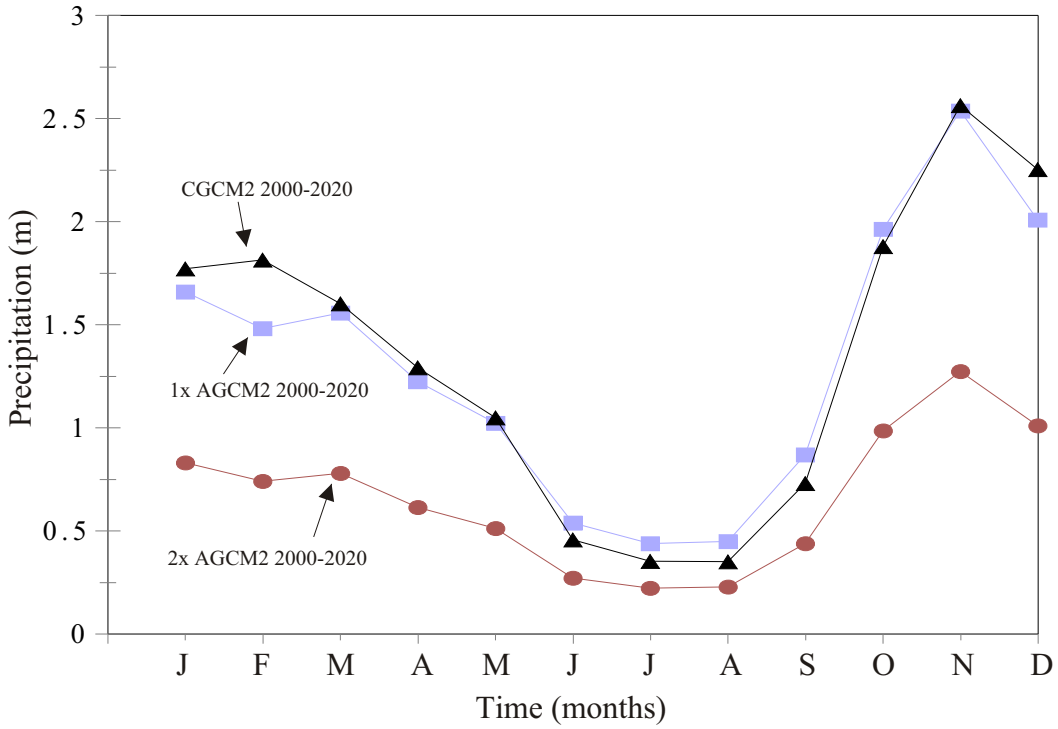

Figure 8.7 - Average monthly precipitation data from the grid square for the ACCM2 1x, AGCM2 2x and CGCM2 models over the period 2000-2020.

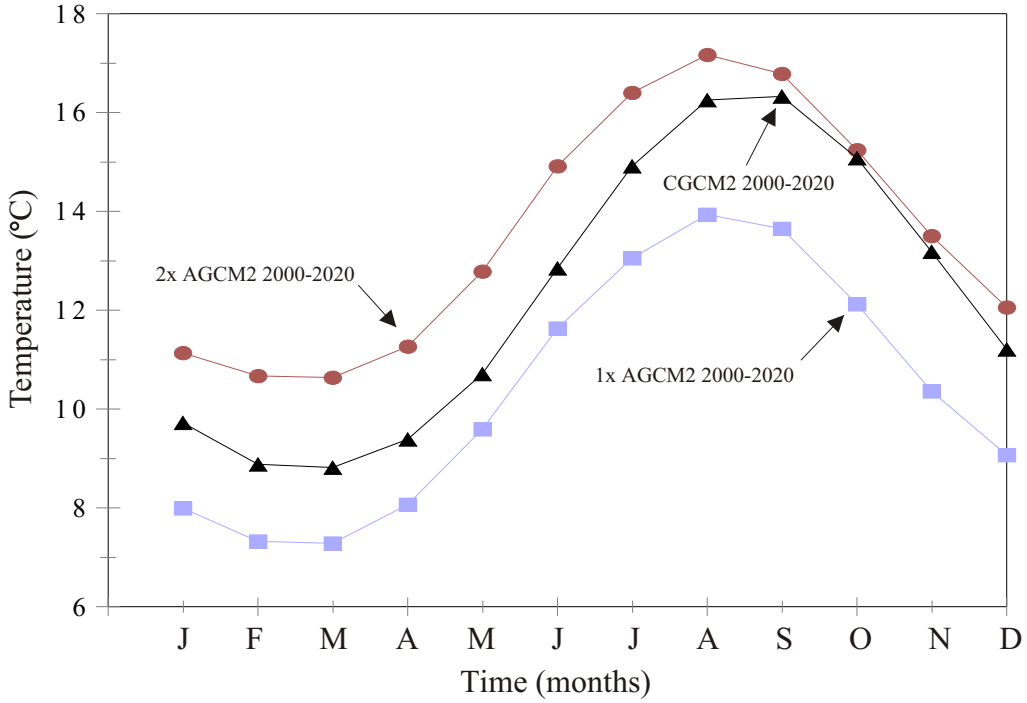

Figure 8.8 - Average monthly temperature data from the grid square for the ACCM2 1x, AGCM2 2x and CGCM2 models over the period 2000-2020.

Table 8.3 - Results of a stepwise multiple regression analysis predicting radial growth using precipitation and temperature variables from GCM data (1900-1995). All models have a one year lag parameter included in each model and are significant at $p < 0.0001$.

Dependant variable	Explained r (r^2)	Equations
Master mountain hemlock	0.68 (0.46)	MH = (Apr temp*0.0009713) + (Aug precip * -0.000164) + (Dec temp * -0.0068) + (July temp * -0.000756) + (June temp * 0.002581) + (March temp * 0.001146) + (May precip * -0.0000529) + (previous Dec precip * -0.0000279) + (previous July precip * -0.0000531) + (Previous July temp * -0.00532) + (previous June precip * 0.0000711) + (MH lag * 0.43) + (Constant) 1.798
Master yellow-cedar	0.67 (0.46)	YC = (Aug temp * -0.002814) + (Feb precip * -0.000000 09007) + (July temp * 0.001224) + (previous July temp * -0.004403) + (previous Nov Precip * -0.00000823) + (previous Oct temp * 0.008047) + (previous Sept temp * -0.002886) + (YC lag * 0.614) + (Constant) 0.601
Master western hemlock	0.71 (0.50)	WH = (Apr temp * -0.0001762) + (Aug precip * -0.0000 5854) + (Jan precip * 0.000008 454) + (June temp*0.0008377)+ (previous Aug precip * -0.00002815) + (previous July temp * -0.001095) + (previous Sept precip * -0.00003183) + (WH lag * 0.672) + (Constant) 0.434
Master western red-cedar	0.67 (0.45)	WRC = (Feb temp * 0.002756) + (June temp * 0.001086) + (July precip * 0.00004456) + (May precip * 0.00001717) + (previous Aug temp * 0.007483) + (previous Dec precip * 0.00002349) + (previous July precip * 0.00005170) + (previous July temp * -0.00323) + (previous Nov precip * -0.00001205) + (previous Oct precip * -0.000009412) + (previous Oct temp * -0.00004719) + (previous Sept temp * -0.008824) + (WRC lag * 0.655) + (Constant) 0.598
Master Douglas-fir	0.63 (0.40)	DF = (May precip * 0.000005043) + (Nov precip + -0.00002028) + (Previous June precip * -0.0000117) + (previous July precip * -0.00003991) + (previous May temp * -0.001692) + (Sept precip * 0.00003080) + (DF lag * 0.625) + (Constant) 0.575

radial-growth indices allows for standard calibration and verification procedures to be conducted, allowing for further modelling. The same climate variables that were used in the *TREE* model regression equations (Table 8.1) were entered into SPSS (Version 7.5, 1996) to produce new long-term radial-growth regression equations using the GCM data (Table 8.3).

A 60/40 split of the data set was again used for the calibration/verification procedure for the same period as the short-term analysis (Table 8.3). The models explain between 40 and 50 percent of the variance in radial growth, with all models passing five of the six goodness-of- fit tests in the VFY program (Holmes 1999)(Table 8.4).

Table 8.4 - Results of the goodness-of-fit tests for the forecast models developed by the GCM calibrated data. Each test is listed as pass or fail with the statistical values in brackets.

	Mountain hemlock	Yellow-cedar	Western hemlock	Western red-cedar	Douglas-fir
[a]Correlation (r)	pass (0.60)	pass (0.55)	pass (0.81)	pass (0.34)	pass (0.63)
[b]Correlation (r)	pass (0.60)	pass (0.55)	pass (0.81)	pass (0.34)	pass (0.63)
[a]Reduction of Error test	pass (0.62)	pass (0.33)	pass (0.68)	pass (0.17)	pass (0.45)
[a]T-Value test	pass (4.44)	pass (2.83)	pass (3.86)	pass (1.49)	pass (2.72)
[a]Sign-product test	pass (7)	pass (11)	pass (4)	pass (9)	pass (4)
[a]Negative first differential test	fail (14)	fail (24)	fail (15)	fail (18)	fail (18)

Calibration intervals and significance levels for each test are noted as follows: Calibration time period = 1937-1995 and verification time period = 1901-1936, [a]Significant at $p < 0.05$, [b]Significant at $p < 0.025$. Significance levels for the six tests are as follows: $r = 0.95 > 0.27$, $r = 0.975 > 0.32$, RE >0.07 T-value>1.69, S-P<= 12, Neg F.D.<= 12.

8.3.2 Results

The actual radial-growth increments and the predicted growth from the CGCM2 data set for mountain hemlock are displayed in Figure 8.9a. The mountain hemlock model explains a low amount of explained variance, but the equation is still thought to effectively predict future growth (46 % of the variance explained). Mountain hemlock radial growth remains near its long-term mean range of variation until approximately 2030, when a steepening decline in ring width is initiated. From 2030 until 2100, mountain hemlock radial growth continues to decline until eventually surpassing even the worst recorded growth for the species by the 2060s.

The response of yellow-cedar to future climates is displayed in Figure 8.9b. For the first 40 years the radial growth of yellow-cedar is near the historical average and never exceeds the recorded range of variation. For the following 60 years, radial growth remains at or near the low end of the long-term range of variation.

The response of western hemlock to future climates is shown in Figure 8.9c. Similar to mountain hemlock, western hemlock radial-growth is reduced from the beginning of the 21st century. Radial growth returns to values near the long-term mean by 2040, and from there the two hemlock species growth patterns differ greatly. While the radial growth of mountain hemlock is greatly reduced, western hemlock growth increments slowly decrease in size, but still match a range of variation that characterized 20th century growth.

Figure 8.9d displays the predicted radial growth trend of western red-cedar based on future CGCM2 climate data. Western red-cedar exhibits a sudden increase in radial

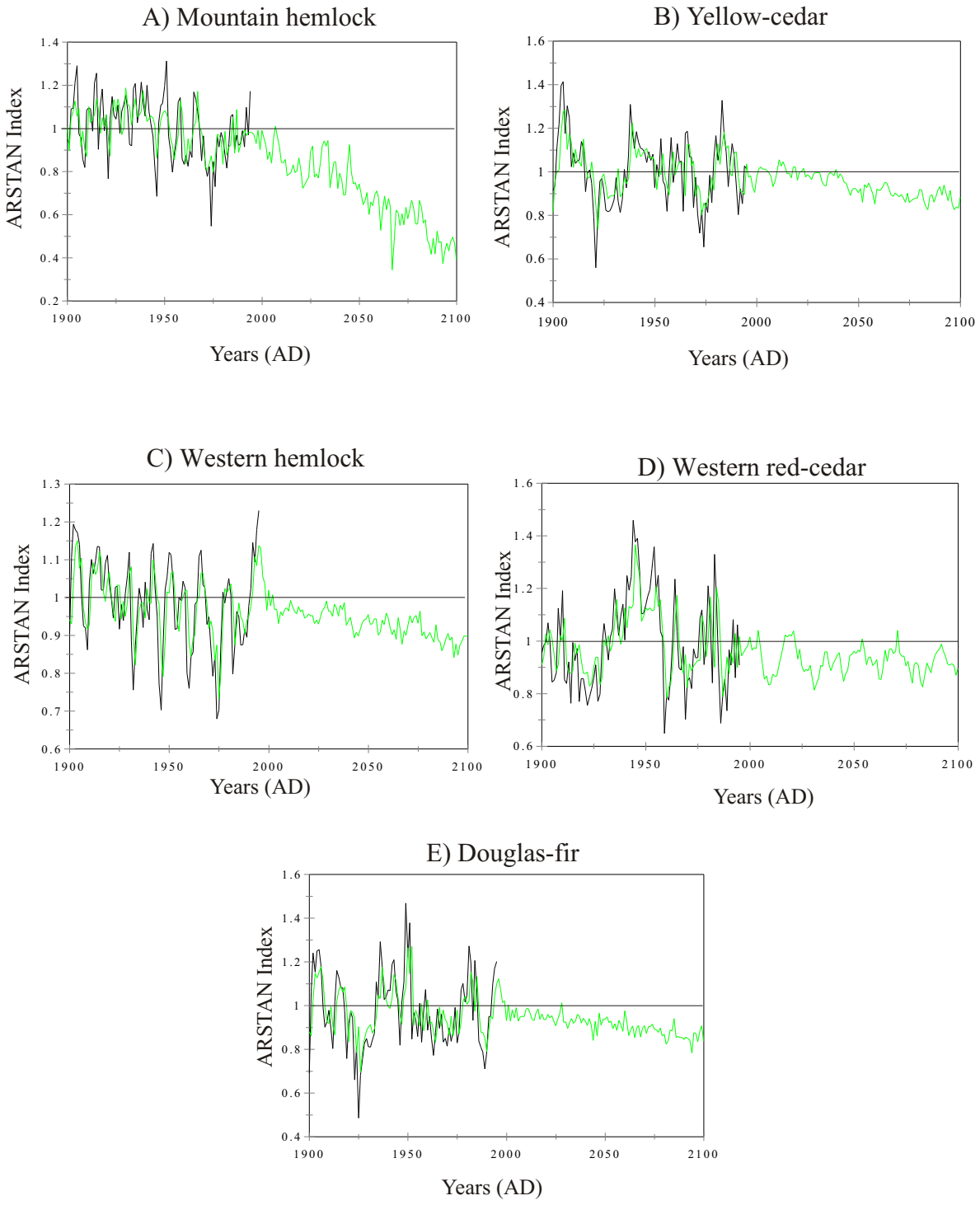

Figure 8.9 - Actual and predicted long-term radial growth trends for all species in the study. Predicted radial growth is based on CGCM2 data.

growth, followed by an equally sudden reduction in growth in the first 10 years of the new century. Radial growth slowly recovers throughout the 2010s and 2020s, until it regains a position slightly above the historical 20th century average. In the 2030s, the western red-cedar radial-growth rate again decreases, only to increase to average levels throughout the late 2050s and the 2060s. Western red-cedar radial growth maintains near average levels until 2100, where it has a below-average growth rate at the end of the forecast.

The forecasted long-term radial growth behaviour of upper-elevation Douglas-fir is shown in Figure 8.9e. The annual increments have values slightly below the long-term mean for almost the entire record. In the years immediately after the turn of the 21st century, Douglas-fir has a few years when growth at the historical average is exhibited. However, by 2010 annual radial growth slowly decreases until 2100, despite a series of minor increases and decreases in increments throughout the interval.

Test results for the 1x and 2x CO_2 changes to the atmosphere from the AGCM2 data are represented in Figures 8.10 and 8.11. The 1x atmospheric CO_2 increase to climate, maintains radial-growth increments near the long-term mean values for two of the species (western hemlock, and Douglas-fir) (Figure 8.10). Under these conditions, mountain hemlock and western red-cedar show a considerable increase in radial growth and maintain these elevated levels throughout the record (Figure 8.10). Yellow-cedar displays a reduction in its radial-growth increments based on the predicted 1x CO_2 climates and maintains a slightly reduced increment throughout the forecast period (Figure 8.10).

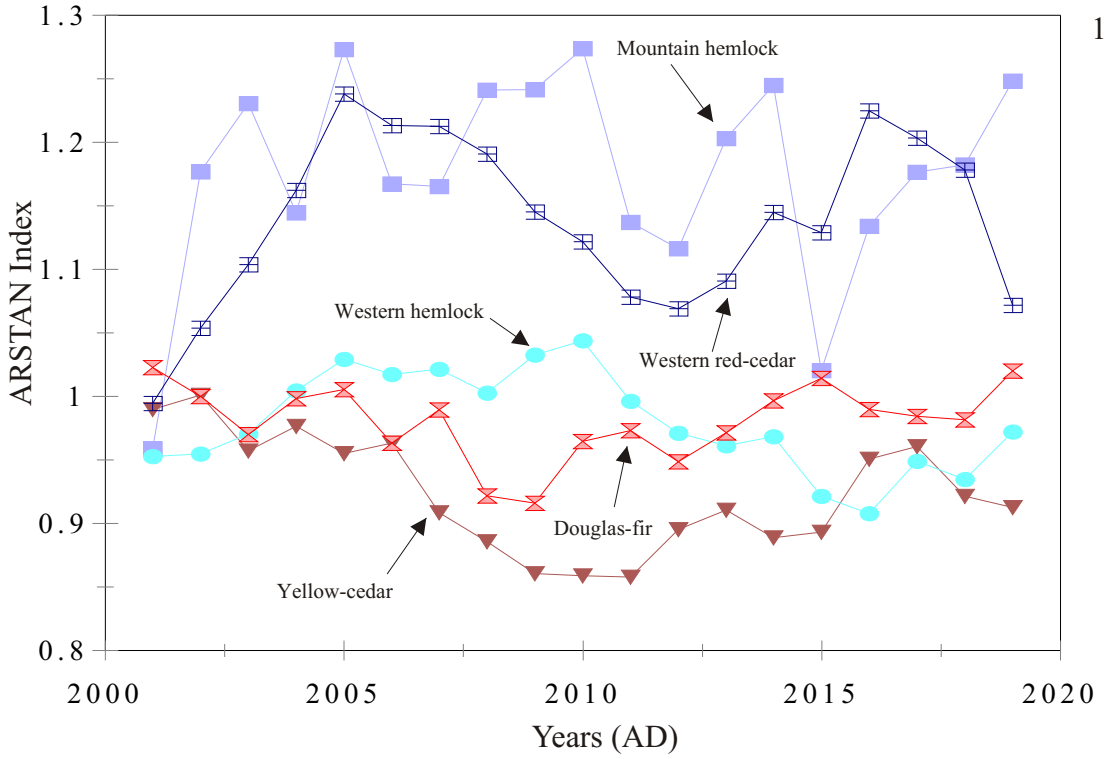

Figure 8.10 - Predicted radial growth trends for all species. Radial growth is based on the 1x CO2 AGCM climate data.

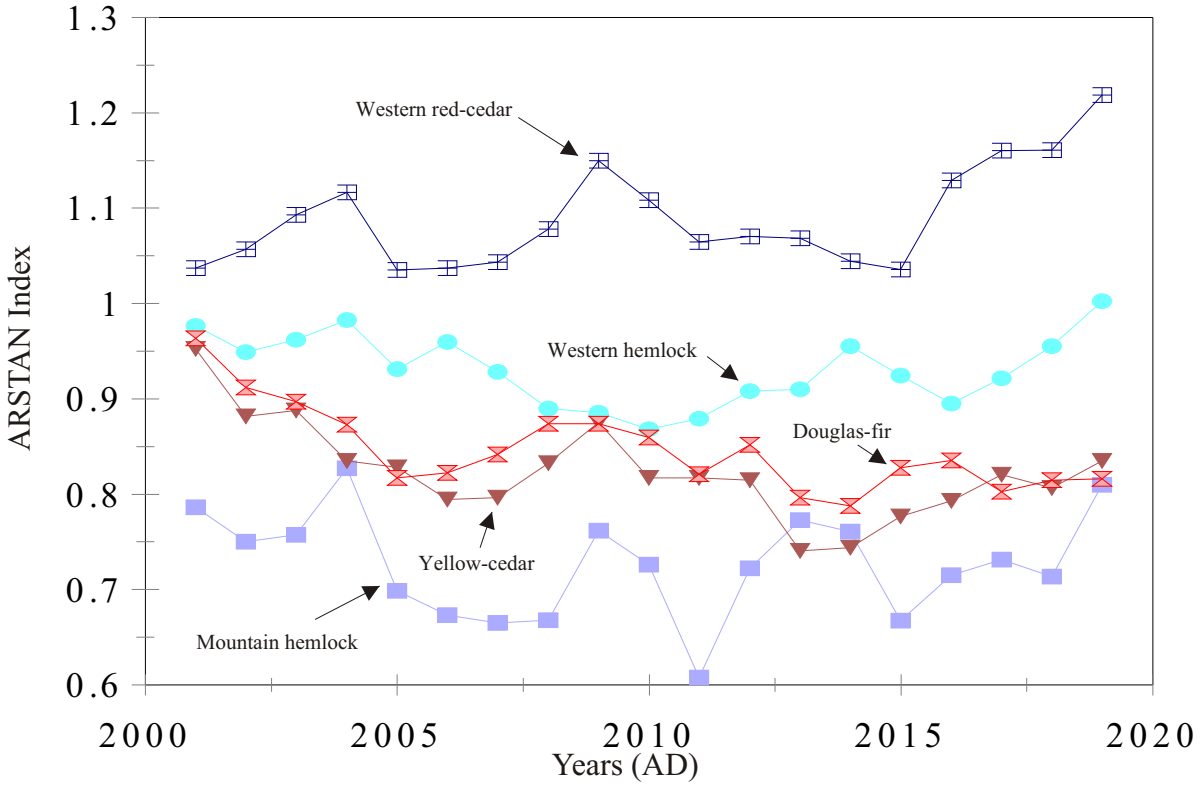

Figure 8.11 - Predicted radial growth trends for all species. Radial growth is based on the predicted 2x CO2 AGCM data.

Two x CO_2 changes to the atmosphere result in growth responses that are moderate compared to those of a 1x CO_2 environment. Western red-cedar continues to demonstrate enhanced radial-growth, but the elevated level is less pronounced when compared to that accompanying a 1x CO_2 atmospheric changes (Figure 8.11). Mountain hemlock attains below-average radial growth throughout the record, which differs markedly from the 1x CO_2 forecast (Figure 8.11). Western hemlock experiences a reduction in radial growth in the middle portions of the forecast, but recovers to near-average radial growth by 2020 (Figure 8.11). Douglas-fir and yellow-cedar continue to exhibit a reduction in radial growth under a 2x CO_2 environment, but the level of reduction is slightly more than was predicted under the 1x CO_2 environment (Figure 8.10).

8.4 Discussion

8.4.1 Short-term Forecasting

Experimentation with the *TREE* model highlights the capacity of forests to respond to future climate changes. It is apparent that generalist species such as yellow-cedar (Antos and Zobel 1986, Russell 1993) are better able to adjust to climatic changes, since no single factor limits their growth to a high degree. Conversely, a species like mountain hemlock will be able to cope with the short-term climatic changes provided alterations do not positively or negatively affect a crucial parameter in their radial-growth cycle.

8.4.2 Long-term Forecasting

The CGCM2 data set is not a perfect replicate of any single land-based station on

Vancouver Island, but it does provide a consistent interpretation of the known climate pattern for use in modelling radial growth. The precipitation extremes in the data set are all matched or exceeded in land-based records, but the temperature extremes are higher than what is generally seen on land, especially in winter months.

The CGCM2 data predicts that most high-elevation tree species on Vancouver Island will continue to grow well. An exception to this is mountain hemlock which shows more degeneration in radial growth over time than any other species. The effect of a drier springtime (when mountain hemlock usually enjoys a wetter environment) is partly driving the reduced growth potential of the species. Figure 8.2 illustrates reduced April, May, and June precipitation from the 20th to 21st century in the modelled data. The response function created in Chapter 5 from 20th-century data put an emphasis on the importance of April, May, and June spring precipitation for radial growth in mountain hemlock trees. Changes in precipitation totals manifest themselves in greatly reduced radial growth later in the 21st century. It is also unknown how the state of the precipitation (i.e., snow vs rain) will affect the growth of mountain hemlock since both forms of precipitation have been shown to have different effects on radial growth (Peterson and Peterson 2001). The last unknown, is whether mountain hemlock already has the ability to adjust its tree-time to take advantage of the forecasted wetter months before April to maintain an average rate of radial growth.

The second factor that may be responsible for the forecasted reduction in the radial growth in mountain hemlock is the lag factor that was built into the regression model to explain a large amount of the variance in its radial growth. The high

autocorrelation values from Chapter 3 suggest that poor growth in the previous year should have a strong negative effect on radial growth in the current year. Compounding negative inputs to the growth equations will then make a current year s radial growth continually susceptible to the previous year s reduced growth. What is not known is if the natural one year lag in radial growth behaves as predicted, or will it react differently when unusually small rings are produced in multiple consecutive years.

Lag factors are common parameters to incorporate into forecast models (Abraham and Ledolter 1983, Geisser 1993, Aitchison and Dunsmore 1975), but to determine if the lag variable coefficient was driving the model to a greater degree than the climate variables, an additional examination of the data was necessary. The same three step procedure, as outline above, for the selection of variables to be included into the regression equations was conducted. In this analysis, the one year lag variable was intentionally excluded from the stepwise selection of the most significant climate variables on radial growth. To select a similar number of climate variables for the equation, the F to enter and F to remove limitations in the stepwise multiple regression were set at less restrictive boundaries of 0.20 and 0.25 respectively.

Table 8.5 displays the new regression equations for each species, while Figure 8.12 displays the forecasted growth for each tree species without using the lag variables. A comparison between the two scenarios suggests that they display similar trends. For instance, in both scenarios mountain hemlock radial growth declines through time. This behaviour is interpreted to signal that, although lag factor mechanics do contribute to the downward trend in radial growth within one scenario, the climate forecast scenario shows

Table 8.5 - Results of a stepwise multiple regression analysis predicting radial growth using precipitation and temperature variables from GCM data (1900-1995). All models ***do not*** have a lag parameter included to determine the effects of the lag parameter from previous models.

Dependant variable	Explained r (r^2)	Equations
Master mountain hemlock	0.48 (0.23)	MH = (Apr temp*-0.00266) + (Dec temp * -0.00649) + (July temp * -0.00231) + (June temp * 0.01008) + (Oct temp * -0.00169) + (previous Dec precip * -0.0000342) + (previous July temp * -0.00231) + (Previous June precip * 0.00002676) + (previous Nov precip * -0.0000404) + (previous Nov temp * -0.00552) + (Constant) 2.164
Master yellow-cedar	0.28 (0.08)	YC = (Aug precip * -0.0002) + (Aug temp * -0.012) + (Dec temp * 0.0005637) + (Feb precip * -0.00000165) + (July temp * 0.006907) + (Nov precip * -0.00000473) + (previous Jun precip * 0.00007536) + (previous Oct temp * 0.006292) + (Sept precip * -0.0000117) + (Constant) 0.997
Master western hemlock	0.26 (0.06)	WH = (Apr temp * 0.0002792) + (Dec temp * -0.00265) + (Mar precip *- 0.0000113) + (Oct temp * -0.000747) + (previous Aug precip * -0.000129) + (previous July precip * -0.0000586) + (previous July temp * 0.002098) + (previous Nov temp * -0.00244) + (Constant) 1.427
Master western red-cedar	0.41 (0.17)	WRC = (Feb temp * -0.00107) + (July precip * 0.0001564) + (June precip * -0.0000727) + (June temp * 0.0005966) + (Mar precip * 0.00006542) + (Nov precip * -0.0000142) + (previous Aug temp * 0.0009004) + (previous July precip * 0.000181 9) + (previous Oct precip * -0.0000109) + (previous Oct temp * -0.0027) + (Constant) 1.113
Master Douglas-fir	0.19 (0.04)	DF = (Nov precip * -0.000021) + (previous July precip + 0.0000548) + (Previous June precip * -0.0000732) + (previous May precip * 0.00002144) + (previous Nov precip * -0.0000065) + (Sept precip * 0.00004303) + (Sept temp * 0.002373) + (Constant) 0.635

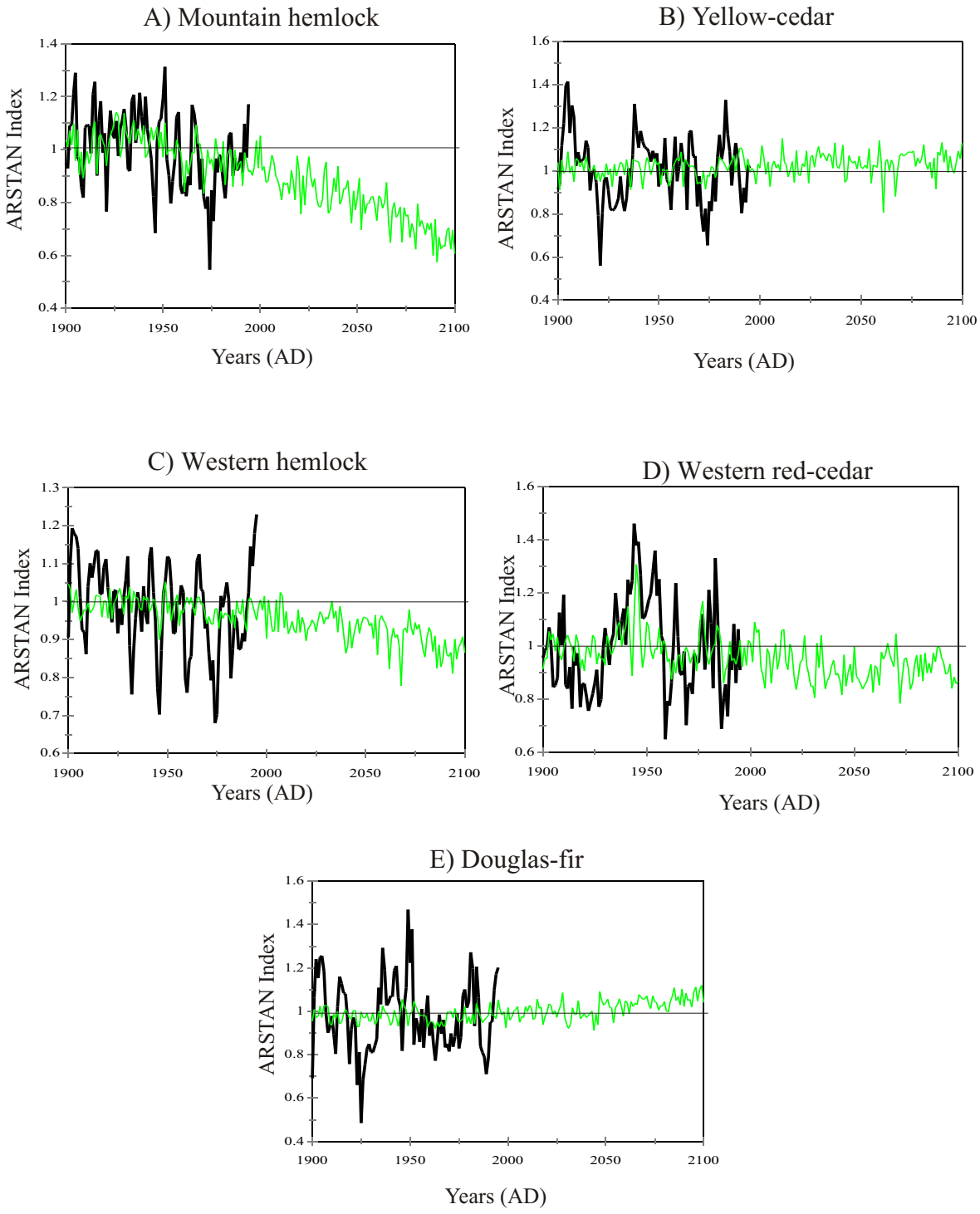

Figure 8.12 - Actual and predicted long-term radial growth trends for all species in the study. Predicted radial growth is based on CGCM2 data. All models do not have a lag parameter included in the regression equation.

the same trend. The offset of spring-like conditions to earlier in the season, is thus considered to be the single most important factor driving the continuing decline in the radial growth of mountain hemlock. As previously mentioned, it is impossible for the model to predict if mountain hemlock on Vancouver Island will produce normal radial growth increments under shifting spring climates, as this type of displacement is unprecedented in the historical record.

Both short-term and long-term forecast models can never adequately model the natural ecological amplitude or plasticity inherent to each tree species. Nevertheless, if mountain hemlock is not able to adjust to the forecasted climate changes, then it is anticipated that lower elevational stands are likely to become increasingly senescent and eventually die. There is also some probability that the elevation extent of mountain hemlock trees may increase as more favourable conditions for germination become commonplace beyond the present altitudinal treeline. For the case of Vancouver Island though, this reaction would be somewhat diminished as there is no higher terrain to move too.

The radial growth trends for the remaining tree species show similar trends under both model conditions (Figures 8.9 and 8.12). Western hemlock shows a slightly larger reduction in growth than the other species (Figure 8.12c), similar to Figure 8.9c. Yellow-cedar, western red-cedar and Douglas-fir all show little difference in the radial growth trends over the forecast period from one growth scenario to the other (Figure 8.12b, 8.12d, and 8.12e).

9.0 Conclusions

The aim of this research program was to examine the growth response of high-elevation conifers on Vancouver Island to climate. To do this, multiple species from a high-elevation coastal network were used to: describe radial-growth changes over time and space on Vancouver Island; to establish individual tree-times of each species by relating the timing and responses of the radial growth of these trees to known climatic parameters; and, to develop improved climate/radial-growth models capable of predicting the effects of past, present and future climates on selected conifer species. The results of these analyses suggest that better proxy climate records can be developed in Pacific North America by using selected chronologies from multiple tree species to shed light on the natural range of past climates.

Chapter 3 details the first thorough dendrochronological examination of upper-elevation tree species on Vancouver Island. With more than 30 chronologies developed for mountain hemlock and yellow-cedar, the dendroclimatological potential of both species is better understood. Mountain hemlock was found to be the most consistently useful species with high mean series correlations (mean = 0.490), strong mean sensitivity values (mean = 0.251), and relatively low autocorrelation values (mean = 0.729). Yellow-cedar followed closely with mean series correlation (mean = 0.433), mean sensitivity (mean = 0.253), and mean autocorrelation values (mean = 0.764). Western hemlock, western red-cedar and Douglas-fir, were found to lag behind mountain hemlock and yellow-cedar in usefulness, but the low numbers of trees sampled, and difficulties encountered when crossdating (especially with western hemlock), are factors affecting

this result.

The number of cores needed to develop adequate dendroclimatic reconstructions has never been investigated in this setting. This study determined that most of these species are well suited for dendroclimatic research, particularly when 18 or more cores are present in a chronology. This figure must be treated as a guideline only, as some species crossdate poorly (i.e., western hemlock), and may require as many as 25 cores for confident chronology development.

Chapter 4 reveals that the radial growth trends of high-elevation trees on Vancouver Island are consistent across the entire island in most years. Because common growth trends have existed for at least the last 500 years, connections were sought to climate systems in Pacific North America. Master chronologies for each species were constructed and examined to see if there were any links to the three most common oceanic forcing mechanisms (i.e., ENSO, PDO, and PNA). All of the tree species examined (except Douglas-fir) showed a connection to at least one ocean forcing mechanism. No two species displayed the same level of connection to a single mechanism and, as such, point toward each capturing a unique climate signal in their radial growth. Clearly the interactions between radial growth and the various forcing mechanisms are complex, but because the links are present, this finding offers an area for further investigation.

Chapter 5 examined the relationship of the timing of radial growth and to the environment in the Vancouver Island MH zone. This investigation was designed to elucidate the approximate tree-time that determines the physiological behaviour of each

of the five species examined. Initiation of earlywood and latewood cell production, as well as cessation of these radial-growth processes were established. The distinct timing of these events is seen as key to a determination of how each tree species incorporates the environmental parameters that are active at the time of radial growth. A major finding was an understanding of how each species radial-growth cycle was offset. Tree-time cycles showed that mountain hemlock was the first tree species to initiate and cease radial-growth, and as such, early season climate parameters were best captured. Yellow-cedar and western hemlock lagged behind mountain hemlock in initiating radial growth by as much as two or three weeks. The ability to more precisely link specific species to calendar time periods was an essential starting point in developing a multi-species methodology.

By using multiple tree species, and by understanding each species growth response to its environment, multiple aggregate chronologies (MACs) were developed to reconstruct climate parameters. Four specific tests were conducted in order to enhance the climate signal of two seasonal and two monthly parameters. Like single-species chronologies, MACs were better able to predict seasonal parameters then individual monthly parameters. MACs were able to improve climatic models compared to single-species reconstructions, except when the strongest single-species chronologies were used. In all cases, correlations between single-species chronologies and climate parameters culminated in an upper threshold for the relationship. MACs improved the strength of a relationships between radial growth and climate at an average site, up to, or closer to, this threshold. MACs were unable to improve upon the single-species indices that were

already at or near the relationship threshold, but they were able to significantly improve the weak chronologies tested. It is concluded that if the ability to choose the best-correlated index from a large set of indices (e.g., > 25) is not available, then developing MACs by sampling multiple species from a site will likely produce a stronger relationships to climate than a single index can provide.

By selecting and averaging the top five MAC models, calibrated and verified paleoclimatic reconstructions were developed. Two seasonal parameters produced reconstructions with more explained variance than the two single-monthly climate parameters. A 500-year April 1 snowpack reconstruction showed prolonged intervals above and below the historical average snowdepth throughout the reconstruction. These cyclical patterns have modes of variability on various scales and seem to be closely linked to the dominant climate influences from the nearby Pacific ocean. The average June-July temperature reconstruction extends over a 350-year interval and also shows links to cyclical ocean climates. The July precipitation and temperature paleoreconstructions produced significant models, but both were not high in explained variance. Individual monthly parameters continue to be problematic for reconstruction, with extreme event years causing the most trouble in the relationship. The July precipitation model produced a 350-year paleoreconstruction, while the July temperature model produced the longest reconstruction of 800-years. Although not as highly significant as the two seasonal reconstructions, both single monthly reconstructions display common cyclical modes of variability linked to the ocean. Evidence from the long-duration July reconstruction also suggests a mode of variability with an

approximately 130-150-year return period.

Further research needs to be undertaken to determine whether the MAC technique is applicable to other settings where climate-growth relationships have been used to develop proxy models (e.g., PDO, CTI, PNA reconstructions). Theoretically, the MAC technique should display a similar pattern in reconstructing oceanic indices as was seen with seasonal and monthly climate relationships.

Forecast models for radial growth of trees have never before been attempted with climate data. Both short-term and long-term models were developed in Chapter 8. *TREE* (Tree-ring Radial Expansion Estimator) is a short-term model that allows users to define climate change scenarios for up to 20 years to project the effect of the induced set of changes upon one or more selected species. Five species models were built, developing relationships based on Nanaimo climate station data, and were able to explain from 55 to 68 percent of the variance in radial growth. The models were able to account for alterations to yearly precipitation and temperature variables, giving the user the ability to investigate the radial-growth impacts of a wide range of possible climate change scenarios.

Long-term radial growth models were developed using GCM data from the Canadian Climate Centre. Regression analyses established climate-growth relationships for all master chronologies to the GCM data. The strength of these relationships ranged from a low of 40 percent of the variance explained for mountain hemlock to a high of 50 percent for yellow-cedar. Forecasts were made from the data for the years 2000 to 2100 AD.

Mountain hemlock was shown to be the tree species most susceptible to impact from the forecasted climate changes. While the radial growth of the other species examined were shown to experience slight reductions in radial growth over this interval, these were comparably minor when compared to the potential impact on mountain hemlock populations. A test was conducted to see if the reduction in increment of all models was driven by the mechanics of the model or by the changing climate variables. Once the lag variables were taken out of the models, similar tends in overall growth were seen for all scenarios, even though the explanatory power of the models was drastically reduced.

Long-term forecasting as presented in this dissertation is by no means highly certain, as it focusses only on the impact generated by forecasted changes inherent within the Canadian Climate Model. Nevertheless, these predictions of future forest productivity break new ground in that it they use forecasted data to predict growth instead of using growth trend scenarios. Despite any shortcomings of this application, it does provide a starting point for forest managers and forest ecologists to consider what effect future climates may have on tree growth.

References

Aitchison, J., and Dunsmore, I.R., 1975. *Statistical Prediction Analysis*. Cambridge University Press, Cambridge.

Alfaro, R.I., and MacDonald, R.N., 1988. Effects of defoliation by western false looper on Douglas-fir tree-ring chronologies. *Tree-Ring Bulletin*, 48: 3-11.

Allen, G.S., and Owens, J.N., 1972. *The life history of Douglas-fir*. Forestry Service, Environment Canada. Ottawa, Ontario.

Allen, M.R., Stott, P.A., Mitchell, J.F.B., Schnur, R., and Delworth, T.L., 2000. Quantifying the uncertainty in forecasts of anthropogenic climate change. *Nature*, 407: 617-620.

Antos, J.A., and Zobel, D.B., 1986. Habitat relationship of Chamaecyparis nootkatensis in southern Washington, Oregon, and California. *Canadian Journal of Botany*, 64: 1898-1909.

British Columbia Ministry of Forests, 1993. *Biogeoclimatic units of the Vancouver forest region, Map 4 and 5.* 1:250 000 Map Sheet.

Beaubien, E.G., and Freeland, H.J., 2000. Spring phemology trends in Alberta, Canada: links to ocean temperature. *International Journal of Biometeorology*, 44: 53-59.

Biondi, F., Gershunov, A., and Cayan, D.R., 2001. North Pacific decadal climate variability since 1661. *Journal of Climate*, 14: 5-10.

Blasing, T.J., and Fritts, H.C., 1976. Reconstructing past climatic anomalies in the north Pacific and western North America from tree-ring data. *Quaternary Research*, 6: 563-579.

Blasing, T.J., Solomon, A.M., and Duvick, D.N., 1984. Response functions revisited. *Tree-Ring Bulletin*, 44: 1-15.

Boer, G.J., McFarlane, N.A., and M. Lazare, 1992. Greenhouse gas-induced climate change simulated with the CCC second-generation general circulation model. *Journal of Climate*, 5: 1045-1077.

Bovas, A., and Ledolter, J., 1983. *Statistical Methods for Forecasting*. Wiley and Sons, New York.

Briffa, K.R., and Jones, P.D., 1990. Basic chronology statistics and assessment. In: Cook, E.R. and Kairiukstis, L.A., (Eds.). *Methods of Dendrochronology, Applications in the Environmental Sciences*. Kluwer Academic Publishers, Dordrecht Holland, 137-152.

Briffa, K.R., Jones, P.D., and Schweingruber, F.H., 1992. Tree-ring density reconstructions of summer temperature patterns across western North America since 1600. *Journal of Climate*, 5: 735-754.

Carter, G. A., and Smith, W.K., 1987. Microhabitat comparisons of transpiration and photosynthesis in three subalpine conifers. *Canadian Journal of Botany*, 66: 963-969.

Charles, C., 1998. The ends of an era. *Nature* 394: 122-1232.

CONVERT, 1996. Program, version 1.3, February, 1996. Regent Instruments, Quebec, Quebec.

Coleman, M.D., Hinckley, T.M., McNaughton, G., and Smit, B.A., 1992. Root cold hardiness and native distribution of subalpine conifers. *Canadian Journal of Forest Research*, 22: 932-938.

Cook, E.R. 1999. TurboARSTAN program and reference manual, V 2.0.7 February, 1999. Tree-ring Laboratory, Lamont-Doherty Earth Observatory, Palisades, New York.

Cook, E.R., and Briffa, K., 1990. Data Analysis. In: *Methods of Dendrochronology, Applications in the Environmental Sciences*. Cook, E.R. and Kairiukstis, L.A., (Eds.), Kluwer Academic Publishers, Dordrecht Holland, 97-153.

Cook, E.R, and Peters, K., 1981. The smoothing spline: A new approach to standardizing forest interior tree-ring width series for dendroclimatic studies. *Tree-Ring Bulletin*, 41: 45-54.

Colenutt, M.E., and Luckman, B.H., 1991. Dendrochronological investigation of *Larix lyallii* at Larch Valley, Alberta. *Canadian Journal of Forest Research*, 21: 1222-1233.

Cropper, J.P., and Fritts, H.C., 1982. Density of tree-ring grids in western North America. *Tree-Ring Bulletin*, 42: 3-10.

D Arrigo, R., Wiles,G., Jacoby, G., and Villalba, R., 1999. North Pacific seas surface temperatures: Past variations inferred from tree rings. *Geophysical Reaserch Letters*, 26: 2757-2760.

Douglass, A.E., 1936. Climatic cycles and tree growth, Vol. III. A study of cycles. *Carnegie Institute of Washington Publications*, 289 pp.

Efron, B., 1979. Bootstrap methods: Another look at the jackknife. *The Annals of Statistics*, 7: 1-26.

Ettl, G.J., and Peterson, D.L., 1995. Growth response of subalpine fir (*Abies lasiocarpa*) to climate in the Olympic Mountains, Washington, USA. *Global Change Biology* 1: 213-230.

Environment Canada, 1996: MANOBS - Manual of surface weather observations. Seventh Edition, 3-9.

Fielder, P., and Owens, J.N., 1989. A comparative study of shoot and root development of interior and coastal Douglas-fir seedlings. *Canadian Journal of Forest Research*, 19: 539-549.

Flato, G.M., and G.J. Boer, 2001. Warming asymmetry in climate change simulations. *Geophysical Research Letters*, 28: 195-198.

Flato, G.M., Boer, G.J., Lee, W.G., McFarlane, N.A., Ramsden, D., Reader, M.C., and Weaver, A.J., 2000. The Canadian centre for climate modelling and analysis global coupled model and its climate. *Climate Dynamics*, 16: 451-467.

Fonda, R.W., and Bliss, L.C., 1969. Forest vegetation of the montane and subalpine zones, Olympic Mountains, Washington. *Ecological Monographs*, 39: 271-301.

Fowells, H.A., 1965. *Silvics of Forest Trees of The United States*. United States Department of Agriculture Handbook, Number 271, 146-150.

Fritts, H.C., 1976. *Tree Rings and Climate.* Academic Press, London.

Fritts, H.C., 1991. *Reconstructing large-scale climatic patterns from tree-ring data.* University of Arizona Press, Tucson.

Fritts, H.C., Guiot, J., Gordon, G.A., and Schweingruber, F., 1990. Methods of calibration, verification, and reconstruction. In: *Methods of Dendrochronology, Applications in the Environmental Sciences*. Cook, E.R. and Kairiukstis, L.A., (Eds.).

Kluwer Academic Publishers, Dordrecht Holland, 163-217.

Fritts, H.C., Blasing, T.J., Hayden, B.P., and Kutzbach, J.E., 1971. Multivariate techniques for specifying tree-growth and climate relationships and for reconstructing anomalies in paleoclimate. *Journal of Applied Meteorology*, 10: 845-864.

Fry, D. J., and Phillips, I.D.J., 1977. Photosynthesis of conifers in relation to annual growth cycles and dry matter production. *Physiologia Plantarum*, 40: 300-306.

Gavin, D.G., 2000. Holocene fire history of a coastal temperate rain forest, Vancouver Island, British Columbia, Canada. Unpublished Ph.D., University of Washington, Seattle, Washington.

Grassl, H., 2000. Status and improvements of coupled general circulation models. *Science*, 288: 1991-1997.

Gedalof, Z.M., 1999. Low frequency climate variability in the northeast Pacific interpreted from the annual growth-rings of mountain hemlock. Unpublished M.Sc. thesis, University of Victoria, Victoria, British Columbia.

Gedalof, Z.M., and Smith, D.J., 2001a. Interdecadal climate variability and regime-scale shifts in Pacific North America. *Geophysical Research Letters*, 28: 1515-1518.

Gedalof, Z.M., and Smith, D.J., 2001b. Dendroclimatic response of mountain hemlock (*Tsuga mertensiana*) in Pacific North America. *Canadian Journal of Forest Research*, 31: 322-332.

Geisser, S., 1993. *Predictive Inference: An Introduction.* Chapman and Hall, New York.

Graumlich, L.J., and Brubaker, L.B., 1986. Reconstruction of annual temperature (1590-1979) for Longmire, Washington, derived from tree rings. *Quaternary Research*, 25: 223-234.

Graumlich, L.J., Brubaker, L.B., and Grier, C.C., 1989. Long term trends in forest net primary productivity: Cascade Mountains, Washington. *Ecology*, 70: 405-410.

Grossnickle, S.C., 1992. Physiological and environmental tolerances of yellow cypress. In: *Yellow cypress: Can we grow it? Can we sell it?* Canada-British Columbia Partnership Agreement on Forest Research Development: FRDA Report 171: 31-33.

Grossnickle, S.C., and Russell, J.H., 1991. Gas exchange processes of yellow-cedar (*Chamaecyparis nootkatensis*) in response to environmental variables. *Canadian Journal of Botany*, 69: 2684-2691.

Guiot, J., 1991. The bootstrapped response function. *Tree-Ring Bulletin*, 51: 39-41.

Guiot, J., 1990. Methods of calabration. In: Cook, E.R. and Kairiukstis, L.A., (Eds.). *Methods of Dendrochronology, Applications in the Environmental Sciences*. Kluwer Academic Publishers, Dordrecht Holland, 165-177.

Guiot, J., Berger, A.L., and Munaut, A.V., 1982. Response functions. In: Hughes, M.K., Kelly, P.M., Pilcher, J.R., and LaMarche, V.C. Jr., (Eds.). *Climate From Tree Rings*. Cambridge University Press, Cambridge, 38-50.

Hale, M.G., and Orcutt, D.M., 1987. *The physiology of plants under stress*. Wiley (Interscience), New York.

Hanawa, K., 1995. Long-term variations in SST fields of the north Pacific Ocean. In:

R.J. Beamish (ed.). *Climate Change and Northern Fish Populations*. Ottawa, National Research Council, 25-36.

Hare, S.R., 1996. Low frequency climate variability and salmon production. Unpublished Ph.D. University of Washington, Seattle, Washington.

Havranek, W.M., and Tranquillini, W., 1995. Physiological processes during winter dormancy and their ecological significance. In: Smith, W.K. and Hinckley, T.M., (Eds.). *Ecophysiology of coniferous forests*. Academic Press, San Diego, California, 96-124.

Hawkins, B.J., 1993. Photoperiod and night frost influence the frost hardiness of *Chamaecyparis nootkatensis* clones. *Canadian Journal of Forest Research*, 23: 1408-1414.

Hegerl, G.C., Stott, P.A., Allen, M.R., Mitchell, J.F.B., Tett, S.F.B., and Cubasch, U., 2000. Optimal detection and attribution of climate change: sensitivity of results to climate model differences. *Climate Dynamics*, 16: 737-754.

Heikkinen, O., 1985. Relationships between tree growth and climate in the subalpine Cascade Range of Washington, U.S.A. *Annals of Botany Fennici*, 22: 1-14.

Heikkinen, O., 1984. Dendrochronological evidence of variations of Coleman Glacier, Mount Baker, Washington, U.S.A. *Arctic and Alpine Research*, 16: 53-64.

Holmes, R.L., 1999. Dendrochronology program library users manual. Laboratory of Tree-Ring Research. University of Arizona. February, 1999.

Holmes, R.L., Adams, R.K., and Fritts, H.C., 1986. Tree-ring chronologies of western North America: California, eastern Oregon and northern Great Basin, with procedures

used in the chronology development work, including users manuals for computer programs COFECHA and ARSTAN. *Chronology Series VI.* Laboratory of Tree-Ring Research, University of Arizona, Tucson.

Holzer, M., 1999. Analysis of passive tracer transport as modelled by an atmospheric general circulation model. *Journal of Climate*, 12: 1659-1684.

Hnytka, J., 1990. *Strathcona Park / Strathcona - Westmin Park: Master Plan*. Omni Environmental Consultants, Vancouver, British Columbia, 176 pp.

Jozsa, L.A., 1992. Yellow cypress wood quality and the hinoki connection. In: *Yellow Cypress: Can We Grow It? Can We Sell It?*. Canada-British Columbia Partnership Agreement on Forest Resource Developement: FRDA Report 171, 9-12.

Kadonaga, L.K., Podlaha, O., Whiticar, M.J., 1999. Time series analyses of tree ring chronologies from Pacific North America: evidence for sub-century climate oscillations. *Chemical Geology*, 161: 339-363.

Keller, T., Guiot, J., and Tessier, L., 1998. The artificial neural networks: a new advance in response function calculation. In: C. Urbinati and M Carrer (eds.). *Dendrochronologia: una scienza per l ambiente tra passato e presente*. Atti del XXXIV Corso di Cultura in Ecologia, Dipartmento Territorio e Sistemi Agroforestali, Universita degli Studi di Padova, Italy, 43-53.

Kellner, A.E., Laroque, C.P., Smith, D.J., and Harestad, A.S., 2000. Chronological dating of high-elevation dead and dying trees on northern Vancouver Island, British Columbia. *Northwest Science*, 74: 242-247.

Kellog, R.M., and Rowe, S., 1981. An anatomical method for differentiating woods of

western and mountain hemlock: a research note. *Wood and Fiber,* 13: 166-168.

Klinka, K., and Chourmouzis, C., 2001. The Mountain Hemlock Zone of British Columbia: Classification, Vegetation Environment Relationships, and Silvicultural Implications. Scientia Silvica Extension Series Number 28.

Klinka, K., Pojar, J., and Meidinger, D.V., 1991. Revision of Biogeoclimatic units of Coastal British Columbia. *Northwest Science*, 65: 32-47.

Koppenaal, R.S., and Mitchell, A.K., 1992. *Regeneration of Montane Forests in the Coastal Western Hemlock Zone of British Columbia: A Literature Review*. Canada-British Columbia Partnership Agreement on Forest Resourse Developement: FRDA II, Report 192.

Krajina, V.J., 1965. Biogeoclimatic zones and biogeocoenoses of British Columbia. *Ecology of Western North America*, 1: 1-17.

Krajina, V.J., 1969. Ecology of forest trees in British Columbia. *Ecology of Western North America*, 2: 1-146.

Laroque, C. P., 1995. The dendrochronology and dendroclimatology of yellow-cedar on Vancouver Island, British Columbia. Unpublished M.Sc. thesis, University of Victoria, Victoria, British Columbia.

Laroque, C.P., and Smith, D.J., 1999. Tree-ring analysis of yellow-cedar (*Chamaecyparis nootkatensis*) on Vancouver Island, British Columbia. *Canadian Journal of Forest Research*, 29: 115-123.

Laroque, C.P., Lewis, D.H., and Smith, D. J., 2000/01. Treeline dynamics on southern

Vancouver Island, British Columbia. *Western Geography*, 10/11: 43-63.

Leung, L.R., and Ghan, S.J., 1999. Pacific northwest climate sensitivity simulated by a regional climate model driven by a GCM. Part II: 2 x CO2 simulations. *Journal of Climate*, 12: 2031-2053.

Lewis, D.H., and Smith, D.J., 1999. Little Ice Age climate trends at treeline in Strathcona Provincial Park, Vancouver Island: Insights from glaciers and trees. In: D. C. MacIver (ed.). *Proceedings of the Workshop on Decoding Canada's Environmental Past: Adaptation Lessons Based on Changing Trends and Extremes in Climate Biodiversity*. Downsview: Atmospheric Enviroment Service, 19-29.

Lewis, D.H., 2001. Little Ice Age of Strathcona Provincial Park. Unpublished M.Sc. thesis, University of Victoria, Victoria, British Columbia.

Livingston, N.J., and Spittlehouse, D.L., 1996. Carbon isotope fractionation in tree ring early and late wood in relation to intra-growing season water balance. *Plant, Cell and Environment*, 19: 768-774.

Malamud, B.D., 2001. Using wavelet to quantify long-range persistence in tree rings and precipitation. Programme and abstracts of the European Geophysical Society meeting, Nice, France. March 25-30, 2001.

Margolis, H., Oren R., Whitehead, D., and Kaufmann, M.R., 1995. Leaf area dynamics of conifer forests. In: Smith, W.K. and Hinckley, T.M., (Eds.). *Ecophysiology of coniferous forests.* Academic Press, San Diego, California, 181-223.

Mantua, N.J., Hare, S.R., Zhang, Y., Wallace, J.M., and Francis, R.C., 1997. A Pacific interdecadal climate oscillation with impacts on salmon production. *Bulletin of the*

American Meteorological Society, 78: 1069-1079.

Mekis, E., and Hogg, W.D., 1999. Rehabilitation and analysis of Canadian daily precipitation time series. *Atmosphere-Ocean*, 37: 53-85.

McFarlane, N.A., Boer, G.J., Blanchet, J.P., and Lazare, M., 1992. The Canadian climate centre second generation general circulation model and its equilibrium climate. *Journal of Climate*, 5: 1013-1044.

McMinn, R.G., 1960. *Water relations and forest distribution in the Douglas-fir region on Vancouver Island.* Publication 1091. Forest Biology Laboratory Victoria, BC. Canada Department of Agriculture, Ottawa Ontario, 71pp.

Moore, R.D., and McKendry, I.G, 1996. Spring snowpack anomaly patterns and winter climatic variability, British Columbia, Canada. *Water Resources Research*, 32: 623-632.

Nuszdorfer, F.C., Klinka, K., and Demarchi, D.A., 1991. Coastal Douglas-fir zone. In: Meidinger, D., and Pojar, J., (eds.). *Ecosystems of British Columbia*, British Columbia Ministry of Forests Special report series No. 6. Victoria BC, 81-94.

Oquist, G., 1983. Effects of low temperature on photosynthesis. *Plant, Cell and Environment*, 6: 281-300.

Owens, J. N., 1984. Bud development in mountain hemlock (*Tsuga mertensiana*). I. Vegetative bud and shoot development. *Canadian Journal of Botany*, 62: 475-483.

Owens, J.N., 1973. *The reproductive cycle of Douglas-fir.* Environment Canada, Forestry service. Ottawa, Ontario.

Owens, J.N., 1968. Initiation and development of leaves in Douglas-fir. *Canadian Journal of Botany*, 46: 271-278.

Owens, J.N., and Molder, M., 1985. *The reproductive cycles of true firs.* British Columbia Ministry of Forests, Victoria, British Columbia.

Owens, J.N., and Molder, M., 1984a. *The reproductive cycles of western and mountain hemlock*. British Columbia Ministry of Forests, Victoria, British Columbia.

Owens, J.N., and Molder, M., 1984b. *The reproductive cycles of western redcedar and yellow-cedar.* British Columbia Ministry of Forests, Victoria, British Columbia.

Owens, J.N., and Molder, M., 1980. Sexual reproduction of western red cedar (*Thuja plicata*). *Canadian Journal of Botany*, 58: 1376-1393.

Owens, J.N., and Molder, M., 1975. Sexual reproduction of mountain hemlock (*Tsuga mertensiana*). *Canadian Journal of Botany*, 53: 1811-1826.

Owens, J. N., and Molder, M., 1974a. Cone initiation and development before dormancy in yellow cedar (*Chamaecyparis nootkatensis*). *Canadian Journal of Botany*, 52: 2075-2084.

Owens, J. N., and Molder, M., 1974b. Bud development in western hemlock. II. Initiation and early development of pollen cones and seed cones. Canadian Journal of Botany, 52: 283-294.

Owens, J. N., and Molder, M., 1973. Bud development in western hemlock. I. Annual growth cycle of vegetative buds. *Canadian Journal of Botany*, 51: 2223-2231.

Owens, J.N., and Pharis, R.P., 1971. Initiation and development of western red cedar cones in response to gibberellin induction and under natural conditions. Canadian Journal of Botany, 49: 1165-1175.

Owens, J.N., Simpson, S.J., and Molder, M., 1980. The pollination mechanism in yellow cypress (*Chamaecyparis nootkatensis*). *Canadian Journal of Forestry Research*, 10: 564-572.

Parminter, J. 1990. Fire history and effects on vegetation in three biogeoclimatic zones of British Columbia. In: *Fire and the environment: ecological and cultural perspectives*. Proceedings of an intemational symposium, 20-24 March, Knoxville, Tennessee. USDA Forest Service General Technical Report SE-69. Asheville, N.C., 263-272.

Peters, K., Jacoby, G.C., and Cook, E.R., 1981. Principal components analysis of tree-ring sites. *Tree-Ring Bulletin*, 41: 1-20.

Peterson, D.W., and Peterson, D.L., 2001. Mountain hemlock growth responds to climatic variability at annual and decadal time scales. *Ecology*, 82: 3330-3345.

Peterson, D.L., Silsbee, D.G., and Redmond, K.T., 1999. Detecting long-term hydrological patterns at Crater lake, Oregon. *Northwest Science*, 73: 121-130.

Pew, K.L., and Larson, C.P.S., 2001. GIS analysis of spatial and temporal patterns of human-caused wildfires in the temperate rain forest of Vancouver Island, Canada. *Forest Ecology and Management*, 140: 1-18.

Pojar, J., and Meidinger, D., 1991. Introduction. In: Meidinger, D., and Pojar, J., (eds.). *Ecosystems of British Columbia*, British Columbia Ministry of Forests Special report series no. 6. Victoria BC., 1-8.

Pojar, J., and Stewart, A.C., 1991. Alpine Tundra Zone. In: Meidinger, D., and Pojar, J., (eds.). *Ecosystems of British Columbia*, British Columbia Ministry of Forests Special report series no. 6. Victoria BC., 263-274.

Pojar, J., Klinka, K., and Demarchi, D.A., 1991a. Coastal Western Hemlock Zone. In: Meidinger, D., and Pojar, J., (eds.). *Ecosystems of British Columbia*, British Columbia Ministry of Forests Special report series no. 6. Victoria BC., 95-112.

Pojar, J., Klinka, K., and Demarchi, D.A., 1991b. Mountian Hemlock Zone. In: Meidinger, D., and Pojar, J., (eds.). Ecosystems of British Columbia, British Columbia Ministry of Forests Special report series no. 6. Victoria BC., 113-124.

Pojar, J., Klinka, K., and Meidinger, D., 1987. Biogeoclimatic ecosystem classification in British Columbia. *Forest Ecology and Management*, 22: 119-154.

PRECON, 1999. Quick help for PRECON Version 5.17. Dendrochronology modelling. Tuscon, Arizona. Version 5.17, April, 1999.

Pregitzer, K.S., King, J.S., Burton, A. J., and Brown, S.E., 2000. Response of tree fine roots to temperature. New Phytologist, 147: 105-115.

Reader, C., and Boer, G. J., 1998. The modification of greenhouse gas warming by the direct effect of sulphate aerosols. *Climate Dynamics*, 14: 593-608.

Rensing, K.H., and Owens, J.N., 1994. Bud and cambial zone phenology of lateral branches from Douglas-fir (*Pseudotsuga menziesii*) seedlings. *Canadian Journal of Forest Research*, 24: 286-296.

Rigozo, N.R., Nordemann, D.J.R., and Gonzalez, W.D., 2001. Solar variability effects

studied by tree-ring data wavelet analysis. Programme and abstracts of the European Geophysical Society meeting, Nice, France. March 25-30, 2001.

Robertson, E.O., Jozsa, L.A., and Spittlehouse, D.L., 1990. Estimating Douglas-fir wood production from soil and climate data. *Canadian Journal of Forest Research*, 20: 357-364.

Russell, J.H., 1993. Genetic architecture, genecology and phenotypic plasticity in seed and seedling traits of yellow-cedar. Unpublished Ph.D. dissertation, University of British Columbia, Vancouver, British Columbia.

Schmidt, R.L., 1957. *The silvics and plant geography of the genus Abies in the coastal forests of British Columbia.* Technical Publication T-46. Department of Lands and Forests British Columbia Forest Service. Victoria.

Schweingruber, F.H., 1996. *Tree rings and environment dendroecology.* Paul Haupt Publishers, Berne.

Schweingruber, F.H., 1993. *Trees and Wood in Dendrochronology*. Springer-Verlag, Berlin, Germany.

Schweingruber, F.H., 1988. *Tree Rings, Basics and Applications of Dendrochronology.* Kluwer Academic Publishers, Dordrecht Holland.

Silim, S.N., and Lavender, D.P., 1994. Seasonal patterns and environmental regulation of frost hardiness in shoots of seedlings of *Thuja plicata*, *Chamaecyparis nootkatensis*, and *Picea glauca. Canadian Journal of Botany*, 72: 309-316.

Smith, D. J., and Laroque, C. P., 1998a. Mountain hemlock growth dynamics on

Vancouver Island. *Northwest Science*, 72: 67-70.

Smith, D. J., Laroque, C. P., 1998b. High-elevation dendroclimatic records from Vancouver Island. In: MacIver, D.C., and Meyer, R.E., (eds.). *Proceedings of the Workshop on Decoding Canada's Environmental Past: Climate Variations and Biodiversity Change during the Last Millennium.* Atmospheric Enviroment Service, Downsview: 33-44.

Smith, D.J., and Laroque, C.P., 1996. Dendroglaciological dating of a little ice age glacial advance at Moving Glacier, Vancouver Island, British Columbia. *Géographie physique et Quaternaire*, 50: 47-55.

Smith, D.J., and Lewis, D.H., 1996. *Reconnaissance tree-ring studies at CFB Esquimalt.* UVTRL Report 96-04. Prepared for Trudy Chatwin, Ministry of Environment, Lands and Parks.

Smith, T.M., Reynolds, R.E., Livezey, R.E., and Stokes, D.C., 1996. Reconstruction of historical sea surface temperatures using empirical orthoginal functions. *Journal of Climate*, 9: 1403-1420.

SPSS, 1996. Program and reference manual, version 7.5.1, December, 1996. SPSS Incorporated.

Stokes, M.A., and Smiley, T.L., 1968. *An Introduction to Tree-Ring Dating.* University of Chicago Press, Chicago, USA.

SURFER, 1997. Program and reference manual, version 6.04, February, 1997. Golden Software Incorporated, Golden, Colorado.

Taylor, R.J., 1972. The relationship and origin of *Tsuga heterophylla* and *Tsuga mertensiana* based on phytochemical and morphological interpretations. *American Journal of Botany*, 59: 149-157.

Teskey, R.O., Hinckley, T.M., and Grier, C.G., 1984. Temperature-induced change in water relations of *Abies amabilis* (Dougl.) Forbes. *Plant Physiology*, 74: 77-80.

Torrence, C., and Compo, G.P., 1998. A practical guide to wavelet analysis. *Bulletin of the American Meteorological Society*, 79: 61-78.

van den Driessche, R., 1969. Influence of moisture supply, temperature, and light on frost-hardiness changes in Douglas-fir seedlings. *Canadian Journal of Botany*, 47: 1765-1772.

van Pelt, R., and Franklin, J.F., 1999. Response of understory trees to experimental gaps in old-growth Douglas-fir forests. *Ecological Applications*, 9: 504-512.

Vincent, L.A., 1998. A technique for the identification of inhomogeneities in Canadian temperature series. *Journal of Climate*, 5: 1094-1104.

Vincent, L.A., and Gullett, D. W., 1999. Canadian historical and homogeneous temperature datasets for climate change analyses. *International Journal of Climatology*, 19: 1375-1388.

Wallace, J.M., and Gutzler, D.S., 1981. Teleconnections in the geopotential height field during the northern hemisphere winter. *Monthly Weather Review*, 109: 784-812.

Watson, E., Youngblut, D., Luckman, B.H., and Froelich, N., 2000. *Dendroclimatic investigations in British Columbia, Alberta and the southwest Yukon.* Final report to

Meteorological Services of Canada, 99DD-011.

Wigley, T.M.L., Briffa, K.R., and Jones, P.D., 1984. On the average of correlated time series, with applications in dendroclimatology and hydrometeorology. *Journal of Climate and Applied Meteorology*. 23: 201-213.

Wiles, G.C., D Arrigo, R.D., and Jacoby, G.C., 1998. Gulf of Alaska atmosphere-ocean variability over recent centuries inferred from coastal tree-ring records. *Climate Change*, 38: 159-205.

Wiles, G.C., D Arrigo, R.D., and Jacoby, G.C., 1996. Temperature changes along the Gulf of Alaska and the Pacific northwest coast modelled from coastal tree rings. *Canadian Journal of Forest Research* 26: 474-481.

Woodhouse, C.A., 1999. Artificial neural networks and dendroclimatic reconstructions: an example from the Front Ranges, Colorado, USA. *The Holocene,* 9: 521-529.

WinDENDRO, 1996. WinDENDRO reference manual, V 6.1b February, 1996. Regent Instruments, Quebec, Quebec.

Zhang, Q., 1996. A 2,122-year tree-ring chronology of Douglas-fir and spring precipitation reconstruction at Heal Lake, southern Vancouver Island, British Columbia. Unpublished M.Sc. thesis, University of Victoria, Victoria, British Columbia.

Zhang, Q., 2000. Modern and late holocene climate-tree-ring growth relationships and growth patterns in Douglas-fir, Coastal British Columbia, Canada. Unpublished Ph.D. dissertation, University of Victoria, Victoria, British Columbia.

Zhang, Q.B., Hebda,, R.J., Zhang, Q.J., and Alfaro, R.I., 2000. Modeling tree-ring

growth responses to climatic variables using artificial neural networks. *Forest Science*, 46: 229-239.

Zhang, Y., Wallace, J.M., and Battisti, D., 1997. ENSO-like interdecadal variability: 1900-93. *Journal of Climate*, 9: 1468-1478.

Zwiers, F.W., 1996. Interannual variability and predictability in an ensemble of AMIP climate simulations conducted with the CCC GCM2. *Climate Dynamics*, 12: 825-847.

Appendix A **- Scientific Name of Trees in Text**

mountain hemlock, *Tsuga mertensiana* (Bong.) Carr.

yellow-cedar, *Chamaecyparis nootkatensis* (D. Don) Spach

western hemlock, *Tsuga heterophylla* (Raf.) Sarg.

Douglas-fir, *Pseudotsuga menziesii* (Mirb.) Franco

western red-cedar, *Thuja plicata* Donn

subalpine fir, *Abies lasiocarpa* (Hook.) Nutt.

amabilis fir, *Abies amabilis* (Dougl.) Forbes

grand fir, *Abies grandis* (Dougl.) Lindl.

shore pine, *Pinus contorta* var. *contorta* Dougl.

Garry oak, *Quercus garryana* Dougl.

western yew, *Taxus brevifolia* Nutt.

bigleaf maple, *Acer macrophyllum* Pursh

red alder, *Alnus rubra* Bong.

black cottonwood, *Populus trichocarpa* Torr. & Gray

arbutus, *Arbutus menziesii* Pursh

western white pine, *Pinus monticola* Dougl.

Sitka spruce, *Picea sitchensis* (Bong.) Carr.

Appendix B

The 88 x 88 Correlation Matrix

The 88 x 88 chronology correlation matrix is described below. Each series is described by a code. The series codes can be defined as follows: Site code (see Table 2.1) followed by a three number code describing the species. The species codes are as follows - 000 = western hemlock, 100 = yellow-cedar, 200 = mountain hemlock, 300 = Douglas-fir, 400 = subalpine-fir, 700 = western red-cedar.

	94Mila	94Cain	94Arro	94Heat	94Wash	96A100	96B100	96C100
94Mila	1.0000							
94Cain	0.5667	1.0000						
94Arro	0.6743	0.5610	1.0000					
94Heat	0.4153	0.5000	0.4402	1.0000				
94Wash	0.6925	0.6027	0.8010	0.3898	1.0000			
96A100	0.3589	0.4020	0.4076	0.6535	0.4078	1.0000		
96B100	0.4315	0.3244	0.5158	0.4413	0.4659	0.5349	1.0000	
96C100	0.3464	0.3030	0.4573	0.4220	0.4542	0.4254	0.4696	1.0000
96E100	0.3602	0.2938	0.5672	0.4540	0.5202	0.4136	0.5033	0.4003
96F100	0.4358	0.4767	0.6235	0.4611	0.6569	0.5668	0.6334	0.5822
96G100	0.0812	0.3005	0.2855	0.5578	0.2589	0.4967	0.5160	0.2446
96H100	0.3106	0.1371	0.3678	0.3748	0.2927	0.5897	0.6746	0.4051
96I100	0.3952	0.5129	0.4047	0.7375	0.3815	0.6732	0.6421	0.3781
96J100	0.3683	0.4549	0.5720	0.4917	0.5461	0.5698	0.7063	0.4569
96K100	0.2947	0.2339	0.1663	0.4843	0.1937	0.4370	0.3330	0.1248
96L100	0.4608	0.5182	0.5553	0.5080	0.4813	0.5207	0.5563	0.3439
96M100	0.4345	0.6502	0.4174	0.6052	0.4437	0.5222	0.4390	0.3272
96O100	0.3551	0.4996	0.3504	0.5492	0.3584	0.6318	0.5702	0.3397
96P100	0.2667	0.4488	0.2009	0.5049	0.1970	0.5892	0.4079	0.1932
96Q100	0.2392	0.3757	0.2144	0.6244	0.2156	0.6266	0.4373	0.3263
96S100	0.2866	0.3695	0.1618	0.4059	0.1470	0.3698	0.1743	0.1230
96V100	0.4312	0.4841	0.5778	0.7249	0.5169	0.4460	0.4225	0.3639
96X100	0.3270	0.4463	0.4451	0.5129	0.3924	0.6557	0.6946	0.4366
97B100	-0.0744	0.0478	-0.1149	0.0625	-0.0929	0.1343	0.0073	-0.0863
97D100	0.6129	0.4260	0.6065	0.3958	0.6716	0.3097	0.4638	0.2609
97E100	0.6148	0.5952	0.6795	0.2663	0.7068	0.3672	0.4390	0.3844
97F100	0.3527	0.4425	0.3463	0.5465	0.3729	0.6003	0.6868	0.4261
97I100	0.5465	0.5959	0.7042	0.4441	0.7137	0.5467	0.5923	0.4829
97J100	0.3859	0.3120	0.5807	0.5051	0.4942	0.6253	0.7822	0.6114
97K100	0.3225	0.5070	0.2347	0.5302	0.2607	0.5408	0.4275	0.2115
97L100	0.1125	0.3855	0.0690	0.4675	0.0157	0.4494	0.4109	0.0637
97M100	0.2464	0.4967	0.3623	0.5651	0.3324	0.4925	0.5524	0.2803
97O100	0.4860	0.5706	0.5123	0.6041	0.5244	0.6144	0.6399	0.3777
97P100	0.1330	0.2930	0.1332	0.4903	0.1906	0.5091	0.3518	0.2314
97Q100	-0.1011	0.1467	0.0673	0.2191	0.1319	0.3570	0.2910	0.2502

	94Mila	94Cain	94Arro	94Heat	94Wash	96A100	96B100	96C100
97N000	-0.2083	0.0330	-0.0671	0.1223	-0.1701	0.0586	0.0166	-0.0059
97C000	0.1494	0.1064	0.2214	0.1514	0.2385	0.0647	0.4209	0.0958
97Q000	0.0142	-0.0415	-0.0222	0.0035	-0.0473	-0.0474	0.0769	0.0527
97A000	0.1645	0.1744	0.3189	0.0995	0.2100	0.0809	0.3005	0.0721
97B000	0.0122	0.0306	0.0054	0.0009	-0.0956	-0.0031	-0.0985	-0.0969
97E000	0.0980	0.1159	-0.0244	0.1279	0.0190	-0.0353	0.1622	0.0293
96C000	0.1035	0.0852	0.0698	0.0182	0.1163	0.0362	0.2233	-0.0037
96U000	-0.0092	0.1273	0.0644	0.1736	0.0153	0.0590	0.0831	0.2231
96B000	0.0692	0.0976	-0.0764	0.1829	-0.1030	-0.0218	0.1102	-0.0926
96I000	-0.1503	0.1607	-0.0739	0.1668	-0.0548	0.1085	0.1869	-0.0445
96A000	0.0130	0.1200	0.0488	0.1097	0.0352	0.0175	0.1276	0.0002
93MP300	0.0410	-0.0826	-0.0362	0.0117	0.0257	0.0876	0.0738	0.1957
96D300	-0.0209	0.0685	-0.0160	0.1144	-0.0032	0.0836	0.1730	0.0352
97Q700	0.1525	0.0701	-0.0661	0.1883	0.0162	0.2149	0.3172	0.0957
97B700	0.3512	0.2897	0.1269	0.2978	0.1429	0.3603	0.2853	0.2172
96W400	0.3131	0.2537	0.1414	0.2738	0.2837	0.0035	0.0377	0.1927
96N200	0.3892	0.3990	0.3726	0.5040	0.3256	0.3215	0.0631	0.1629
94HM200	0.0796	0.0454	0.1066	0.2720	0.0850	0.0164	-0.0157	0.1781
96A200	-0.0397	0.0675	-0.0471	0.3479	-0.1076	0.3003	-0.0884	-0.0085
96B200	0.0798	0.0399	0.1165	0.1310	0.0881	0.0779	0.4300	0.1179
96C200	0.0887	0.0903	0.2348	0.1574	0.2090	0.0416	0.3679	0.2868
96D200	-0.0337	-0.1304	0.1585	-0.0221	0.0372	0.0298	0.3628	0.1657
96E200	0.3171	0.3752	0.4177	0.4351	0.4249	0.1673	0.1950	0.3059
96F200	0.3424	0.2853	0.4274	0.2961	0.3605	0.2425	0.5043	0.2062
96G200	0.3279	0.4862	0.4141	0.2495	0.3519	0.1096	0.3459	0.2150
96H200	0.1402	0.0071	0.1965	-0.0086	0.1209	-0.0004	0.3622	0.2831
96I200	-0.0815	0.1564	0.0968	0.2144	-0.0319	0.1165	0.1160	-0.0195
96J200	0.0971	0.0918	0.1839	0.2977	0.1060	0.1651	0.2368	0.1354
96K200	0.4568	0.2499	0.3830	0.2324	0.3503	0.1925	0.1024	0.1686
96L200	0.0139	-0.0722	-0.0235	0.2744	-0.1308	0.1252	-0.0381	-0.0746
96M200	0.4440	0.4167	0.3629	0.5110	0.2942	0.3302	0.0859	0.1911
96O200	0.0284	0.1162	0.0916	0.4369	-0.0094	0.2451	0.0616	0.0176
96P200	-0.1089	0.0186	-0.1628	0.2989	-0.2513	0.1701	-0.1837	-0.1684
96Q200	-0.1154	-0.0324	-0.0004	0.0656	-0.0858	0.0013	0.1153	-0.1316
96T200	0.3865	0.3699	0.2847	0.3783	0.2822	0.4481	0.2695	0.3255
96U200	0.2458	0.1934	0.1448	0.3202	0.1267	0.0194	0.0797	0.2786
96V200	0.3030	0.2727	0.3754	0.4638	0.2747	0.1708	0.2423	0.2943
96W200	0.4198	0.4679	0.4075	0.5493	0.3370	0.2891	0.2209	0.2747
96X200	-0.2232	0.0367	0.0025	0.0982	-0.1406	-0.0557	-0.1344	-0.1083
97A200	0.2831	0.1579	0.3397	0.3401	0.2428	0.0923	0.2854	0.0538
97D200	0.0662	0.2421	0.0699	0.0263	0.1029	0.0194	0.2183	-0.0043
97E200	0.2166	0.3110	0.1925	0.5006	0.1478	0.4005	0.1414	0.1600
97F200	0.1023	0.0216	0.2755	0.2280	0.1776	0.1575	0.2662	0.1058
97H200	0.3458	0.2976	0.2824	0.4892	0.1812	0.1993	0.1423	0.1572
97I200	0.3284	0.2882	0.2691	0.4182	0.1146	0.2313	0.2444	0.2333
97J200	0.1893	0.1727	0.2773	0.2097	0.1848	0.1992	0.4219	0.1331
97K200	0.4210	0.2783	0.3503	0.3029	0.2742	0.2143	0.1761	0.1667
97L200	0.0134	0.2217	0.2042	0.1997	0.1250	0.0479	0.2602	0.0839
97M200	0.0360	0.0823	0.1958	0.2485	0.0776	0.1416	0.0788	0.1818
97O200	-0.0049	0.1191	0.2386	-0.0008	0.1670	-0.1606	0.2424	-0.0008
97P200	0.0401	0.1863	0.1821	0.3453	0.1238	0.1917	0.2248	0.1412

	96E100	96F100	96G100	96H100	96I100	96J100	96K100	96L100
94Mila								
94Cain								
94Arro								
94Heat								
94Wash								
96A100								
96B100								
96C100								
96E100	1							
96F100	0.4778	1						
96G100	0.2791	0.478	1					
96H100	0.364	0.5341	0.3442	1				
96I100	0.5132	0.558	0.6529	0.5273	1			
96J100	0.5141	0.6987	0.5564	0.525	0.6335	1		
96K100	0.3787	0.1906	0.2028	0.2968	0.5237	0.2018	1	
96L100	0.4731	0.4734	0.3232	0.3863	0.5563	0.5667	0.4539	1
96M100	0.1801	0.5635	0.538	0.3581	0.6373	0.501	0.2819	0.5585
96O100	0.4397	0.4566	0.4026	0.4312	0.6834	0.4433	0.6084	0.7609
96P100	0.2265	0.3743	0.3924	0.4086	0.6811	0.3512	0.5462	0.5622
96Q100	0.2529	0.4035	0.5151	0.5177	0.7087	0.3635	0.4999	0.5317
96S100	0.2571	0.1344	0.2024	0.2085	0.4827	0.1659	0.5534	0.4018
96V100	0.632	0.5251	0.5268	0.2903	0.6299	0.528	0.3745	0.4786
96X100	0.4034	0.6551	0.5115	0.6425	0.6944	0.6473	0.4312	0.6026
97B100	0.1952	-0.0242	-0.0122	0.0927	0.2533	0.0529	0.2795	0.0606
97D100	0.4614	0.4639	0.3041	0.2375	0.4447	0.4603	0.2523	0.484
97E100	0.3822	0.5303	0.1847	0.2396	0.3383	0.425	0.1691	0.6808
97F100	0.3562	0.5629	0.598	0.5637	0.7477	0.6079	0.4767	0.6848
97I100	0.4253	0.6978	0.4398	0.4787	0.5133	0.6315	0.1453	0.4311
97J100	0.5627	0.6537	0.4649	0.5997	0.6124	0.6701	0.3576	0.5975
97K100	0.3412	0.324	0.3112	0.3119	0.6165	0.3449	0.6298	0.6573
97L100	0.201	0.2462	0.3801	0.3978	0.6623	0.3326	0.5064	0.4853
97M100	0.4326	0.4817	0.4425	0.4649	0.6989	0.5557	0.4766	0.6988
97O100	0.5187	0.5423	0.5022	0.5156	0.7719	0.5833	0.4688	0.6866
97P100	0.3075	0.3706	0.4665	0.4402	0.61	0.3922	0.4258	0.4421
97Q100	0.2453	0.4291	0.4197	0.2814	0.3197	0.4347	0.1408	0.1379

	96E100	96F100	96G100	96H100	96I100	96J100	96K100	96L100
97N000	-0.031	0.0152	0.1595	0.1031	0.1574	-0.0142	0.0124	0.1506
97C000	0.309	0.3809	0.2443	0.2171	0.2296	0.351	0.1581	0.2394
97Q000	0.1393	-0.0627	-0.1283	-0.0405	0.0728	-0.0669	0.1102	0.0432
97A000	0.3347	0.2822	0.1516	0.0512	0.1684	0.3206	0.2368	0.4123
97B000	0.0051	-0.0601	0.0627	-0.0837	-0.0493	-0.0861	0.0356	-0.0135
97E000	0.1353	0.0012	0.0815	0.0996	0.1332	0.1066	0.0764	0.0479
96C000	0.0764	0.1421	0.1906	0.1546	0.1598	0.2408	-0.0278	0.1658
96U000	0.0471	0.1799	0.1198	0.0497	0.2106	0.1824	0.0511	0.1263
96B000	0.1071	-0.0453	-0.0348	0.118	0.2467	0.1064	0.1754	0.1591
96I000	-0.0257	0.1201	0.2366	0.1052	0.2884	0.2584	0.0498	0.1305
96A000	0.142	0.0304	0.092	0.1208	0.1702	0.1812	0.0948	0.1306
93MP300	0.2065	0.1057	-0.1251	0.2058	0.0122	0.052	-0.0072	0.0488
96D300	0.0442	0.2648	0.0787	0.1978	0.1777	0.2108	0.0791	0.0866
97Q700	0.1741	0.1537	0.1642	0.2959	0.2812	0.0819	0.2827	0.1463
97B700	0.0516	0.2782	0.1568	0.3234	0.3541	0.0786	0.3654	0.1993
96W400	0.1801	0.1592	0.0486	-0.1454	0.1455	0.0716	0.0233	0.1222
96N200	0.2853	0.2356	0.1931	0.0646	0.3415	0.2289	0.3169	0.385
94HM200	0.2781	0.0719	0.0325	-0.0398	0.1744	0.0707	0.2229	0.2176
96A200	0.1836	-0.0085	0.153	0.1027	0.3461	-0.0454	0.4169	0.0956
96B200	0.2811	0.3076	0.1802	0.3091	0.2894	0.284	0.1686	0.2733
96C200	0.4077	0.3702	0.1992	0.2041	0.2418	0.2457	0.0934	0.2247
96D200	0.2065	0.2788	0.0937	0.3712	0.1202	0.2452	-0.0159	0.1193
96E200	0.3438	0.3762	0.3087	0.0053	0.3011	0.3128	0.2083	0.3995
96F200	0.3273	0.5786	0.2835	0.372	0.3719	0.4144	0.2029	0.4487
96G200	0.2449	0.3065	0.2532	0.0348	0.3195	0.349	0.0818	0.4214
96H200	0.2325	0.2192	0.0033	0.3423	0.0774	0.2112	0.0537	0.1365
96I200	0.2327	0.1034	0.1891	0.0924	0.3776	0.1146	0.195	0.1822
96J200	0.305	0.2649	0.2849	0.2029	0.3711	0.3793	0.2088	0.1958
96K200	0.4002	0.0953	-0.2256	0.094	0.1228	0.1267	0.3995	0.4607
96L200	0.227	-0.0617	-0.0718	0.1947	0.2477	-0.0371	0.3645	0.1149
96M200	0.3577	0.2163	0.1325	0.0749	0.3995	0.2045	0.4025	0.3998
96O200	0.3697	0.0369	0.1221	0.1607	0.3582	0.1262	0.413	0.4257
96P200	0.082	-0.0941	0.0965	0.0882	0.3151	-0.075	0.3625	0.0697
96Q200	0.2033	-0.0498	0.0494	0.1145	0.1831	0.0369	0.2145	0.1889
96T200	0.2405	0.2297	0.1315	0.1855	0.3402	0.2028	0.3936	0.5533
96U200	0.3146	0.1162	0.0972	0.0009	0.2691	0.1061	0.0969	0.1719
96V200	0.3617	0.3198	0.2769	0.1182	0.3529	0.3307	0.3231	0.3887
96W200	0.3378	0.2839	0.3124	0.0718	0.4302	0.3529	0.3488	0.432
96X200	0.1669	-0.1168	0.0519	-0.1321	0.0948	0.0133	0.1314	0.1255
97A200	0.3686	0.2919	0.1975	0.1264	0.2894	0.2881	0.2637	0.3247
97D200	-0.0073	0.2807	0.1068	0.1295	0.2017	0.2207	0.013	0.2826
97E200	0.2214	0.2605	0.3381	0.2686	0.4529	0.2159	0.3468	0.3086
97F200	0.4817	0.1911	0.0731	0.3012	0.2131	0.2429	0.2613	0.3252
97H200	0.2607	0.1741	0.1509	0.1176	0.3375	0.1976	0.4055	0.3501
97I200	0.2973	0.2512	0.1603	0.2092	0.3935	0.2176	0.3189	0.4508
97J200	0.4163	0.3823	0.1832	0.233	0.3509	0.3596	0.2211	0.4323
97K200	0.4893	0.12	-0.1	0.1065	0.2784	0.1748	0.4803	0.5907
97L200	0.3414	0.2451	0.2247	0.1224	0.3137	0.2766	0.1604	0.3615
97M200	0.3126	0.1352	0.0531	0.1737	0.1764	0.1214	0.2454	0.2113
97O200	0.0896	0.2015	0.1516	0.0213	0.0995	0.1772	-0.118	0.1198
97P200	0.1851	0.342	0.344	0.247	0.3123	0.3261	0.1256	0.3193

	96M100	96O100	96P100	96Q100	96S100	96V100	96X100	97B100
94Mila								
94Cain								
94Arro								
94Heat								
94Wash								
96A100								
96B100								
96C100								
96E100								
96F100								
96G100								
96H100								
96I100								
96J100								
96K100								
96L100								
96M100	1							
96O100	0.5409	1						
96P100	0.5743	0.7342	1					
96Q100	0.6405	0.646	0.6435	1				
96S100	0.3278	0.5726	0.5335	0.4118	1			
96V100	0.4633	0.4537	0.3946	0.3831	0.3901	1		
96X100	0.5655	0.7081	0.5868	0.6538	0.3588	0.4167	1	
97B100	-0.0788	0.2211	0.1734	0.1062	0.3528	0.1773	0.1463	1
97D100	0.484	0.2972	0.207	0.3452	0.1243	0.3834	0.3262	-0.2351
97E100	0.5529	0.4992	0.3656	0.3136	0.2222	0.3629	0.4256	-0.1238
97F100	0.6539	0.7955	0.6891	0.7548	0.3785	0.4123	0.7748	0.0918
97I100	0.6092	0.3862	0.2937	0.3659	0.1276	0.4458	0.5908	-0.056
97J100	0.4179	0.6046	0.4637	0.4233	0.2471	0.499	0.6535	0.019
97K100	0.5266	0.8382	0.7258	0.5381	0.675	0.4165	0.5733	0.1729
97L100	0.5161	0.7091	0.8544	0.5761	0.5321	0.3784	0.5695	0.2613
97M100	0.5161	0.7195	0.6361	0.5527	0.4491	0.5043	0.6603	0.2281
97O100	0.5899	0.7554	0.5972	0.6321	0.4541	0.5244	0.6804	0.1593
97P100	0.5923	0.5034	0.5436	0.7329	0.3854	0.3082	0.4839	0.025
97Q100	0.2363	0.2525	0.2768	0.2022	0.2045	0.2822	0.3472	0.0198

	96M100	96O100	96P100	96Q100	96S100	96V100	96X100	97B100
97N000	0.1596	0.1009	0.3459	0.2878	0.1467	0.1351	0.0302	0.1291
97C000	0.2397	0.1553	0.1787	0.1444	0.0766	0.297	0.2013	0.0155
97Q000	-0.0719	0.013	0.0519	0.1374	0.0655	0.0413	-0.0177	0.0939
97A000	0.1126	0.3085	0.1609	0.0085	0.1862	0.2928	0.244	0.1431
97B000	-0.0106	-0.0582	0.044	-0.0484	0.093	0.1528	-0.1489	0.1274
97E000	0.0707	0.0974	0.0831	0.0525	0.0896	0.127	-0.0223	-0.0137
96C000	0.1036	0.1224	0.1129	0.1082	0.0202	0.141	0.1005	0.008
96U000	0.1373	0.136	0.1789	0.1135	0.094	0.1999	0.1726	0.0929
96B000	0.1082	0.1639	0.1727	0.211	0.2499	0.1476	0.0711	0.2322
96I000	0.2447	0.1303	0.2985	0.2027	0.1562	0.188	0.126	0.134
96A000	0.0532	0.1913	0.0517	0.0453	0.1369	0.1453	0.1067	0.2081
93MP300	-0.0591	0.0975	0.0225	0.0571	0.0615	0.0659	0.0325	0.0886
96D300	0.1982	0.1315	0.2389	0.2818	0.0207	0.0791	0.1911	0.0815
97Q700	0.1597	0.2991	0.2308	0.2819	0.2247	0.1664	0.2747	0.1514
97B700	0.3883	0.3164	0.4704	0.4115	0.285	0.1603	0.3584	0.0901
96W400	0.2855	0.0306	-0.0684	0.0752	-0.0681	0.3769	-0.01	0.0817
96N200	0.4249	0.2454	0.2875	0.2779	0.4281	0.5231	0.1279	0.1334
94HM200	0.0389	0.1714	0.0848	0.0764	0.2575	0.3615	0.0179	0.1518
96A200	0.1725	0.2859	0.4422	0.3397	0.4931	0.3649	0.1095	0.3126
96B200	0.2025	0.2423	0.1999	0.278	0.0873	0.2671	0.2722	0.2303
96C200	0.1513	0.1912	0.0653	0.168	0.1461	0.3596	0.2014	0.1709
96D200	-0.0018	0.0181	0.0581	0.1132	-0.0596	0.1231	0.1777	0.138
96E200	0.3767	0.2646	0.1563	0.2505	0.2777	0.5015	0.1879	0.0069
96F200	0.4644	0.331	0.291	0.2948	0.1626	0.3624	0.415	0.0367
96G200	0.306	0.2882	0.1668	0.1485	0.101	0.3588	0.2633	0.1398
96H200	0.0037	0.1117	0.0774	0.0318	0.0008	0.1314	0.1797	0.0267
96I200	0.1412	0.2237	0.409	0.2218	0.2986	0.3766	0.182	0.3812
96J200	0.2091	0.121	0.1281	0.2796	0.1953	0.3809	0.2232	0.2694
96K200	0.0311	0.3935	0.1597	0.101	0.4813	0.2596	0.1415	0.1781
96L200	0.0419	0.1395	0.2222	0.3215	0.331	0.2302	0.0394	0.3375
96M200	0.3743	0.3515	0.3504	0.2733	0.5245	0.5174	0.1325	0.1656
96O200	0.1705	0.3918	0.4016	0.4066	0.453	0.4025	0.1378	0.3296
96P200	0.167	0.1637	0.4732	0.3646	0.4206	0.2469	0.02	0.3376
96Q200	-0.0679	0.1296	0.222	0.1377	0.2197	0.226	0.0587	0.3851
96T200	0.4542	0.5776	0.4657	0.4243	0.5764	0.3272	0.3245	0.0944
96U200	0.2207	0.1138	0.0408	0.2795	0.1206	0.4317	-0.0042	0.1669
96V200	0.2928	0.2732	0.2151	0.2421	0.3445	0.528	0.2152	0.0988
96W200	0.402	0.3189	0.2366	0.3118	0.3565	0.5508	0.2363	0.1384
96X200	-0.1255	0.0824	0.1072	-0.0195	0.2349	0.2075	-0.0056	0.3649
97A200	0.2224	0.2182	0.0788	0.0787	0.234	0.4407	0.163	0.0763
97D200	0.4032	0.2133	0.2986	0.2093	0.1202	0.0576	0.2714	0.0569
97E200	0.4998	0.3332	0.461	0.5042	0.4804	0.4621	0.2356	0.1518
97F200	-0.0941	0.2435	0.117	0.1099	0.1753	0.353	0.1534	0.2766
97H200	0.3446	0.2801	0.1826	0.3484	0.3988	0.4371	0.1629	0.1345
97I200	0.3311	0.4089	0.4153	0.3071	0.3763	0.4593	0.2525	0.1488
97J200	0.1997	0.4098	0.2944	0.2243	0.2357	0.3768	0.3839	0.2629
97K200	0.1627	0.526	0.3146	0.2004	0.5337	0.3535	0.1957	0.1773
97L200	0.1687	0.3276	0.3061	0.1405	0.3518	0.4056	0.2066	0.3067
97M200	0.0368	0.1859	0.1849	0.1126	0.2344	0.3704	0.1361	0.3566
97O200	0.0837	-0.0147	-0.0605	-0.1374	-0.1607	0.1245	0.1294	0.0248
97P200	0.3729	0.2085	0.3325	0.2609	0.1524	0.3471	0.1669	0.0801

	97D100	97E100	97F100	97I100	97J100	97K100	97L100	97M100
94Mila								
94Cain								
94Arro								
94Heat								
94Wash								
96A100								
96B100								
96C100								
96E100								
96F100								
96G100								
96H100								
96I100								
96J100								
96K100								
96L100								
96M100								
96O100								
96P100								
96Q100								
96S100								
96V100								
96X100								
97B100								
97D100	1							
97E100	0.6384	1						
97F100	0.459	0.5092	1					
97I100	0.54	0.6065	0.4977	1				
97J100	0.3848	0.51	0.6064	0.5346	1			
97K100	0.2611	0.4359	0.6697	0.2659	0.4679	1		
97L100	0.0779	0.2074	0.6569	0.188	0.3706	0.7543	1	
97M100	0.3156	0.3387	0.6557	0.3867	0.5344	0.6873	0.6669	1
97O100	0.4774	0.5655	0.7416	0.6272	0.5948	0.6272	0.537	0.6551
97P100	0.3635	0.2784	0.6214	0.2982	0.3584	0.5167	0.5555	0.4767
97Q100	0.0627	0.0609	0.2762	0.1806	0.4217	0.2791	0.2829	0.2796

	97D100	97E100	97F100	97I100	97J100	97K100	97L100	97M100
97N000	-0.1512	0.0061	0.1455	-0.0454	0.0152	0.0442	0.336	0.1427
97C000	0.3526	0.203	0.2872	0.1936	0.2837	0.0518	0.1609	0.2091
97Q000	0.1005	0.0059	0.0229	-0.0337	-0.0024	-0.047	0.0808	0.0132
97A000	0.1984	0.3128	0.2391	0.1699	0.3168	0.221	0.1841	0.3104
97B000	-0.1219	0.0015	-0.0911	-0.0057	-0.0964	-0.0584	0.0729	-0.0886
97E000	0.0385	-0.0786	0.1255	-0.0237	0.0774	0.0638	0.1195	0.1617
96C000	0.1361	0.1025	0.2397	0.0421	0.0942	0.0184	0.0823	0.1721
96U000	-0.1224	0.0239	0.1384	0.0306	0.1858	0.1663	0.192	0.2368
96B000	0.014	-0.0655	0.1937	-0.1265	0.0336	0.1792	0.2858	0.2066
96I000	-0.1169	-0.0102	0.195	0.007	0.1397	0.1761	0.392	0.2552
96A000	0.0095	-0.0157	0.1281	0.0069	0.0996	0.1406	0.1202	0.2645
93MP300	-0.0844	0.0626	0.051	-0.0318	0.2168	0.079	-0.0057	0.019
96D300	0.0546	0.0099	0.2694	0.0355	0.1102	0.0619	0.2544	0.1415
97Q700	0.0617	-0.0662	0.3108	0.1149	0.1692	0.2291	0.2418	0.2167
97B700	0.1122	0.1849	0.3545	0.2459	0.2139	0.3375	0.3369	0.1952
96W400	0.0832	0.2338	0.0078	0.1508	0.0116	0.1209	0.0016	0.0615
96N200	0.2374	0.2539	0.138	0.2145	0.1803	0.2331	0.1714	0.2553
94HM200	0.113	0.0464	0.0419	-0.0384	0.1053	0.1497	0.086	0.2324
96A200	-0.1218	-0.1168	0.1185	-0.0923	0.1125	0.3013	0.3943	0.2022
96B200	0.1758	0.111	0.3519	0.1145	0.282	0.0647	0.2761	0.2779
96C200	0.1491	0.1834	0.1921	0.2349	0.3222	0.031	0.136	0.2534
96D200	0.0553	0.0571	0.152	0.1304	0.3054	-0.1647	0.0801	0.147
96E200	0.3949	0.3742	0.2123	0.3363	0.2739	0.2032	0.0813	0.3539
96F200	0.3884	0.4268	0.4194	0.4016	0.4331	0.1749	0.2578	0.328
96G200	0.2163	0.4118	0.2391	0.3884	0.3233	0.1538	0.1343	0.3711
96H200	0.0513	0.1383	0.1778	0.1485	0.3325	-0.0483	0.11	0.1204
96I200	-0.0636	0.0402	0.1304	0.0054	0.1529	0.161	0.4478	0.3331
96J200	0.1599	-0.0364	0.2124	0.0975	0.1808	0.003	0.128	0.2725
96K200	0.2198	0.3877	0.1203	0.1016	0.2121	0.3337	0.0591	0.2046
96L200	-0.0582	-0.2338	0.0283	-0.1612	0.0087	0.104	0.2542	0.2501
96M200	0.2158	0.2292	0.1776	0.2008	0.2181	0.336	0.2435	0.3084
96O200	0.1002	0.0453	0.2596	-0.1059	0.1554	0.3686	0.4237	0.4151
96P200	-0.145	-0.2064	0.0988	-0.245	-0.0846	0.2414	0.4927	0.2338
96Q200	-0.0518	-0.0374	0.0869	-0.1811	0.0832	0.104	0.3012	0.2471
96T200	0.2018	0.496	0.3821	0.294	0.3829	0.505	0.3443	0.3106
96U200	0.1207	0.1156	0.0545	0.0948	0.1083	-0.0049	0.1178	0.2053
96V200	0.2984	0.2123	0.2313	0.2099	0.3392	0.2338	0.213	0.4016
96W200	0.327	0.2776	0.2818	0.3004	0.2475	0.3037	0.2221	0.3719
96X200	-0.1457	-0.1295	-0.0519	-0.2273	-0.0314	0.1371	0.2159	0.2866
97A200	0.3453	0.1428	0.1303	0.1516	0.2794	0.1335	0.0821	0.3304
97D200	0.1668	0.3332	0.3393	0.132	0.1368	0.1415	0.3382	0.1665
97E200	0.1513	0.1572	0.3122	0.1908	0.2294	0.3026	0.4036	0.2844
97F200	0.0972	0.053	0.1242	-0.0377	0.3315	0.1346	0.1217	0.3204
97H200	0.1709	0.1017	0.1772	0.1832	0.1549	0.2327	0.1973	0.3014
97I200	0.1286	0.2788	0.3106	0.1572	0.399	0.3101	0.3931	0.3401
97J200	0.1303	0.2797	0.3334	0.1968	0.4317	0.2103	0.339	0.3675
97K200	0.3393	0.4158	0.2675	0.0651	0.3181	0.5158	0.2675	0.3513
97L200	0.04	0.2009	0.2276	0.0029	0.2976	0.3036	0.3967	0.4202
97M200	-0.1292	-0.0153	0.0069	-0.0466	0.2593	0.1586	0.1961	0.3528
97O200	0.177	0.1879	0.041	0.1321	0.1388	-0.0601	0.0326	0.2184
97P200	0.1259	0.1493	0.2917	0.0852	0.3276	0.1924	0.3313	0.3546

	97O100	97P100	97Q100	97N000	97C000	97Q000	97A000	97B000
94Mila								
94Cain								
94Arro								
94Heat								
94Wash								
96A100								
96B100								
96C100								
96E100								
96F100								
96G100								
96H100								
96I100								
96J100								
96K100								
96L100								
96M100								
96O100								
96P100								
96Q100								
96S100								
96V100								
96X100								
97B100								
97D100								
97E100								
97F100								
97I100								
97J100								
97K100								
97L100								
97M100								
97O100	1							
97P100	0.5196	1						
97Q100	0.2225	0.3551	1					

	97O100	97P100	97Q100	97N000	97C000	97Q000	97A000	97B000
97N000	0.0634	0.2151	0.0199	1				
97C000	0.1696	0.158	0.3505	0.2321	1			
97Q000	0.0006	-0.0158	-0.112	0.2713	0.2513	1		
97A000	0.1867	-0.0206	0.1014	0.0528	0.4679	0.1825	1	
97B000	-0.1016	-0.0719	-0.0823	0.2736	0.1931	0.4855	0.2093	1
97E000	0.0729	0.0496	0.0982	0.1008	0.2932	0.1531	0.0982	0.0587
96C000	0.0964	0.0366	0.1147	0.0595	0.2894	0.0652	0.203	-0.0044
96U000	0.1314	0.0679	0.1976	0.1662	0.0088	-0.0399	-0.0002	0.0065
96B000	0.1171	0.1265	-0.0042	0.2571	0.286	0.2719	0.147	0.0721
96I000	0.1127	0.2161	0.2977	0.4085	0.2934	0.1656	0.1141	0.1385
96A000	0.1018	0.0042	0.0941	-0.0111	0.1342	-0.0381	0.1731	-0.0385
93MP300	0.0085	-0.0033	0.2107	0.0804	0.0805	-0.011	-0.0061	-0.0652
96D300	0.0284	0.2386	0.1544	0.2861	0.322	0.211	0.0649	0.0723
97Q700	0.2696	0.2176	0.236	-0.0137	0.2227	0.2352	0.095	0.0561
97B700	0.3276	0.3302	0.1179	0.0384	0.1689	0.1342	0.0547	0.1321
96W400	0.1274	-0.0533	0.0238	0.2357	0.1513	0.309	0.139	0.1896
96N200	0.2412	0.2868	0.0363	0.2834	0.2598	0.0518	0.1978	0.2791
94HM200	0.0697	0.0182	0.0289	0.0584	0.1923	0.0818	0.3193	0.0171
96A200	0.1167	0.2906	0.17	0.3415	0.1309	0.0665	0.0498	0.1472
96B200	0.1993	0.1713	0.1901	0.3291	0.6796	0.3722	0.3641	0.2106
96C200	0.1888	0.0772	0.1274	0.2898	0.6152	0.3337	0.424	0.2308
96D200	0.0296	0.0044	0.1519	0.3625	0.6394	0.3523	0.3519	0.2644
96E200	0.3015	0.2066	0.1903	0.1774	0.4439	0.0942	0.3927	0.1152
96F200	0.3606	0.219	0.1567	0.2275	0.7262	0.2184	0.5291	0.1685
96G200	0.3311	-0.0251	-0.0307	0.1994	0.3194	0.1859	0.4883	0.1925
96H200	0.1273	-0.0852	0.0843	0.2042	0.4923	0.3641	0.3733	0.264
96I200	0.1563	0.1294	0.1264	0.6141	0.3764	0.2541	0.3307	0.2668
96J200	0.1337	0.1889	0.1806	0.2405	0.5166	0.1675	0.3105	0.1335
96K200	0.3417	0.0562	-0.0739	-0.0401	0.0755	0.0786	0.2762	0.0545
96L200	0.0419	0.231	-0.1572	0.3466	0.1217	0.2975	0.1123	0.1686
96M200	0.3004	0.24	-0.0001	0.2402	0.1903	0.0816	0.2244	0.265
96O200	0.2278	0.3401	0.032	0.4466	0.2923	0.2507	0.2004	0.1839
96P200	0.0226	0.3701	0.0187	0.4761	0.0993	0.2163	0.0442	0.2678
96Q200	-0.0027	0.0364	-0.0064	0.5353	0.3606	0.4445	0.341	0.3664
96T200	0.4917	0.3119	0.1286	0.1835	0.1168	0.1546	0.2452	0.2053
96U200	0.1117	0.1738	0.0519	0.1924	0.287	0.3367	0.2351	0.2363
96V200	0.2091	0.168	0.1258	0.2266	0.4803	0.1823	0.486	0.176
96W200	0.3436	0.2468	0.0493	0.129	0.2561	0.0842	0.347	0.1793
96X200	-0.1247	-0.0233	0.0636	0.3313	0.1597	0.1921	0.34	0.2607
97A200	0.1832	0.0615	0.0351	0.0583	0.5223	0.1487	0.5696	0.1339
97D200	0.1875	0.2471	0.1628	0.2636	0.484	0.2048	0.3011	0.0809
97E200	0.2758	0.4857	0.1654	0.4651	0.3578	0.158	0.1699	0.3151
97F200	0.1279	0.0436	0.1291	0.2482	0.4393	0.1637	0.3963	0.1436
97H200	0.2539	0.2675	-0.0495	0.1987	0.2322	0.1969	0.2734	0.2435
97I200	0.2861	0.1723	0.0628	0.3281	0.4008	0.2266	0.4663	0.3284
97J200	0.3015	0.087	0.1079	0.2826	0.5165	0.2653	0.5646	0.2454
97K200	0.3704	0.195	-0.0257	-0.005	0.1716	0.0705	0.416	0.0176
97L200	0.2281	0.1586	0.264	0.4006	0.4077	0.1564	0.3788	0.1617
97M200	0.0151	0.0623	0.0921	0.3228	0.1946	0.1069	0.2513	0.243
97O200	0.0491	-0.2257	0.0517	0.0672	0.3832	0.1298	0.311	0.0383
97P200	0.1247	0.3376	0.2669	0.5309	0.4627	0.0553	0.2998	0.1068

	97E000	96C000	96U000	96B000	96I000	96A000	93MP300	96D300
97N000								
97C000								
97Q000								
97A000								
97B000								
97E000	1							
96C000	0.5951	1						
96U000	0.1414	0.1004	1					
96B000	0.5683	0.4436	0.1803	1				
96I000	0.3741	0.427	0.2683	0.5882	1			
96A000	0.4967	0.6051	0.2616	0.5447	0.4238	1		
93MP300	0.2001	0.1437	0.0556	0.21	0.1214	0.0628	1	
96D300	0.3384	0.4346	0.1454	0.4626	0.4627	0.2287	0.2871	1
97Q700	0.1886	0.0367	-0.0466	0.2634	0.0479	0.0284	0.106	0.15
97B700	0.077	-0.0656	-0.0144	0.1376	0.0405	-0.0835	-0.0563	0.1483
96W400	-0.1123	-0.1969	0.4058	0.089	0.152	-0.0623	0.0712	-0.0886
96N200	0.1174	0.0378	0.0503	0.1673	0.1241	0.0407	-0.019	0.0483
94HM200	0.141	0.1106	0.0612	0.1289	0.0495	0.1885	0.13	-0.0164
96A200	0.1637	0.0934	0.0777	0.3033	0.2761	0.2562	0.1019	0.1502
96B200	0.3114	0.33	0.0873	0.4094	0.3613	0.1763	0.2642	0.4738
96C200	0.2706	0.2248	0.0324	0.2215	0.2367	0.1882	0.1804	0.2324
96D200	0.1862	0.2465	0.0404	0.2393	0.2573	0.104	0.2415	0.3927
96E200	0.1406	0.1239	0.1199	0.1311	0.113	0.1242	-0.0005	0.005
96F200	0.2375	0.2929	0.0709	0.258	0.2747	0.1834	0.0546	0.3254
96G200	0.2294	0.2837	0.2167	0.2294	0.3053	0.295	-0.0881	0.0214
96H200	0.2609	0.1401	0.0795	0.1256	0.1233	0.0686	0.1794	0.1515
96I200	0.1501	0.1842	0.1814	0.3512	0.4531	0.2094	0.1022	0.2638
96J200	0.2895	0.3335	0.18	0.3993	0.3247	0.3269	0.1197	0.3313
96K200	0.0718	-0.0119	-0.0241	0.165	-0.1205	0.0557	0.1451	-0.1128
96L200	0.1873	0.0098	-0.0044	0.3728	0.1	0.1246	0.0548	0.1888
96M200	0.1654	0.0205	0.0706	0.2002	0.0583	0.0876	0.016	-0.0069
96O200	0.2518	0.1504	0.0868	0.4499	0.2981	0.2582	0.1131	0.269
96P200	0.1867	0.0374	0.096	0.3463	0.2998	0.1216	-0.0238	0.2481
96Q200	0.3162	0.2771	0.1296	0.4469	0.4311	0.3376	0.1215	0.3135
96T200	0.0849	0.0196	0.0592	0.1279	0.1234	0.0217	0.1619	-0.0499
96U200	0.2103	0.2257	0.2585	0.3324	0.2093	0.2358	0.139	0.2235
96V200	0.1739	0.1298	0.0958	0.2578	0.1579	0.1707	0.048	0.0752
96W200	0.1606	0.1138	0.1389	0.2193	0.1232	0.1433	-0.0818	0.0338
96X200	0.1824	0.1471	0.1773	0.2453	0.2804	0.3489	0.0333	0.1019
97A200	0.2279	0.1871	-0.047	0.2686	0.0686	0.2467	-0.021	0.0472
97D200	0.0905	0.1637	0.0398	0.2398	0.3486	0.0543	0.0884	0.4027
97E200	0.1664	0.0473	0.0731	0.251	0.2549	0.0497	0.0324	0.1742
97F200	0.3356	0.2641	0.091	0.3358	0.1692	0.333	0.2762	0.2416
97H200	0.1421	-0.0314	0.003	0.256	0.0482	0.0557	-0.0406	0.0325
97I200	0.2957	0.2116	0.1977	0.3757	0.2509	0.2342	0.1765	0.1869
97J200	0.25	0.2539	0.0974	0.3264	0.2714	0.1947	0.1275	0.2452
97K200	0.0909	-0.0013	-0.0137	0.2025	-0.0896	0.1335	0.1225	-0.0835
97L200	0.3381	0.3274	0.2431	0.3844	0.4433	0.3394	0.1717	0.2868
97M200	0.199	0.0689	0.1957	0.1586	0.1723	0.2268	0.1823	0.0982
97O200	0.1493	0.2871	0.1146	0.1771	0.2785	0.3496	-0.1162	0.0932
97P200	0.3046	0.2565	0.1466	0.3192	0.4107	0.1901	0.1257	0.4191

	97Q700	97B700	96W400	96N200	94HM200	96A200	96B200	96C200
97N000								
97C000								
97Q000								
97A000								
97B000								
96E000								
96C000								
96U000								
96B000								
96I000								
96A000								
93MP300								
96D300								
97Q700	1							
97B700	0.5922	1						
96W400	0.0267	0.0196	1					
96N200	0.0444	0.271	0.2317	1				
94HM200	-0.0129	-0.1219	0.2965	0.348	1			
96A200	0.1671	0.283	-0.0777	0.5263	0.3304	1		
96B200	0.3378	0.1245	0.0373	0.1676	0.1946	0.2212	1	
96C200	0.1792	0.0044	0.1811	0.2545	0.3638	0.2228	0.6931	1
96D200	0.1515	0.0201	-0.0846	0.0731	0.1227	0.103	0.75	0.6864
96E200	0.0048	0.0602	0.4217	0.5929	0.4529	0.2307	0.2537	0.472
96F200	0.1922	0.2493	0.1374	0.3995	0.2247	0.1921	0.6256	0.6747
96G200	-0.0305	0.0463	0.3027	0.3168	0.2402	0.0577	0.2927	0.4263
96H200	0.2058	0.0779	-0.0963	-0.0451	0.0748	-0.0042	0.5456	0.5505
96I200	-0.0004	0.0947	0.1099	0.4095	0.2984	0.5821	0.5251	0.5021
96J200	0.16	0.0568	0.0868	0.4555	0.3354	0.3833	0.6035	0.4805
96K200	0.0604	0.0876	-0.0107	0.4225	0.2948	0.1866	0.0645	0.0811
96L200	0.1964	0.1866	-0.006	0.4844	0.2899	0.5538	0.2915	0.2998
96M200	0.1034	0.3048	0.1888	0.8957	0.4075	0.5673	0.1436	0.2745
96O200	0.0929	0.0616	0.0327	0.5426	0.3933	0.6064	0.429	0.3953
96P200	0.0805	0.2396	0.0135	0.4671	0.2673	0.7275	0.2176	0.1539
96Q200	0.0732	0.0205	0.1592	0.2375	0.2785	0.3862	0.5412	0.4743
96T200	0.1859	0.3369	0.1608	0.4293	0.2129	0.3138	0.1414	0.2144
96U200	0.1283	0.0695	0.4511	0.4827	0.6994	0.2379	0.3708	0.4784
96V200	0.0363	0.0998	0.3558	0.624	0.5221	0.355	0.3364	0.5012
96W200	0.0802	0.2312	0.4583	0.6978	0.4304	0.3099	0.1932	0.2705
96X200	-0.177	-0.1587	0.0978	0.2553	0.356	0.3512	0.2275	0.2768
97A200	0.1462	0.0613	0.135	0.5098	0.4356	0.2942	0.3842	0.5073
97D200	0.1145	0.1837	0.0474	0.0894	-0.0153	0.0301	0.4349	0.3037
97E200	0.1905	0.4007	0.1893	0.802	0.2871	0.6398	0.3304	0.3644
97F200	0.1156	-0.016	0.0064	0.3763	0.3851	0.3757	0.5341	0.5446
97H200	0.1943	0.2569	0.2391	0.7416	0.3315	0.4252	0.2633	0.3366
97I200	0.1066	0.2394	0.182	0.5577	0.4141	0.4877	0.4249	0.4965
97J200	0.1471	0.063	0.0751	0.3341	0.3526	0.2739	0.5936	0.6897
97K200	0.0907	0.1464	-0.0029	0.4582	0.4374	0.3559	0.1755	0.2214
97L200	0.0215	0.0007	0.0904	0.3479	0.3457	0.3671	0.5172	0.5205
97M200	-0.0033	0.0544	0.1814	0.5271	0.4003	0.4836	0.3372	0.4183
97O200	-0.1353	-0.1491	0.0244	-0.0082	0.1005	-0.0892	0.3258	0.396
97P200	0.0689	0.15	0.1748	0.4812	0.1944	0.3214	0.4188	0.3701

	96D200	96E200	96F200	96G200	96H200	96I200	96J200	96K200
97N000								
97C000								
97Q000								
97A000								
97B000								
97E000								
96C000								
96U000								
96B000								
96I000								
96A000								
93MP300								
96D300								
97Q700								
97B700								
96W400								
96N200								
94HM200								
96A200								
96B200								
96C200								
96D200	1							
96E200	0.1979	1						
96F200	0.564	0.5181	1					
96G200	0.2172	0.557	0.4848	1				
96H200	0.6595	0.0866	0.4419	0.249	1			
96I200	0.4542	0.3205	0.3867	0.3923	0.2263	1		
96J200	0.4809	0.4571	0.5174	0.3514	0.189	0.4942	1	
96K200	-0.0325	0.3018	0.1742	0.1968	0.1028	0.0779	0.1306	1
96L200	0.2379	0.1663	0.1984	0.0343	0.0672	0.4971	0.4824	0.2649
96M200	0.0167	0.5457	0.3517	0.3157	-0.0032	0.4114	0.4285	0.5193
96O200	0.2729	0.3612	0.3456	0.1705	0.1191	0.5618	0.5008	0.3679
96P200	0.1069	0.1089	0.1446	-0.0232	-0.0278	0.5873	0.3804	0.0956
96Q200	0.4558	0.1641	0.3567	0.3043	0.318	0.7039	0.4802	0.0769
96T200	0.0157	0.3955	0.3018	0.3153	0.1482	0.1545	0.1209	0.5719
96U200	0.2857	0.6107	0.3337	0.3201	0.1484	0.4389	0.4212	0.2016
96V200	0.3286	0.816	0.5437	0.5136	0.1974	0.4416	0.5442	0.2767
96W200	0.0478	0.7202	0.3762	0.4322	-0.0185	0.3058	0.4359	0.2595
96X200	0.1726	0.2855	0.1313	0.32	0.0702	0.5966	0.3968	0.0707
97A200	0.2937	0.6017	0.6348	0.4831	0.2134	0.3605	0.551	0.295
97D200	0.3533	0.1731	0.5626	0.3098	0.2568	0.2834	0.2578	0.019
97E200	0.2494	0.5035	0.4865	0.2056	0.0965	0.5056	0.4655	0.213
97F200	0.4877	0.2823	0.4468	0.3131	0.3584	0.5267	0.4908	0.3451
97H200	0.12	0.6286	0.3955	0.3499	0.0722	0.3301	0.4956	0.3795
97I200	0.3314	0.5417	0.5954	0.5149	0.3639	0.5413	0.4233	0.2967
97J200	0.5399	0.4191	0.677	0.537	0.4436	0.559	0.4877	0.2835
97K200	-0.0022	0.4025	0.3051	0.2656	0.1438	0.1971	0.2012	0.7338
97L200	0.3324	0.3371	0.4534	0.4047	0.2781	0.6176	0.3965	0.2789
97M200	0.2855	0.3213	0.2906	0.2873	0.2022	0.5714	0.4329	0.2743
97O200	0.3689	0.2607	0.4835	0.4632	0.2421	0.3532	0.2655	-0.0998
97P200	0.3811	0.3717	0.5224	0.3016	0.212	0.4855	0.4	0.0117

	96L200	96M200	96O200	96P200	96Q200	96T200	96U200	96V200
97N000								
97C000								
97Q000								
97A000								
97B000								
97E000								
96C000								
96U000								
96B000								
96I000								
96A000								
93MP300								
96D300								
97Q700								
97B700								
96W400								
96N200								
94HM200								
96A200								
96B200								
96C200								
96D200								
96E200								
96F200								
96G200								
96H200								
96I200								
96J200								
96K200								
96L200	1							
96M200	0.5728	1						
96O200	0.6583	0.5649	1					
96P200	0.75	0.5098	0.7087	1				
96Q200	0.5167	0.2554	0.5947	0.5498	1			
96T200	0.137	0.5069	0.2954	0.1363	0.0806	1		
96U200	0.3533	0.4874	0.3455	0.2546	0.2966	0.2725	1	
96V200	0.3799	0.6191	0.4782	0.2824	0.3199	0.3044	0.6547	1
96W200	0.2868	0.6728	0.4105	0.2548	0.1912	0.3571	0.663	0.7215
96X200	0.3757	0.2709	0.5579	0.4898	0.6943	-0.0395	0.2026	0.4193
97A200	0.4189	0.5287	0.387	0.1996	0.3387	0.2162	0.4141	0.7152
97D200	-0.0031	0.0146	0.1187	0.1272	0.2457	0.2195	0.1237	0.189
97E200	0.5555	0.7638	0.6047	0.6437	0.3336	0.4653	0.4296	0.5661
97F200	0.5161	0.4041	0.6421	0.3672	0.6749	0.0883	0.3295	0.4221
97H200	0.5782	0.7476	0.5095	0.4226	0.2374	0.3939	0.5832	0.6944
97I200	0.3969	0.6106	0.5186	0.4145	0.4299	0.4971	0.5783	0.6616
97J200	0.3821	0.3847	0.4471	0.2617	0.5063	0.3569	0.3956	0.5129
97K200	0.3344	0.6067	0.558	0.2495	0.2178	0.5618	0.2247	0.4512
97L200	0.2601	0.361	0.5716	0.3885	0.6336	0.2371	0.3024	0.3931
97M200	0.597	0.5585	0.5768	0.5162	0.5911	0.1687	0.5024	0.4635
97O200	-0.0954	-0.0614	0.1026	-0.1139	0.3534	-0.1264	0.1439	0.2552
97P200	0.3569	0.3901	0.5352	0.422	0.4315	0.1341	0.3284	0.4889

	96W200	96X200	97A200	97D200	97E200	97F200	97H200	97I200
97N000								
97C000								
97Q000								
97A000								
97B000								
97E000								
96C000								
96U000								
96B000								
96I000								
96A000								
93MP300								
96D300								
97Q700								
97B700								
96W400								
96N200								
94HM200								
96A200								
96B200								
96C200								
96D200								
96E200								
96F200								
96G200								
96H200								
96I200								
96J200								
96K200								
96L200								
96M200								
96O200								
96P200								
96Q200								
96T200								
96U200								
96V200								
96W200	1							
96X200	0.2722	1						
97A200	0.5213	0.3414	1					
97D200	0.0395	0.0617	0.2156	1				
97E200	0.6015	0.2414	0.4171	0.2106	1			
97F200	0.2602	0.5494	0.537	0.0523	0.3641	1		
97H200	0.6957	0.2432	0.6003	0.0786	0.6515	0.3158	1	
97I200	0.5497	0.3551	0.5394	0.2929	0.6118	0.464	0.5909	1
97J200	0.3402	0.3029	0.5801	0.3748	0.371	0.5689	0.3888	0.6313
97K200	0.4017	0.276	0.4518	0.0595	0.3512	0.4578	0.4534	0.5026
97L200	0.2697	0.5338	0.3924	0.2964	0.3619	0.6481	0.2618	0.448
97M200	0.3747	0.5772	0.4048	-0.0661	0.5031	0.7126	0.4467	0.4936
97O200	0.0814	0.3291	0.3451	0.3528	-0.0826	0.2831	0.0024	0.208
97P200	0.3488	0.3602	0.4211	0.3666	0.5864	0.5357	0.3489	0.5069

	97J200	97K200	97L200	97M200	97O200	97P200
97N000						
97C000						
97Q000						
97A000						
97B000						
97E000						
96C000						
96U000						
96B000						
96I000						
96A000						
93MP300						
96D300						
97Q700						
97B700						
96W400						
96N200						
94HM200						
96A200						
96B200						
96C200						
96D200						
96E200						
96F200						
96G200						
96H200						
96I200						
96J200						
96K200						
96L200						
96M200						
96O200						
96P200						
96Q200						
96T200						
96U200						
96V200						
96W200						
96X200						
97A200						
97D200						
97E200						
97F200						
97H200						
97I200						
97J200	1					
97K200	0.4048	1				
97L200	0.5744	0.3837	1			
97M200	0.4736	0.3332	0.5758	1		
97O200	0.3616	-0.0213	0.4011	0.2023	1	
97P200	0.4072	0.175	0.5778	0.5115	0.2811	1

Appendix C - PERL Script for ***TREE*** model

```
#! c:\perl\bin\perl

##############################################
#             TREE 2.1  (A Colin et al. project)             #
##############################################

$title = "Tree-ring Radial Expansion Estimator";  # Title of the page
$form  = "treeform";            # Name of the file with form inside.
$home  = "http://cgrg.geog.uvic.ca";
$action= "/cgi-bin/tree.cgi";     # Name of the script file
$root  = "c:/progra~1/apache~1/apache/htdocs";

###################################
#           Start of Program                  #
###################################

print "Content-type: text/html\n\n";
&Header;
$length = $ENV{'CONTENT_LENGTH'};
$method = $ENV{'REQUEST_METHOD'};
if ("$length")  { &RunEngine;  }
else  {
open(FORM,$form) || &Footer("<h6>Cannot open $form!\n</h6>");
print STDOUT <FORM>;
close(FORM);
&Footer;
}
if ($sector eq "Mountain hemlock" ) { &MHCALC  }
if ($sector eq "Yellow-cedar" ) { &YCCALC  }
if ($sector eq "Western hemlock" ) { &WHCALC  }
if ($sector eq "Western red-cedar" ) { &WRCCALC  }
if ($sector eq "Douglas-fir" ) { &DFCALC  }
if ($sector eq "All montane tree species") { &ALL  }
if ($sector eq "Mountain hemlock" ) { &MHOUT  }
if ($sector eq "Yellow-cedar" ) { &YCOUT  }
if ($sector eq "Western hemlock" ) { &WHOUT  }
if ($sector eq "Western red-cedar" ) { &WRCOUT  }
if ($sector eq "Douglas-fir" ) { &DFOUT  }
if ($sector eq "All montane tree species") { &ALLOUT  }
&Footer;
###############
# Sub-routines  #
##############
sub Header {
print<<"EOHEADER";
<HTML>
<HEAD>
<TITLE>TREE Modeller Version 2.1</TITLE>
</HEAD>
<BODY bgcolor="FFFFCC"><center>
```

```
<A HREF="http://office.geog.uvic.ca/dept/uvtrl/uvtrl.htm"><IMG border="0" SRC="/uvtrl.gif"></A>
<P><P>
<IMG src="/title.gif">
<HR><P>
EOHEADER
}
sub RunEngine {

        &footer("Request Method must be POST") if ($method ne "POST");
        if(read(STDIN,$entries,$length)     < $length) { print "<h4>Short Read</h4>"; }
        @entries = split(/&/,$entries);
        foreach $nxt (@entries) {
                $nxt =~ s/\+/ /g;
                $nxt =~ s/%([A-Fa-f0-9]{2})/pack("c",hex($1))/ge;

                if  ($nxt =~ /jan-temp=(.*)/) {
                        $jantemp   = $1;
                } elsif ($nxt =~ /feb-temp=(.*)/) {
                        $febtemp   = $1;
                } elsif ($nxt =~ /march-temp=(.*)/) {
                        $marchtemp   = $1;
                } elsif ($nxt =~ /april-temp=(.*)/) {
                        $aprtemp   = $1;
                } elsif ($nxt =~ /may-temp=(.*)/) {
                        $maytemp   = $1;
                } elsif ($nxt =~ /june-temp=(.*)/) {
                        $junetemp   = $1;
                } elsif ($nxt =~ /july-temp=(.*)/) {
                        $julytemp   = $1;
                } elsif ($nxt =~ /aug-temp=(.*)/) {
                        $augtemp   = $1;
                } elsif ($nxt =~ /sept-temp=(.*)/) {
                        $septtemp   = $1;
                } elsif ($nxt =~ /oct-temp=(.*)/) {
                        $octtemp   = $1;
                } elsif ($nxt =~ /nov-temp=(.*)/) {
                        $novtemp   = $1;
                } elsif ($nxt =~ /dec-temp=(.*)/) {
                        $dectemp   = $1;
                } elsif($nxt =~ /jan-precip=(.*)/) {
                        $janprecip   = $1;
                } elsif ($nxt =~ /feb-precip=(.*)/) {
                        $febprecip   = $1;
                } elsif ($nxt =~ /march-precip=(.*)/) {
                        $marchprecip   = $1;
                } elsif ($nxt =~ /april-precip=(.*)/) {
                        $aprilprecip   = $1;
                } elsif ($nxt =~ /may-precip=(.*)/) {
                        $mayprecip   = $1;
                } elsif ($nxt =~ /june-precip=(.*)/) {
                        $juneprecip   = $1;
                } elsif ($nxt =~ /july-precip=(.*)/) {
```

```
                $julyprecip   = $1;
            } elsif ($nxt =~ /aug-precip=(.*)/) {
                $augprecip   = $1;
            } elsif ($nxt =~ /sept-precip=(.*)/) {
                $septprecip   = $1;
            } elsif ($nxt =~ /oct-precip=(.*)/) {
                $octprecip   = $1;
            } elsif ($nxt =~ /nov-precip=(.*)/) {
                $novprecip   = $1;
            } elsif ($nxt =~ /dec-precip=(.*)/) {
                $decprecip   = $1;
            } elsif ($nxt =~ /sector=(.*)/) {
                $sector   = $1;
            } elsif ($nxt =~ /years=(.*)/) {
                $years   = $1;
            } else {
                print "<h4>Unknown search item $nxt</h4><br>\n";
            }
    }

if ($jantemp eq "100 yr. Average") { $jantemp = 26.07  } elsif ($jantemp ne "100 yr. Average") {$jantemp
= 26.07 + ($jantemp*10) }
if ($febtemp eq "100 yr. Average") { $febtemp = 40.07  } elsif ($febtemp ne "100 yr. Average")
{$febtemp = 40.07 + ($febtemp*10) }
if ($marchtemp eq "100 yr. Average") { $marchtemp = 58.19  } elsif ($marchtemp ne "100 yr. Average")
{$marchtemp = 58.19 + ($marchtemp*10) }
if ($apriltemp eq "100 yr. Average")  { $apriltemp = 86.62  } elsif ($apriltemp ne "100 yr. Average")
{$apriltemp = 86.62 + ($apriltemp*10) }
if ($maytemp eq "100 yr. Average")  { $maytemp = 122.66  } elsif ($maytemp ne "100 yr. Average")
{ $maytemp = 122.66 + ($maytemp*10) }
if ($junetemp eq "100 yr. Average")  { $junetemp = 151.52  } elsif ($junetemp ne "100 yr. Average")
{ $junetemp = 151.52 + ($junetemp*10) }
if ($julytemp eq "100 yr. Average")  { $julytemp = 177.71  } elsif ($jultemp ne "100 yr. Average")
{ $julytemp = 177.71 + ($julytemp*10) }
if ($augtemp eq "100 yr. Average")  { $augtemp = 176.96  } elsif ($augtemp ne "100 yr. Average")
{ $augtemp = 176.96 + ($augtemp*10) }
if ($septtemp eq "100 yr. Average") { $septtemp = 145.11  } elsif ($septtemp ne "100 yr. Average")
{$septtemp = 145.11 + ($septtemp*10) }
if ($octtemp eq "100 yr. Average")  { $octtemp = 99.40  } elsif ($octtemp ne "100 yr. Average")
{$octtemp = 99.40 + ($octtemp*10) }
if ($novtemp eq "100 yr. Average") { $novtemp = 57.43  } elsif ($novtemp ne "100 yr. Average")
{$novtemp = 57.43 + ($novtemp*10) }
if ($dectemp eq "100 yr. Average") { $dectemp = 35.11  } elsif ($dectemp ne "100 yr. Average")
{$dectemp = 35.11 + ($dectemp*10) }
if ($janprecip eq "100 yr. Average") { $janprecip = 1592.21  } elsif ($janprecip ne "100 yr. Average")
{ $janprecip = 1592.21 + ($janprecip*10) }
if ($febprecip eq "100 yr. Average") { $febprecip = 1179.56  } elsif ($febprecip ne "100 yr. Average")
{ $febprecip = 1179.56 + ($febprecip*10) }
if ($marchprecip eq "100 yr. Average"){$marchpecip = 908.52} elsif ($marchprecip ne "100 yr. Average")
{ $marchprecip = 908.52 + ($marchprecip*10) }
if ($aprilprecip eq "100 yr. Average") { $aprilprecip = 551.45  } elsif ($aprilprecip ne "100 yr. Average")
{ $aprilprecip = 551.45 + ($aprilprecip*10) }
```

```
if ($mayprecip eq "100 yr. Average") { $mayprecip = 421.63  } elsif ($mayprecip ne "100 yr. Average")
{ $mayprecip = 421.63 + ($mayprecip*10) }
if ($juneprecip eq "100 yr. Average") { $juneprecip = 418.54  } elsif ($juneprecip ne "100 yr. Average")
{ $juneprecip = 418.54 + ($juneprecip*10) }
if ($julyprecip eq "100 yr. Average") { $julyprecip = 251.79  } elsif ($julyprecip ne "100 yr. Average")
{ $julyprecip = 251.79 + ($julyprecip*10) }
if ($augprecip eq "100 yr. Average") { $augprecip = 280.24    } elsif ($augprecip ne "100 yr. Average")
{ $augprecip = 280.24 + ($augprecip*10) }
if ($septprecip eq "100 yr. Average") { $septprecip = 445.07  } elsif ($septprecip ne "100 yr. Average")
{ $septprecip = 445.07 + ($septprecip*10) }
if ($octprecip eq "100 yr. Average") { $octprecip = 965.90  } elsif ($octprecip ne "100 yr. Average")
{ $octprecip = 965.90  + ($octprecip*10) }
if ($novprecip eq "100 yr. Average") { $novprecip = 1665.29  } elsif ($novprecip ne "100 yr. Average")
{ $novprecip = 1665.29 + ($novprecip*10) }
if ($decprecip eq "100 yr. Average") { $decprecip = 1771.17  } elsif ($decprecip ne "100 yr. Average")
{ $decprecip = 1771.17  + ($decprecip*10) }

$pmayprecip  = 421.63; $pjuneprecip = 418.54; $pjulyprecip = 251.79; $paugprecip =   280.24;
$pseptprecip = 445.07; $poctprecip  = 965.90; $pnovprecip  = 1665.29; $pdecprecip =   1771.17;
$pmaytemp =122.66; $pjunetemp = 151.52; $pjulytemp = 177.71; $paugtemp =176.96;
$pseptemp = 145.11; $pocttemp = 99.40; $pnovtemp = 57.43; $pdectemp = 35.11;
$lag = 1.00;
}

sub MHCALC {
                    $twig1 = "/mh1.gif";
                    $TREE = "Mountain ";
                    $SPECIES = "Hemlock ";
                    $JPG = "/mh.gif";
                    RUN_LOOP: for ($count = 1; $count <= $years; $count++){
                    { $mh1 =
($apriltemp*0.0017)+($augprecip*0.0001362)+($dectemp*0.001423)+($julytemp*0.001287)+
($junetemp*0.002033)+($marchtemp*0.001764)+($mayprecip*-0.00007374)+($pdecprecip*-0.00003426)
+($pjulyprecip*-0.0001392)+($pjulytemp*-0.006888)+($pjuneprecip*0.0001224)+($lag*0.600)+(0.82488
);
          $pjuneprecip = $juneprecip;  $pjulyprecip = $julyprecip;  $pdecprecip  = $decprecip;
          $pjulytemp =  $julytemp;

          &Trunk;
          push (@mh,$mh1);
          $mh_sum1 += $mh1;
          $lag = $mh1;
          if ($count eq $years){
          last RUN_LOOP;}
          next RUN_LOOP;
          }
          }
          $mh_total1 = $mh_sum1/$years;
          &Trunk;
          if ($mh_total1 > 1.05) {$mh_rad="rad1.gif";} elsif ($mh_total1 < 0.95){$mh_rad="rad3.gif";}
          else {($mh_rad ="rad2.gif");}
          if ($mh_total1 > 1.05) {$mh_norm="above normal growth.";} elsif
```

```
($mh_total1 < 0.95){$mh_norm="below normal growth.";} else
{($mh_norm ="close to average growth.");}
}

sub YCCALC {
        $twig1 = "/yc1.gif";
        $TREE = "Yellow ";
        $SPECIES = "Cedar ";
        $JPG = "/yc.gif";
        RUN_LOOP: for ($count = 1; $count <= $years; $count++){

        { $yc1 =
($augtemp*-0.002083)+($febprecip*0.00004853)+($julytemp*0.002375)+($pjulytemp*-0.002667)+
($pnovprecip*-0.00003721)+($pocttemp*0.00325)+($pseptttemp*-0.00217)+($lag*0.703)+(0.714060);



        $pnovprecip  =  $novprecip;        $pjulytemp =     $julytemp;
        $pseptttemp  =   $septtemp;        $pocttemp  =     $octtemp;


        &Trunk;
        push (@yc,$yc1);
        $yc_sum1 += $yc1;
        $lag = $yc1;
        if ($count eq $years){
        last RUN_LOOP;}
        next RUN_LOOP;
        }
        }
        $yc_total1 = $yc_sum1/$years;
        &Trunk;
        if ($yc_total1 > 1.05) {$yc_rad="rad1.gif";} elsif ($yc_total1 < 0.95){$yc_rad="rad3.gif";} else
        {($yc_rad ="rad2.gif");}
        if ($yc_total1 > 1.05) {$yc_norm="above normal growth.";} elsif
         ($yc_total1 < 0.95){$yc_norm="below normal growth.";} else
        {($yc_norm ="close to average growth.");}
        }

sub WHCALC {
        {
        $twig1 = "/wh1.gif";
        $TREE = "Western ";
        $SPECIES = "Hemlock ";
        $JPG = "/wh.gif";
        RUN_LOOP: for ($count = 1; $count <= $years; $count++)

        {$wh1 =
($apriltemp*0.001748)+($augprecip*0.00007632)+($janprecip*-0.00002267)+($junetemp*-0.001128)+($
paugprecip*0.0001395)+($pjulytemp*-0.002621)+($pseptprecip*-0.00002694)+
($lag*0.765)+(0.707885);
```

```
        $paugprecip  = $augprecip;  $pseptprecip = $septprecip;  $pjulytemp =  $julytemp;


        &Trunk;
        push (@wh,$wh1);
        $wh_sum1 += $wh1;
        $lag = $wh1;
        if ($count eq $years){
        last RUN_LOOP;}
        next RUN_LOOP;
        }
        }
        $wh_total1 = $wh_sum1/$years;
        &Trunk;
        if ($wh_total1 > 1.05) {$wh_rad="rad1.gif";} elsif ($wh_total1 < 0.95){$wh_rad="rad3.gif";}
        else {($wh_rad ="rad2.gif");}
        if ($wh_total1 > 1.05) {$wh_norm="above normal growth.";} elsif
        ($wh_total1 < 0.95){$wh_norm="below normal growth.";} else
        {($wh_norm ="close to average growth.");}
        }

sub WRCCALC {
                $twig1 = "/wrc1.gif";
                $TREE = "Western ";
                $SPECIES = "red-cedar ";
                $JPG = "/wrc.gif";
                RUN_LOOP: for ($count = 1; $count <= $years; $count++){

                { $wrc1 =
($febtemp*0.003154)+($junetemp*-0.003885)+($julyprecip*0.0001133)+($mayprecip*-0.000543)+
($paugtemp*-0.001977)+($pdecprecip*-0.0000246)+($pjulyprecip*0.002131)+($pjulytemp*-0.001369)+
($pnovprecip*-0.00002821)+($poctprecip*0.00003589)+($pocttemp*0.002782)+($psepttemp*0.001995)+
($lag*0.580)+(0.9059768);

        $pjulyprecip =   $julyprecip; $poctprecip  = $octprecip;  $pnovprecip  = $novprecip;
        $pdecprecip  =   $decprecip;  $pjulytemp = $julytemp; $paugtemp =   $augtemp;
        $pseptemp =      $septtemp;   $pocttemp =  $octtemp;


        &Trunk;
        push (@wrc,$wrc1);
        $wrc_sum1 += $wrc1;
        $lag = $wrc1;
        if ($count eq $years){
        last RUN_LOOP;}
        next RUN_LOOP;
        }
        }
        $wrc_total1 = $wrc_sum1/$years;
        &Trunk;
        if ($wrc_total1 > 1.05) {$wrc_rad="rad1.gif";} elsif ($wrc_total1 < 0.95){$wrc_rad="rad3.gif";}
        else {($wrc_rad ="rad2.gif");}
```

```
        if ($wrc_total1 > 1.05){$wrc_norm="above normal growth.";} elsif
        ($wrc_total1 < 0.95){$wrc_norm="below normal growth.";} else
        {($wrc_norm ="close to average growth.");}
        }

sub DFCALC {
                {
                $twig1 = "/df1.gif";
                $TREE = "Douglas-";
                $SPECIES = "fir";
                $JPG = "/df.gif";
                RUN_LOOP: for ($count = 1; $count <= $years; $count++)

                {$df1 =
($mayprecip*0.00008060)+($novprecip*0.00001835)+($pjuneprecip*0.0002227)+($pjulyprecip*0.00018
01)+ ($pmaytemp*-0.001733)+($septprecip*0.00006149)+($lag*0.551)+(0.4311048) ;

        $pjuneprecip = $juneprecip; $pjulyprecip = $julyprecip; $pmaytemp = $maytemp;


        &Trunk;
        push (@df,$df1);
        $df_sum1 += $df1;
        $lag = $df1;
        if ($count eq $years){
                last RUN_LOOP;}
                next RUN_LOOP;
                }
                }
        $df_total1 = $df_sum1/$years;
        &Trunk;
        if ($df_total1 > 1.05) {$df_rad="rad1.gif";} elsif ($df_total1 < 0.95){$df_rad="rad3.gif";} else
        {($df_rad ="rad2.gif");}
        if ($df_total1 > 1.05) {$df_norm="above normal growth.";} elsif
        ($df_total1 < 0.95){$df_norm="below normal growth.";} else
        {($df_norm ="close to average growth.");}
        }

sub ALL  {
                &MHCALC;
                &YCCALC;
                &WHCALC;
                &WRCCALC;
                &DFCALC;
}

sub MHOUT {

print<<"EOMODEL";
        <P> <HR width= 550> <TABLE border=0 align="center">
        <P><CENTER><IMG src="/vi3.gif"></CENTER><P><P>
        <H2><UND> Results for $sector</UND></H2> <TR>
```

```
        <TD height="150" width="100" align="center" valign="middle">
        <IMG src="/mh.gif"><BR><B>Mountain<BR>Hemlock</B></TD>
        <TD height="150"  width="100" align="center" valign="middle">
        <IMG src="/$mh_rad">  </TD>
        <TD height="150"  width="300" align="left" valign="middle">
        Based on average growth of 1.0, the climate parameters you have selected
        for the $years years of growth, suggest the average tree growth would be $mh_totall
        or $mh_norm </TD> </TR> </TABLE>
        <TABLE border=0 align="center"> <TR> <TD height=\"50\" align="center" valign="bottom">
EOMODEL
        JPG_LOOP: for ($loop = 0; $loop <= $years; $loop++){
        {$value = @mh[$loop];
        if ($value > 1.05) {$PIC ="mh1.gif";} elsif ($value < 0.95){$PIC="mh3.gif";} else
        {($PIC ="mh2.gif");}
        $timeA = $timeA + 1;
        print "Year $timeA<spacer type=\"horizontal\" size=\"7\"> <BR>
        <IMG SRC=\"/$PIC\"><BR>$value</TD>
        <TD height=\"50\" align=\"center\" valign=\"bottom\">";
        if ($loop == 9)  {print "</TD></TR></TABLE><P>
        <TABLE border=0 align=\"center\"><TR>
        <TD height=\"50\" align=\"center\" valign=\"bottom\">";}
        if ($loop == 19) {print "</TD></TR></TABLE><P>
        <TABLE border=0 align=\"center\"><TR>
        <TD height=\"50\" align=\"center\" valign=\"bottom\">";}
        if ($loop == $years-1) {last JPG_LOOP;}
        next JPG_LOOP;
                }
                }
        if ($value == @mh[0]) {$stabyr = "1st";} elsif ($value == @mh[1]) {$stabyr = "2nd";}elsif
        ($value == @mh[2]) {$stabyr= "3rd";} elsif ($value == @mh[3]) {$stabyr = "4th";} elsif ($value
        == @mh[4]) {$stabyr = "5th";} elsif ($value == @mh[5]) {$stabyr = "6th";} elsif ($value ==
        @mh[6]) {$stabyr = "7th";} elsif ($value == @mh[7]) {$stabyr = "8th";}elsif
        ($value == @mh[8]) {$stabyr = "9th";}else {($stabyr = "10th");}
        if ($years >9){print "The climate scenario you have defined remains static in its inputs, therefore
        the growth increment stabilizes at $value in the $stabyr year and remains the same through the
        time period you have selected.";}
print<<"EOMODEL";
        </TD></TR> </TABLE>
EOMODEL
}

sub YCOUT {

print<<"EOMODEL";
        <HR width= 550> <TABLE border=0 align="center"> <P><CENTER>
        <IMG src="/vi3.jpg"></CENTER><P><P>
        <H2><UND> Results for $sector</UND></H2>
        <TR><TD height="150"  width="100" align="center" valign="middle">
        <IMG src="/yc.gif"><BR><B>Yellow<BR>Cedar</B></TD>
        <TD height="150"  width="100" align="center" valign="middle">
        <IMG src="/$yc_rad"> </TD>
        <TD height="150"  width="300" align="left" valign="middle">
```

```
        Based on average growth of 1.0, the climate parameters you have selected
        for the $years years of growth, suggest the average tree growth would be $yc_total1
        or $yc_norm  </TD> </TR> </TABLE>
        <TABLE border=0 align="center">
        <TR><TD align="center" valign="bottom">
EOMODEL
        JPG_LOOP: for ($loop = 0; $loop <= $years; $loop++){
        {$value = @yc[$loop];
        if ($value > 1.05) {$PIC ="yc1.gif";} elsif ($value < 0.95){$PIC="yc3.gif";} else
        {($PIC ="yc2.gif");}
        $timeB = $timeB + 1;
        print "Year $timeB<spacer type=\"horizontal\" size=\"7\"> <BR>
        <IMG SRC=\"/$PIC\"><BR>$value</TD><TD align=\"center\" valign=\"bottom\">";
        if ($loop == 9) {print "</TD></TR></TABLE><P>
        <TABLE border=0 align=\"center\"><TR><TD align=\"center\" valign=\"bottom\">";}
        if ($loop == 19) {print "</TD></TR></TABLE><P>
        <TABLE border=0 align=\"center\"><TR><TD align=\"center\" valign=\"bottom\">";}
        if ($loop == $years-1) {last JPG_LOOP;}
        next JPG_LOOP;
        }
        }
        if ($value == @yc[0]) {$stabyr = "1st";} elsif ($value == @yc[1]) {$stabyr = "2nd";}elsif
        ($value == @yc[2]) {$stabyr = "3rd";} elsif ($value == @yc[3]) {$stabyr = "4th";} elsif
        ($value == @yc[4]) {$stabyr = "5th";} elsif ($value == @yc[5]) {$stabyr = "6th";} elsif
        ($value == @yc[6]) {$stabyr = "7th";} elsif ($value == @yc[7]) {$stabyr = "8th";}elsif
        ($value == @yc[8]) {$stabyr = "9th";}else {($stabyr = "10th");}
        if ($years >9){print "The climate scenario you have defined remains static in its inputs, therefore
        the growth increment stabilizes at $value in the $stabyr year and remains the same through the
        time period you have selected.";}
print<<"EOMODEL";
        </TD></TR></TABLE>
EOMODEL
}

sub WHOUT {

print<<"EOMODEL";
        <HR width= 550><TABLE border=0 align="center"><P><CENTER>
        <IMG src="/vi3.jpg"></CENTER><P><P>
        <H2><UND> Results for $sector</UND></H2>
        <TR><TD height="150"  width="100" align="center" valign="middle">
        <IMG src="/wh.gif"><BR><B>Western<BR>Hemlock</B></TD>
        <TD height="150"  width="100" align="center" valign="middle">
        <IMG src="/$wh_rad"></TD>
        <TD height="150"  width="300" align="left" valign="middle">
        Based on average growth of 1.0, the climate parameters you have selected
        for the $years years of growth, suggest the average tree growth would be $wh_total1
        or $wh_norm </TD> </TR> </TABLE>
        <TABLE border=0 align="center">
        <TR> <TD align="center" valign="bottom">
EOMODEL
        JPG_LOOP: for ($loop = 0; $loop <= $years; $loop++){
```

```
        {$value = @wh[$loop];
        if ($value > 1.05) {$PIC ="wh1.gif";} elsif ($value < 0.95){$PIC="wh3.gif";} else
        {($PIC ="wh2.gif");}
        $timeC = $timeC + 1;
        print "Year $timeC<spacer type=\"horizontal\" size=\"7\"> <BR>
        <IMG SRC=\"/$PIC\"><BR>$value</TD><TD align=\"center\" valign=\"bottom\">";
        if ($loop == 9) {print "</TD></TR></TABLE><P>
        <TABLE border=0 align=\"center\"><TR><TD align=\"center\" valign=\"bottom\">";}
        if ($loop == 19) {print "</TD></TR></TABLE><P>
        <TABLE border=0 align=\"center\"><TR><TD align=\"center\" valign=\"bottom\">";}
        if ($loop == $years-1) {last JPG_LOOP;}
        next JPG_LOOP;
        }
        }
        if($value == @wh[0]) {$stabyr = "1st";} elsif ($value == @wh[1]) {$stabyr = "2nd";}elsif
        ($value == @wh[2]) {$stabyr = "3rd";} elsif ($value == @wh[3]) {$stabyr = "4th";} elsif
        ($value == @wh[4]) {$stabyr = "5th";} elsif ($value == @wh[5]) {$stabyr = "6th";} elsif
        ($value == @wh[6]) {$stabyr = "7th";} elsif ($value == @wh[7]) {$stabyr = "8th";}elsif
        ($value == @wh[8]) {$stabyr = "9th";}else {($stabyr = "10th");}
        if ($years >9){print "The climate scenario you have defined remains static in its inputs, therefore
        the growth increment stabilizes at $value in the $stabyr year and remains the same through the
        time period you have selected.";}
print<<"EOMODEL";
        </TD></TR></TABLE>
EOMODEL
}

sub WRCOUT {

print<<"EOMODEL";
        <P><HR width= 550><TABLE border=0 align="center"><P><CENTER>
        <IMG src="/vi3.gif"></CENTER><P><P>
        <H2><UND> Results for $sector</UND></H2>
        <TR> <TD height="150" width="100" align="center" valign="middle">
        <IMG src="/wrc.gif"><BR><B>Western<BR>Red-cedar</B></TD>
        <TD height="150"  width="100" align="center" valign="middle">
        <IMG src="/$wrc_rad">  </TD>
        <TD height="150"  width="300" align="left" valign="middle">
        Based on average growth of 1.0, the climate parameters you have selected
        for the $years years of growth, suggest the average tree growth would be $wrc_total1
        or $wrc_norm </TD> </TR> </TABLE>
        <TABLE border=0 align="center"> <TR> <TD align="center" valign="bottom">
EOMODEL
        JPG_LOOP: for ($loop = 0; $loop <= $years; $loop++){
        {$value = @wrc[$loop];
        if ($value > 1.05) {$PIC ="wrc1.gif";} elsif($value < 0.95){$PIC="wrc3.gif";} else
        {($PIC ="wrc2.gif");}
        $timeD = $timeD + 1;
        print "Year $timeD<spacer type=\"horizontal\" size=\"7\"> <BR>
        <IMG SRC=\"/$PIC\"><BR>$value</TD><TD align=\"center\" valign=\"bottom\">";
        if ($loop == 9) {print "</TD></TR></TABLE><P>
        <TABLE border=0 align=\"center\"><TR><TD align=\"center\" valign=\"bottom\">";}
```

```
        if ($loop == 19) {print "</TD></TR></TABLE><P>
        <TABLE border=0 align=\"center\"><TR><TD align=\"center\" valign=\"bottom\">";}
        if ($loop == $years-1) {last JPG_LOOP;}
        next JPG_LOOP;
        }
        }
        if ($value == @wrc[0]) {$stabyr = "1st";} elsif($value == @wrc[1]) {$stabyr = "2nd";}elsif
        ($value == @wrc[2]) {$stabyr = "3rd";} elsif ($value == @wrc[3]) {$stabyr = "4th";} elsif
        ($value == @wrc[4]) {$stabyr = "5th";} elsif ($value == @wrc[5]) {$stabyr = "6th";} elsif
        ($value == @wrc[6]) {$stabyr = "7th";} elsif ($value == @wrc[7]) {$stabyr = "8th";}elsif ($value
        == @wrc[8]) {$stabyr = "9th";}else {($stabyr = "10th");}
        if ($years >9){print "The climate scenario you have defined remains static in its inputs, therefore
        the growth increment stabilizes at $value in the $stabyr year and remains the same through the
        time period you have selected.";}
print<<"EOMODEL";
        </TD> </TR> </TABLE>
EOMODEL
}

sub DFOUT {

print<<"EOMODEL";
        <P> <HR width= 550> <TABLE border=0 align="center">
        <P><CENTER><IMG src="/vi3.gif"></CENTER><P><P>
        <H2><UND> Results for $sector</UND></H2>
        <TR> <TD height="150" width="100" align="center" valign="middle">
        <IMG src="/df.gif"><BR><B>Douglas-<BR>fir</B> </TD>
        <TD height="150"  width="100" align="center" valign="middle">
        <IMG src="/$df_rad">  </TD>
        <TD height="150"  width="300" align="left" valign="middle">
        Based on average growth of 1.0, the climate parameters you have selected
        for the $years years of growth, suggest the average tree growth would be $df_total1
        or $df_norm  </TD> </TR> </TABLE>
        <TABLE border=0 align="center"> <TR> <TD align="center" valign="bottom">
EOMODEL
        JPG_LOOP: for ($loop = 0; $loop <= $years; $loop++){
        {$value = @df[$loop];
        if ($value > 1.05) {$PIC ="df1.gif";} elsif ($value < 0.95){$PIC="df3.gif";} else
        {($PIC ="df2.gif");}
        $timeE = $timeE + 1;
        print "Year $timeE<spacer type=\"horizontal\" size=\"7\"> <BR>
        <IMG SRC=\"/$PIC\"><BR>$value</TD><TD align=\"center\" valign=\"bottom\">";
        if ($loop == 9) {print "</TD></TR></TABLE><P>
        <TABLE border=0 align=\"center\"><TR><TD align=\"center\" valign=\"bottom\">";}
        if ($loop == 19) {print "</TD></TR></TABLE><P>
        <TABLE border=0 align=\"center\"><TR><TD align=\"center\" valign=\"bottom\">";}
        if ($loop == $years-1) {last JPG_LOOP;}
        next JPG_LOOP;
        }
        }
        if ($value == @df[0]) {$stabyr = "1st";} elsif ($value == @df[1]) {$stabyr = "2nd";}elsif
        ($value == @df[2]) {$stabyr = "3rd";} elsif ($value == @df[3]) {$stabyr = "4th";} elsif
```

```
        ($value == @df[4]) {$stabyr = "5th";} elsif ($value == @df[5]) {$stabyr = "6th";} elsif
        ($value == @df[6]) {$stabyr = "7th";} elsif ($value == @df[7]) {$stabyr = "8th";}elsif
        ($value == @df[8]) {$stabyr = "9th";} else {($stabyr = "10th");}
        if ($years >9){print "The climate scenario you have defined remains static in its inputs, therefore
        the growth increment stabilizes at $value in the $stabyr year and remains the same through the
        time period you have selected.";}
print<<"EOMODEL";
        </TD> </TR> </TABLE>
EOMODEL

sub ALLOUT {

print<<"EOMODEL";
        <HR width= 550> <TABLE border=0 align="center"> <P> <CENTER>
        <IMG src="/vi3.jpg"></CENTER><P><P>
        <H2><UND> Results for $sector</UND></H2>
        <TR> <TD height="150" width="100" align="center" valign="middle">
        <IMG src="/mh.gif"><BR><B>Mountain<BR>Hemlock</B> </TD>
        <TD height="150" width="100" align="center" valign="middle">
        <IMG src="/$mh_rad"> </TD>
        <TD height="150" width="300" align="left" valign="middle">
        Based on average growth of 1.0, the climate parameters you have selected
        for the $years years of growth, suggest the average tree growth would be $mh_totall
        or $mh_norm </TD> </TR> </TABLE>
        <TABLE border=0 align="center">
        <TR> <TD align="center" valign="bottom">
EOMODEL
        JPG_LOOP: for ($loop = 0; $loop <= $years; $loop++){
        {$value = @mh[$loop];
        if ($value > 1.05) {$PIC ="mh1.gif";} elsif ($value < 0.95){$PIC="mh3.gif";} else
        {($PIC ="mh2.gif");}
        $timeA = $timeA + 1;
        print "Year $timeA<spacer type=\"horizontal\" size=\"7\"> <BR>
        <IMG SRC=\"/$PIC\"><BR>$value</TD><TD align=\"center\" valign=\"bottom\">";
        if ($loop == 9) {print "</TD></TR></TABLE><P>
        <TABLE border=0 align=\"center\"><TR><TD align=\"center\" valign=\"bottom\">";}
        if ($loop == 19) {print "</TD></TR></TABLE><P>
        <TABLE border=0 align=\"center\"><TR><TD align=\"center\" valign=\"bottom\">";}
        if ($loop == $years-1) {last JPG_LOOP;}
        next JPG_LOOP;
        }
        }
print<<"EOMODEL";
        </TD> </TR> </TABLE> <HR width= 550> <TABLE border=0 align="center">
        <TR> <TD height="150" width="100" align="center" valign="middle">
        <IMG src="/yc.gif"><BR><B>Yellow<BR>Cedar</B> </TD>
        <TD height="150" width="100" align="center" valign="middle">
        <IMG src="/$yc_rad"> </TD>
        <TD height="150" width="300" align="left" valign="middle">
        Based on average growth of 1.0, the climate parameters you have selected
        for the $years years of growth, suggest the average tree growth would be $yc_totall
        or $yc_norm </TD> </TR> </TABLE>
```

```
        <TABLE border=0 align="center"> <TR>
        <TD align="center" valign="bottom">
EOMODEL
        JPG_LOOP: for ($loop = 0; $loop <= $years; $loop++){
        {$value = @yc[$loop];
        if ($value > 1.05) {$PIC ="yc1.gif";} elsif ($value < 0.95){$PIC="yc3.gif";} else
        {($PIC ="yc2.gif");}
        $timeB = $timeB + 1;
        print "Year $timeB<spacer type=\"horizontal\" size=\"7\"> <BR>
        <IMG SRC=\"/$PIC\"><BR>$value</TD><TD align=\"center\" valign=\"bottom\">";
        if ($loop == 9) {print "</TD></TR></TABLE><P><TABLE border=0
        align=\"center\"><TR><TD align=\"center\" valign=\"bottom\">";}
        if ($loop == 19) {print "</TD></TR></TABLE><P><TABLE border=0
        align=\"center\"><TR><TD align=\"center\" valign=\"bottom\">";}
        if ($loop == $years-1) {last JPG_LOOP;}
        next JPG_LOOP;
        }
        }
print<<"EOMODEL";
        </TD> </TR> </TABLE> <HR width= 550> <TABLE> <TR>
        <TD height="150"  width="100" align="center" valign="middle">
        <IMG src="/wh.gif"><BR><B>Western<BR>Hemlock</B> </TD>
        <TD height="150"  width="100" align="center" valign="middle">
        <IMG src="/$wh_rad"></TD>
        <TD height="150"  width="300" align="left" valign="middle">
        Based on average growth of 1.0, the climate parameters you have selected
        for the $years years of growth, suggest the average tree growth would be $wh_totall
        or $wh_norm </TD> </TR> </TABLE>
        <TABLE border=0 align="center"> <TR> <TD align="center" valign="bottom">
EOMODEL
        JPG_LOOP: for ($loop = 0; $loop <= $years; $loop++){
        {$value = @wh[$loop];
        if ($value > 1.05) {$PIC ="wh1.gif";} elsif ($value < 0.95){$PIC="wh3.gif";} else {($PIC
        ="wh2.gif");}
        $timeC = $timeC + 1;
        print "Year $timeC<spacer type=\"horizontal\" size=\"7\"> <BR>
        <IMG SRC=\"/$PIC\"><BR>$value</TD><TD align=\"center\" valign=\"bottom\">";
        if ($loop == 9) {print "</TD></TR></TABLE><P><TABLE border=0
        align=\"center\"><TR><TD align=\"center\" valign=\"bottom\">";}
        if ($loop == 19) {print "</TD></TR></TABLE><P><TABLE border=0
        align=\"center\"><TR><TD align=\"center\" valign=\"bottom\">";}
        if ($loop == $years-1) {last JPG_LOOP;}
        next JPG_LOOP;
        }
        }
print<<"EOMODEL";
        </TD> </TR></TABLE> <HR width= 550> <TABLE border=0 align="center">
        <TR> <TD height="150" width="100" align="center" valign="middle">
        <IMG SRC="/wrc.gif"><BR><B>Western<BR>Red-cedar</B> </TD>
        <TD height="150"  width="100" align="center" valign="middle">
        <IMG src="/$wrc_rad"> </TD>
        <TD height="150"  width="300" align="left" valign="middle">
```

```
        Based on average growth of 1.0, the climate parameters you have selected
        for the $years years of growth, suggest the average tree growth would be $wrc_total1
        or $wrc_norm
        </TD> </TR> </TABLE> <TABLE border=0 align="center">
        <TR> <TD align="center" valign="bottom">
EOMODEL
        JPG_LOOP: for ($loop = 0; $loop <= $years; $loop++){
        {$value = @wrc[$loop];
        if ($value > 1.05) {$PIC ="wrc1.gif";} elsif ($value < 0.95){$PIC="wrc3.gif";} else {($PIC
        ="wrc2.gif");}
        $timeD = $timeD + 1;
        print "Year $timeD<spacer type=\"horizontal\" size=\"7\"> <BR>
        <IMG SRC=\"/$PIC\"><BR>$value</TD><TD align=\"center\" valign=\"bottom\">";
        if ($loop == 9) {print "</TD></TR></TABLE><P>
        <TABLE border=0 align=\"center\"><TR><TD align=\"center\" valign=\"bottom\">";}
        if ($loop == 19) {print "</TD></TR></TABLE><P>
        <TABLE border=0 align=\"center\"><TR><TD align=\"center\" valign=\"bottom\">";}
        if ($loop == $years-1) {last JPG_LOOP;}
        next JPG_LOOP;
        }
        }
print<<"EOMODEL";
        </TD> </TR> </TABLE> <HR width= 550> <TABLE border=0 align="center">
        <TR> <TD height="150" width="100" align="center" valign="middle">
        <IMG SRC="/df.gif"><BR><B>Douglas-<BR>fir</B> </TD>
        <TD height="150"  width="100" align="center" valign="middle">
        <IMG src="/$df_rad">  </TD>
        <TD height="150"  width="300" align="left" valign="middle">
        Based on average growth of 1.0, the climate parameters you have selected
        for the $years years of growth, suggest the average tree growth would be $df_total1
        or $df_norm
        </TD> </TR> </TABLE> <TABLE border=0 align="center">
        <TR> <TD align="center" valign="bottom">
EOMODEL
        JPG_LOOP: for ($loop = 0; $loop <= $years; $loop++){
        {$value = @df[$loop];
        if ($value > 1.05) {$PIC ="df1.gif";} elsif ($value < 0.95){$PIC="df3.gif";} else
        {($PIC ="df2.gif");}
        $timeE = $timeE + 1;
        print "Year $timeE<spacer type=\"horizontal\" size=\"7\"> <BR>
        <IMG SRC=\"/$PIC\"><BR>$value</TD><TD align=\"center\" valign=\"bottom\">";
        if ($loop == 9) {print "</TD></TR></TABLE><P>
        <TABLE border=0 align=\"center\"><TR><TD align=\"center\" valign=\"bottom\">";}
        if ($loop == 19) {print "</TD></TR></TABLE><P>
        <TABLE border=0 align=\"center\"><TR><TD align=\"center\" valign=\"bottom\">";}
        if ($loop == $years-1) {last JPG_LOOP;}
        next JPG_LOOP;
        }
        }
print<<"EOMODEL";
        </TD> </TR> </TABLE> <HR width= 550>
EOMODEL
```

```
}

sub Trunk {
        $mh = sprintf("%1.2f",$mh);
        $yc = sprintf("%1.2f",$yc);
        $wh = sprintf("%1.2f",$wh);
        $wrc = sprintf("%1.2f",$wrc);
        $df = sprintf("%1.2f",$df);
        $mh_total1 = sprintf("%1.2f",$mh_total1);
        $yc_total1 = sprintf("%1.2f",$yc_total1);
        $wh_total1 = sprintf("%1.2f",$wh_total1);
        $wrc_total1 = sprintf("%1.2f",$wrc_total1);
        $df_total1 = sprintf("%1.2f",$df_total1);
        $total1 = sprintf("%1.2f",$total1);
        $mh1 = sprintf("%1.2f",$mh1);
        $yc1 = sprintf("%1.2f",$yc1);
        $wh1 = sprintf("%1.2f",$wh1);
        $wrc1 = sprintf("%1.2f",$wrc1);
        $df1 = sprintf("%1.2f",$df1);
}

sub Count {

        open (COUNTFILE, "treecount3.txt") || die "Can not open COUNTFILE";
        $runs = (<COUNTFILE>);
        close (COUNTFILE);
        unless ($runs > 0) { return; }
        open (OUTFILE, ">treecount3.txt") || die "Can not open OUTFILE";
        $runs += 1;
        print OUTFILE $runs;
        close (OUTFILE);
}
sub Footer {
        print $_[0] if "$_[0]";
        print $endmessage if "$endmessage";
print<<"EOFOOTER";
        <P> <CENTER> <HR width = 260><BR>
         Please forward any questions to
         <A HREF="mailto:colin\@uvtrl.geog.uvic.ca">Colin</A><BR><P>
         <HR width = 150><BR> <P><A HREF="http://cgrg.geog.uvic.ca/cgi-bin/tree.cgi">
        <B>Return to the <I><FONT COLOR="GREEN">TREE</I></FONT> Model</B></A>
        </CENTER>
EOFOOTER
        &Count;
print<<"EOFOOTER";
        <P><P> There have been $runs runs of the <I><FONT COLOR="GREEN">TREE</I>
        <FONT> model Version 2.1 since we went online January 1st, 2002! <P><P>
        </BODY>
        </HTML>
EOFOOTER
        exit (1);
}
```

Appendix D - **HTML code - *TREE* Forms**

```
<FORM METHOD=POST ACTION="/cgi-bin/tree.cgi">
<BODY bgcolor="FFFFCC"> <center> <P> <HR width = 550><BR><P>
<P><H3><BOLD> STEP 1:</H3></BOLD><TABLE border=0 align="center">
        <TR> <TD width="150" align="center" valign="middle">
        <B>Select a high elevation species on Vancouver Island which you wish to apply the
        <I><FONT COLOR="GREEN">TREE</I></FONT> model. </B><BR>
        <CENTER><P> <B>Sector Selector</B><BR><P> </CENTER>
        <SELECT NAME="sector" TYPE ="text" SIZE= 1>
        <OPTION>Mountain hemlock <OPTION> Yellow-cedar <OPTION>Western hemlock
        <OPTION>Western red-cedar <OPTION>Douglas-fir <OPTION>All montane tree species
        </SELECT> </TD> <TD width="150" align="center" valign="middle">
        <IMG src="/vi3.jpg"> </TD> </TR> </TABLE> <P><HR width = 550><BR><P>

<P><H3><BOLD> STEP 2:</H3></BOLD>
        <CENTER><B>The following portion of the form allows you to alter a set of climate paramaters
        for future growth.  You are allowed to deviate future climates from the average established
        pattern. </B></CENTER><P><P> <P><H3><B><U> Current Year's Climate </H3></B></U>
        <TABLE border=0 align="center">
        <TD width="170" align="right" valign="middle"  bgcolor="FF8000">
       <B>January Temperature</B> </TD> <TD width="200" align="left" valign="middle"
        bgcolor="FF8000">  <SELECT NAME="jan-temp" VALUE="equals" SIZE= 1>
        <OPTION> 100 yr. Average <OPTION>2.0 <OPTION>1.5 <OPTION> 1.0 <OPTION>0.5
        <OPTION>-0.5 <OPTION>-1.0  <OPTION>-1.5 <OPTION>-2.0 </SELECT>
        <B> degrees C</B> </TD>

        <TD width="170" align="right" valign="middle" bgcolor="FF8000">
       <B>February Temperature</B> </TD>
        <TD width="200" align="left" valign="middle" bgcolor="FF8000">
         <SELECT NAME="feb-temp" VALUE="equals" SIZE= 1>
        <OPTION> 100 yr. Average <OPTION>2.0 <OPTION>1.5 <OPTION> 1.0 <OPTION>0.5
        <OPTION>-0.5 <OPTION>-1.0 <OPTION>-1.5 <OPTION>-2.0 </SELECT>
        <B> degrees C</B> </TD> </TR>
```

```
<TR><TD width="170" align="right" valign="middle" bgcolor="FF6000">
 <B>March Temperature</B></TD>
<TD width="200" align="left" valign="middle" bgcolor="FF6000">
 <SELECT NAME="march-temp" VALUE="equals" SIZE= 1>
<OPTION>100 yr. Average <OPTION>2.0 <OPTION>1.5 <OPTION>1.0 <OPTION>0.5
<OPTION>-0.5 <OPTION>-1.0 <OPTION>-1.5 <OPTION>-2.0 </SELECT>
<B> degrees C</B> </TD>

<TD width="170" align="right" valign="middle" bgcolor="FF6000">
<B>April Temperature</B> </TD>
<TD width="200" align="left" valign="middle"  bgcolor="FF6000">
 <SELECT NAME="april-temp" VALUE="equals" SIZE= 1>
<OPTION>100 yr. Average <OPTION>2.0 <OPTION>1.5 <OPTION>1.0 <OPTION>0.5
<OPTION>-0.5 <OPTION>-1.0 <OPTION>-1.5 <OPTION>-2.0 </SELECT>
<B> degrees C</B> </TD> </TR> <TR>

<TD width="175" align="right" valign="middle" bgcolor="FF1000">
<B>May Temperature</B> </TD>
 <TD width="200" align="left" valign="middle" bgcolor="FF1000">
 <SELECT NAME="may-temp" VALUE="depth" SIZE= 1>
<OPTION>100 yr. Average <OPTION>2.0 <OPTION>1.5 <OPTION>1.0 <OPTION>0.5
<OPTION>-0.5 <OPTION>-1.0 <OPTION>-1.5 <OPTION>-2.0 </SELECT>
<B> degrees C</B> </TD>

<TD width="175" align="right" valign="middle" bgcolor="FF1000">
<B>June Temperature</B> </TD>
 <TD width="200" align="left" valign="middle"  bgcolor="FF1000">
 <SELECT NAME="june-temp" VALUE="depth" SIZE= 1>
<OPTION>100 yr. Average <OPTION>2.0 <OPTION>1.5 <OPTION>1.0 <OPTION>0.5
<OPTION>-0.5 <OPTION>-1.0 <OPTION>-1.5 <OPTION>-2.0 </SELECT>
<B> degrees C</B></TD></TR><TR>

<TD width="175" align="right" valign="middle" bgcolor="FF1000">
<B>July Temperature</B></TD>
```

```
 <TD width="200" align="left" valign="middle" bgcolor="FF1000">
 <SELECT NAME="july-temp" VALUE="depth" SIZE= 1>
<OPTION>100 yr. Average <OPTION>2.0 <OPTION>1.5 <OPTION>1.0 <OPTION>0.5
<OPTION>-0.5  <OPTION>-1.0    <OPTION>-1.5   <OPTION>-2.0   </SELECT>
<B> degrees C</B>
</TD>

<TD width="175" align="right" valign="middle" bgcolor="FF1000">
<B>August Temperature</B></TD>
 <TD width="200" align="left" valign="middle" bgcolor="FF1000">
 <SELECT NAME="aug-temp" VALUE="depth" SIZE= 1>
<OPTION>100 yr. Average <OPTION>2.0 <OPTION>1.5 <OPTION>1.0 <OPTION>0.5
<OPTION>-0.5   <OPTION>-1.0 <OPTION>-1.5 <OPTION>-2.0 </SELECT>
<B> degrees C</B> </TD> </TR>

<TR><TD width="170" align="right" valign="middle" bgcolor="FF6000">
<B>September Temperature</B> </TD>
<TD width="200" align="left" valign="middle" bgcolor="FF6000">
 <SELECT NAME="sept-temp" VALUE="equals" SIZE= 1>
<OPTION>100 yr. Average <OPTION>2.0 <OPTION>1.5 <OPTION>1.0 <OPTION>0.5
<OPTION>-0.5   <OPTION>-1.0   <OPTION>-1.5   <OPTION>-2.0   </SELECT>
<B> degrees C</B> </TD>

<TD width="170" align="right" valign="middle" bgcolor="FF6000">
 <B>October Temperature</B></TD>
<TD width="200" align="left" valign="middle" bgcolor="FF6000">
 <SELECT NAME="oct-temp" VALUE="equals" SIZE= 1>
<OPTION>100 yr. Average <OPTION>2.0 <OPTION>1.5 <OPTION>1.0 <OPTION>0.5
<OPTION>-0.5 <OPTION>-1.0 <OPTION>-1.5 <OPTION>-2.0 </SELECT>
<B> degrees C</B> </TD> </TR>

<TR><TD width="170" align="right" valign="middle" bgcolor="FF8000">
<B>November Temperature</B> </TD>
<TD width="200" align="left" valign="middle" bgcolor="FF8000">
 <SELECT NAME="nov-temp" VALUE="equals" SIZE= 1>
```

```
<OPTION>100 yr. Average <OPTION>2.0 <OPTION>1.5 <OPTION>1.0 <OPTION>0.5
<OPTION>-0.5 <OPTION>-1.0 <OPTION>-1.5 <OPTION>-2.0 </SELECT>
<B> degrees C</B> </TD>

<TD width="170" align="right" valign="middle" bgcolor="FF8000">
<B>December Temperature</B> </TD>
<TD width="200" align="left" valign="middle" bgcolor="FF8000">
<SELECT NAME="dec-temp" VALUE="equals" SIZE= 1>
<OPTION>100 yr. Average <OPTION>2.0 <OPTION>1.5 <OPTION>1.0 <OPTION>0.5
<OPTION>-0.5 <OPTION>-1.0 <OPTION>-1.5<OPTION>-2.0 </SELECT>
<B> degrees C</B> </TD> </TR> </TABLE><P><P>

<TABLE border=0 align="center"><TR>
<TD width="170" align="right" valign="middle" bgcolor="3060FF">
<B>January Precipitation</B> </TD>
<TD width="200" align="left" valign="middle" bgcolor="3060FF">
 <SELECT NAME="jan-precip" VALUE="equals" SIZE= 1>
<OPTION>100 yr. Average <OPTION>75.0 <OPTION>50.0 <OPTION>20.0 <OPTION>10.0
<OPTION>5.0 <OPTION>3.0 <OPTION>-3.0 <OPTION>-5.0 <OPTION>-10.0
<OPTION>-20.0 <OPTION>-50.0 <OPTION>-75.0 </SELECT>
<B> mm</B></TD>

<TD width="170" align="right" valign="middle" bgcolor="3060FF">
 <B>February Precipitation</B> </TD>
<TD width="200" align="left" valign="middle" bgcolor="3060FF">
 <SELECT NAME="feb-precip" VALUE="equals" SIZE= 1>
<OPTION>100 yr. Average <OPTION>75.0 <OPTION>50.0 <OPTION>20.0 <OPTION>10.0
<OPTION>5.0 <OPTION>3.0 <OPTION>-3.0 <OPTION>-5.0 <OPTION>-10.0
<OPTION>-20.0 <OPTION>-50.0 <OPTION>-75.0 </SELECT>
<B> mm</B></TD></TR> <TR>

<TD width="170" align="right" valign="middle" bgcolor="30A0FF">
<B>March Precipitation</B></TD>

<TD width="200" align="left" valign="middle" bgcolor="30A0FF">
```

```
 <SELECT NAME="march-precip" VALUE="equals" SIZE= 1>
<OPTION>100 yr. Average <OPTION>50.0 <OPTION>30.0 <OPTION>20.0 <OPTION>10.0
<OPTION>5.0 <OPTION>3.0 <OPTION>-3.0 <OPTION>-5.0 <OPTION>-10.0
<OPTION>-20.0 <OPTION>-30.0 <OPTION>-50.0 </SELECT>
<B> mm</B> </TD>

<TD width="170" align="right" valign="middle" bgcolor="30A0FF">
<B>April Precipitation</B></TD>
<TD width="200" align="left" valign="middle" bgcolor="30A0FF">
<SELECT NAME="april-precip" VALUE="equals" SIZE= 1>
<OPTION>100 yr. Average<OPTION>30.0 <OPTION>20.0 <OPTION>10.0 <OPTION>5.0
<OPTION>3.0 <OPTION>1.0 <OPTION>-1.0 <OPTION>-3.0 <OPTION>-5.0 OPTION>-10.0
<OPTION>-20.0 <OPTION>-30.0 </SELECT>
<B> mm</B></TD></TR><TR>

<TD width="170" align="right" valign="middle" bgcolor="30C0FF">
<B>May Precipitation</B> </TD>
<TD width="200" align="left" valign="middle" bgcolor="30C0FF">
 <SELECT NAME="may-precip" VALUE="equals" SIZE= 1>
<OPTION>100 yr. Average <OPTION>30.0 <OPTION>20.0 <OPTION>10.0 <OPTION>5.0
<OPTION>3.0 <OPTION>1.0 <OPTION>-1.0 <OPTION>-3.0 <OPTION>-5.0 <OPTION>-10.0
<OPTION>-20.0 <OPTION>-30.0 </SELECT>
<B> mm</B> </TD>

<TD width="170" align="right" valign="middle" bgcolor="30C0FF">
<B>June Precipitation</B>  </TD>
<TD width="200" align="left" valign="middle" bgcolor="30C0FF">
 <SELECT NAME="june-precip" VALUE="equals" SIZE= 1>
<OPTION>100 yr. Average <OPTION>30.0 <OPTION>20.0 <OPTION>10.0 <OPTION>5.0
<OPTION>3.0 <OPTION>1.0 <OPTION>-1.0 <OPTION>-3.0 <OPTION>-5.0
<OPTION>-10.0 <OPTION>-20.0 <OPTION>-30.0 </SELECT>
<B> mm</B> </TD> </TR>

<TR><TD width="170" align="right" valign="middle" bgcolor="30C0FF">
<B>July Precipitation</B> </TD>
```

```
<TD width="200" align="left" valign="middle" bgcolor="30C0FF">
 <SELECT NAME="july-precip" VALUE="equals" SIZE= 1>
<OPTION>100 yr. Average <OPTION>30.0 <OPTION>20.0 <OPTION>10.0 <OPTION>5.0
<OPTION>3.0 <OPTION>1.0 <OPTION>-1.0 <OPTION>-3.0 <OPTION>-5.0
<OPTION>-10.0 <OPTION>-20.0 <OPTION>-30.0 </SELECT>
<B> mm</B> </TD>

<TD width="170" align="right" valign="middle" bgcolor="30C0FF">
 <B>August Precipitation</B> </TD>
<TD width="200" align="left" valign="middle" bgcolor="30C0FF">
 <SELECT NAME="aug-precip" VALUE="equals" SIZE= 1>
<OPTION>100 yr. Average <OPTION>30.0 <OPTION>20.0 <OPTION>10.0 <OPTION>5.0
<OPTION>3.0 <OPTION>1.0 <OPTION>-1.0 <OPTION>-3.0 <OPTION>-5.0
<OPTION>-10.0 <OPTION>-20.0 <OPTION>-30.0 </SELECT>
<B> mm</B> </TD> </TR>

<TR><TD width="170" align="right" valign="middle" bgcolor="30A0FF">
<B>September Precipitation</B> </TD>
<TD width="200" align="left" valign="middle" bgcolor="30A0FF">
 <SELECT NAME="sept-precip" VALUE="equals" SIZE= 1>
<OPTION>100 yr. Average <OPTION>40.0 <OPTION>30.0 <OPTION>20.0 <OPTION>10.0
<OPTION>5.0 <OPTION>3.0 <OPTION>-3.0 <OPTION>-5.0 <OPTION>-10.0
<OPTION>-20.0 <OPTION>-30.0 <OPTION>-40.0 </SELECT>
<B> mm</B></TD>

<TD width="170" align="right" valign="middle" bgcolor="30A0FF">
<B>October Precipitation</B> </TD>
<TD width="200" align="left" valign="middle" bgcolor="30A0FF">
<SELECT NAME="oct-precip" VALUE="equals" SIZE= 1>
<OPTION>100 yr. Average <OPTION>50.0 <OPTION>30.0 <OPTION>20.0 <OPTION>10.0
<OPTION>5.0 <OPTION>3.0 <OPTION>-3.0 <OPTION>-5.0 <OPTION>-10.0
<OPTION>-20.0 <OPTION>-30.0 <OPTION>-50.0 </SELECT>
<B> mm</B></TD> </TR>

<TR> <TD width="170" align="right" valign="middle" bgcolor="3060FF">
```

```
<B>Novemebr Precipitation</B> </TD>
<TD width="200" align="left" valign="middle" bgcolor="3060FF">
<SELECT NAME="nov-precip" VALUE="equals" SIZE= 1>
<OPTION> 100 yr. Average <OPTION>75.0 <OPTION>50.0 <OPTION>20.0 <OPTION>10.0
<OPTION> 5.0 <OPTION>3.0 <OPTION>-3.0 <OPTION>-5.0 <OPTION>-10.0
<OPTION>-20.0 <OPTION>-50.0 <OPTION>-75.0 </SELECT>
<B> mm</B> </TD>

<TD width="170" align="right" valign="middle" bgcolor="3060FF">
 <B>December Precipitation</B> </TD>
<TD width="200" align="left" valign="middle" bgcolor="3060FF">
<SELECT NAME="dec-precip" VALUE="equals" SIZE= 1>
<OPTION> 100 yr. Average <OPTION>75.0 <OPTION>50.0 <OPTION>20.0 <OPTION>10.0
<OPTION> 5.0  <OPTION>3.0 <OPTION>-3.0 <OPTION>-5.0 <OPTION>-10.0
<OPTION>-20.0 <OPTION>-50.0 <OPTION>-75.0 </SELECT>
<B> mm</B> </TD> </TR> </TABLE>

<BR><P><HR width = 260><BR><P><P>

<H3><BOLD> STEP 3:</H3></BOLD>
<CENTER><B>Lastly you are allowed to choose the number of years that you
would like these climatic conditons to persist.  Intervals from 1 to 20 years
are avaiable to be selected.  Year-to-year effects will slowly compound and alter the radial growth
conditions of the tree species, so a lag effect is also calculated and applied to the radial
growth if you select an interval of more than one year. </B></CENTER><P><P>

<TABLE border=0 align="center"> <TR>
<TD width="20%" align="CENTER" valign="middle"> <CENTER>
<B>Modelled<BR>Years</B><BR>  <SELECT NAME="years" TYPE ="text" SIZE= 1>
<OPTION> 1 <OPTION> 5 <OPTION> 10 <OPTION> 20 </SELECT> </CENTER>
</TD> </TR> </TABLE><P><HR width = 260><BR><P><P>

<TABLE><TR> <TD align="center">
<INPUT TYPE="SUBMIT" value="RUN MODEL"></TD> <TD align="center">
 <INPUT NAME="RESET" TYPE="RESET"></TD></TR></TABLE></FORM><P>
```

VITA

SURNAME: Laroque **GIVEN NAMES**: Colin Peter

PLACE OF BIRTH: Saskatoon, Saskatchewan

EDUCATIONAL INSTITUTIONS ATTENDED:

University of Victoria	1996 to 2001
University of Victoria	1993 to 1995
University of Saskatchewan	1988 to 1993

DEGREES AWARDED

M.Sc.	University of Victoria	1995
B.Sc. (Honours)	University of Saskatchewan	1993

HONOURS AND AWARDS

- WCAG Student Presentation Award (honourable mention), 1999
- WCAG Student Presentation Award (honourable mention), 1998
- Derek Sewell Graduate Scholarship, 1997
- B.C. Environmental Research Scholarship, 1996
- Griffith Taylor Prize in Geography, 1993
- Undergraduate College Travel Grant, 1993
- R.C.G.S Undergraduate Project Bursary, 1993
- Alumni Challenge Undergraduate Scholarship, 1992
- R.C.G.S Undergraduate Project Bursary, 1991

PUBLICATIONS:

Laroque, C.P., Lewis, D.H., and Smith, D. J., 2000/01. Treeline dynamics on southern Vancouver Island, British Columbia. *Western Geography*, 10/11: 43-63.

Kellner, A.E., Laroque, C.P., Smith, D.J., and Harestad, A.S., 2000. Chronological dating of high-elevation dead and dying trees on Northern Vancouver Island, British Columbia. *Northwest Science*, 74: 242-247.

Carter, R., LeRoy, S., Nelson, T., Laroque, C.P., and Smith, D.J., 1999. Dendroglaciological investigations at Hilda Creek rock glacier, Banff National Park, Canadian Rocky Mountains. *Géographie physique et Quaternaire*, 53: 365-371.

Laroque, C.P., and Smith, D.J., 1999. Tree-ring analysis of yellow-cedar (*Chamaecyparis nootkatensis*) on Vancouver Island, British Columbia. *Canadian Journal of Forest Research*, 29: 115-123.

Smith, D.J., and Laroque, C.P., 1998. Mountain hemlock growth dynamics on Vancouver Island. *Northwest Science*, 72 (Special Issue 2): 67-70.

Smith, D.J., and Laroque, C.P., 1998. High-elevation dendroclimatic records from Vancouver Island. *In: Decoding Canada s Past: Climate Variations and Biodiversity Change During the Last Millennium*. MacIver, D.C. and Meyer, R.E. (eds.). Atmospheric and Environment Services, Downsview, Ontario, 33-44.

Smith, D.J., and Laroque, C.P., 1996. Dendroglaciological dating of a Little Ice Age glacial advance at Moving Glacier, Vancouver Island, British Columbia. *Géographie physique et Quaternaire*, 50: 47-55.

Denton, J.J., Laroque, C.P., Williams, A.E., and Wilson, P.J., 1995. Proglacial sedimentation in the Loss Creek valley, southwestern Vancouver Island, British Columbia. *Western Geography*, 5: 1-12.

Lawby, C.P., Smith, D.J, Laroque, C.P., and Brugman, M.M., 1995. Glaciological studies at Rae Glacier, Canadian Rocky Mountains. *Physical Geography*, 15: 425-441.

Conference Presentations:

Laroque, C.P., and Smith, D.J., 2001. A 900 Year Record of Pacific Decadal Oscillations in Pacific North America. Annual Meeting, Western Division Canadian Association of Geographers, Calgary, Alberta. March 8-10, 2001.

Challies, M., Cormier, L., Fric, C., George, L., Laroque, C.P., Smith, D.J., 2001. Bathymetric Analysis of Sunwapta Lake. Annual Meeting, Western Division Canadian Association of Geographers, Calgary, Alberta. March 8-10, 2001.

Laroque, C.P., and Smith, D.J. Effects of climate on radial growth of high-elevation coastal conifers, British Columbia, Canada. International Conference on Dendrochronology for the Third Millennium, Mendoza, Argentina. April 2000.

Bachrach, T., Jakobsen, K., Kinney, J., Laroque, C.P., Nishimura, P., Reyes, A., and Smith, D.J. Dendroglaciological and morphological evidence of active movement of Hilda Rock Glacier, Banff National Park, Canadian Rocky Mountains. Annual Meeting, Western Division Canadian Association of Geographers, Abbotsford, British Columbia. March 2000.

Day, C., Elmieh, N., Huisman, L., Larson, C., Wood, C., Smith, D.J. and Laroque, C.P. Neoglaciation at Saskatchewan Glacier, Banff National Park. Western Division Canadian Association of Geographers, Abbotsford, British Columbia. March 2000.

Laroque, C.P., and Smith, D.J. Applied dendroclimatology: estimating radial growth trends under changing climates at high-elevational sites on Vancouver Island, British Columbia. Annual Meeting, Canadian Association of Geographers, Lethbridge, Alberta. June 1999.

Ferby, T., Smith, D.J., and Laroque C.P. Dendrochronological study of historical log cabins in Jasper National Park: an appraisal of the Tangle Creek cabin. Annual Meeting, Western Division Canadian Association of Geographers, Kelowna, British Columbia. March 1999.

Laroque, C.P., and Smith, D.J., Understanding Tree Time : dendroclimatological baby steps in the Pacific Northwest. Annual Meeting, Western Division Canadian Association of Geographers, Kelowna, British Columbia. March 1999.

LeRoy, S., Nelson, T., Carter, R., Laroque, C.P., and Smith, D.J., Calender-dated Little Ice Age advance of the Hilda Glacier terminal moraine complex, Banff National Park, Alberta. Annual Meeting, Western Division Canadian Association of Geographers, Richmond, British Columbia. March 1998.

Laroque, C.P., Zhang, Q., Smith, D.J., and Hebda, R. Reconstruction of Little Ice Age climates on Vancouver Island: an index to glaciological responses in the southern Canadian Cordillera? Annual Meeting, Western Division Canadian Association of Geographers, Richmond, British Columbia. March 1998.

Lewis, D.H., Laroque, C.P., and Smith, D.J. Tree invasion and regeneration patterns in endangered Vancouver Island marmot habitat. Annual Meeting, Western Division Canadian Association of Geographers, Prince George, British Columbia. March 1997.

Laroque, C.P., and Smith, D.J. A dendrochronological analysis of yellow-cedar from timberline sites on Vancouver Island. Annual Meeting, Canadian Association of Geographers, Saskatoon, Saskatchewan. May 1996.

Laroque, C.P., and Smith, D.J. A millennium-long record of climatic change on Vancouver Island, B.C. Annual Meeting, Western Division Canadian Association of Geographers, Lethbridge, Alberta. March 1996.

Smith, D.J., and Laroque, C.P. High-elevation dendroclimatic records from Vancouver Island. Workshop on Climate and Biodiversity in Canada, Ottawa, Ontario. January 1996.

Smith, D.J., and Laroque, C.P. Dendroclimatic records of climate change over the last millennium at high-elevation sites in Strathcona Provincial Park, Vancouver Island. Annual Meeting, Canadian Meteorological and Oceanographic Society, Kelowna, British Columbia, May-June 1995.

Laroque, C.P., and Smith, D.J. Establishing a millennium-aged tree species, yellow-cedar (*Chamaecyparis nootkatensis*), for dendroglaciological analysis on Vancouver Island, British Columbia. Annual Meeting, Western Division Canadian Association of Geographers, Victoria, British Columbia. March 1995.

Smith, D.J., and Laroque, C.P. The untold story of Little Ice Age glacial activity on Vancouver Island, British Columbia. Annual Meeting, Western Division Canadian

Association of Geographers, Victoria, British Columbia. March 1995.

Smith, D.J., and Laroque, C.P. The growth responses of mountain hemlock and yellow-cedar to changes in climate at high-elevation sites on Vancouver Island. Fifteenth Annual Forest and Tree Related Research Colloquium, Victoria, British Columbia. April 1995.

Laroque, C.P., and Smith, D.J. Dendroclimatological index of climatic fluctuations in the Forbidden Plateau area, Strathcona Provincial Park, Vancouver Island, British Columbia. Annual Meeting, Western Division Canadian Association of Geographers, Kamloops, British Columbia. March 1994.

PARTIAL COPYRIGHT LICENSE

I hereby grant the right to lend my thesis to users of the University of Victoria Library, and to make single copies for such users or in response to a request from the Library of any other university, or similar institution, on its behalf or for one of its users. I further agree that permission for extensive copying of this thesis for scholarly purposes may be granted by me or a member of the University designated by me. It is understood that copying or publication of this thesis for financial gain shall not be allowed without my written permission.

Title of Dissertation:

Dendroclimatic Response of High-Elevation Conifers, Vancouver Island, British Columbia

Author 

Colin Peter Laroque
February 8, 2002